“Engineering and characterization of single chain antibody fragments (scFvs) specific to key enzymes in polyamine biosynthesis and manipulation of polyamine pathway by constitutive expression of recombinant ODC and SDE enzymes in transgenic tobacco”

Von der Fakultät für Mathematik, Informatik and Naturwissenschaften der Rheinisch-Westfälischen Technischen Hochschule Aachen zur Erlangung des akademischen Grades einer Doktorin der Naturwissenschaften genehmigte Dissertation

vorgelegt von

Master of Science

Greta Nölke

aus

Korce (Albanien)

Berichter: Universitätsprofessor Dr. rer. nat. R. Fischer
Universitätsprofessor Dr. rer. nat. F. Kreuzaler

Tag der mündlichen Prüfung: 20. September 2002

Für Daniel

I Introduction ... 1
I.1 Characteristics and biosynthesis of polyamines ... 1
I.1.1 Polyamines and their cellular localisation ... 1
I.1.2 Polyamines in animal cells ... 2
I.1.3 Exogenous polyamines - implications for growth and health ... 3
I.1.4 Polyamine function in plants ... 4
I.1.5 Polyamine biosynthesis pathway ... 5
I.1.6 Ornithine decarboxylase ... 7
I.1.7 Molecular and genetic approaches for modulating the levels of polyamines in plants ... 9
I.2 Engineering of recombinant antibodies by phage display technology ... 10
I.2.1 General structure of antibodies ... 10
I.2.2 Immunoglobulin genetics ... 13
I.2.3 Selection of recombinant antibodies by phage display ... 14
I.2.4 Antibody libraries ... 15
I.2.5 Expression of antibody genes in plants: immunomodulation ... 17
I.3 Aim of this thesis ... 19

II Material and Methods ... 22
II.1 Material ... 22
II.1.1 Chemicals and consumables ... 22
II.1.2 Enzymes and reaction kits ... 22
II.1.3 Primary antibodies, secondary antibodies and substrates ... 22
II.1.4 Bacterial strains ... 23
II.1.5 Plants and animals ... 24
II.1.6 Phage ... 24
II.1.7 Vectors ... 24
II.1.8 Oligonucleotides ... 25
II.1.9 Buffers, media and solutions ... 28
II.1.10 Matrices and membranes ... 29
II.1.11 Equipment and applications ... 29
II.2 Methods ... 31
II.2.1 Recombinant DNA technologies ... 31
II.2.1.1 Competent cells for RbCl-mediated transformation ... 31
II.2.1.2 Transformation of *E. coli* by heat-shock ... 32

II.2.1.3 Preparation of electrocompetent *E. coli* 32
II.2.1.4 Transformation of *E. coli* by electroporation 32
II.2.1.5 Preparation of electrocompetent *Agrobacterium* cells 32
II.2.1.6 Transformation of *Agrobacterium* by electroporation 33
II.2.1.7 Determination of the efficiency of recombinant bacteria transformation 33
II.2.1.8 Culturing of *E. coli* and glycerol stock preparation 33
II.2.1.9 Growth of recombinant *A. tumefaciens* and preparation of glycerol stocks 33
II.2.1.10 Isolation of plasmid-DNA from *E.coli* 34
II.2.1.11 Agarose gel electrophoresis of DNA 34
II.2.1.12 Preparative agarose gel electrophoresis 34
II.2.1.13 PCR amplification 34
II.2.1.14 DNA sequencing 36
II.2.1.15 Sequence analysis 36
II.2.2 Generation and characterisation of transgenic plants 36
II.2.2.1 Transient assay in tobacco leaves by vacuum infiltration 36
II.2.2.2 Preparation of recombinant Agrobacteria 36
II.2.2.3 Vacuum infiltration of intact leaves 37
II.2.2.4 Recombinant agrobacterium-mediated stable transformation of tobacco plants 37
II.2.2.5 Growth of *N. tabacum* cv. Petite Havana SR1 38
II.2.2.6 Preparation of total soluble proteins from plant leaves 38
II.2.2.7 Extraction of RNA from transgenic plants 39
II.2.2.8 Northern-blot analysis 39
II.2.3 Expression and purification of recombinant proteins 40
II.2.3.1 Expression and purification of polyamine-GST fusion proteins from *E. coli* 40
II.2.3.2 Expression and purification of ODC and PAO proteins 40
II.2.3.3 Large scale expression of scFv in pSyn and purification of soluble scFv by IMAC 41
II.2.4 Protein analysis 42
II.2.4.1 Quantification of proteins 42
II.2.4.2 SDS-PAA gel electrophoresis and Coomassie brillant blue staining 42
II.2.4.3 Immunoblot analysis 43
II.2.4.4 Dot blot analysis 44
II.2.5 Immunization of mice 44

II.2.5.1 Determination of antisera titers by ELISA 44
II.2.6 Construction of phage displayed scFv libraries 45
II.2.6.1 Isolation of total RNA from spleen cells 45
II.2.6.2 First strand cDNA synthesis 45
II.2.6.3 Construction of scFv libraries 45
II.2.6.4 *Bst*NI fingerprinting 45
II.2.7 Phage displayed antibody selection 46
II.2.8 Characterisation of phage displayed scFv fragments 46
II.2.8.1 Soluble expression of scFv fragments and direct ELISA 46
II.2.8.2 Capture ELISA of selected scFv fragments 47
II.2.8.3 Biotinylation of scFv 47
II.2.8.4 Competition ELISA of biotinylated scFv fragments 47
II.2.8.5 Electrophoretic mobility shift assay (EMSA) 47
II.2.8.6 Gel Filtration 48
II.2.8.7 Characterisation of scFv fragments by BIACORE 48
II.2.9 Determination of ODC activity 48
II.2.10 Extraction of polyamines from tobacco plants 49
II.2.10.1 Analysis of free polyamine levels from stable transformed tobacco 49

III Results 51
III.1 Cloning of human ornithine decarboxylase (ODC) a key enzyme in polyamine biosynthesis 51
III.2 Expression and purification of ADC, ODC and PAO from bacterial cultures 52
III.3 Cloning of ODC in bacteria expression vector pET22b and purification of the expressed protein via IMAC 53
III.4 Generation and characterization of transgenic plants 54
III.4.1 Engineering of constructs for targeting of human ODC to different plant cell compartments 54
III.4.1.1 Cloning of ODC into plant expression vector pSSH1 54
III.4.1.2 Transient expression of ODC in different plant cell compartments 56
III.4.2 Generation and screening of stable transformed tobacco plants expressing human ODC 58
III.4.3 Generation of transgenic tobacco plants co-expressing human ODC and chimeric mouse/human SDE enzymes 60
III.5 Polyamine analysis 61
III.5.1 Polyamine levels in stable transformed plants overexpressing ODC 61
III.5.2 Polyamine levels in transgenic plants co-expressing apoplasmic ODC and SDE enzymes 63

III.6 Enzymatic activity of ODC in stable transformed plants overexpressing human ODC 64
III.7 Immunization of mice with recombinant ADC, ODC and PAO 66
III.8 Construction of phage displayed libraries 67
III.8.1 Isolation of total RNA from mouse spleen cells 67
III.8.2 cDNA synthesis and PCR amplification of variable heavy and light chain fragments 68
III.8.3 Construction of phagemid-scFv libraries 70
III.9 Selection and characterisation of specific scFvs 73
III.9.1 Solid phase panning of libraries HA_1LA_2 and HO_1LO_2 against recombinant fusion proteins ADC and ODC-GST 73
III.9.2 Screening and characterisation of scFv-fragments against ODC-GST fusion protein 74
III.9.3 Sequence analysis of scFv fragments specific to ODC clones 76
III.9.4 Screening and characterisation of scFv-fragments against ADC-GST fusion protein 78
III.9.5 Sequence analysis of selected scFv-ADC clones 80
III.10 Characterization of biological and physical features of the ODC-specific scFv antibodies 83
III.10.1 Cloning and expression of scFvODC1, scFvODC3, scFvODC7 and scFvODC15 in *E. coli* 83
III.10.2 Stability of affinity purified scFvODCs 84
III.10.3 Reactivity of ODC-specific scFvs with ODC-GST and GST 85
III.10.4 Epitope mapping of scFvODC1, scFvODC3 and scFvODC7 by surface plasmon resonance 87
III.10.5 Comparative analysis of binding activity of scFvODC1 preincubated with ODC-GST 88
III.10.6 Electrophoretic mobility shift assay (EMSA) 90
III.10.7 *In vitro* effect of scFvODC1 and scFvODC3 on the enzymatic activity of bacterial purified ODC-GST 91
III.10.8 Transient expression of scFvODC1, 3, 7 and 15 in vacuum-infiltrated tobacco leaves 93
III.10.9 Functional analyses of the cytosolic expressed scFvODC1 and scFvODC3 94
III.10.10 Generation and screening of stable transformed plants overexpressing scFvODCs 97
III.11 Cloning and expression of scFvADC3 and scFvADC7 in *E.coli* 99
III.11.1 Reactivity of purified scFvADC3 and scFvADC7 100
III.12 Epitope mapping of scFvADC3 and scFvADC7 101
III.13 Transient expression of scFvADC3 in tobacco plants 102

IV Discussion 104
IV.1 Generation and characterization of transgenic plants 105
IV.2 Enzymatic activity and polyamine analyses of stable transformed plants overexpressing human ODC 106
IV.3 Polyamine analyses of transgenic tobacco plants co-expressing apoplasmic ODC and SDE enzymes 108
IV.4 Generation and Characterization of scFv-fragments specific to ADC, ODC and PAO 109
IV.4.1 Expression and purification of recombinant antigens 110
IV.4.2 Immunization of mice with ADC, ODC-GST and PAO-GST inclusion bodies 111
IV.4.3 Phage displayed antibody selection 112
IV.4.4 Expression and purification of scFvs in *E. coli* 115
IV.4.5 Characterization of engineered scFvs 116
IV.4.6 Generation of stable transformed tobacco plants overexpressing ODC-specific scFvs 119
IV.5 Conclusion and future prospects 121

V Summary 123

VI References 125

VII Appendices 145

I Introduction

I.1 Characteristics and biosynthesis of polyamines

I.1.1 Polyamines and their cellular localisation

The polyamines represent a group of naturally occurring compounds ubiquitous in all living cells of prokaryotes, eukaryotes, plants and animals. They play essential roles in a wide range of biological processes, including cell growth and differentiation (Pegg, 1986; Tabor and Tabor, 1984). Inhibition of polyamine synthesis results in growth arrest and eventually, cell death (Seidenfeld *et al*., 1986; Snyder *et al*., 1989; Anehus *et al*., 1984a; Quemener *et al*., 1994; Aziz *et al*., 1996). *In vivo* polyamines occur either in their free form (positively charged), or bound as conjugates with hydroxycinnamic acids (Tiburcio *et al*., 1990; Evans *et al*., 1989) and many types of proteins including numerous enzymes whose activities are directly modulated by polyamine binding (Corley *et al*., 1983, Datta *et al*., 1987, Igarashi *et al*., 1989). Chemically polyamines are organic aliphatic cations with two (putrescine), three (spermidine) or four (spermine) amino groups that are fully protonated at physiological pH. Unlike inorganic molecules or ions, the positive charges on polyamines are spaced out at intervals and, despite the hydrocarbon chains being flexible, have steric as well as cationic properties. The structure of the three most commonly occurring natural polyamines, putrescine, spermidine, and spermine, together with those of 1,3-diaminopropane and cadaverine (1,5-diaminopropane), are shown in Figure I-1.

Putrescine	NH_3^+-CH_2-CH_2-CH_2-CH_2-NH_3^+
Cadaverine	NH_3^+-CH_2-CH_2-CH_2-CH_2-CH_2-NH_3^+
Spermidine	NH_3^+-CH_2-CH_2-CH_2- NH^+-CH_2-CH_2-CH_2-NH_3^+
Spermine	NH_3^+-CH_2-CH_2-CH_2- NH^+-CH_2-CH_2-CH_2- NH^+-CH_2-CH_2-CH_2-NH_3^+
1,3-diaminopropane	NH_3^+-CH_2-CH_2-CH_2-NH_3^+

Figure I-1 Structure of polyamines.

The diamine putrescine and the polyamines spermidine and spermine are found at concentrations from micromoles to millimoles in almost any living cell (Tabor and Tabor, 1984; Pegg and McCann, 1982; Russell, 1980). Intracellular polyamine concentrations vary throughout the cell cycle. An increase in polyamine synthesis is a very early event in cell proliferation and takes place before any increase in protein or nucleic acid synthesis (Morgan, 1998) is detectable.

Understanding the biological role of polyamines in plants is hampered by the lack of knowledge about their tissue- and subcellular distribution (Kumar *et al*., 1997). The difficulties experienced in attempting to identify and measure the amounts of polyamines in biological materials are related with their size, the concentrations in which they are present and that their only reactive centers are the amino groups. In mature plant tissues polyamines are associated primarily with the cell wall, bound to polyuronic acids and lignin (Goldberg and Perdrizer, 1984). They are localized in the vacuole (Pistocchi *et al*., 1988; Jokela *et al*., 1997), mitochondria and chloroplast (Slocum, 1991a). The polyamines have also been detected in thylakoid membranes of spinach, associated with the light harvesting complex and photosystem II (Kotzabasis *et al*., 1993). In normal secretory cell systems, the polyamines are concentrated in cytoplasmic structures (Hougaard, 1992). Ultrastructural studies using immunogold labelling have shown that polyamines, primarily spermine and to a lesser extent spermidine, are concentrated in regions of high density chromatin in the interphase nucleus (Roch *et al*., 1997). The polyamine transport across the plasmalemma is energy–dependent and influenced by calcium through a cascade pathway involving protein kinase and phosphatase activities (Antognoni *et al*., 1995).

I.1.2 Polyamines in animal cells

Polyamines, primarily putrescine, spermidine and spermine, play critical roles in cell proliferation (Pegg, 1986; Piacenza *et al*., 2001), including tumor growth (Hobbs and Gilmour, 2000), differentiation, maintenance and neoplastic transformation.

In mammalian cells, polyamines play an important role in promoting S-phase progression and also facilitate the G1-S transition. Several studies have indicated the role of polyamines in inducing and prevention of apoptosis (Dypbukt *et al*., 1994, Takahashi *et al*., 2000; Piacenza *et al*., 2001; Thomas and Thomas, 2001). Polyamines induce bends and transitions in DNA from B to Z and/or A isoforms (Thomas *et al*., 1995; Korolev *et al*., 2001), and promote associations or cause release of a variety of DNA binding proteins (Bryans *et al*., 1996). They may play a critical role in stabilisation of histone interactions in formation of the nucleosome and higher chromatin structures (Ballestar *et al*., 1996; Basu *et al*., 1999; Hobbs and Gilmour, 2000). The specific interactions of polyamines with a number of different types of ion channels have also been reported (Williams, 1997). Overexpression of ornithine decarboxylase (ODC), a key enzyme in polyamine biosynthesis, leads to greater overall protein phosphorylation (Shore *et al*., 1997), suggesting that high intracellular polyamine concentration might have major impact on signalling pathways.

The polyamines have been observed to enhance transcription of a number of genes, including protooncogenes (Celano *et al*., 1989). Rapidly growing cells such as tumor cells

and regenerating cells produce greater amounts of polyamines than normal tissue (Nishioka *et al*., 1996; Takahashi *et al*., 2000), therefore polyamines can be possible biomarkers of tumor progression (Nishioka *et al*., 1995). Many studies indicate that the polyamine pathway is a molecular target for therapeutic intervention in several types of cancer. Cells are able to take up polyamines from the diets and from the polyamines produced by the intestinal mucosa and bacteria (Leveque *et al*., 1998). Thus, complete control of polyamines may require a polyamine free diet and inhibition of uptake from gastrointestinal sources (Quemener *et al*., 1994; Kumar *et al*., 1997; Thomas and Thomas, 2001). Inhibitors of polyamine biosynthesis, polyamine analoges as well as oligonucleotide polyamine analog combinations are promising drug candidates for chemoprevention and/or treatment of cancer (Thomas and Thomas, 2001).

The polyamines have a significant importance in human health. They have important neurophysiological functions (Williams *et al*., 1991; Williams, 1994; Carter, 1994) and roles in both post-natal brain development and in mature brain function (Slotkin, and Bartolome, 1986; Morrison *et al*., 1995). Polyamines also enhance the survival of sympathetic neurons (Gilad and Gilad, 1988). Studies have indicated participation of polyamines in the cortical development especially in the layer formation (Ichikawa *et al*., 1997). Abnormal polyamine activity is involved in the neurodegenerative processes occurring in the brain of patients with Alzheimer's disease (Morrison and Kish, 1995).

I.1.3 Exogenous polyamines - implications for growth and health

Exogenous polyamines play an important role in the growth process of body tissues and organs. Every organ of the body requires polyamines for growth, renewal and metabolism. The polyamine content of an organ correlates with its metabolic activity. The gut epithelium has one of the highest cell turnover and hence the highest metabolic activity of the body. Polyamines are essential for the maintenance of the high metabolic activity of the normally functioning and healthy gut. Although every cell has capacity to synthesise polyamines (Jänne et al., 1978; Pegg, 1986; Tabor and Tabor, 1984), the body also relies on a continuous supply of polyamines from food, most of which are not retained by the gut tissues, but distributed in different organs of the body. Thus the polyamine requirements that cannot be met by biosynthesis have to be satisfied by exogenous polyamines derived from food. Food varies widely in its polyamine content and distribution. Cereal grains represent the primary diet for most people in the world, yet having low levels of all polyamines (Bardoz *et al*., 1993). Rice is probably the most important, accounting for most of the energy uptake for up to 50% of the world's population (Christou, 1994). However, it contains very low levels of nutrients such as iron, calcium and polyamines (Bardocz *et al*., 1993).

The importance of different polyamine sources for growth and health changes with the physiological or pathological states of the person. With age, cell proliferation slows and the activity of ODC decreases. Therefore, dietary polyamines might be more important later in life than in growing individuals, whose polyamine requirement can be satisfied to a larger extend by more active biosynthesis. In contrast, to inhibit unwanted growth, such as neoplastic proliferation of any of the tissues, the uptake of polyamines should be minimised to slow down the growth and progression of the tumour (Molinoux *et al*., 1991; Sarah and Seiler, 1991). Thus, manipulation of polyamine biosynthetic pathway by combining genetic engineering and antibody approach could lead to the establishment of transgenic food plants with altered polyamine levels, increasing their nutritional and health values.

I.1.4 Polyamine function in plants

Molecular analysis of polyamine biosynthesis in plants was initiated in 1990 when Bell and Malmberg isolated the first ADC cDNA from oat. The polyamines have been demonstrated to play important roles in many plant metabolic processes by virtue of their polybasic nature (Rajam, 1997; Galston and Kaur-Sawhney, 1990). In addition to their involvement in plant growth and development, they play a role in plant stress tolerance (Young and Galston, 1983; 1984; Besford *et al*., 1993; Borrell *et al*., 1996), senescence (Drolet *et al*., 1986; Carbonell and Navarro, 1989), modulation of enzyme activity, and stabilization of nucleic acids and cell membranes (Tiburcio *et al*., 1989; Evans and Malmberg, 1989; Bajaj and Rajam, 1995, 1996; Sharma and Rajam, 1995; Zheliaskova *et al*., 2000). Polyamine levels in plant cells increase in response to various stresses (Galston and Kaur-Sawhney, 1990). The localisation of ADC in the chloroplast indicates the role of polyamine biosynthesis in the maintenance of photosynthetic activity during senescence responses induced by osmotic stress (Borrell *et al*., 1995). The polyamines also protect cells and cell compartments from oxidative damage (Drolet *et al*., 1986; Balasundaram, *et al*., 1993). They play a role in controlling the flux between primary and secondary metabolism (Lamberts *et al*., 1959). Many plants form toxic alkaloids from polyamines (Guggisberg and Hesse, 1983; Burtin and Michael, 1997), and the principal alkaloid of tobacco is nicotine.

At their physiological concentrations polyamines control the currents through the plant ion channels, namely through the tonoplast FV and SV channels (Dobrovinskaya *et al*., 1999). Polyamines have been implicated in somatic embryogenesis (Feirer *et al*., 1984; Minocha and Minocha, 1995), flowering (Caffaro *et al*., 1994; Caffaro and Vicente, 1994; Tarenghi and Martin-Tanguy, 1995; Havelange *et al*., 1996), floral development (Kaur-Sawhney *et al*., 1990; Rastogi and Sawhney, 1990; Perez-Amador and Carbonell, 1995), root growth

and differentiation of lateral roots (Sharma *et al*., 1997). Putrescine enhances xylogenesis of xylem cells in *Helianthus* tuber (Phillips *et al*., 1988) and it influences cambial activity in gymnosperms (Königshofer, 1991).

I.1.5 Polyamine biosynthesis pathway

The biosynthetic pathways for polyamines have been well documented. The initial key enzymes in polyamine biosynthesis are arginine decarboxylase (ADC; EC 4.1.1.19) and ornithine decarboxylase (ODC; EC 4.1.1.17). ADC catalyses the decarboxylation of L-arginine to the diamine putrescine, via agmatine and N-carbamoylputrescine. This is one of the main pathways of putrescine synthesis in plants (Tiburcio *et al*., 1990) (Figure I-2) and in some bacteria. In contrast to the pathway in animals and most fungi in which the sole route to putrescine biosynthesis is the direct decarboxylation of L-ornithine in a reaction catalysed by ODC. However, there are several preliminary reports of ADC activity in animals (Li *et al*., 1994; Morrissey *et al*., 1995; Gilad *et al*., 1996; Regunathan and Reis, 2000) and in various fungi (Khan and Minocha, 1989).

In a step common to most organisms, spermidine is formed from putrescine by addition of an aminopropyl group donated by decarboxylated S-adenosylmethionine. This reaction is catalysed by spermidine synthase (SDE), an aminopropyl-transferase. Spermine is formed by addition of the second aminopropyl moiety to spermidine, catalyzed by a different aminopropyl transferase namely, spermine synthase (SME) (Tiburcio *et al*., 1990).

Polyamines are oxidatively deaminated by the action of amine oxidases including the copper diamine oxidase (DAO; EC 1.4.3.6), and the flavoprotein polyamine oxidase (PAO; EC 1.5.3.3). Putrescine can be oxidised to pyrroline in a reaction catalized by DAO. The diamine oxidase is characterised by its substrate specificity toward diamines. The polyamine oxidase oxidises spermidine and spermine at their secondary amino groups to 1,3-diaminopropane and pyrroline or 1-(3-1-aminopropyl)-pyrroline (Smith, 1988; Tiburcio *et al*., 1997). 1,3-Diaminopropane can be converted into alanine (Terano and Suzuki, 1978), whereas pyrroline can be further catabolized to gamma-aminobutiric acid (GABA) (Flores and Filner, 1985). GABA is subsequently transaminated and oxidised to succinic acid, which is incorporated into the Krebs cycle. This pathway ensures the recycling of carbon and nitrogen from putrescine and spermidine (Flores and Filner, 1985).

Although one or both of the pathways may be active in different plant tissues, their relative contribution to the biosynthesis of putrescine in higher plants is controversial (Tiburcio *et al*., 1990). The activity of ADC is considered to be responsible for putrescine biosynthesis upon stress (Smith, 1990) or nutrient deficiency and in tissues undergoing cell elongation and morphogenesis (Flores and Galston, 1982; 1984; Pandit and Ghosh, 1988; Slocum and Weinstein, 1990; Besford *et al*., 1993; Borrell *et al*., 1995, 1996). The rise in putrescine

titers, observed in rapidly proliferating plant cells is due to ODC activity (Cohen *et al*., 1982; Hiatt *et al*., 1986). ODC and ADC are responsible for different physiological processes in plant development (Kwak and Lee, 2001).

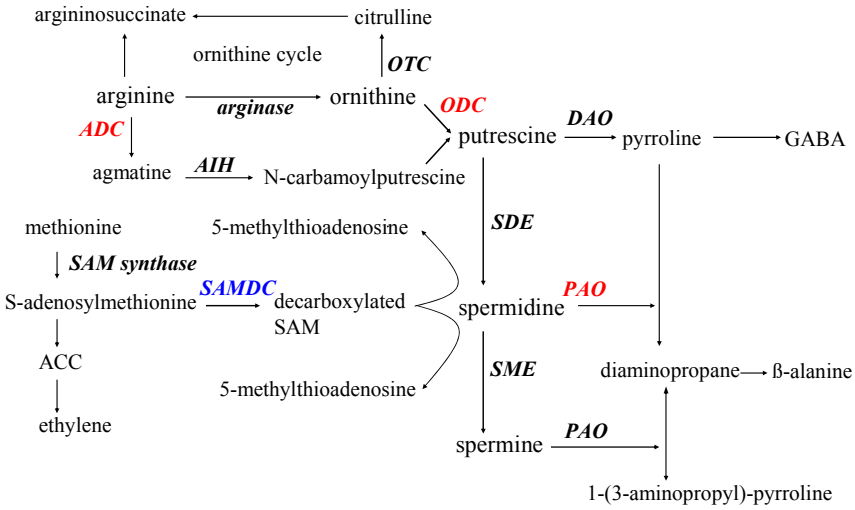

Figure I-2 Schematic representation of the polyamine biosynthetic pathway and its interrelationship with the ethylene pathway.

SAMDC, the key enzyme for both pathways is indicated in blue. The target enzymes are indicated in red. Abbreviations: *OTC*, ornithine transcarbamylase; *ADC*, arginine decarboxylase; *SAMDC*, S-adenosylmethionine decarboxylase; *ACC*, 1-aminocyclopropane-1-carboxylic acid, *ODC*, ornithine decarboxylase; *SDE*, spermidine synthase; *SME*, spermine synthase; *DAO*, diamine oxidase, *PAO*, polyamine oxidase, *AIH*, agmatine iminohydrolase; GABA, gamma-aminobutiric acid.

S-adenosynmethionine decarboxylase (SAMDC) is a further key enzyme in the biosynthesis of the polyamines spermidine and spermine from putrescine and its activity has been shown to be rate limiting in this pathway (Slocum *et al*., 1984; Tabor and Tabor, 1984; Slocum, 1991; Pegg and McCann, 1992). SAMDC influences the rate of ethylene biosynthesis (Apelbaum *et al*., 1985) as the polyamine and ethylene pathways are biosynthetically related by sharing a common precursor, SAM (Biondi *et al*., 1990; Kushad and Dumroff, 1991).

Many studies indicated that ODC activity is regulated at the transcriptional, translational and post-translational levels (Hayashi and Murakami, 1995). The protein levels and/or enzymatic activity of plant ADC and SDE are regulated post-translationally (Coleman *et al*., 1993; Schröder and Schröder, 1995; Malmberg and Cellino, 1994; Borrell *et al*., 1996; Primikiros and Roubelakis-Angelakis, 2001). The intracellular free polyamine pools do not only dependent on polyamine synthesis, but also on several other processes including: 1.) the activities of enzymes that regulate the synthesis of arginine and ornithine, like arginase (L-arginine aminohydrolase; EC 3.5.3.1) and ornithine transcarbamylase (EC 2.1.3.3) which can supply ornithine from arginine and vice versa, respectively; 2.) the catalysis of

polyamines by the respective catabolic enzymes (oxidative deamination); 3.) the interconvertion of free putrescine, spermidine and spermine to their soluble and insoluble forms; 4.) the size of the intracellular polyamine pools; 5.) polyamine transport (Tiburcio *et al*., 1990; Slocum and Flores, 1991; Bagni and Torrigiani, 1992); 6.) the rate of conversion of free putrescine to spermidine and spermine (Bouchereau *et al*., 1999; Primikirios *et al*., 1999).

I.1.6 Ornithine decarboxylase

Ornithine decarboxylase (ODC) (EC 4.1.1.17), a key enzyme of polyamine biosynthesis is one of the most highly regulated eukaryotic enzymes. ODC is an extremely labile enzyme present in low concentration. cDNA clones of ODC have been obtained from a number of species (McCann and Pegg, 1992; Michael *et al*., 1996; Alabadi and Carbonell, 1998; Kwak and Lee, 2001). The homology among eukaryotic ODC genes is greater than 90% suggesting that their structural and catalytic properties are similar. In contrast, the similarity to bacterial ODC genes is low.

Eukaryotic ODCs require pyridoxal 5′-phosphate (PLP) as a cofactor and the amino acid residues Lys^{69} and Cys^{360} are critical at the active site of ODC (Jackson *et al*., 2000). Lys^{69} in the mouse ODC is important for PLP binding (Heby and Persson, 1990). The Cys^{360} is the key residue that binds difluoromethylornithine (DFMO) a specific 'suicide' inhibitor of ODC (Metcalf *et al*., 1978). The enzyme forms a homodimer (Figure I-3), with Lys^{69} of one of the subunits forming an active site in trans with Cys^{360} of the other subunit (Tobias and Khahana, 1993; Coleman *et al*., 1993). Most ODC genes code for about 460 amino acids, except the bacterial and *Leishmania* enzymes, which are 40% bigger.

Mammalian ODC has an extremely short intracellular half-life of 15 min to 1 h (Ghoda et al., 1989; Hölttä and Pohjanpelto, 1986; Isomaa et al., 1983; McConlogue et al., 1986). Turnover of ODC is extremely rapid and highly regulated, and is accelerated when polyamine levels increase (Satriano *et al*., 1998; Babal *et al*., 2001). The polyamine-mediated degradation of ODC is associated with the antizyme (AZ), an ODC inhibitory protein induced by polyamines (Fong *et al*., 1976; Heller *et al*., 1976; Matsufuji *et al*., 1995). AZ binds to the N-terminal region of the monomeric subunit of ODC inducing conformational changes that expose the C-terminal region to the 26S proteosome-dependent degradation (Li and Coffino 1992; 1993; Murakami *et al*., 2000) without ubiquitylation (Murakami *et al*., 1992; 1999). The carboxyl terminal domain of mouse ODC contains a specific amino acid sequence PEST (residues 423-449) which makes the enzyme sensitive to cellular proteases (Rogers *et al*., 1986; Rechsteiner, 1987). Deletion of some or all of the 36 residues at the carboxyl end of the mouse enzyme does not alter

enzyme activity, but greatly increases the stability of the protein (Ghoda *et al*., 1989; Lu *et al*., 1991).

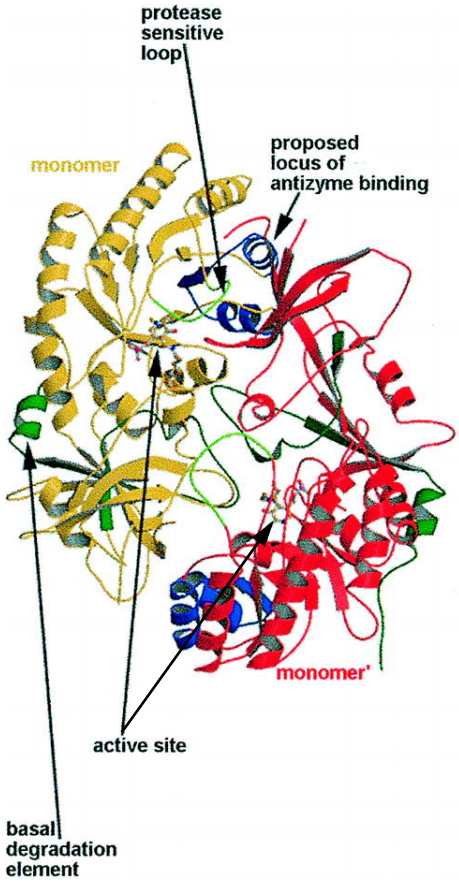

Figure I-3 Crystal structure of human ODC homodimer with the PLP as cofactor.

The two subunits are coloured yellow and red. The localization of the putative antizyme-binding element is coloured blue, the protease-sensitive loops are light green, and the basal PEST degradation motifs (residues 376-427) are dark green (Almrud et al., 2000).

Trypanosoma ODC does not have a PEST sequence, but its stability was reduced when fused to the C-terminus of mouse ornithine decarboxylase and expressed in Chinese hamster ovary cells (Ghoda *et al*., 1990). Thus, the degradation pathway of ODC proceeds as a sequence of multiple distinct processes, including recognition, sequestration, unfolding, translocation, and ultimate degradation mediated by the 26S proteasome (Murakami *et al*., 2000). The plant ODC does not posses the C-terminal extension found in the mammalian enzyme, suggesting that the plant ODC may have a longer half life (Michael *et al*., 1996).

In normal mammalian cells (non proliferating cells) ODC activity is low and only 100-200 molecules of the enzyme are present (Pegg *et al*., 1982a). ODC activity is closely associated with the cellular proliferation and the enzyme is essential for normal cell growth (Pegg, 1988; Pegg and McCann, 1992). The human ODC promoter is directly regulated by the product of *c-myc* (Bello-Fernandes *et al*., 1993; Wagner *et al*., 1993; Iyengar *et al*., 2001) and overexpression of human ODC in NIH3T3 cells resulted in cell transformation (Auvinen *et al*., 1992; Moshier *et al*., 1993). This and other studies (Packham and Cleveland, 1994; Guo *et al*., 1999) have indicated that ODC is a proto-oncogene crucial for regulation of cellular growth and transformation. Inhibition of ODC activity has been shown to be associated with a decrease in polyamine levels, DNA synthesis and carcinogenesis in various cancer types.

I.1.7 Molecular and genetic approaches for modulating the levels of polyamines in plants

In recent years, several genes encoding polyamine biosynthetic enzymes have been cloned from different plants. Availability of cloned genes for polyamine biosynthesis enzymes provides a unique opportunity to manipulate cellular polyamine metabolism.

In early experiments, DeScenzo and Minocha (1993) and Bastola and Minocha (1995) expressed a mammalian ODC gene in carrot and transgenic tobacco under the control of plant specific promoters. This caused a 2.5-fold increase in cellular putrescine levels. Putrescine levels were also increased in tobacco roots (Hamill *et al*., 1990) by expressing transgenic yeast ODC. Transgenic cells of poplar (*Populus nigra x maximowiczii*) expressing a mouse ODC gene showed elevated activity of mouse ODC and increased levels of polyamines (Bhatnagar *et al*., 2001).

An increase in cellular levels of spermidine has been achieved by introduction of a human SAMDC cDNA into tobacco plants. In these transgenic plants, putrescine levels were significantly reduced, whereas the spermidine content was two to three times higher compared to control plants (Noh and Minocha, 1994). Transgenic tobacco plants containing sense and antisense constructs of the potato SAMDC cDNA under the control of the cauliflower mosaic virus (CaMV) 35S promoter have been generated (Kumar *et al*., 1996). Reduction in the levels of SAMDC transcripts in the antisense plants were observed resulting in stunted phenotypes with highly branched stems, short internodes, small and chlorotic leaves and inhibited root growth. Attempts to produce transgenic plants with the sense SAMDC construct were unsuccessful, suggesting that a constitutive overexpression of the enzyme may be lethal (Kumar *et al*., 1996).

Overexpression of oat ADC cDNA in tobacco caused a 65-fold increase in agmatine accumulation but no concomitant changes in putrescine levels (Burtin and Michael, 1997).

Inducible overexpression of oat ADC in transgenic tobacco led to an accumulation of ADC mRNA, increased ADC activity and changes in polyamine levels (Masgrau *et al*., 1997). Biochemical analysis of cellular polyamines resulted in up to fourfold increase in putrescine levels in transgenic callus and regenerated rice plants (Capell *et al*., 1998; Noury *et al*., 2000).

Transgenic rice cell lines, engineered with the pea diamine oxidase cDNA in antisense orientation under the control of two different promoters (Bassie *et al*., 2000), have demonstrated for the first time the down regulation of DAO catabolic enzyme involved in polyamine metabolism accompanied by concomitant increase in putrescine and spermidine concentrations.

Although plant PAO genes have been cloned and characterised from a few plant species (Federico and Angelini, 1991; Tavaldoraki *et al*., 1998) no results for overexpression of this enzyme in transgenic plants have been reported.

Thus, with the ability of the key genes involved in the biosynthetic pathways and catabolic processes, it has become possible to manipulate the polyamine metabolism using antisense and sense transgenic approaches (Taylor *et al*., 1992; Bastola and Minocha, 1995; Koc *et al*., 1995; Kumar *et al*., 1997; Malmberg *et al*., 1998). However, alternative approaches based on antibodies stabilizing or destabilizing key enzymes in polyamine biosynthesis have not been addressed so far.

I.2 Engineering of recombinant antibodies by phage display technology

I.2.1 General structure of antibodies

Human immunoglobulins are a group of structurally and functionally similar glycoproteins that confer humoral immunity in humans (Spiegelberg, 1974). Five classes (isotypes) of immunoglobulins (IgG, IgA, IgM, IgD, and IgE) have been distinguished, each of which has a distinct heavy-chain C region encoded by a distinct C-region gene. The isotype of an antibody determines the effector mechanisms that it can engage on binding antigen.

The general structure of an antibody (immunoglobulin) is that of a bifunctional molecule, comprising two antigen binding domain on one side of the molecule and an effector domain on the other side. The antigen binding domains are highly diverse and are produced by somatic recombinations and mutaions, which create the variable domain of the antibody molecule. The effector functions are part of the constant region of the antibody. The antibodies are multichain proteins, consisting of two pairs of light chains

(either κ or λ isotype) and two pairs of heavy chains (isotype γ, ε, δ, α, or μ) organized into three structural units as presented in Figure 1-4. Two of these units called Fab for **F**ragment **a**ntigen **b**inding are identical and enable the binding to an antigen. The other unit has no antigen binding activity and was originally observed to crystallize readily, and for that reason was named the Fc fragment for **F**ragment **c**rystalline. The Fc fragment interacts with effector systems such as the complement system. The light chain (L) is formed by two domains of about 100 residues in length, called the variable (V_L) and the constant (C_L) domain. The heavy chain (H) contains a variable domain (V_H) and three or four constant (C_{H1}, C_{H2}, C_{H3}, C_{H4}) domains, depending on the isotype (Alberts *et al*., 1989). Each domain is formed by two β sheets packed face to face and linked together by conserved disulfide bridge and by interstrand loops (Lesk and Chothia, 1982). Disulfide bridges are an important component of the IgG structure. Intrachain disulfide bonds stabilize domain folding and interchain disulfide bonds stabilize the interaction of H and L chains and the interaction of H chains (Burton., 2001). The antigen binding sites of most antibodies are formed by six loops called 'complementary determining regions' (CDRs) (Kabat *et al*., 1977; Kabat, 1978), three from the V_L domain (L1, L2, L3) and three from the V_H domain (H1, H2, H3) (Al-Lazikani *et al*., 1997). The CDR with the greatest variation in terms of length and sequence is the heavy-chain CDR3 (HCDR3) (Sanz, 1991). Comparison of the crystal structures of a number of antibodies suggests that CDRs, with the exception of HCDR3, adopt a limited number of confirmations or 'canonical structures'. In each antibody, 3-5 residues of the CDR loops contribute contact sites to the antigen interaction. The regions of variable domains outside these loops are called framework. They are highly conserved in sequence and their conformation can be predicted using standard homology modelling techniques (Morea *et al*., 1998; Morea *et al*., 2000).

By limited proteolytic digestion, it is possible to obtain smaller antibody fragments containing only a subset of the domains of a complete antibody, of which they maintain either the antigen binding ability ($F(ab')_2$, Fab, Fv) or the effector unit (Fc) (Winter and Milstein, 1991). Recent improvements in heterologous gene expression and the development of phage display technologies permit the design and expression of recombinant antibodies (rAb) with multiple specificity such as: scFv fragment, bispecific scFv, diabody (Holliger *et al*., 1993; Holliger and Winter, 1997; Hudson, 1999; Breitling and Dübel, 2000) (Figure 1-4).

As antibodies are very large molecules, the use of small fragments can be advantageous for research and *in vivo* applications, due to their ability to penetrate tissues and faster clearance from tissues and serum (Yokota *et al*., 1992; Cumber *et al*., 1992). Recombinant antibody fragments have been fused with a range of molecules including enzymes for prodrug therapy, toxins for cancer therapy, viruses for gene therapy, ligands to guide them

to specific cellular targets (Michael et al., 1996; Douglas and Curiel 1997; Brinkmann, 2000).

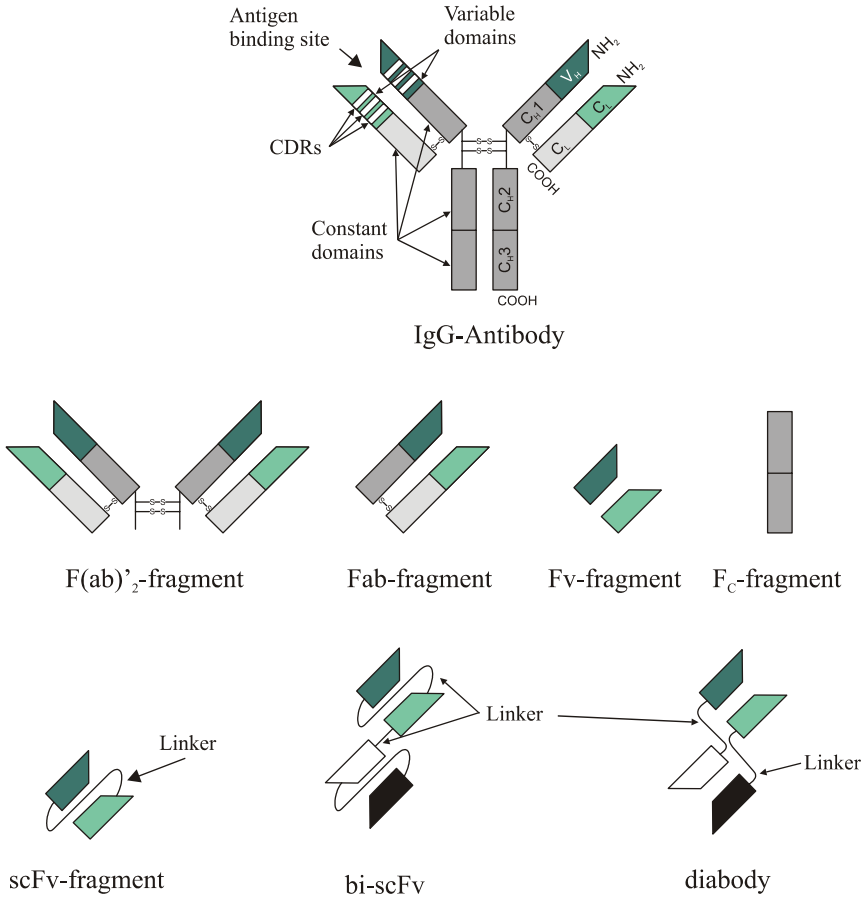

Figure I-4 Schematic presentation of IgG molecule and antibody fragments

The recombinant antibody fragment most commonly used in research and therapy is the single chain antibody fragment (scFv) (Bird *et al*., 1988; Huston *et al*., 1988; Skerra and Plückthun, 1988). ScFv fragments (~30 kDa) contain the complete antigen binding site of an antibody. In scFv fragments, the V_H and V_L domains are covalently linked by a flexible peptide linker (Whitlow *et al*., 1993) (usually 15-20 amino acids long, e.g. of the sequence $(Gly_4Ser)_3$, or 218 linker) (Whitlow *et al*., 1993). If no reorientation of the two domains occurs they should have the same monomeric binding affinity as the parental monoclonal antibody as experimentally demonstrated in a number of cases (e. g. Bird *et al*., 1988; Glockshuber *et al*., 1990; Huston *et al*., 1991). The hydrophobic interaction between the V_H and V_L domains is not very strong. This can lead to dimer formation where the V_H of one molecule interacts with the V_L of another and *vice versa*. Consequently, most scFv fragments are found in two forms: monomer and dimer (Kortt *et al*., 1994; Chames and Baty, 2000). This tendency to dimerize has been exploited to create bivalent or bispecific

diabodies (Holliger and Winter 1997; Perisic *et al*., 1994; Plückthun and Pack, 1997) and triabodies (Iliades *et al*., 1997).

Single-chain fragments can be expressed in a variety of hosts (Verma *et al*., 1998), including bacteria (Plückthun *et al*., 1996), yeast (Fischer *et al*., 1999a) and plants (Shimada *et al*., 1999; Fischer *et al*., 1999b; Fischer et al., 1999c; Smith and Glick 2000). Single-chain fragments have found broad applications in medicine (Huston *et al*., 1993; Hudson, 1999) and have also great potential in biotechnology (Harris, 1999). The unique and highly specific antigen-binding ability might, for example, be exploited to block specific enzymes, bacteria or to detect environmental pollutents present in very low concentrations (biosensors) (Wörn and Plückthun, 2001).

I.2.2 Immunoglobulin genetics

In humans, antibody gene loci have been well characterized (Berek and Milstein, 1988; Tomlinson *et al*., 1995; Cook and Tomlinson, 1995). There are approximately 50 potentially functional heavy-chain germ-line sequences (V_H gene segments) that are organized into seven families. The largest family is V_H3 with 22 genes, followed by V_H1 and V_H4. V_H5 has only two members and V_H6 only one. The relative expression of these families is $V_H3>V_H1$, $V_H4>V_H6>V_H5>V_H2$. There are about 40 V_κ and about 30 V_λ human light chain germ-line genes, organized into six κ and ten λ families (Schable and Zachau, 1993). In human antibodies, the κ to λ ratio is typically of the order 3:2.

In mice, there are more than 100 heavy chain germ-line sequences organized into 15 or more families, and a similar number of κ light-chain sequences (Coutinho *et al*., 1992). The expression of λ chains in mice is far less than in humans, with only two potentially functional genes in most strains. In Balb/c mice, light chains are expressed with a typically κ:λ ratio of about 20:1.

Antibody diversity is generated by somatic recombination in B lymphocytes, whereby V gene segments are linked to other gene segments (Dreyer and Bennett, 1965; Schroeder *et al*., 1995a). For the heavy chain, one of 27 diversity (D) gene segments is linked to one of 6 joining (J_H) gene segments. In turn, this D-J_H fusion is linked to a V_H gene segment to produce a V_H rearrangement V_H-D-J_H segment that contains the complete coding region for the heavy chain variable domain. Later, the constant domain coding segment is joined by RNA splicing that determines the isotype of expressed antibody. For the κ chain, a V_κ gene segment is joined to one of 5 Jκ segments; for the λ light chain, a V_λ segment is joined to one of 4 J_λ segments. Additional diversity is generated during recombination by imprecise joining at the junctions of some of the gene segments. The greatest diversity is therefore typically seen at and between these two junctions, which structurally correspond to the

heavy-chain CDR3 region. Finally during an *in vivo* immune response, the interaction of B cells with antigen often results in additional diversity in antibody genes.

I.2.3 Selection of recombinant antibodies by phage display

Phage display is a powerful technique for rapid selection of high affinity recombinant antibody fragments from large repertoires to any protein of interest (Barbas *et al*., 1991; Hogenboom *et al*., 1998). The development of phage display vectors (Smith, 1985) has allowed expression and presentation of antigen-binding antibody fragments on the surface of filamentous phages. In 1990, McCafferty and colleagues demonstrated in a model experiment that it was possible to select antibody fragments from a large population of non-binding proteins by filamentous bacteriophages. A protein, in this case an antibody fragment, is located on the surface of a phage particle by cloning the antibody fragment into the phage genome, fused with a coat protein (pIII, pIV or pVIII). Upon expression, the coat protein fusion will be incorporated into new particles that are assembled in the bacterium. Expression of the fusion product and its subsequent incorporation into the mature phage coat results in the binding structures being present on the phage surface, while its genetic material resides within the phage particle. This relation between genotype and phenotype allows enrichment of specific phages (Barbas, 1993; Burton and Barbas, 1994; Hoogenboom, 1997), which are selected on immobilised targets by a simple *in vitro* selection procedure called 'biopanning'. Phages that display a relevant binding structures will be retained, while non-adherent phage will be washed away. Bound phages are recovered from the surface and used for reinfection of bacteria.

The success of ligand phage display hinges on the combination of this display and enrichment method with the synthesis of large combinatorial repertoires on phage (Hoogenboom *et al*., 1998; Chames and Baty, 2000). Large libraries displaying peptide and proteins have been made using pIII as fusion partner (Smith and Scott, 1993; Winter *et al*., 1994), leading to the development of a number of techniques for selecting the molecule(s) desired from such libraries (Clackson and Wells, 1994; Hoogenboom, 1997). Peptides and proteins have also been fused to the amino-terminal part of the major capsid protein pVIII (Iannolo *et al*., 1995; Malik *et al*., 1996). Recently, heavy and light-chain variable regions have been fused to the amino terminus of pVII and pIX and displayed on phages showing that this two minor coat proteins can also been used for display (Gao *et al*., 1999).

Initially, phage vectors that carried all the genetic information required for the phage life cycle were used (McCafferty *et al*., 1990; Clackson *et al*., 1991). Display of antibodies on smaller filamentous particles called phagemids (Bass *et al*., 1990; Breitling *et al*., 1991) advanced antibody engineering. The phagemid genome contains the filamentous phage intergenic region with its origin of replication for viral and complementary strand synthesis

as well as the hairpin packaging signal. The phagemid also contains an origin for plasmid replication and a resistance marker. The phagemid can maintain itself as a plasmid and function as a bacterial expression vector if desired. Infection of the bacteria with a filamentous helper phage activates the phage origin of replication, resulting in single stranded phagemid DNA being encapsulated into filamentous phage-like particles using helper phage proteins. A helper phage, such as M13KO7 has a defective packaging signal so that the majority of phages produced contain the phagemid single-stranded DNA (Russel *et al*., 1986). Bacteria can be infected with this phage selected via their antibiotic resistance. The phagemid DNA can then be propagated again by infection of the bacteria with helper phage. In phagemids, the scFv may be fused at the N-terminus of the mature gene III protein (McCafferty *et al*., 1990; Hoogenboom *et al*., 1991) or at the N-terminus of truncated pIII lacking the first two N-terminal domains (Garrard *et al*., 1991; Barbas *et al*., 1991). Phagemids have higher transformation efficiency and they are suited for generating very large repertoires. They may also be formatted for direct secretion of the unfused antibody fragment without subcloning (Hoogenboom *et al*., 1991). Many phagemids utilize the *lac*Z promoter to drive expression of the antibody-pIII fusion (Barbas *et al*., 1991; Breitling *et al*., 1991; Hoogenboom *et al*., 1991; Orum *et al*., 1993). The use of a *lac*Z promoter with an additional transcriptional terminator (Krebber *et al*., 1996) or of the phage shock promoter (psp) (Rakonjac et al., 1997) allow display of relatively toxic products and reduce expression-mediated library bases.

I.2.4 Antibody libraries

There are two basic types of phage antibody libraries. One is the antibody library derived from spleen mRNA of immunized donors the other derived from non-immunized donors. With the first library the phage antibody repertoire is enriched for antigen-specific antibodies, because some have undergone affinity maturation by the immune system (Clackson *et al*., 1991; Lorimer *et al*., 1996; Chowdhury *et al*., 1998). This method yields antibodies with higher affinity than these from hybridomas (Chester *et al*., 1994). For immune libraries it is preferable to use a donor with a high serum antibody titer to the antigen of interest. More specific antibodies reflect higher levels of specific mRNA. Therefore, the likelihood of combining heavy and light chain fragments specific for the protein of interest is greater. The construction of immune libraries from a variety of species has been reported, including mouse, human, chicken, rabbit and camel (Hoogenboom *et al*., 1998).

The other type of phage display library are ‘single-pot’ libraries that depend on the source of immunoglobulin genes and are further discriminated in ‘naïve’ and ‘synthetic’ antibody libraries. The naïve library offers the possibility to select high–affinity antibodies of any

desired specificity without the need for immunization (Burton, 2001). V-genes are amplified from B-cell cDNA using V_L and V_H family specific oligonucleotides (Marks *et al*., 1991). The heavy and light chains are randomly combined and cloned to encode a combinatorial library of scFv or Fab antibody fragments. This procedure provides access to antibodies that have not yet encountered antigen, although the frequency of those genuine 'germline antibodies' is depended on the source of B-cells. A large and diverse naïve library can be used to generate antibodies to a large panel of antigens, including self, non-immunogenic and relatively toxic antigens (Griffiths *et al*., 1993; Marks *et al*., 1991; Vaughan et al., 1996). The naïve library has to be extremely large to represent almost the entire immune repertoire and allows selection of antigen binders with sufficient affinity. They must be in the order of 10^{10} or more, a size that is technically difficult to attain (Marks *et al*., 1991; Voughan *et al*., 1996). The affinity of antibodies selected from a naïve library is proportional to the size of the library, ranging from 10^{6-7} M^{-1} for a small library, to 10^{8-10} M^{-1} for a very large repertoire made by brute force cloning (Vaughan *et al*., 1996).

Alternatively, 'synthetic' libraries have been made artificially by *in vitro* assembly of V-gene segments and D/J fragments. PCR techniques and degenerate primers are used to introduce diversity at precise locations, typically CDR3s (Ellman and Gallop, 1998; Hoogenboom and Chames, 2000). The regions and degree of diversity may be chosen to correspond to areas of highest natural diversity of the antibody repertoire.

Ultimately, the value of any library is best determined by its success in yielding specific, high-affinity ligands for a variety of target molecules. However, antibodies with modest affinity can be engineered to bind with higher affinity to a target molecule by constructing multivalent molecules (Plückthun and Pack, 1997; Hoogenboom, 1997) or *in vitro* affinity maturation. Diversity in the antibody genes may be introduced using a variety of methods such as: mutator strains (Low *et al*., 1996; Irving *et al*., 1996), error prone PCR (Hawkins *et al*., 1992), chain shuffling (Clackson *et al*., 1991; Marks *et al*., 1992), DNA shuffling (Stemmer, 1994a,b), codon based mutagenesis (Virnekäs *et al*., 1994). The ability to alter affinity and selectivity by evolution of a parent antibody is a powerful advance in antibody display technology.

Phage display has been mostly used for affinity screening of combinatorial peptide and protein libraries, to define epitopes for monoclonal antibodies, to increase antibody affinity, to select enzyme substrates and to screen cloned antibody repertoires (Clackson *et al*., 1991; Griffith and Duncan, 1998; Hoogenboom *et al*., 1998; Benhar *et al*., 2000). Phage display systems have also been used to provide an understanding of the structural bases of an interaction in systems in which insights is limited (Wright *et al*., 1995; McConnell *et al*., 1996). Antibody phage display is versatile in allowing the effective display of scFv (Orlandi *et al*., 1989; McCafferty *et al*., 1990), Fab fragments (Barbas *et*

al., 1991, Hoogenboom *et al*., 1991; Yang *et al*., 1995), and diabody fragments (Holliger *et al*., 1993; McGuinness *et al*., 1996).

I.2.5 Expression of antibody genes in plants: immunomodulation

The first plant expressed antibody, a full length IgG, was described in 1989 (Hiatt et al., 1989). Since then, plants have been engineered to synthesize a wide range of recombinant antibodies, from dAbs (Benvenuto *et al*., 1991), scFv (Fiedler and Conrad, 1995; Artsaenko *et al*., 1998; Zimmermann *et al*., 1998; Vaquero *et al*., 1999; De Wilde *et al*., 1999; Smith and Glick, 2000; Stöger *et al*., 2000) and bispecific scFv (Fischer *et al*., 1999d) to Fab fragments (De Neve *et al*., 1993) and secretory IgA antibodies (Ma *et al*., 1995; Ma and Hein, 1996; Ma and Hiatt, 1996), that can be subsequently used for therapy, diagnosis or laboratory and industrial applications (De Wilde *et al*., 1999, Peeters *et al*., 2001). Although the maximum level of antibody accumulation depends on plant species, tissues and on the intrinsic properties of the antibody itself, recombinant protein accumulation and stability can be optimized by exploiting the protein sorting and targeting mechanisms of plant cells. Directing the target rAbs to the secretory pathway using either plant (De Neve *et al*., 1993) or murine (Hiatt *et al*., 1989) leader peptides, results in their accumulation in the intracellular space beneath the cell wall (apoplast), from where correctly processed, active rAbs can be recovered (De Wilde *et al*., 1998). Many studies have indicated that the full size antibodies and Fab fragments are accumulated at high levels (more than 0.1% of TSP) upon secretion by adding an N-terminal signal leader peptide sequence. Currently scFvs have been targeted to the apoplast, the ER and the cytosol. Targeting of scFvs torwards the apoplast or cytosol can result in large variation of accumulation levels ranging from 0.5 to 0.1% of TSP or even undetectable levels (De Wilde *et al*., 1999). The highest levels of scFv fragments (1-6.8% of total soluble protein) are obtained when they are retained in the ER by adding an N-terminal signal sequence and a C-terminal KDEL retention signal (De Jaeger *et al*., 2000). The scFv antibody fragments have a higher chance of being correctly folded in the cytosol because the two variable domains are interconnected by a flexible peptide linker, avoiding the need for assembly of different chains and the formation of inter-chain disulfide bridges.

The capability of plant cells to synthesize, process and target large, complex mammalian proteins in a manner very similar to their natural hosts makes them an attractive alternative for rAb production. Antibodies or antibody fragments produced in plants are often referred to as ‘plantibodies’ and they can be exploited for applications in the field of molecular farming (Fischer *et al*., 1999c; Peeters *et al*., 2001). After isolation and purification from the plant tissue, the rAbs can be used in industrial processes, as diagnostic tools, for immunochromatography, or in medical therapy. In addition, there is a growing interest for

immunomodulation strategy of *in planta* applications, in which antibodies or antibody fragments are produced to modulate the function of a corresponding antigen (De Jaeger *et al*., 2000). Immunomodulation is defined as a molecular protein based technique that allows interference with cellular metabolism, signal transduction or pathogen infectivity by the ectopic expression of genes encoding recombinant antibodies (Conrad and Manteuffel, 2001). Recombinant antibodies that specifically recognize soluble or membrane associated receptors, enzymes or DNA-binding proteins can interfere with the functions of these proteins by generating antigen-antibody complexes, or cause steric changes of the molecular structure combined with a loss of function. Finally, the antigen can be mistargeted as a result of antibody binding.

The expression of specific scFv's in different plant species, plant organs and cellular compartments offers the possibility of manipulating plant metabolism, changing the agronomic traits, or blocking regulatory factors, such as the immunomodulation of enzyme or signal molecule activity (Conrad and Fiedler, 1998; Franken *et al*., 1997; De Jaeger *et al*., 2000; Giddings *et al*., 2000; Schillberg *et al*., 2001; Fischer *et al*., 2001). The immunomodulation approach has been shown to be also applicable for modulating the infection process of plant viruses (Tavladoraki *et al*., 1993; Voss *et al*., 1995; Zimmerman *et al*., 1998; Fecker *et al*., 1997; Schillberg *et al*., 2000).

Owen *et al*. (1996) demonstrated the immunomodulation of the activity of the endogenous photoregulatory protein phytochrome by the use of a cytosolic scFv. A similar approach was used to block the biological activity of the phytohormone abscisic acid by accumulating high concentrations of an anti-ABA-scFv in the ER of tobacco leaf cells. Those plants wilted under ambient conditions (Artsaenko *et al*., 1995) because of an increased transpiration rate, which indicated that they were unable to close their stomata. Philips *et al*. (1997) enabled for the first time the seed specific immunomodulation of ABA activity. In this study the tobacco plants had normal vegetative growth and development patterns while the seeds displayed an altered phenotype due to the reduction of ABA activity. Transgenic tobacco lines that accumulate high levels of an anti-gibberellin scFv in the ER showed a dwarf phenotype and lower gibberellin (Shimada *et al*., 1999).

The feasibility and flexibility of recombinant antibody technology makes the plantibody approach one of the most recent innovations in the field of molecular techniques for the analysis and manipulation of plant metabolic pathways, pathogen infections and development.

I.3 Aim of this thesis

The fast moving field of recombinant antibody technology and expression has opened new opportunities, not only for the medical sciences, but also for applied and fundamental agronomic research. The immunomodulation of regulatory processes in physiology and development is an interesting and powerful tool for plant cell biology. Furthermore, the advantage of immunomodulation versus the use of existing mutants or conventional inhibitor and antisense techniques is, that antibody binding can activate or inactivate the end product of a biosynthetic pathway without affecting the function of any precursors (Artsaenko et al., 1999; Conrad and Manteuffel, 2001).

The objective of the present study was to modify levels of polyamine biosynthesis by using genetic engineering and antibody technology for altering polyamine production thereby developing transgenic plants to increase their nutritional and health value. Tobacco plants were initially used as a model plant prior to moving into crops. The aim of the study will be achieved by the following approaches:

- Overexpression of ODC and SDE genes: The ODC gene will be amplified from a human prostate cDNA library and integrated into plant expression vectors for generation of transgenic tobacco. The enzymes will be targeted in different plant cell compartments to verify expression rate and integrity of the protein in these compartments. Stable transformed tobacco lines expressing apoplastic and cytosolic ODC and co-expressing ODC and SDE enzymes in apoplast will be generated. Immunoblot analyses will be performed to investigate the accumulation levels and the stability of the heterologous enzymes. The effect of recombinant proteins on the polyamine metabolism will be investigated by analysis of putrescine, spermidine and spermine levels. The enzymatic activity of ODC will be determined to investigate whether the overexpressed human ODC is a functional and active enzyme.
- Inhibition of PAO activity and stabilisation of ADC and ODC using specific scFv fragments with high affinity generated by phage display technology: The antibody mediated regulation of ADC and ODC enzymes will enable enhanced production of putrescine while maintaining and/or improving their catalytic activity. Antibodies that inhibit PAO function could increase the spermidine pool by blocking the degradation of polyamines (Figure I-2). Recombinant scFv antibodies will be constructed by generation of phage displayed libraries from animals immunized with bacterial produced GST polyamine fusion proteins. Selected scFv-fragments will be tested for their reactivity and functionality to the specific target molecule in ELISA. The candidate scFvs will be characterised in surface plasmon resonance experiments to determine the affinity binding constant and epitope mapping. Electrophoretic mobility shift assays (EMSA) will be performed to test the functionality of engineered scFv. The effect of selected scFv-fragments on the enzymatic activity of target molecule will be

analysed by *in vitro* assays. Promising scFv-fragments will be subcloned into plant expression vectors and targeted to the apoplasm and the ER as control. Stable transformed tobacco lines accumulating ODC-specific scFv will be generated to investigate the biological effect of plant produced scFvs upon down or up regulation of ODC enzymatic activity.

A schematic overview of this Ph.D thesis is presented in Figure I-5.

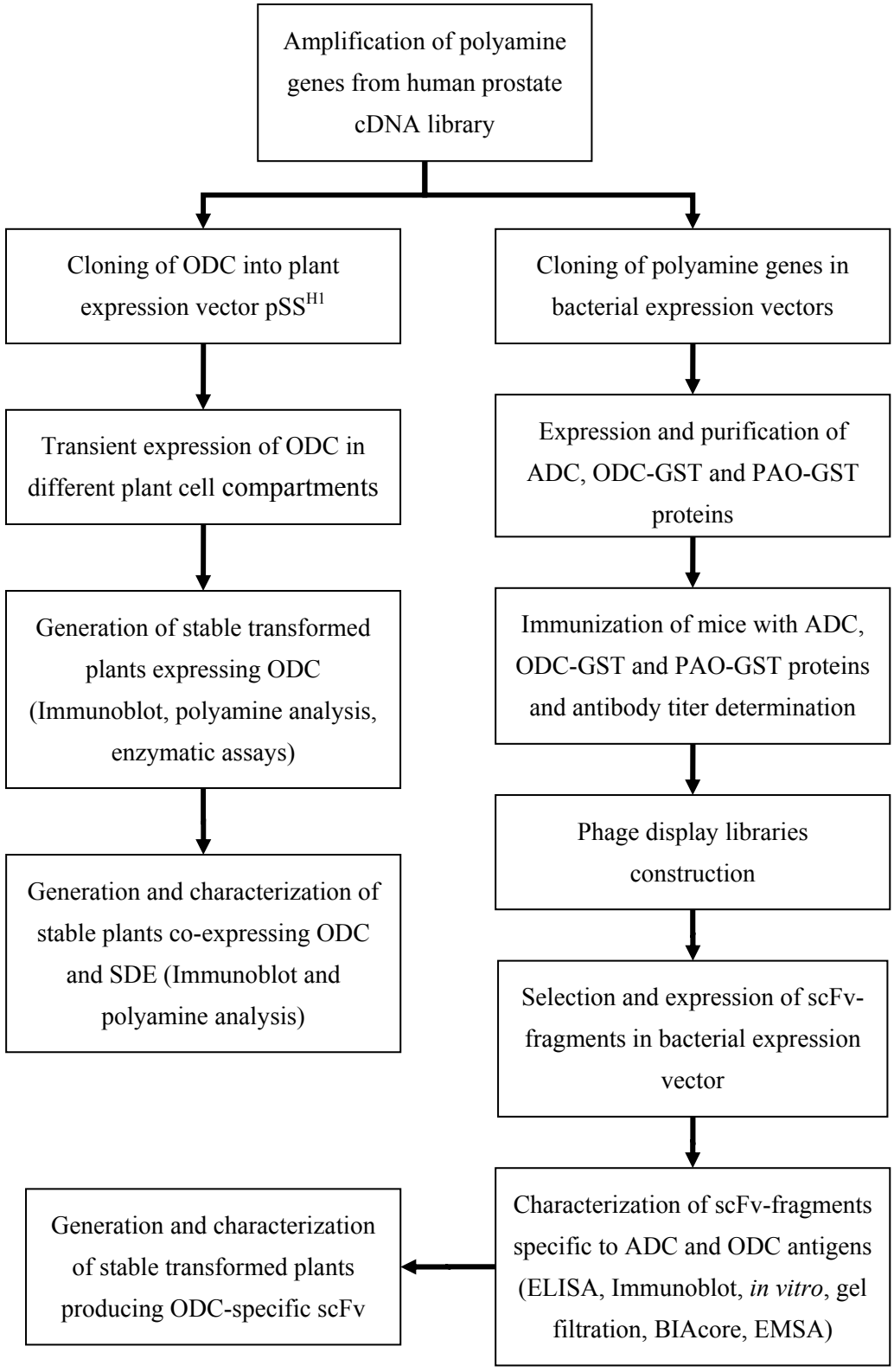

Figure I-5 Schematic overview of the project

II Material and Methods

II.1 Material

II.1.1 Chemicals and consumables

The chemicals used throughout the work were purchased from the following companies: Bio-Rad (München), Roche (Mannheim), Fluka (Neu-Ulm), Gibco BRL (Eggenstein), Merck (Darmstadt), Amersham Pharmacia Biotech (Freiburg), Roth (Karlsruhe), Serva (Heidelberg), Sigma (Deisenhofen). The consumables were from: Amicon (Witten), Biozym (Hess. Oldendorf), Eppendorf (Hamburg), Greiner (Solingen), Kodak (Stuttgart), Millipore (Eschborn), Nunc (Bieberach), Schott Glaswerke (Mainz), Serva (Heidelberg), USB/Amersham (Braunschweig), Whatman (Bender & Hobein, Bruchsal) and Zeiss (Oberkochem).

II.1.2 Enzymes and reaction kits

Restriction enzymes either from New England Biolabs (Schwalbach) or GibcoBRL were used for DNA digestion. Expand™ high fidelity DNA *Taq* polymerase from Roche was used for PCR amplification from cDNA libraries. *Taq* polymerase from Gibco BRL was used for amplification of mouse heavy and light chain fragments and for amplification of cloned DNA (‘‘check-PCR’’).

The following kits were used:

Plasmid isolation kits (Mini, Midi, Maxi)	Qiagen (Hilden)
QIAquick gel extraction kit	Qiagen
QIAquick PCR purification kit	Qiagen
RNeasy mini kit	Qiagen
Superscript™ preamplification system kit	GibcoBRL
BCA protein assay kit	Pierce (Rockford)
Bradford protein assay kit	Bio-Rad
PCR DIG probe synthesis kit	Roche
DIG luminescent detection kit	Roche (Mannheim)

II.1.3 Primary antibodies, secondary antibodies and substrates

Mouse anti-GST monoclonal antibody and rabbit anti-GST polyclonal antibodies, provided by Dr. Michael Monecke (RWTH Aachen, Institut für Biologie VII, Germany) were used for analyses of GST and GST fusion protein expression. Rabbit anti-GST antibody was

also used as capture antibody for epitope mapping in BIAcore analyses (II.2.8.7). Mouse anti-c-myc tag monoclonal antibody (9E10) (ATCC clone number CRL-1729) was used for detection of scFv-fragments by dot blot (II.2.4.4), immunoblot (II.2.4.3) and ELISA (II.2.8.1). Mouse anti-his6 (Qiagen) and mouse anti-Grp78 (KDEL) (StressGen Biotechnologies Corp. Victoria, Canada) antibodies were also used for detection of scFv-fragments in transient protein expression experiments. IgY's from chicken raised against ODC-GST and ADC-GST fusion proteins, provided by Dr. Bernd Schneider, Institut für Biologie VII, Germany) were used in capture ELISA analyses (II.2.8.2) of scFv-fragments. Streptavidin alkaline phosphatase conjugated ($Strep^{AP}$) polyclonal antibody (Dianova) was used for detection of biotinylated scFv fragments in competition ELISA (II.2.8.4). Alkaline phosphatase (AP) or horseradish peroxidase (HRP)-conjugated to goat anti-mouse IgG (H+L, Fc) (Dianova) antibodies were used as secondary antibody in immunoblot analysis (II.2.4.3) and ELISA (II.2.8.1) NBT/BCIP (Bio-Rad) and pNPP (Bio-Rad) were used as substrate for detection of immobilized proteins in Immunoblot (II.2.4.3) and ELISA (II.2.8.1), respectively.

II.1.4 Bacterial strains

E. coli strains DH5α and XL1-Blue were used as a host cells for all intermediate cloning constructs; BL21 was used for expression of GST fusion proteins (II.2.3.1); TG1 was used for generation of phage-displayed antibody libraries used in solid-phase panning (II.2.7). HB2151 was used for expression of soluble scFv-fragments (II.2.3.3) (Table II-1).

Table II-1 Names, suppliers and genotypes of *Escherichia coli* strains used throughout the work.

Strain	Source	Genotype
DH5α	Ausubel et al., 1994	F^- (*f80d Lac* 2Δ*M*15) Δ(*LacZYA-argF*) *U*169*end A*1 *rec*1 *hsdR*17(r_k^- m_k^+) *deoR thi*-1 *supE*44 *gyrA*96 *relA1* λ^-
HB2151	Ausubel et al., 1994	K12, *ara,* Δ(*lac-pro), thi*/ F´ *pro* A^+B^+, *lacIqz*Δ*M15*
BL21(λDE3)	Novagen	F^- *ompT hsdS*$_B$ (r_B^- m_B^-) *gal dcm* (DE3)
XL1-Blue	Stratagene	*recA*1 *endA*1 *gyrA*96 *thi*-1 *hsdR*17 *supE*44 *relA*1 *lac* [F´ *proAB laclI*^{q} *Z*Δ*M*15 Tn10 (Tet^r)]
TG1	Stratagene	*supE thi*-1 Δ(*lac-proAB*) Δ(*mcrB-hsdSM*) 5(r_K^- m_K^-) [F´*traD*36 *proAB lacI*^{q} *Z*Δ*M*15]
SCS 110	Stratagene	*rpsL* (^{Str}r) *thr leu endA thi*-1 *lacY galK galT ara tonA tsx dam dcm supE*44 Δ*(lac-proAB)* [F´ *traD*36 *proAB lacIq Z*Δ^{M15}]

Agrobacteria strains:

Agrobacterium tumefaciens GV 3101 (pMP90RK Gm^R, Km^R, Rif^R (Koncz and Schell, 1986) was used for agrobacterium-mediated gene transfer (II.2.1.6).

II.1.5 Plants and animals

Nicotiana tabacum L. cv. Petite Havana SR1 was used for transient protein expression after vacuum infiltration of agrobacteria (II.2.2.1), and generation of stable transformed plants (II2.2.4). Stable transformed tobacco plants targeting recombinant spermidine synthase (SDE) to the apoplast were provided by Dr. Bernd Schneider (RWTH Aachen, Institut für Biologie VII, Germany).

6-8 weeks old female BALB/c mice were used for immunization with ADC, GST-ODC and GST-PAO fusion proteins (II.2.5). Brown Leghorn chicken about 12 weeks old were immunized with GST-ADC, GST-ODC and GST-PAO.

II.1.6 Phage

M13KO7 helper phage (Amersham Pharmacia Biotech) is an M13mp1 derivative containing a modified gene 11 [G changed to T at position 6125, giving a methionine to isoleucine change at codon 40 of the gene 11 protein]. The p15A origin of replication and the kanamycin resistance gene from Tn903 are present in M13KO7.

II.1.7 Vectors

Schematic presentation of the vector maps are presented in the Appendix.

pGEM-3zf (Promega) was used for cloning the human ODC gene amplified from prostate cDNA library.

pGEX-5X-3 from Amersham Pharmacia Biotech, modified at the multiple cloning site by insertion of a *Nco*I site was used for subcloning the ODC gene and expression of the GST fusion protein.

pET22b(+) from Novagen, was used for cloning and purification of recombinant proteins via IMAC (immobilized metal ion affinity chromatography).

pHEN4II phagemid vector containing *Sfi*I-*Bst*EII, *Asc*I-*Not*I cloning sites, the 218* linker was used to establish the mouse phage display libraries. The pHEN4II vector (Zhang *et al*., 2001) based on the pHEN4C vector (Hoogenboom, et al., 1991).

pSynI used for cloning and expression of soluble scFv-fragments was generated from pHEN1 phagemid vector (Hoogenboom et al., 1991) by removing the fd-gene III and addition of a C-terminal His6 tag (Dr. Ricarda Finnern, Fraunhofer IME, Aachen, Germany)

pUC18 (Yanisch-Perron and Messing, 1985) containing the SCA24OmW cassette (Dr. Sabine Zimmermann, Institut für Biologie VII, RWTH, Aachen, Germany) (see III.4.1.1) was used for subcloning of the ODC gene.

PSS^{H1} plant expression [10,3 kBp, Amp^R Cb^R, Km^R] (Voss et al., 1995) was used for transformation of *A. tumefaciens* and expression of ODC in different plant cell compartment. pSS^{H1} plasmid is a derivative from the binary vector pPCV002 (Koncz and Schell, 1986). It contains the CaMV-35S expression cassette from pRT101 (Töpfer et al., 1988) with a duplicated 35S enhancer region (Kay et al., 1987; Becker, 1990) and the 3' UTR.

pTRA (Thomas Rademacher, Institut für Biology VII, RWTH Aachen, Germany) is a optimized plant expression vector containing the 35SS promoter and the pA35S untranslated region from CaMV. A matrix attachment region was introduced to improve transcription.

II.1.8 Oligonucleotides

Oligonucleotides used for sequence analysis and amplification of DNA are listed below. All oligonucleotides were synthesized by MWG (Ebersberg, Germany).

1. Primers used for amplification of human ODC from prostate cDNA library

forward ODC: 5′ – CCG GAA TTC CCC ATG GGT AAC TTT GGT AAT GAA GAG T - 3′ (37-mer)

reverse ODC: 5′ – GGG AAG CTT GTC GAC CAC ATT AAT ACT AGC CGA AGC AGC A - 3′ (40 -mer)

2. Primers used for PCR amplification of recombinant DNA (*E. coli* and *A. tumefaciens)* from:

- pSS and pTRA:

forward pSS 5′: 5′ - GAC CCT TCC TCT ATA TAA GG (20-mer)

reverse pSS 3′: 5′ - C AC ACA TTA TTC TGG AGA AA (20-mer)

- pHEN4II:

LMB3: 5′- CAG GAA ACA GCT ATG AC - 3′ (17-mer)

fdseq: 5′- GAA TTT TCT GTA GG - 3′ (14-mer)

3. Primers used for cDNA synthesis and PCR amplification of mouse V_H- and V_L-domains

Table II-2 Murine phage display primer sequences for first strand cDNA generation from total RNA in 5′-3′ orientation.

COH 30 (C_{H1} IgG_1)	GGC CAG TGG ATA GAC AGA
COH 32 (C_{H1} $IgG_{2a/2b}$)	TAA CCC TWG ACC AGG CAT CC
Mu PD 31 (C_{L1} κ)	GCT GAT GCT GCA CCA ACT GTA TCC GTC GAC GCG GCC GCG ACT AGT
Mu PD 32 (C_{L1} λ)	TTT CCA CCT TCC TCT GAR GAG CTT GTC GAC GCG GCC GCG ACT AGT

Table II-3 Sequences of murine V_H domain specific front primers MPDVHF1-MPDVHF16 in 5′-3′ orientation.

Name	Overhang region	Restriction enzymes (*Sfi*I/*Nco*I)	Binding region
MPDVHF1	C ATG CCA TGA CTC GC	G GCC CAG CCG GCC ATG GCC	GAK GTR CAG CTT CAG GAG TCR GGA
MPDVHF2	C ATG CCA TGA CTC GC	G GCC CAG CCG GCC ATG GCC	CAG GTG MAG CTG AWG GAR TCT GG
MPDVHF3	C ATG CCA TGA CTC GC	G GCC CAG CCG GCC ATG GCC	GAG GTC CAG CTR CAR CAR TCT GGA CC
MPDVHF4	C ATG CCA TGA CTC GC	G GCC CAG CCG GCC ATG GCC	CAG GTW CAG CTS CAG CAG TCT G
MPDVHF5	C ATG CCA TGA CTC GC	G GCC CAG CCG GCC ATG GCC	SAG GTC CAR CTG CAG SAR YCT G
MPDVHF6	C ATG CCA TGA CTC GC	G GCC CAG CCG GCC ATG GCC	GAG GTT CAG CTG CAG SAR YCT GGR
MPDVHF7	C ATG CCA TGA CTC GC	G GCC CAG CCG GCC ATG GCC	GAR GTG AAG CTG GTG GAR TCT GGR
MPDVHF8	C ATG CCA TGA CTC GC	G GCC CAG CCG GCC ATG GCC	GAG GTG AAG STY MTC GAG TCT GGA
MPDVHF9	C ATG CCA TGA CTC GC	G GCC CAG CCG GCC ATG GCC	GAR GTG AAG CTK GAK GAG WCT GR
MPDVHF10	C ATG CCA TGA CTC GC	G GCC CAG CCG GCC ATG GCC	GAV GTG MWG CTK GTG GAG TCT GGK
MPDVHF11	C ATG CCA TGA CTC GC	G GCC CAG CCG GCC ATG GCC	GAG GTG CAR CTK GTT GAG TCT GGK
MPDVHF12	C ATG CCA TGA CTC GC	G GCC CAG CCG GCC ATG GCC	SAG GTY CAG CTK CAG CAG TCT GGA
MPDVHF13	C ATG CCA TGA CTC GC	G GCC CAG CCG GCC ATG GCC	CAG ATC CAG TTG GTG CAG TCT GGA
MPDVHF14	C ATG CCA TGA CTC GC	G GCC CAG CCG GCC ATG GCC	CAG GTS CAC STG RWG SAG TCT GGG
MPDVHF15	C ATG CCA TGA CTC GC	G GCC CAG CCG GCC ATG GCC	CAG GTT ACT CTR AAA GWG TST GGC C
MPDVHF16	C ATG CCA TGA CTC GC	G GCC CAG CCG GCC ATG GCC	GAT GTG AAC TTG GAA GTG TCT GG

Note: degeneracy codes: K= G or T; M = A or C; S = C or G; R = A or G; W = A or T

Table II-4 Sequences of murine V_L-domain specific front primers MPDVLF1-MPDVLF15 in 5′-3′ orientation.

Name	Overhang region	Restriction enzymes (*Asc*I)	Binding region
MPDVLF1	CAT GCC ATG ACT CGC	GGC GCG CCT	GAC ATT GTG MTG WCH CAG TCC CCA
MPDVLF2	CAT GCC ATG ACT CGC	GGC GCG CCT	GAC ATT CAG ATG ATT CAG TCT CC
MPDVLF3	CAT GCC ATG ACT CGC	GGC GCG CCT	GAC ATT GTT CTC WHC CAG TCT CC
MPDVLF4	CAT GCC ATG ACT CGC	GGC GCG CCT	GAC ATT GTG MTG WCH CAG TCT CAA
MPDVLF5	CAT GCC ATG ACT CGC	GGC GCG CCT	GAT RTT KTG ATG ACC CAR RCK GCA
MPDVLF6	CAT GCC ATG ACT CGC	GGC GCG CCT	GAT RTT KTG ATG ACC CAR RCK CCA
MPDVLF7	CAT GCC ATG ACT CGC	GGC GCG CCT	GAC ATT GTG ATG ACC CAR BHT G
MPDVLF8	CAT GCC ATG ACT CGC	GGC GCG CCT	GAT ATT KTG ATG ACC CAR AYT CC
MPDVLF9	CAT GCC ATG ACT CGC	GGC GCG CCT	RAM ATT GTG MTG ACC CAA TYT CCW
MPDVLF10	CAT GCC ATG ACT CGC	GGC GCG CCT	SAA AWT GTK CTS ACC CAG TCT CCA
MPDVLF11	CAT GCC ATG ACT CGC	GGC GCG CCT	GAY ATY CAG ATG ACM CAG WCT AC
MPDVLF12	CAT GCC ATG ACT CGC	GGC GCG CCT	GAY ATY CAG ATG ACH CAG WCT CC
MPDVLF13	CAT GCC ATG ACT CGC	GGC GCG CCT	GAC ATT GTG ATG ACT CAG GCT AC
MPDVLF14	CAT GCC ATG ACT CGC	GGC GCG CCT	CAR SYT GTK STS ACT CAG KAA T
MPDVLF15	CAT GCC ATG ACT CGC	GGC GCG CCT	CAR SYT GTK STS ACT CAG KCA T

Note: degeneracy codes: K= G or T; M = A or C; S = C or G; R = A or G; W = A or T

Table II-5 Sequences of murine VH-domain specific back primers MPDVHB1-MPDVHB5 in 5′-3′ orientation

Name	Overhang region	Restriction enzymes (*Bst*EII)	Binding region
MPDVHB1	CTA GTG GTA CTC CAC	GGC GCG CCT	MRG AGA CDG TGA SMG TRG TC
MPDVHB2	CTA GTG GTA CTC CAC	GGC GCG CCT	MRG AGA CDG TGA SRG TRG TG
MPDVHB3	CTA GTG GTA CTC CAC	GGC GCG CCT	MRG AGA CDG TGA SCA GRG TC
MPDVHB4	CTA GTG GTA CTC CAC	GGC GCG CCT	MRG AGA CDG TGA STG AGG TT
MPDVHB5	CTA GTG GTA CTC CAC	GGC GCG CCT	MRG AGA CDG TGA STG ARA TT

Note: degeneracy codes: K= G or T; M = A or C; S = C or G; R = A or G; W = A or T

Table II-6 Sequences of murine κ V_L-domain specific back primers MPDVLB1-MPDVLB5 in 5′-3′ orientation

Name	Overhang region	Restriction enzymes (*Sal*I/*Not*I)	Binding region
MPDVLB1	CT AGT GGT ACT CCA C	GC GGC CGC GTC GAC	AGC MCG TTT CAG YTC CAR YTT
MPDVLB2	CT AGT GGT ACT CCA C	GC GGC CGC GTC GAC	AGC MCG TTT KAT YTC CAR YTT
MPDVLB3	CT AGT GGT ACT CCA C	GC GGC CGC GTC GAC	AGC MCG TTT BAK YTC TAT CTT TGT
MPDVLB4	CT AGT GGT ACT CCA C	GC GGC CGC GTC GAC	AGC MCG AGC MCG TTT TAT TTC CAA MKT
MPDVLB5 (λ)	CT AGT GGT ACT CCA C	GC GGC CGC GTC GAC	CTG RCC TAG GAC AGT SAS YTT GGT

Note: degeneracy codes: K= G or T; M = A or C; S = C or G; R = A or G; W = A or T

Table II-7 Primers used for DNA sequencing [LI-COR IR2-DNA sequencer, labelled with IRD 700 or IRD 800 (USB/Amersham)]. Sequences given in 5′-3′ direction.

Universe	GTT GTA AAA CGA CGG CCA GT
Reverse (P_4)	ACA CAG GAA ACA GCT ATG AC
pHEN forward	GCC GCT GGA TTG TTA TTA CTC GC
pHEN backward	TTT CAA CAG TCT ATG CGG CCC C
pSS 5′	ATC CTT CGC AAG ACC CTT CCT CT
pSS 3′	AGA GAG AGA TAG ATT TGT AGA GA
pGEX forward	GGG CTG GCA AGC CAC GTT TGG TG
pGEX backward	TTT CAA CAG TCT ATG CGG CCC C
P_{62} Myc.SeqRic.	GCC CCA TTC AGA TCC TCT TCT G

II.1.9 Buffers, media and solutions

All standard solutions, buffers, and media were prepared according to Sambrook *et al.* (1989), Ausubel *et al.* (1995) and Coligan *et al,* (1995). Compositions of non-standard solutions or buffers are listed at the end of the respective method section. Media for cultivating bacteria were sterilized by autoclaving (121°C/1-2 bar), all other solutions were sterile filtered (0.2 µm). Thermo labile components such as antibiotics were sterile filtered and added to the media after autoclaving and cooling to 50°C.

II.1.10 Matrices and membranes

Glutathione sepharose 4B from Amersham Pharmacia Biotech was used for purification of GST fusion proteins (II.2.3.1).

Ni-NTA agarose matrix from Bio-RAD was used for purification of scFv fragments from large scale cultures by immobilized metal ion affinity chromatography (IMAC) (II.2.3.3).

Immobilon^{TM}-P transfer membrane (PVDF) (0.45µm) from Millipore, Hybond^{TM}-C nitrocellulose membrane (0.45µm) from Amersham Life Science and Whatman no.1 paper from Whatman (Maidstone, England) were used in immunoblot analysis (II.2.4.3). Hybond N^+ nylon transfer membrane (0.45µm) from Amersham Life Science was used in Northern blot analysis (II.2.2.8)

II.1.11 Equipment and applications

Biochrom 20 amino acid analyser (Amersham Pharmacia Biotech) and EZchrom V 6.7 data system software (Amersham Pharmacia Biotech).

Cameras: MP4 (Polaroid, Cambridge, MA, USA). E.A.S.Y 429K camera (Herolab, Wiesloch).

Centrifuges: Avanti^{TM} 30 and Avanti^{TM}J-25 (Beckman, California, USA), Biofuge A (Heraeus, Hanau), Sigma 3-10 and Sigma 4-10 (Sigma, St. Louis, Missouri, USA), RC5C and RC5B plus (Sorval instruments, Du Pont, Bad Homburg). Rotors: F0650, F2402H, JLA 10.500 and JA 25.50 (Beckman), #1140 and #11222 (Sigma), RLA-300, SS-34 and GS-3 (Du Pont).

Chromatography equipment: ÄKTA explorer 10xT (Amersham Pharmacia Biotech), Gel filtration XK26 column 26 mm inside diameter, 20 cm length (Amersham Pharmacia Biotech), 150 ml super-loop (Amersham Pharmacia Biotech) and UNICORN control, evaluation and documentation software (Amersham Pharmacia Biotech).

DNA gel electrophoresis apparatus: wide mini and mini cells for DNA agarose electrophoresis and power supplies (Bio-Rad).

DNA-sequencing machine: LI-COR IR2-4200 Sequencer (LI-COR, MWG-Biotech) and Base ImageIR^{TM} 4.0 software (LI-COR).

Electroporation apparatus: "Gene pulser^{TM}", "Pulse controller" unit, Extender unit (BioRad) and 0.2 cm cuvettes (Bio-Rad).

Innova^{TM} 4340 incubator shaker (New Brunswick Scientific, Nürtingen).

PCR Thermocyclers: Primus and Primus 96 plus (MWG-Biotech).

Photometers: Spectrophotometer Uvikon 930 (Kontron, Neufahrn) and multi-channel spectrophotometer Spectromax 340 (Molecular Devices, Sunnyvale, Kalifornien).

Probe sonicator: (Braun Biotech, Melsungen).

Protein gel electrophoresis equipment: Mini PROTEAN II™ from BioRad. Gel Air Dryer (Bio-Rad).

Surface plasmon resonance: BIACORE® 2000 (BIACORE®, Uppsala, Schweden) + PC, Windows NT 4.0 operating system (Microsoft) and Software (BIAControl 1.3 and BIAEvaluation 3.0).

UV-Transilluminators: wavelength 302 nm and UVT-20M (Herolab). UV-chamber (Bio-Rad).

Software: Windows NT 4.0 operating system (Microsoft); Microsoft Office 2000 (Microsoft); Adobe Photoshop 6.0 (Adobe); Chromas; Origin 6.0 (Data analysis and technical graphics, Microcal Software, Inc.); GCG (Wisconsin Package TM of Genetic Computer Group).

II.2 Methods

All experiments related to the genetic engineering were performed according to the regulations of "S1-Richtlinien" and were officially approved by the "Regierungspräsidium des Landes NRW" (RP-Nr.: 23.203.2 AC 12, 21/95) and "BGA" [AZ 521-K-1-8/98:AI3-04/1/0866/88 (S1) and 55.8867/-4/93 (greenhouse)].

General recombinant DNA techniques, i.e. PCI (phenol/chloroform/isoamyl alcohol) and CI (chloroform/isoamyl/alcohol) extraction, DNA precipitation, restriction enzyme digestion, DNA ligation, DNA agarose gel electrophoresis, were according to the standard protocols described in Sambrook *et al*. (1989) and Ausubel *et al.* (1995).

II.2.1 Recombinant DNA technologies

II.2.1.1 Competent cells for RbCl-mediated transformation

E. coli strain DH5α competent cells were prepared for RbCl-mediated transformation by heat-shock as described by Hanahan (1985). A single bacterial colony was inoculated in 5 ml of LB broth and cultured at 37°C overnight (o/n). 0.5 ml of the o/n culture was transferred into 50 ml of LB broth containing 20 mM $MgSO_4$ and 10 mM KCl. The cells were cultured at 37°C for 3-4 hours until the OD_{600nm} reached 0.4-0.5 and then transferred to an ice-cold tube. After incubation on ice for 10 min, the cells were recovered by centrifugation (2000g/4°C/10 min). The pellets were resuspended in 15 ml ice-cold TfB-I solution by gentle vortexing and stored on ice for 10 min. The cells were recovered by centrifugation as described above and resuspended in 2 ml ice-cold TfB-II. 200 µl-aliquots of the suspension were dispensed into prechilled microcentrifugation tubes, frozen immediately in liquid nitrogen and stored at -80°C.

TfB-I pH 5.8:

Potassium acetate	30 mM
$MnCl_2$	50 mM
$CaCl_2$	10 mM
Glycerol	15% (v/v)

TfB-II pH 6.8:

MOPS	30 mM
$CaCl_2$	75 mM
RbCl	10 mM
Glycerol	15% (v/v)

II.2.1.2 Transformation of *E. coli* by heat-shock

As soon as the competent cells (II.2.1.1) were thawed, plasmid DNA (up to 100 ng) (II.2.1.10) or ligation products (Sambrook *et al.*, 1989) were mixed gently with the competent cells and incubated on ice for 30 min. The cells were then exposed to 42°C for 90 seconds and placed on ice for 2 min. 800 µl of LB medium were added to the tubes and incubated at 37°C for 45 min. 200 µl of cells were plated onto a LB-agar plate supplemented with appropriate antibiotics and incubated at 37°C overnight.

II.2.1.3 Preparation of electrocompetent *E. coli*

Electrocompetent *E. coli* were prepared from the following strains, DH5α, BL21(DE3), SCS110, HB101, XL1-blue, and TG1 as described by Dower *et al.* (1988). A single bacterial colony from an LB plate was inoculated in 5 ml LB-broth and cultured at 37°C o/n. Three ml of fresh o/n culture was transferred into 500 ml of LB broth. The cells were cultured at 37°C for 3-4 hours until the mid-log phase (OD_{600nm} = 0.5-0.8). Then the cells were placed on ice for 15-20 min and harvested by centrifugation (3000g/4°C/10 min). Cells were washed three times with sterile water and resuspended in ice-cold 10% (v/v) glycerol to a 300-fold concentration from the original culture volume (at $>10^{10}$ cells/ml). 40 µl aliquots were stored at -80°C.

II.2.1.4 Transformation of *E. coli* by electroporation

Electrocompetent cells (II.2.1.3) were thawed on ice and mixed with 1 pg to 300 ng of DNA in sterile dH_2O. The cell/DNA mixture was transferred into a prechilled electroporation cuvette (0.2 cm) and assembled into a safety chamber. After application of the pulse (25 µF, 2.5 kV, 200 Ω), the cells were diluted in 1 ml of SOC medium and incubated at 37°C with shaking for 1 h. Finally, 100 µl of the cells were plated onto LB-agar containing appropriate antibiotics and incubated at 37°C o/n.

II.2.1.5 Preparation of electrocompetent *Agrobacterium* cells

A single colony of *Agrobacterium tumefaciens* strain GV3101 grown on YEB-agar plate containing 100 µg/ml rifampicin (Rif) and 25 µg/ml kanamycin (Km) (YEB-Rif-Km) was inoculated in 5 ml of YEB-Rif-Km medium in a 100 ml Erlenmeyer flask and incubated at 28°C for two days with shaking (250 rpm). 1 ml of the culture was transferred into 100 ml of YEB-Rif-Km medium and cultivated at 28°C for 15-20 h with shaking (250 rpm) until the OD_{600nm} reached 1-1.5. The cells were chilled on ice for 15 min and spun down by centrifugation (4,000g/4°C/5 min). The culture medium was decanted and the cells were washed three times with 10 ml of dH_2O by centrifugation and resuspended in 500 µl of sterile 10% (v/v) glycerol. 45 µl-aliquots of the suspension were dispensed into prechilled microcentrifugation tubes, frozen immediately in liquid nitrogen and stored at -80°C.

YEB-Rif-Km medium:

Nutrient Broth	0.5% (w/v)
Yeast Extract	0.1% (w/v)
Peptone	0.5% (w/v)
Sucrose	0.5% (w/v)

2 mM $MgSO_4$, 100 μg/ml rifampicin, 25 μg/ml kanamycin were added after autoclaving and cooling.

II.2.1.6 Transformation of *Agrobacterium* by electroporation

0.2-1.0 μg of plasmid DNA (II.2.1.10) in sterile dH_2O was added to a thawed aliquot of electrocompetent *Agrobacterium* cells (II.2.1.5) and incubated on ice for 3 min. The cell/DNA mixture was transferred into a prechilled electroporation cuvette (0.2 cm) and assembled into a safety chamber. After application of the pulse (25 μF, 2.5 kV, 200 Ω), the cells were diluted in 1 ml of SOC medium in a 4.0-ml tube and incubated at 28°C with shaking (250 rpm) for 1 h. Finally, 1-10 μl of the cells were plated on YEB-agar containing 100 μg/ml rifampicin (Rif), 25 μg/ml kanamycin (Km) and 100 μg/ml carbenicillin (Carb) (YEB-Rif-Km-Carb) and incubated at 28°C for 2-3 days. As a control transformation of Agrobacterium cells with H_2O was performed.

II.2.1.7 Determination of the efficiency of recombinant bacteria transformation

Efficiency of transformation of each new batch of competent cells was measured by test transformations with known concentrations of supercoiled plasmid pUC18 for *E. coli* and pSS^{H1} for *A. tumefaciens* cells. The following transformation rates were obtained; RbCl $>10^7$/μg pUC18, electrocompetent *E. coli* $>10^8$/μg pUC18 and *A. tumefaciens* $>10^3$/μg pSS^{H1}.

II.2.1.8 Culturing of *E. coli* and glycerol stock preparation

Individual colonies of all strains were obtained by plating the pertaining strain on LB agar plates. Strains carrying an F′ factor were spread on M9 plates. Incubation was performed at 37°C. The plates were stored at 4°C for short periods (less than 2 weeks). LB medium containing the suitable antibiotics and 2% glucose was inoculated with a single recombinant colony of *E. coli* and grown o/n at 37°C with vigorous shaking (225 rpm). Glycerol stocks were prepared by mixing 600 μl of a fresh overnight culture with 600 μl of 40% sterile glycerol. Bacteria glycerol stocks were stored at -80°C.

II.2.1.9 Growth of recombinant *A. tumefaciens* and preparation of glycerol stocks

Single colonies of *A. tumefaciens* were examined for the presence of plasmids by control PCR (II.2.1.13). Positive colonies were inoculated in 10 ml of YEB-Rif-Km-Carb medium and cultivated at 28°C for 2-3 days with vigorous shaking at 250 rpm. The culture was transferred to Falcon tubes and *Agrobacteria* cells were pellet by centrifugation at 4000g for 10 min at 15°C. The cells were resuspended in a 1:1 volume of YEB Rif-Km-Carb

medium and glycerol stock media (GSM). The suspension was aliquoted (100µl) and stored at –80°C for further experiments.

Glycerol stock media (GSM):

Glycerol	50% (v/v)
MgSO4	100 mM
Tris, pH 7.4	25 mM

II.2.1.10 Isolation of plasmid-DNA from *E.coli*

Recombinant plasmid DNA was purified with the Qiagen plasmid DNA Mini-and Midi-prep kits according to the manufacturers instructions based on the alkaline lysis method (Sambrook *et al.,* 1989). Quality and yield of plasmid DNA was examined by reading the absorbance at 260 nm and 280 nm in a spectrophotometer according to Müller *et al*., (1993) and Sambrook *et al*. (1996). The integrity of DNA was verified by a control restriction digest followed by agarose gel electrophoresis (II.2.1.11). Isolated plasmid DNA was stored at -20°C.

II.2.1.11 Agarose gel electrophoresis of DNA

Plasmid DNA and PCR-fragments were separated in 0.8-1.2% (w/v) agarose gels. Preparation of agarose gels and electrophoresis of the samples were carried out as described by Sambrook *et al*., (1989). Ethidium bromide was added to the gel solution and TBE electrophoreses running buffer prior to the experiment. Known amounts of DNA molecular markers such as 1 Kb ladder, 100 bp ladder and λ-digested with *Pst*I were used for evaluation and determination of DNA concentration and size. The DNA bands were visualised directly upon illumination with a UV transilluminator at 302 nm. Documentation of the DNA gels was performed by using a black and white E.A.S.Y 429K camera (Herolab) and a photo printer (Mitsubishi).

II.2.1.12 Preparative agarose gel electrophoresis

Preparative gel electrophoresis was used for large scale purification of a particular DNA fragment from a mixture of DNA fragments after restriction enzyme digestion. The agarose containing the DNA fragment of interest was excised from the gel on an UV transilluminator with a sterile scalpel. The DNA extraction was performed with QIAquick Gel extraction kit according to the manufacturers guidelines. The concentration of recovered DNA was measured by spectrophotometer or determined by agarose gel electrophoresis and was used in further experiments.

II.2.1.13 PCR amplification

Polymerase chain reaction (PCR) was used for amplification of ODC gene from a human prostate cDNA library using synthetic oligonucleotides based on the ODC database

sequence (Gen-bank accession number M16650). DNA was amplified, based on the protocol of Sambrook *et al*. (1989), with *Taq*- or high fidelity DNA-polymerase and DNA polymerase buffer from Roche. The reactions were performed in 0.2 ml PCR reaction tubes (Biozym Diagnostik GmbH, Hessisch Oldendorf), using a DNA thermal Cycler (MWG). The cycler contained a heated lid to avoid the use of mineral oil.

For generation of highly sensitive hybridization probes suitable for detection of low copy target sequences in Northen-blot hybridization (II.2.2.8), DIG-dUTP (alkali-labile) was incorporated into ODC-PCR product according to the manufacturers instructions (Roche).

For rapid identification of recombinant *E. coli* and Agrobacteria control-PCR was carried out to detect plasmids as described by Jesnowski *et al.* (1995).

The optimal annealing temperature (T_p) of the primers was experimentally optimised or calculated based on the empiric formula (Wu *et al*., 1991):

$T_p = \{22 + 1{,}46\ [2^* (G + C) + (A + T)]\}$

PCR reactions were carried out in a total volume of 50 µl as described below:

Components	Volume	Final concentration
10X PCR buffer	5 µl	1X
50 mM $MgCl_2$	1.5 µl	1.5 mM
10 mM dNTPs	1 µl	0.2 mM each
10 pmol forward Primer	0.5-1 µl	10 pmol
10 pmol backward primer	0.5-1 µl	10 pmol
Template DNA	0.5-5 µl	10-100 ng
Taq DNA polymerase (5U/µl)	0.25 µl	1.25 units
dd H_2O	to 50 µl	

Amplification was carried out under the following conditions:

5 min 95°C
1 min 94°C
1 min 55°C } x 20-35
1 min 72°C
5 min 72°C

The annealing temperature and the time for denaturation, were changed according to T_p value of primers and the length of the target gene.

The performance of each PCR reaction was checked by running 5µl of each reaction on agarose gels (II.2.1.11), with appropriate DNA markers.

II.2.1.14 DNA sequencing

Fluorescently labeled primers were used for sequence analysis by chain terminating inhibitors (Sanger *et al*., 1977) using the "Thermosequenase sequencing kit'' and the LI-COR 4200 IR2 automated DNA sequencer. For evaluation of sequencing data the Base ImageIR 4.0 software package was used.

pGEX forward and pGEX backward primers were used for sequencing the ODC gene cloned in the pGEX-5X-3 vector. Forward and backward pHEN primers were used for sequencing of scFv-fragments in the pHEN4II phagemid vector. Universal and reverse primers were employed for sequencing genes in pUC- or pGEM vectors. pSS 5' and pSS 3' were used for sequence analysis of genes in pSSH1 vector and pTRA vector. P_4 (reverse) and P_{62} (Myc.SeqRic) were used for sequence analysis of scFv-fragments cloned into pSyn vector.

II.2.1.15 Sequence analysis

Chromas software package was used for displaying the chromatogram files from LI-COR automated DNA sequencer. The sequences were edited and exported for further analysis with the Wisconsin Package ^{TM} of Genetic Computer Group (GCG).

II.2.2 Generation and characterisation of transgenic plants

II.2.2.1 Transient assay in tobacco leaves by vacuum infiltration

Growth of recombinant *Agrobacterium* (II.2.1.9) and vacuum infiltration of tobacco leaves was performed as described by Kapila *et al.* (1996) and Vaquero *et al*. (1999).

II.2.2.2 Preparation of recombinant Agrobacteria

100 ml of YEB-Km-Rif-Carb medium was inoculated with 100 µl of glycerol stock of the selected recombinant Agrobacteria carrying with a plant expression vector. The culture was grown at 28°C o/n with shaking at 250 rpm. Next day the cells were pelleted by centrifugation at 5000 g for 10 min at 15°C and transferred into 250 ml of induction medium and cultivated at 28°C o/n with shaking at 250 rpm. Agrobacteria cells were centrifuged (4000g/15-25°C/15 min) and resuspended in 50 ml of MMA solution and kept at RT for 2 h. The OD_{600nm} was measured after 1:10 dilution and the cell suspension was adjusted to an OD_{600nm} of 1. 100 ml of the diluted cell suspension was used for vacuum infiltration of plant leaves (II.2.2.1).

Induction medium:

YEB medium pH 5.6	
MES	10mM

2 mM $MgSO_4$, 25 μg/ml kanamycin, 100 μg/ml rifampicin, 100 μg/ml carbenicillin, 20 μM acetosyringone were added after autoclaving and cooling.

MMA buffer:

MS-salts (Murashige & Skoog, basic salt mixture)	0.43% (w/v)
MES; pH 5.6	10 mM
Sucrose	2% (w/v)
Acetosyringone was added directly before use	200 μM

II.2.2.3 Vacuum infiltration of intact leaves

Young *N. tabacum* cv. Petite Havana SR1 leaves (4 leaves for each construct) were placed in 100 ml of agrobacteria suspension in a "Weck" glass and a continuous vacuum (60-80 mbar) was applied for 15-20 min. The applied vacuum was released rapidly, the leaves were briefly rinsed in tap water and kept on wet Whatman paper no. 1 with adaxial side upwards. The plastic tray was sealed with saran wrap and placed at 22°C with a 16 h photoperiod for 60 h. Leaves were weighed, frozen in liquid nitrogen and stored at -80°C until analysis. As control, leaves were infiltrated with agrobacteria suspension, which did not contain the pSS^{H1} or pTRA plasmid.

II.2.2.4 Recombinant agrobacterium-mediated stable transformation of tobacco plants

Stable transformation of *N. tabacum* was performed with the help of Dr. Flora Schuster (RWTH Aachen, Institute für Biology VII). Transgenic *N. tabacum* cv. Petite Havana SR1 were generated by leaf disc transformation using recombinant Agrobacteria transformed with pSS^{H1} plasmid carrying apoplasmic ODC gene (II.2.1.5). Transgenic T_0 plants were regenerated from transformed callus (Fraley *et al.*, 1983; Horsch *et al.*, 1985). Briefly, wild type plants were grown on MS medium in "Weck" glasses and the youngest leaves (length up to 4 cm) were used for transformation. The agrobacteria suspension was prepared as described above and the OD_{600nm} was adjusted to at least 1.0 after dilution in MMA buffer. The leaves were cut into 8-10 pieces and transferred into "Weck" glasses containing 50-100 ml of agrobacteria suspension and incubated at RT for 30 min. The leaf pieces were then transferred onto sterile pre-wetted Whatman filters in petri dishes closed with saran wrap and incubated at 26-28°C in the dark for two days. Following washing with distilled water containing 100 μg/ml kanamycin, 200 μg/ml claforan and 200 μg/ml Betabactyl (Ticarcillin/Clavulanic acid, 25:1), leaf pieces were transferred onto MS II-plates and incubated at 25°C in the dark for one week and with a 16 h photoperiod for 2-3 weeks. After shooting, the shoots were removed and transferred onto MS-III-plates and incubated at 25°C with a 16 h photoperiod for 10-14 days until roots developed. The small plants were transferred into "Weck'' glasses containing MS-III medium and incubated at 25°C in

16 h light rhythm for 2 weeks until transferred into soil. The young leaves from regenerated transgenic plants were used for immunoblot analysis of expressed scFvs.

MS medium:

MS-salts	0.43% (w/v)
Myo-Inosite (SERVA)	0.1% (w/v)
Sucrose	2% (w/v)
Thiamin-HCl	0.4 mg/l
A. bidest	add to 1000 ml

The pH was adjusted to 5.8 with 1 N NaOH (for preparation of solid medium, 0.8% (w/v) agar were added), autoclaved and 500 µl of vitamin solution I were added upon cooling to 55°C.

MS-II medium:

MS medium supplemented with:

BAP (in DMSO, from Sigma)	1 mg/l
NAA (from Sigma)	0.1 mg/l
Kanamycin	100 mg/l
Claforan	200 mg/l
Betabactyl	200 mg/l

MS-III medium:

MS medium supplemented with:

Kanamycin	100 mg/l
Claforan	200-250 mg/l
Betabactyl	200-250 mg/l

Vitamin solution I:

Glycin	0.4% (w/v)
Nicotinic acid	0.1% (w/v)
Pyridoxin	0.1% (w/v)

Filter sterilized and stored at 4°C.

II.2.2.5 Growth of *N. tabacum* cv. Petite Havana SR1

Tobacco plants were grown in ED73 standard soil (Patzer, Sinntal-Jossa) with 0-30% (v/v) sand under the following conditions: 16 h artificial light, 25°C (or higher depending on the outside temperature), 10 000 Lux (plus the sun light) and 70-90% humidity. To prevent pollination from other plants flowers were covered with plastic bags with micro pores. Mature, dried seeds were stored in paper bags at RT.

II.2.2.6 Preparation of total soluble proteins from plant leaves

For the extraction of transiently expressed ODC and scFv in vacuum infiltrated tobacco leaves (II.2.2.3) or in stable transformed tobacco plant (II.2.3.4), frozen leaves were

ground in liquid nitrogen to a fine powder with a mortar and pestle. Total soluble proteins were extracted using 2 ml of extraction buffer per gram leaf material. Cell debris was removed by two rounds of centrifugation (16000g/4°C/30 min) and the supernatant was used for expression analyses by immunoblot (II.2.4.3).

Extraction buffer:

Tris-HCl, pH 7.5	200 mM
EDTA	5 mM
DTT	0.1 mM
Tween 20	0.1% (v/v)

II.2.2.7 Extraction of RNA from transgenic plants

Total RNA was isolated from vacuum infiltrated tobacco leaves expressing apoplasmic and ER retained ODC. Young infiltrated leaves were ground in liquid nitrogen to a fine powder using mortar and pestle (baked at 180°C). The powder was transferred to a 2 ml RNase free tube and extraction of total RNA was performed using RNeasy mini kit (Qiagen) according to the manufacturers instructions. 3 µl of extracted total RNA were run on an agarose gel to check quantity and purity of RNA.

II.2.2.8 Northern-blot analysis

RNA samples, in different concentrations were mixed 1:3 (v/v) with RNA loading buffer, denaturated for 10 min at 65°C and separated in 1% (w/v) agarose gel with 2.4 M formaldehyde in MOPS buffer. The gel was run at 65 volts for 2 h, then equilibrated two times in 20x SSC buffer for 15 min. The transfer of RNA-samples from the agarose gel onto Hybond N^+ nylon membrane was performed by a 'downward' alkaline capillary transfer for 3 h at RT (Chomczynski, 1992). UV transilluminator was used for cross-linking the RNA samples to the membrane and then the membrane was air dried. The membrane was prehybridized at 54°C for 2 h and hybridized o/n in standard hybridization solution containing 1 µl of ODC-DIG-dUTP labelled probe.

After hybridization the membrane was washed with the following washing buffers. Detection of dioxigenin labeled ODC was performed by DIG luminescent detection kit according to the manufacturers instructions.

10x MOPS buffer (pH 7.0):

MOPS	200 mM
NaAc	50 mM
EDTA	10 mM

RNA-loading buffer (750 µl):

10x MOPS	100 µl
Formamide	465 µl

37% Formaldehyde	135 µl
88% Glycerol	50 µl
Bromophenol-Blue	1 µg

20x SSC pH 7.4:

NaCl	3 M
Tri-Sodiumcitrate	0.3 M

Washing buffer:

2x SSC/0.1% (v/v) SDS
0.2x SSC/0.1% (v/v) SDS

II.2.3 Expression and purification of recombinant proteins

II.2.3.1 Expression and purification of polyamine-GST fusion proteins from *E. coli*

GST and GST-fusion proteins were expressed and purified according to a modified protocol based on Smith (1993).

A freshly transformed single colony of *E. coli* strain BL21(λDE3) (Novagen) harbouring recombinant plasmid DNA was inoculated in 10 ml of 2YT medium containing 1% (w/v) glucose and 100 µg/ml ampicillin and cultivated o/n at 37°C with vigorous shaking. The following day 400 ml of fresh 2YT/0.1% (w/v) glucose media were inoculated with 3 ml overnight culture and grown at 30°C and 225 rpm to an $OD_{600\ nm}$ of 0.8-1. Expression of recombinant proteins was then induced by addition of IPTG to a final concentration of 0.1 mM. Cells were cultured o/n at 18°C. The cells were harvested by centrifugation (10 min/7700 g/4°C) and the supernatant discarded. The pellet was dried, resuspended in cold PBS buffer (20 ml/400 ml bacterial culture) and sonicated on ice 4 times for 40 sec (150W with 30 sec intervals). Triton X-100 (20% (v/v) stock solution) was added to 1% final concentration. The cell lysate was incubated for 30 min at 4°C on a rotary shaker. Cell debris and insoluble components were removed by centrifugation (20 min/15000 g/4°C) and the supernatant subjected to glutathione affinity chromatography according to the manufacturers instructions (Amersham Pharmacia Biotech).

II.2.3.2 Expression and purification of ODC and PAO proteins

The pET22b in BL21(λDE3) carrying the ODC and PAO genes (kind provided by Dr. B. Schneider, RWTH Aachen, Institut für Biologie VII, Germany) were grown in 10 ml of LB medium at 37°C containing 100 µg/ml ampicillin (LBA). The following day, the non-induced o/n culture was diluted 1:60 with fresh LBA medium and grown at 37°C with vigorous shaking until OD_{600} reached 0.6. IPTG at a final concentration of 1 mM was added and the culture was grown at 37°C for 4 hours. The cells were harvested by centrifugation at 4000 g for 15 min. Polyamine proteins were purified from inclusion

bodies via C-terminal his6 tag using Ni-NTA affinity chromatography under denaturating conditions as described below. The bacterial pellet was resuspended in lysis buffer B containing 8 M urea and incubated for 1 h at room temperature. After centrifugation at 10000 g for 30 min, the supernatant was loaded onto pre-equilibrated Ni-NTA column and passed through the columns twice. After several washing steps with washing buffer, the bound protein was eluted twice with 300 µl of elution buffer and stored in 8 M urea. Fractions were collected and analysed by SDS-PAGE (II.2.4.2) and stored at -20°C for further experiments.

Lysis buffer B: 8 M urea; 0.1 M NaH_2PO_4; 0.01 M Tris HCl pH 8.0
Washing buffer C: 8 M urea; 0.1 M NaH_2PO_4; 0.01 M Tris HCl pH 6.3
Elution buffer E: 8 M urea; 0.1 M NaH_2PO_4; 0.01 M Tris HCl pH 4.5

II.2.3.3 Large scale expression of scFv in pSyn and purification of soluble scFv by IMAC

For large scale expression scFv cDNAs were subcloned into the procaryotic expression vector pSyn using either *Nco*I/*Not*I restriction sites or *Sfi*I/*Not*I restriction sites if an internal *Nco*I restriction site was present. Recombinant pSyn plasmids were transformed into *E. coli* strain HB101. A single recombinant colony was inoculated in 10 ml of 2YT medium containing 1 % (w/v) glucose and 100 µg/ml ampicillin and cultivated at 37°C with shaking (200 rpm).

Three ml of the o/n culture were transferred into 500 ml of 2YT media containing 0.1% (w/v) glucose and 100 µg/ml ampicillin and grown at 37°C until the $OD_{600\ nm}$ reached 0.7-0.8. Expression of scFv fragments were induced by addition of IPTG to a final concentration of 1 mM for 3 hours at 30°C. The culture was centrifuged (4000 g/4°C/20 min) and the pelleted bacteria were resuspended in 10 ml of resuspension buffer (30 mM Tris, 20 % (w/v) sucrose, pH 8.0). EDTA was added to a final concentration of 1 mM. The suspension was incubated at 4°C for 10 min with gentle agitation followed by centrifugation at (8000 g/4°C/20 min). The supernatant S_1 was removed and kept on ice. The pellet was resuspended in 9 ml of cold 5 mM $MgSO_4$ and incubated at 4°C for 8-9 min on a rotatory shaker. EDTA was added to a final concentration of 1 mM and the suspension was agitated for 3 more minutes followed by centrifugation at (8000 g/4°C/20 min). The supernatant (S_2) was mixed with the first supernatant (S_1) and dialysed against PBS prior to IMAC affinity purification.

Ni-NTA-agarose was added in a disposable column and equilibrated with 10-20 volumes of wash buffer. Imidazol and sodium chloride were added into the dialyzed periplasmic fraction to a final concentration of 10 mM and 500 mM, respectively. The sample was

passed twice through the pre-equilibrated Ni-NTA matrix. The column was washed with 20 volumes of wash buffer and the proteins were eluted in three fractions with 700 µl of elution buffer. Collected fractions were immediately dialysed against PBS (pH 7.4) to remove imidazol and salt. To control the yield and purity of dialyzed scFv fragments 5 µl were run in a SDS-PAGE (II.2.4.2). The concentration was determined using the Pierce BCA protein assay (II.2.4.1).

Wash buffer: 1x PBS, 10 mM imidazol; 500 mM NaCl

Elution buffer: 1x PBS, 250 mM imidazol pH 4.5

II.2.4 Protein analysis

II.2.4.1 Quantification of proteins

The concentration of purified protein was determined by Bradford (Bradford, 1976) or BCA (Pierce) assays. For Bradford assay the protein solution of interest was serially diluted. BSA was also serially diluted and used as standard. 10 µl of each dilution was transferred into the wells of a low binding microtiter plate (Greiner, Solingen, Germany). 10 µl of the buffer was used as a blank. 200 µl of Bradford reagent were added to each well, mixed with the proteins and incubated at RT for 10 min followed by the measurement of OD_{595nm}. For each dilution, measurements were performed in duplicate and the average was taken for the calculation of the protein concentration.

The Pierce BCA protein assay is a detergent-compatible formulation based on bicinchoninic acid (BCA) for the colorimetric detection and quantification of proteins (Smith *et al*., 1985; Sorensen and Brodbeck, 1986). This method combines reduction of Cu^{+2} to Cu^{+1} by proteins in an alkaline medium with the sensitive and selective colorimetric detection of the cuprous cation (Cu^{+1}) using bicinchoninic acid (Wiechelman *et al*., 1988). Concentration measurements were done according to the manufacturers instructions, using BSA as standard.

II.2.4.2 SDS-PAA gel electrophoresis and Coomassie brillant blue staining

Discontinuous SDS-polyacrylamide gels (for the stacking gel: T = 4%, C = 2.6%, pH 6.8; for the separating gel: T = 12%, C = 2.6%, pH 8.8) (Ausubel *et al.*, 1995) were used for separation of protein samples. Before loading onto the gel, protein samples were denaturated in the presence of SDS and β-mercaptoethanol. The proteins were separated electrophoretically with 20V/cm for 1 hour. Protein bands were revealed by staining with Coomassie brilliant blue or transfer to nitrocellulose membrane for immunoblot analysis (Ausubel *et al.*, 1995). Proteins were detected after incubating the gel for 30 min in

Coomassie staining solution at RT under constant rocking. Coomassie staining was removed by destaining solution until the protein bands was clearly visible.

SDS-PAGE running buffer (pH 8.3):

Tris	125 mM (w/v)
Glycine	960 mM (v/v)
SDS	0.5% (w/v)

Coomassie staining solution:

Coomassie brillant blue G-250	0.25% (w/v)
Methanol	50% (v/v)
Glacial acetic acid	9% (v/v)

Coomassie destaining solution:

Methanol	10% (v/v)
Glacial acetic acid	10% (v/v)

II.2.4.3 Immunoblot analysis

Separated proteins (II.2.4.2) were transferred from an SDS-PAA gel to PVDF or Hybond^{TM}-C nitrocellulose membrane (0.45 μm). After blotting the membrane was blocked with PBS buffer containing 3% (w/v) skim milk powder (MPBS). As primary antibody either anti c-myc, anti his6 or anti KDEL were used in a dilution of 1:5000 in 1xPBS. Attachment of the primary antibody was detected by addition of the secondary polyclonal antibody coupled to alkaline phosphatase (AP). Both, primary and secondary antibodies were diluted in blocking buffer. The target protein was finally revealed by addition of substrate BCIP/NBT.

PBS buffer (pH 7.3):

NaCl	137 mM
KCl	2.7 mM
$Na_2HPO_4x2H_2O$	8.1 mM
KH_2PO_4	1.5 mM

Transfer buffer (pH 8.3):

Tris-HCl, pH 8.3	25 mM
Glycine	92 mM
Methanol	20% (v/v)

AP buffer (pH 9.6):

Tris-HCl, pH 9.6	100 mM
NaCl	100 mM
$MgCl_2$	5 mM

II.2.4.4 Dot blot analysis

50 µl of supernatant (II.2.8.1) containing soluble scFv fragments expressed on a small-scale were immobilized on Immobilon-P PVDF membrane using a dot blot apparatus. Immobilized scFv fragments were detected using 1:2500 diluted anti-c-myc monoclonal antibody 9E10 followed by 1:5000 diluted AP-labelled goat anti-mouse polyclonal antiserum. Binding of AP-conjugated secondary antibodies was revealed by adding BCIP/NBT substrate.

II.2.5 Immunization of mice

The treatment and maintenance of laboratory animals was approved by the 'Regierungspräsidium des Landes NRW' (RP-Nr.: 23.203.2 AC 12, 21/95) and supervised by Dr. Hirsch as responsible biosafety officer at the Institut für Biologie I, RWTH Aachen.

Two female mice (Balb/c) each were immunized with 50 µg of ADC, ODC-GST and PAO-GST fusion proteins mixed with 40µl GEBRU's adjuvant. Two further injections into the tail vein were given at biweekly intervals with the same amount of antigen and 20µl GEBRU's adjuvant per mouse. The final boost was performed 4 days prior to sacrifice. After the last boost, blood was taken from the tail vein using a 26 gauge needle (1-2 µl) and a capillary for picking up blood. The blood was diluted 1000-fold with PBS for estimation of antibody titers.

II.2.5.1 Determination of antisera titers by ELISA

The determination of polyclonal antibody titers from sera of mice was performed by direct ELISAs (II.2.8.1) using ADC, ODC and PAO proteins as antigens (Fischer, 1990). To determine the titer of ADC-specific antibodies, 10 µg/ml of ADC cleaved from GST with Factor Xa were coated to ELISA plates. For determination of ODC-GST- and PAO-GST-specific antibodies, ODC and PAO proteins (II.2.3.2) were coated in 8 M urea to ELISA plates. GST (10 µg/ml) was included as control. Antigens were coated at 37^{o}C for 1.5 hours and blocked with 1% BSA (w/v) in 1xPBS. Serial dilutions of sera (1:500-1:256000) in blocking buffer were added to the coated plates and incubated at 37°C for 1.5 hours. After three washes with PBST bound antibodies were detected by addition of 1:5000 diluted AP-labelled goat anti-mouse polyclonal antibodies in blocking buffer and p-nitrophenyl phosphate (pNPP) as substrate (Sigma). ELISA plates were incubated at 37°C for 1 h followed by measurement of the OD at 405 nm.

II.2.6 Construction of phage displayed scFv libraries

II.2.6.1 Isolation of total RNA from spleen cells

Spleens from immunised mice (II.2.5) were removed and dissected. Spleenocytes were prepared by disrupting the spleens through a meshing net and washed twice with RPMI 1640 solution. The cells were homogenised in 1xPBS, aliquoted to not more then $1x10^8$ cells and subjected to total RNA isolation using the 'RNeasy Midi kit' followed by a TRIZOL extraction (GibcoBRL) to obtain high yield and pure RNA.

II.2.6.2 First strand cDNA synthesis

First-strand cDNA was synthesised from 5 μg of total RNA using 'Superscript™ preamplification system kit' (GibcoBRL) and gene specific primers COH 30, COH 32, MuPD 31; MuPD 32 that bind to the constant region of mouse IgG1, IgG2a/2b, κ and λ, respectively. cDNA synthesis was performed according to the manufacturers instructions.

II.2.6.3 Construction of scFv libraries

Mouse heavy and light chain variable regions were amplified by PCR using primers specific to murine IgG1, IgG2a/2b heavy chain λ and κ light chain (II.1.9). For each forward primer separate PCR reactions were performed whereas backward primers were used as a cocktail. PCR reactions were carried out in a total volume of 50 μl by adding 10 pmol of each primer(s) and $^1/_{10}$ to $^1/_{16}$ of the first strand cDNA reaction under the following conditions: intial denaturation at 95°C for 5 minutes followed by 35 cycles at 94°C for 1 min, 55°C for 1 min, 72°C for 1 min and a final elongation for 10 min at 72°C.

Heavy (V_H) and light (V_L) chain fragments were gel purified using "QIAquick gel extraction kit" (Qiagen) (II.2.1.12) and digested with *Sfi*I and *Bst*EII, or *Asc*I and *Not*I enzymes, respectively. pHEN4II phagemid DNA was digested with *Sfi*I and *Bst*EII or *Asc*I and *Not*I and gel purified. 200 ng of purified vector were ligated with a five fold molar excess of purified fragments. Ligation products were electroporated into electrocompetent *E. coli* TG1 cells to create the sublibraries. The scFv fragment libraries were constructed by excising V_H or V_L fragments with the respective enzymes and ligating them into the linearised pHEN4II containing V_L or V_H fragments.

II.2.6.4 *Bst*NI fingerprinting

The variability of the generated scFv fragment libraries was tested by restriction with *Bst*NI. PCR-amplified scFv fragments from 20 randomly selected *E. coli* colonies were digested with 5 U *Bst*NI at 60°C for 2 h. This method was first described in phage display protocols by Marks *et al*. (1991) and Hoogenboom *et al*. (1996). Digested fragments were separated in a 2% (w/v) agarose gel (II.2.1.12) and the variability of the library was estimated.

II.2.7 Phage displayed antibody selection

Phage particles were rescued from the scFv-libraries by superinfection with helper phage M13KO7 (Clackson *et al*., 1991). Phage titers were determined by addition of phage dilutions to exponentially growing *E. coli* TG1. For isolation of phages exposing antigen-specific antibodies panning procedures were performed. Polyamine-GST fusion proteins (10 µg/ml) were immobilized o/n to immunotubes. To exclude the binding of phage presenting GST-specific scFv fragments, 10^{12} phages from each library were preincubated with GST (10 µg/ml) in 2% MPBS (w/v) at RT for 30 min. Then the phage solution was added to the antigen-coated immunotubes and incubated for 30 min under rotation and then 1.5 h w/o movement. Phages that showed no or low affinity for the immobilized antigen were washed away by PBS, 0.05% (w/v) Tween20 followed by PBS. Each washing step was performed 20 times by filling the tube and decanting immediately. Phages with affinity to the antigen were eluted from the tube by addition of 1 ml of 100 mM triethylamine (freshly made) while rotating on an under and over turntable for 8-10 min followed by neutralisation with 1 M Tris-HCl pH 7.4. Nine ml of log phase *E. coli* TG1 cells were infected with eluted phages and plated on 2x YT agar plates containing 2% (w/v) glucose and 100 µg/ml ampicillin (2x YTGA-agar). The plates were incubated o/n at 37°C. Cells were scraped off the agar by adding 5 ml of 2x TY medium containing 15% (v/v) glycerol and stored at -70°C for a new round of selection.

The total eluted phage titer indicating the successful binding and elution of phages, was determined after each round of panning by addition of dilutions to exponentially growing *E. coli* TG1. An increasing titer of eluted phages in subsequent round of pannings indicated the enrichment for clones, which bind most strongly to the target antigen.

II.2.8 Characterisation of phage displayed scFv fragments

II.2.8.1 Soluble expression of scFv fragments and direct ELISA

Screening of scFv-fragment libraries was performed after the third round of panning by small scale induction of scFv expression from pHEN4II phagemid vector in ELISA plates. 120 recombinant clones of *E. coli* strain TG1 were randomly selected and inoculated in 100 µl of 2x TY, 100 µg/ml ampicillin, 1% (w/v) glucose in microtiter plates. The plates (master plates) were grown at 37°C overnight. The next day, cells were transferred from the master plate to a second plate containing 125 µl 2x TY, 100 µg/ml ampicillin, 0.1% (w/v) glucose. Bacteria were grown at 37°C until the $OD_{600\ nm}$ reached 0.1-1. Soluble scFv fragment expression was induced at 30°C for 16-24 h by addition of IPTG to a final concentration of 1 mM. The cells were removed by centrifugation and the supernatant was used for soluble ELISA.

A high binding ELISA plate was coated with antigen (10 µg/ml) o/n at 4°C. After blocking with 2% (w/v) MPBS the supernatant was applied to the plate and incubated for 2 h at RT. Bound scFv fragments were detected using 1:5000 diluted anti c-myc monoclonal antibody 9E10 and 1:5000 diluted AP-conjugated goat anti mouse polyclonal antibody. ELISA readings were performed at $OD_{405\ nm}$ after incubation at 37°C with pNPP for 1 h.

II.2.8.2 Capture ELISA of selected scFv fragments

Capture ELISA was performed by o/n coating of chicken IgY's specific to ODC-GST and ADC proteins in two different dilutions 1:1000 and 1:5000. The plate was blocked for 2 h at RT with 2% (w/v) MPBS, then incubated with 10 µg/ml of bacterial purified antigen (ADC-GST, ODC-GST or GST) (II.2.3.1). Finally, supernatant from the periplasmic expression of the 15 selected scFv-fragments (II.2.8.1) was applied and incubated at RT for 2 h. Bound scFv fragments were detected with 9E10 monoclonal antibody and the 1:5000 diluted AP-conjugated goat anti mouse polyclonal antibody. The remaining steps were carried out as described above.

II.2.8.3 Biotinylation of scFv

Affinity purified scFvADC3 (II.2.3.3) was reversibly biotinylated using biotin disulfide N-hydroxysuccinimide ester (Sigma, St Louis, Missouri, USA). 0.5 mg of scFvADC3 in PBS was mixed with 0.25 ml of 1 M $NaHCO_3$ (pH 8.6) and a 15-20 molar excess of biotin solution added at room temperature for 30 min. Free biotinylation reagent was removed by dialysis against PBS at 4°C o/n.

Biotinylation efficiency of the scFvADC3 was determined by immunoblot (II.2.4.3) using the non-biotinylated scFvADC3 and another biotinylated scFv fragment of known concentration as a standard.

II.2.8.4 Competition ELISA of biotinylated scFv fragments

Competition ELISA was used to determine whether the two scFv fragments generated against ADC recognise overlapping or non-overlapping epitopes. ADC-GST fusion protein was coated o/n at 4°C to a microtiter plate at a concentration of 1 µg/ml. scFvADC3 and scFvADC7 were serially diluted in a suitable constant concentration of biotinylated scFvADC3 (1:80), determined from a direct ELISA, in siliconized microtiter plates. All dilutions were transferred to the ADC-GST coated plate. Bound scFvADC was detected with $Strep^{AP}$ antibody. The remaining steps were carried out as described above (II.2.8.1).

II.2.8.5 Electrophoretic mobility shift assay (EMSA)

Varying amounts of ODC-GST antigen were incubated for 1 hr at RT with 2 µg of affinity purified scFv specific to ODC. Then, the electrophoretic mobility was compared to the electrophoretic mobility of purified antigen and scFv alone. Samples were loaded on a

native 9% non-reducing PAGE pH 9 and run at 100 V for 5 hours. Proteins were visualized by Coomassie blue staining (II.2.4.2).

II.2.8.6 Gel Filtration

A Sephadex 200 column (Amersham Pharmacia Biotech) was equilibrated with 1xPBS. Affinity purified scFvs (II.2.8.1) were loaded and run at 1 ml/min. Cytochrome C (12400 Da), carbonic anhydrase (29000 Da), BSA (66000 Da), β-amylase (200000 Da) and Dextran Blue (2000000 Da) were run as molecular weight standards. The eluates were monitored by UV 260 nm and 280 nm and Blue dextran by 610 nm.

II.2.8.7 Characterisation of scFv fragments by BIACORE

Biomolecular interaction analyses of binding of purified scFvODC to ODC-GST antigen were done by surface plasmon resonance (SPR) on a BIACORE® 2000 (BIAcore). All injected samples were diluted in HBS buffer (10 mM HEPES, 150mM NaCl, 3.4 mM EDTA, 0.005% Surfactant P20) and subjected to centrifugation prior to injection (14000 rpm/10 min/4^{o}C) to remove insoluble components.

The ligands were immobilized on a CM5-rg sensor chip using the amine coupling kit (BIAcore). The immobilization of proteins on the chip was performed at a flow rate of 5 µl/min. The carboxyl groups on the sensor surface were activated with an injection of a solution containing 100 mM EDC/NHS (N-Ethyl-N'-(Dimethylaminopropyl)-Carbodimide-Hydrochloride, 400 mM N-Hydroxyl-Succinimide). After each binding experiment the surface was regenerated with 15-20 µl of 1.2 M Guanidine HCl followed by 30 sec injections of HBS. The data were analysed using the BIAevaluation (3.0) software.

II.2.9 Determination of ODC activity

Tobacco leaf tissue was extracted in extraction buffer at ratio 500 mg/ml. Polyvinylpyrrolidone (100 mg) was added during grinding. Following centrifugation at 15000xg for 10 min at 4 ^{o}C, the supernatant was used directly for enzyme activity assays. Tissue was always processed immediately after harvest and all assays were performed using fresh extracts. Enzyme assays were carried out in 2 ml Eppendorff tubes. A 3mm diameter filter paper disc impregnated with 100 µl of 2 M KOH and transfixed with a 3 cm needle was used to trap the $^{14}CO_2$ liberated during the reaction.

The reaction mixture used to determine ODC activity contained 20 µl of extraction buffer (pH 7.0), 160 µl of crude enzyme and 20 µl of the substrate mix [20 µl of DL-(1-^{14}C) ornithine (Moravek Biochemicals, Brea, California) (specific activity 53 mCi/mmol, diluted in distilled water]. Assays were carried out at 37^{o}C for 45 min. Then 200 µl of 10% (v/v) perchloric acid was added to stop the reaction. After further 45 min incubation, the

filter paper was placed in scintillation vials with 1.5 ml scintillation liquid and radioactivity was measured in liquid scintillation counter. Each reaction was performed in four replicates.

Extraction buffer:

HEPES pH 7.5	100mM
DTT	2mM
EDTA	1 mM

II.2.10 Extraction of polyamines from tobacco plants

Young leaves from 1-2 months old tobacco plants were used for extraction of free polyamines. Frozen leaf samples were ground in liquid nitrogen and polyamines extracted in the presence of 10% TCA (1:3 w/v) (Tabor *et al*., 1973). The homogenate was incubated for 4 h on ice and then centrifuged at 15000 rpm at 4°C. The supernatant was filtered sterilised and transferred into a fresh tube. Prior analysis the samples were mixed 1:1 (v/v) with 1.2 M sodium citrate buffer.

II.2.10.1 Analysis of free polyamine levels from stable transformed tobacco

Levels of free polyamines were determined on a Biochrom 20 Amino acid analyser (Amersham Pharmacia Biotech) by post-column derivatisation with ninhydrin (Spackman *et al*., 1958). The polyamine sample was loaded onto a 100 x 4 mm cation-exchange column (Bio 20 Peek, polyamine column, Amersham Pharmacia Biotech) and polyamines eluted according to the manufacturers instructions. The column eluent was mixed with the ninhydrin reagent (Amersham Pharmacia Biotech) and passed through a high temperature (135^{o}C) reaction coil. In the reaction coil ninhydrin reacts with the polyamines present in the eluate to form coloured compounds. The amount of coloured compounds, determined by photometric detection at 570 nm, is directly proportional to the quantity of polyamines in the eluate.

After each sample analysis, the column was regenerated with 0.4 M NaOH followed by the equilibration with 1.2 M sodium citrate buffer (pH 6.45).

Evaluation of amino acid analysis data was performed by using Ezchrom V 6.7 chrom data system (Scientific Software Inc) (Amersham Pharmacia Biotech).

Known concentrations of standard: ornithine, putrescine, spermidine and spermine (Sigma) were run prior to tobacco plants analysis and a calibration analysis was performed based on the manufacturers instructions.

Polyamine buffer:

Tripotassium citrate monohydrate	0.55 M
Sodium chloride anhydrous	0.55 M

Hydrochloric acid (concentrated)	1.78 % (v/v)
Propan-2-ol	6.5 % (v/v)
80% (v/v) solution phenol	0.12 % (v/v)

III Results

III.1 Cloning of human ornithine decarboxylase (ODC) a key enzyme in polyamine biosynthesis

The gene encoding ODC was amplified from a human prostate cDNA library using primers based on the 5' and 3' sequences of human ODC mRNA sequence (Gen-bank accession number M16650). Restriction sites *EcoR*I/*Nco*I and *Sal*I/*Hind*III were introduced into the forward and reverse primers for subcloning, respectively.

The ~1.5 kb PCR product (Figure III-1) was ligated into the *Nco*I/*Sal*I sites of pGEM-3zf vector and the sequence verified from the clone pGEM-3zf-ODC_L. A single point mutation (highlighted in the sequence, please refer to the appendix VII.2) changing glutamic acid to glutamine ($Glu^{417} \rightarrow Gln^{417}$) was observed. To investigate if the original gene from the cDNA library already showed this mutation or if it has been introduced by PCR the ODC gene was amplified from the prostate library using expand high fidelity *Taq* polymerase and ligated into pCR2.1 (TOPO vector). The sequence analysis of six independent transformants confirmed the amino acid change from glutamine to glutamic acid at position 1246. The nucleic acid and the amino acid sequence of amplified ODC gene from clone #103 (ODC_L/TOPO) are presented in appendix VII.2. The ODC fragment of clone #103 was used for subcloning into bacteria (III.2) and plant expression vectors (III.4.1.1).

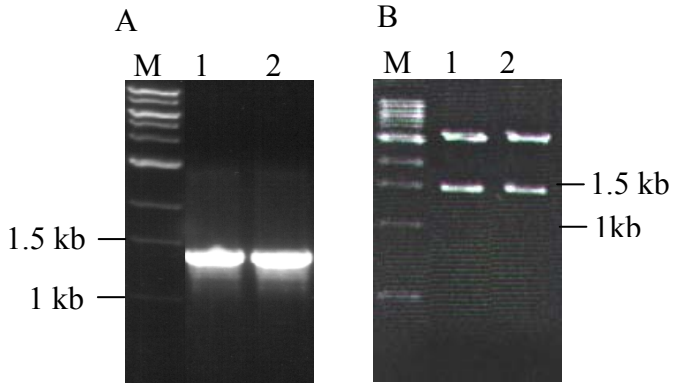

Figure III-1 PCR amplification and cloning of human ODC gene.

Nucleic acids were separated on a 1.2% (w/v) agarose gel. A: 5 µl of PCR amplified ODC gene from human prostate c-DNA library (1 and 2). B: double digestion of the pGEM-3zf-ODC plasmid with *Nco*I/*Sal*I restriction enzymes (1 and 2). M: 1kb ladder.

III.2 Expression and purification of ADC, ODC and PAO from bacterial cultures

In order to obtain polyamine proteins for immunization, panning and scFv characterization, the amplified human ODC (III.1), oat ADC and maize PAO genes (Dr. Bernd Schneider, RWTH Aachen, Institut für Biologie VII, Germany) were ligated into *Nco*I/*Sal*I sites of pGEX-5x-3 bacterial expression vector. The polyamine genes were fused to the C-terminus of GST and expressed in *E. coli* BL21λDE3 (II.2.3.1). The GST fusion proteins contained a Factor Xa cleavage site for removal of the GST fusion part. When protein expression was induced with 1 mM IPTG at 30°C 95% of the fusion proteins were produced as insoluble inclusion bodies (data not shown). The following modifications were employed to obtain improved solubility. First the growth and induction temperatures were lowered from 30°C to 16°C, second the IPTG concentrations were reduced to 0.01-0.1 mM, third longer induction periods, and fourth different induction time (3-12 hr) were tested.

The best parameters to obtain larger quantities of soluble ADC-GST and ODC-GST fusion protein were obtained by increasing the culture volume, decreasing the IPTG concentration to 0.05 mM, reducing the temperature to 18°C after induction and increasing the induction time to 8 hrs.

Cleavage of the polyamine fusion protein from the GST domain with Factor Xa was only successful for ADC (Figure III-2).

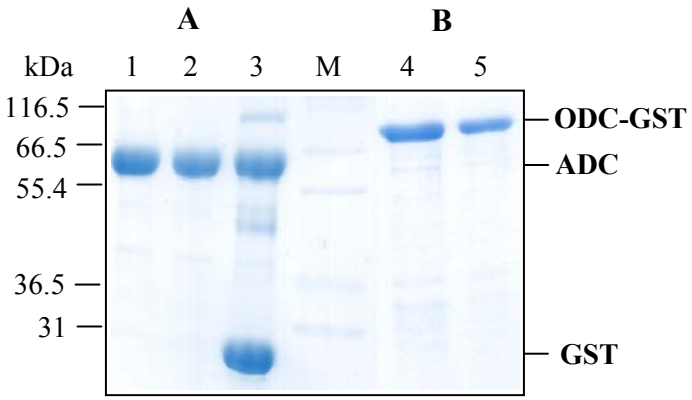

Figure III-2 SDS-PAGE analysis of affinity purified GST fusion proteins.

ADC (A) and ODC-GST (B) fusion proteins were affinity purified using glutathione sepharose matrix (II.2.3.1). Purified proteins were separated on 12% (w/v) SDS-PAA gels then stained with Coomassie brilliant blue (II.2.4.2). A: affinity purified ADC protein after cleavage with Factor Xa; B: affinity purified ODC-GST fusion protein. 1; 2: 5 µl of the first and the second elution fractions of ADC protein after cleavage with Factor Xa; 3: 5 µl of the boiled glutathione sepharose matrix sample after elution of the ADC protein; 4; 5: 5 µl of the first and the second elution fractions of ODC-GST fusion proteins; M: Mark12 protein marker.

Following the elution steps, a significant amount of ADC protein remained bound to the matrix (Figure III-2, line 3). Affinity purified fusion proteins showed high purity in Coomassie-stained SDS-polyacrylamide gels (Figure III-2).

The yields of purified ADC and ODC-GST fusion proteins were 2.0 and 1.5 mg per litre culture medium, respectively. The sizes of the ADC and ODC-GST proteins corresponded with the expected molecular weights of 63 and 78 kDa, respectively.

Attempts to purify soluble PAO fusion protein (MW 83 kDa) with the above mentioned parameters gave no improvements (Figure III-3). The yield of affinity purified PAO-GST was 0.07 mg per litre culture medium. These results suggested that the formation of the PAO-GST inclusion bodies was not affected by the expression conditions used. Efforts for solubilization using 4-8 M urea and N-lauroylsarcosine resulted in low yield of PAO-GST.

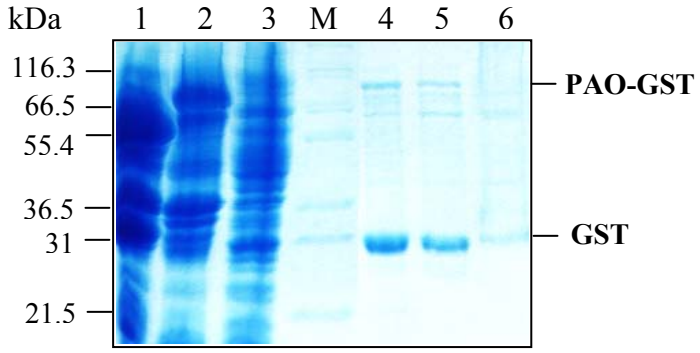

Figure III-3 SDS-PAGE analysis of purified PAO proteins.

Affinity purified PAO-GST fusion protein obtained from the GST expression system was resolved on 12% (w/v) SDS-PAA gel then stained with Coomassie brilliant blue (II.2.4.2). 1: 5 µl of sonicated *E. coli* BL21(λDE3) cells containing the pGEX-5x-3 plasmid that codes for PAO-GST. 2: 5 µl of flow through; 3: 5 µl of wash fraction; 4-6: 10 µl of the first, second and third elution fractions of PAO-GST fusion protein; M: Mark12 protein marker.

Purified ADC, ODC-GST fusion protein and PAO-GST inclusion bodies after suspension in PBS were used as antigens for immunization of mice (III.7) and antibody selection by phage display (III.9.1).

III.3 Cloning of ODC in bacteria expression vector pET22b and purification of the expressed protein via IMAC

To avoid the cross reaction of antibodies against the GST domain during the antibody titer determination of mice immunized with ODC-GST fusion proteins (III.7) the ODC gene was cloned into *Nco*I/*Sal*I sites of pET22b bacterial expression vector and purified via IMAC (II.2.3.2). The pET22b vector contains the IPTG inducible T7 promoter and the

*pel*B leader sequence to enable recombinant protein targeting into the periplasm. The target protein was engineered to contain a C-terminal His tag sequence for Ni-NTA affinity purification. Protein expression was induced with 1 mM IPTG for 4 hr at 37°C. Under these conditions ODC was expressed as insoluble aggregates. The recombinant protein was purified from inclusion bodies via the C-terminal his6 tag under denaturating conditions (II.2.3.2) and stored in 8M urea. The purity was verified on SDS-PAGE. Only about 45% of purified protein showed the expected size of 53 kDa (Figure III-4). Another protein migrating at 37 kDa was observed on SDS-PAGE gels in addition to the full length ODC protein. Both proteins were present in about the same quantity. Immunoblot analysis showed that both purified proteins were recognized by the anti-His6 antibody, indicating that the 37 kDa protein is a truncated form of ODC (data not shown).

The purified 53 kDa and 37 kDa ODC proteins were used in ELISA tests for determination of antibody titer from mice immunized with ODC-GST fusion protein (III.7).

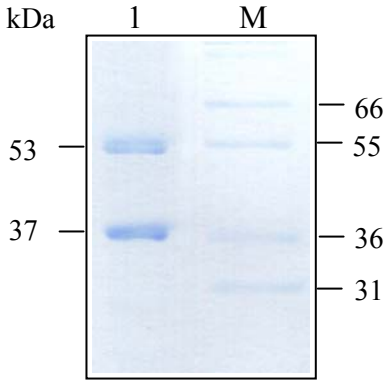

Figure III-4 SDS-PAGE analysis of purified ODC protein from pET22b vector via IMAC.

The affinity purified ODC protein was separated on a 12% (w/v) SDS-PAA gel and stained with Coomassie brilliant blue (II.2.4.2). 1: 5 µl elution fraction; M: Mark12 protein marker. The MW of ODC (53 kDa) and the C-terminal truncated form of ODC (37 kDa) are indicated.

III.4 Generation and characterization of transgenic plants

III.4.1 Engineering of constructs for targeting of human ODC to different plant cell compartments.

III.4.1.1 Cloning of ODC into plant expression vector pSSH1

The human ODC gene was cloned into three plant expression cassettes that enable targeting of expressed recombinant protein to the plant cytosol, secretion to the apoplast and retention in the ER. The strategy for cloning of ODC into the plant expression pSS^{H1} vector is shown Figure III-5. Direct ligation of DNA fragments into plant vector pSS^{H1}

was not possible due to an internal *Nco*I restriction site in the pSS^{H1} vector. Therefore the ODC gene (III.1) had to be subcloned into the *Nco*I/*Sal*I sites of modified pGEM-3zf vector downstream from the 5' untranslated region (UTR) of the chalcone synthase (CHS) and the plant codon-optimized leader peptide derived from the light chain (LPL) of the murine mAb24 (Voss et al., 1995), and upstream from a sequence encoding a his6 tag and the 3' UTR from tobacco mosaic virus (TMV).

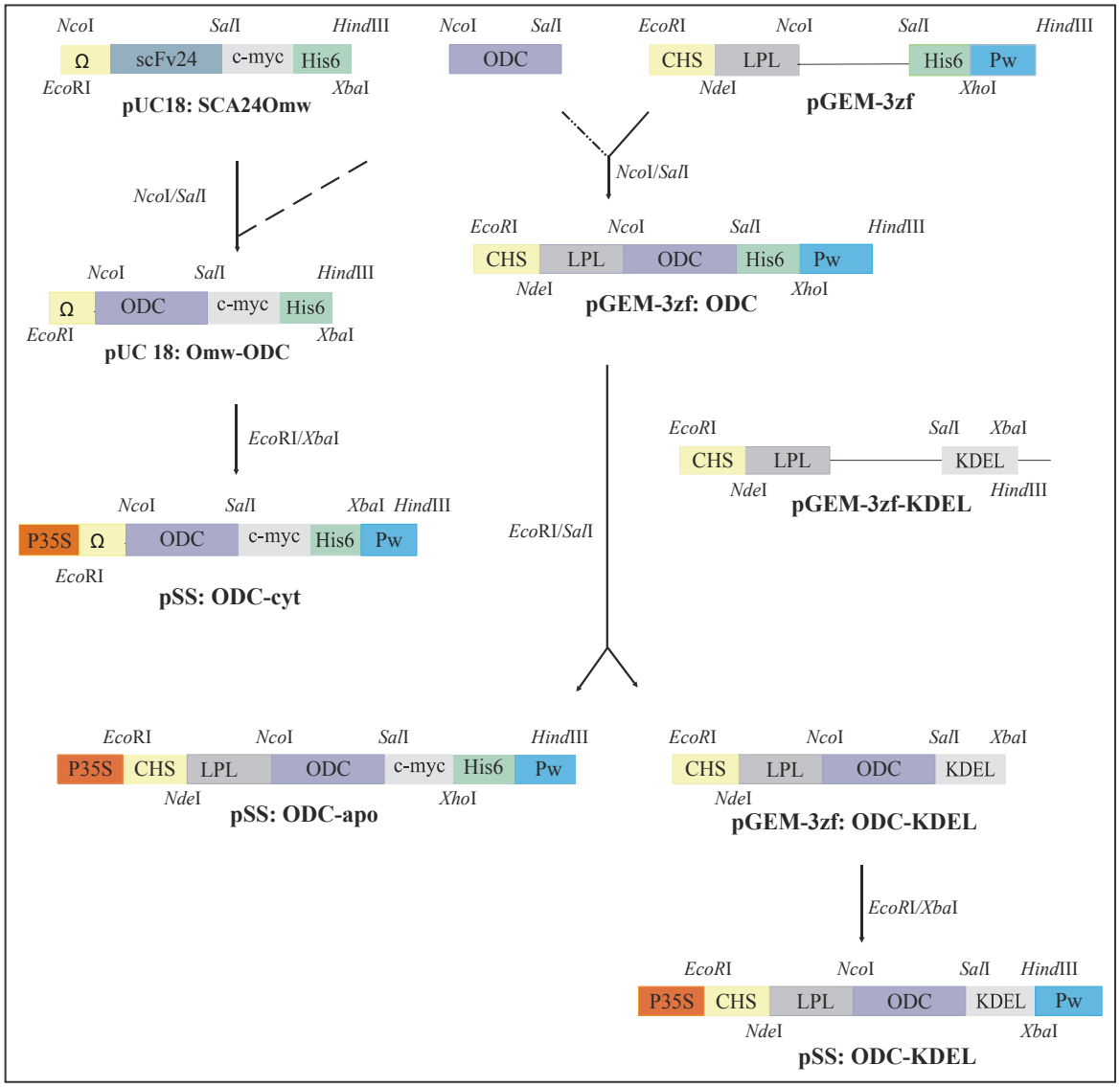

Figure III-5 Strategy for cloning of human ODC gene into pSS plant expression vector for cytosolic, apoplastic expression and ER retention.

P35S: 35SS promoter from CaMV; Ω: omega leader region of TMV RNA; CHS: 5' untranslated region of chalcon synthase; LPL: plant codon optimized leader peptide derived from murine light chain of TMV-specific mAb24; Pw: 3' UTR of TMV RNA: scFv24: TMV specific single chain antibody 24; c-myc: myc epitope for detection; His6: his-6 tag for purification and detection.

For generation of pSS: ODC-apo construct the cassette containing the 5' UTR of CHS, the LPL and ODC gene was excised with *EcoR*I/*Sal*I from ODC-pGEM-3zf vector and cloned downstream of the enhanced 35S promoter and upstream of c-myc/his6 tags and the 3' UTR of tobacco mosaic virus RNA (Pw) of the pSS plant expression vector.

For cytosolic targeting the ODC gene (III.1.1) was cloned *via Nco*I and *Sal*I restriction sites in the SCA24OmW cassette in pUC 18 downstream of an omega leader (Ω) region of TMV, and upstream of the c-myc/his-6 tags. Then, the cassette containing the Ω leader, ODC gene and c-myc/his6 tags was excised with *EcoR*I and *Xba*I and cloned between the enhanced 35S promoter and Pw untranslated region of pSS vector resulting in the pSS: ODC-cyt construct.

To retain the ODC in the lumen of the ER the cassette containing the 5' UTR of CHS, the LPL and ODC gene was excised with *EcoR*I/*Sal*I from pGEM-3zf vector and cloned upstream of the C-terminal KDEL tag (Munro and Pelham, 1987; Nilsson and Warren, 1994) into a modified pGEM-3zf vector. The expression cassette together with the KDEL tag were subcloned into pSS vector *via* the *EcoR*I and *Xba*I restriction sites resulting in the pSS: ODC-ER construct.

The constructs pSS: ODC-apo, pSS: ODC-cyt and pSS: ODC-ER were transformed into *Agrobacterium* by electroporation (II.2.1.6). Seven independent recombinant colonies from each transformation were screened for the presence of insert by PCR (II.2.1.13). Recombinant *Agrobacterium* cultures were prepared from single colonies of each construct (II.2.1.9) and used for transient expression (III.4.1.2) and stable transformation of *N. tabacum* (III.4.2).

III.4.1.2 Transient expression of ODC in different plant cell compartments

Transient expression experiments were performed for the initial analysis because the procedure is fast and not affected by position effects (Kapila *et al*., 1996). Four leaves were infiltrated with recombinant agrobacteria. After three days of incubation soluble proteins were extracted and detected by Immunoblot analysis to verify expression rate and integrity of the recombinant protein in these compartments.

Time-course analyses showed that maximum accumulation of ODC protein was reached at 50-60 h postinfiltration (data not shown). Immunoblot analyses showed a distinct band of approximately 51 kDa, corresponding to the molecular weight of ODC for both, cytosolic and apoplastic constructs (Figure III-6).

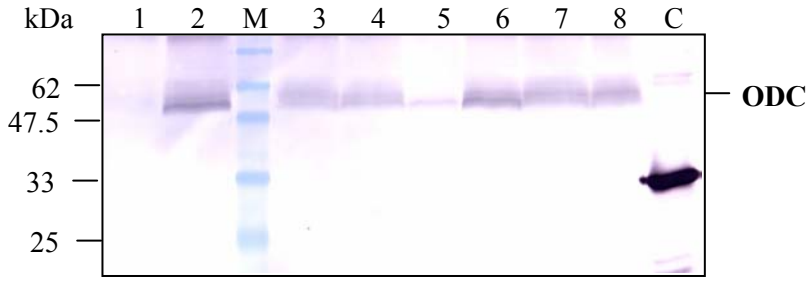

Figure III-6 Transient expression of cytosolic and apoplastic ODC.

Total soluble leaf proteins were extracted by grinding tobacco leaf tissue in two volumes extraction buffer (II.2.2.1), separated by SDS-PAGE (II.2.4.2) and blotted onto a nitrocellulose membrane (II.2.4.3). Immunodetection was carried out with 9E10 as primary antibody in dilution 1:5000, followed by alkaline phosphatase conjugated goat anti mouse as secondary antibody in dilution 1:5000 (II.2.4.3). Detection was performed with NBT/BCIP for 1 min at RT.

1-4: 5 µl of total soluble protein extracted from individual tobacco leaves expressing ODC in the cytoplasm; 5-8: 5 µl of total soluble protein extracted from different infiltrated tobacco leaves secreting ODC into apoplastic space. M: prestained protein marker; C: 1 µg of scFvODC3 carrying c-myc tag used as positive control.

The level of expression of the recombinant protein varied considerably between the constructs. Higher level of expression was shown in cytosol. No size difference was observed between the ODC accumulated in apoplast and cytosol indicating cleavage of the LPL signal peptide for the apoplastic construct pSS: ODC-apo.

ER retained ODC was not detectable by immunoblot analyses although the DNA sequence of the pSS: ODC-ER construct was confirmed (data not shown). RNA extracts of leaves carrying gene constructs for apoplastic and ER retained ODC were analysed by Northern blotting (Figure III-7).

The analysis demonstrated that in both vacuum-infiltrated plants a transcript of about 1.5 kb was synthesized which, hybridized with the human ODC gene used as a probe. This band was absent in the RNA extract of wild type tobacco leaves used as control (Figure III-7, line 3). Although, similar transcript levels were observed for apoplastic and ER constructs, protein expression levels did not correlate with the steady state levels of mRNA.

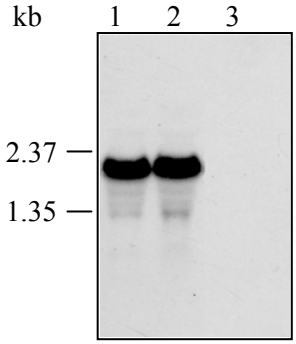

Figure III-7 Northern blot analysis of transcript levels of apoplastic and ER retained ODC. Total RNA was isolated from infiltrated leaves expressing ODC in the apoplast (1), ER (2) and from wild type tobacco plants (3) (II.2.2.7). Per line 10 µg RNA was loaded and separated on a 1% (w/v) agarose gel containing 2.4 M formaldehyde prior to blotting onto a nylon membrane (II.2.2.8). The RNA marker (not shown in the figure) was run simultaneously. DIG labeled 1.5 kb human ODC gene was used as probe for hybridization (II.2.2.8). Detection of dioxigenin labeled ODC was performed by DIG luminescent detection kit for 2 min at RT.

III.4.2 Generation and screening of stable transformed tobacco plants expressing human ODC

Following the transient expression results, pSS: ODC-apo and pSS: ODC-cyt constructs were stably transformed into tobacco plants by *Agrobacterium*-mediated transformation (II.2.2.4). Twenty-five regenerated plants (labeled ODC-apo-1→25) from the transformation experiments with pSS: ODC-apo and 19 plants (labeled ODC-cyt-1→19) expressing pSS: ODC-cyt were planted and screened for accumulation of recombinant protein (Figure III-8/A, C). None of the transformed plants exhibited altered morphology and all set seed normally upon self-fertilization. Recombinant accumulated proteins in tobacco leaves were analyzed by immunoblot using crude extracts of total soluble leaf protein. Immunoblot experiments revealed that 18 out of 25 and 16 out of 19 T_0 transformed plants accumulated the ODC in apoplast and cytosol, respectively (Figure III-8/A, C).

These T_0 plants segregated in a Mendelian manner into siblings with the ODC transgene and those without it. The ODC migrated according to its predicted molecular weight.

Higher expression was observed in tobacco plants accumulating the ODC in cytosol (Figure III-8/C). For apoplasmic ODC the expression was lower. The lines with the highest level of accumulation in the apoplasm (ODC-apo-7; ODC-apo-10) and the cytosol (ODC-cyt-4; ODC-cyt-8; ODC-cyt-10; ODC-cyt-13) (highlighted in the Figure III-8) were selected and self pollinated for establishment of homozygous lines.

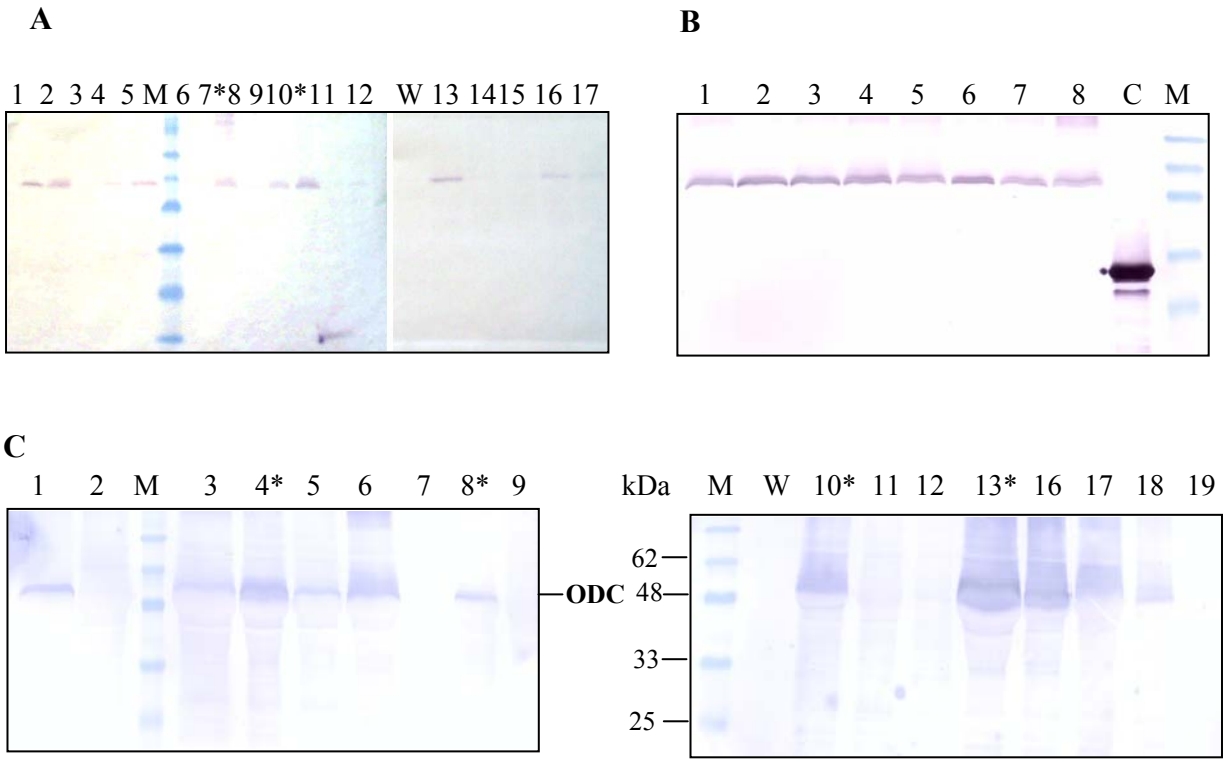

Figure III-8 Screening of stable transgenic tobacco plants expressing apoplastic and cytosolic ODC.

Total soluble leaf proteins were extracted by grinding tobacco leaf tissue in two volumes extraction buffer (II.2.2.6). 5 µl of total soluble protein from each sample was separated by 12% SDS-PAGE (II.2.4.2) and blotted onto a nitrocellulose membrane (II.2.2.3). Immunodetection was carried out with anti-c-myc antibody (1:5000), followed by 1 hr incubation with goat anti-mouse antibody conjugated to alkaline phosphatase (1:5000) and NBT/BCIP detection for 5 min at RT.

A: 1-17: ODC-apo-1→17 T_0 transgenic lines from the transformation experiments expressing apoplasmic ODC. W: 5µl of total soluble protein extracted from wild type fresh leaves; M: prestained protein marker. B: 1-8: T_2 transgenic lines (labeled ODC-apo-7/3-1→8) expressing apoplasmic ODC generated from the T_1 generation of the ODC-apo-7 tobacco plant indicated in the Figure III-8/A; C: 1µg of scFvODC7 carrying the c-myc tag sequence used as positive control; M: prestained protein marker. C: 1-19: ODC-cyt-1→19 T_0 stable transformed tobacco lines expressing cytosolic ODC. Tobacco lines selected for establishment of homozygous lines are indicated by *.

The accumulated levels of the recombinant ODC protein in the T_1 generation of the tobacco plants expressing the ODC in apoplast were similar with the parental T_0 ODC-apo-7 and GR1-10 selected lines (data not shown). The line ODC-apo-7/3 was chosen for further crossing experiments. The T_2 generation of line ODC-apo-7/3 expressing apoplasmic ODC (Figure III-8/B) showed higher level of expression than the T_0 and T_1 generation.

The T_1 generation of ODC-cyt-4; ODC-cyt-8; ODC-cyt-10; ODC-cyt-13 tobacco lines expressing the human ODC in cytosol accumulated comparable levels of the recombinant ODC protein with the T_0 lines (data not shown). Expression levels of the T_2 generation of the ODC-cyt-4; ODC-cyt-8; ODC-cyt-10; ODC-cyt-13 selected lines expressing cytosolic ODC were comparable with the accumulation levels of parental T_0 and T_1 generation (data not shown).

The T_2 generation of tobacco lines overexpressing apoplastic ODC (ODC-apo-7/3) were further analyzed for free polyamine levels (III-5).

III.4.3 Generation of transgenic tobacco plants co-expressing human ODC and chimeric mouse/human SDE enzymes

Non-segregating transgenic lines co-producing apoplasmic ODC and SDE were generated. It was expected that stable transgenic lines coexpressing both polyamine enzymes show an increase in putrescine and spermidine levels. Two T_2 tobacco plants with a high expression of apoplastic SDE (SDE-11/1-2; SDE-11/1-1) (kindly provided by Dr. B. Schneider) were pollinated with two T_2 tobacco plants expressing apoplastic ODC (ODC-apo-7/3-2; ODC-apo-7/3-4). 11 plants of the T_1 generation of each crossing were grown under identical conditions. All plants appeared healthy and there was no noticable change in growth and phenotype compared to wild type plants. Crossed plants were analysed for the expression of ODC and SDE by immunoblots using antibody 9E10 as primary antibody (Figure III-9).

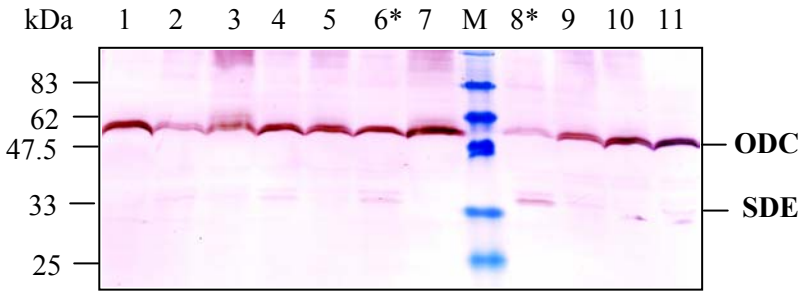

Figure III-9 Analysis of ODC-apo-7/3-2 x SDE-11-1/1 or (ODC x SDE/1→11) stable transformed tobacco plants co-expressing apoplasmic ODC and SDE.

Total soluble leaf proteins were extracted by grinding leaf tissue in two volumes extraction buffer (II.2.2.6), separated by SDS-PAGE (II.2.4.2) and blotted onto a nitrocellulose membrane (II.2.4.3). Immunodetection was carried out with anti-c-myc antibody, followed by goat anti-mouse antibodies conjugated to alkaline phosphatase and NBT/BCIP detection. 1-11: ODC x SDE/1→11 different lines co-expressing both enzymes; M: prestained protein marker. Tobacco lines selected for establishment of homozygous lines are indicated by *.

Non transgenic and ‘‘single transgenic’’ plants were distinguished from ‘‘double transgenic’’ by the absence, by one or both protein band. Immunoblot analyses revealed that more then 80% of the lines tested co-expressed both enzymes. However, as shown in Figure III-9 the expression levels of both enzymes differed significantly, ODC (51.2 kDa) being produced much higher. The enzyme levels were also compared between the T_1 offspring and the parental lines (data not shown). Higher expression of SDE enzyme (33.8) was observed in parental lines, while for ODC similar levels of expression were observed.

Lines ODC x SDE/6 and ODC x SDE/8 (indicated in figure III-9) that showed the strongest signals for both enzymes in immunoblot analysis was kept to establish double transgenic homozygous lines. Analysis of recombinant protein accumulation levels and the free polyamine levels are planned with the T_2 generation of both selected transgenic lines co-expressing both proteins.

III.5 Polyamine analysis

III.5.1 Polyamine levels in stable transformed plants overexpressing ODC

In order to examine if transgenic tobacco plants expressing ODC in apoplast affect the polyamine metabolism, transgenic plants were analyzed for increased levels of putrescine, spermidine and spermine. Polyamine levels were analyzed in transgenic plants in parallel with the immunoblot analyses and ODC enzyme activity measurements. Leaves for polyamine analysis were collected from all transgenic lines at the same time, because abiotic and biotic factors effect the polyamine metabolism and could influence the results. In Figure III-10 the profile of free polyamine levels determined by the amino acid analyser by post-column derivatisation with ninhydrin is presented. The following retention times in minutes were determined: putrescine-17.2; spermidine: 24.1 and spermine: 35.9. The regression curves for each polyamine were calculated using the peak area values and standard concentrations of polyamines (II.2.9.1).

The polyamine profile in Figure III-10 indicates that two transgenic T_2 lines ODC-apo-7/3-3 and GR1-7/3-4 showed 17-20 % higher level of putrescine compared to wild type plants.

The levels of free polyamines were measured in vegetative tissue from six independent transgenic tobacco lines (ODC-apo-7/3-1→6). To exclude errors due to different extraction efficiencies three repetitions for each sample were analyzed.

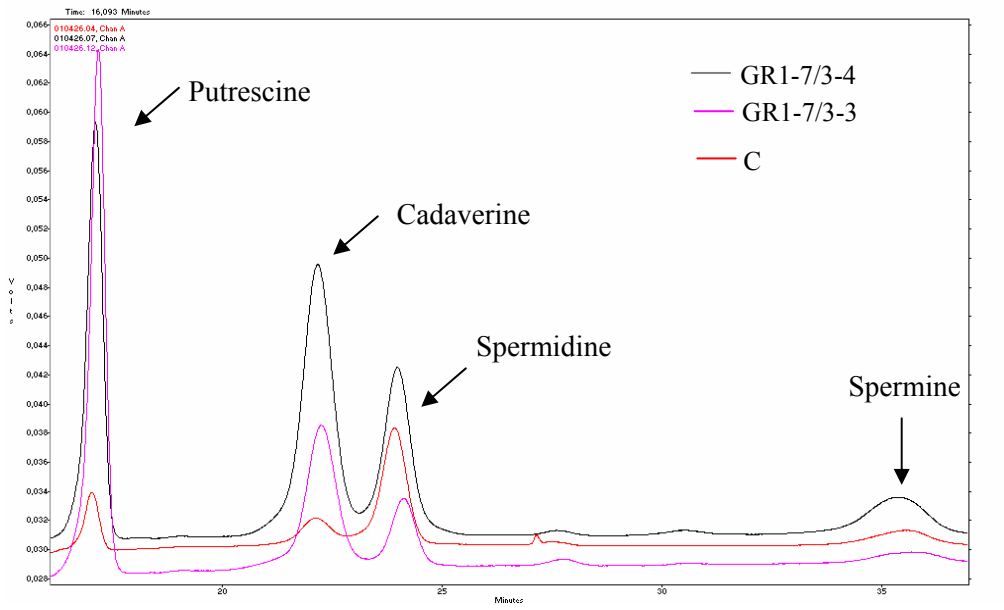

Figure III-10 The polyamine profiles of the two T_2 transgenic lines (ODC-apo-7/3-3 and ODC-apo-7/3-4) compared to wild type tobacco plants.

Free polyamines were extracted by grinding leaf tissue in the presence of 10% TCA (1:3 w/v) (II.2.10). The levels of free polyamines were determined on a Biochrom 20 Amino acid analyser by post-column derivatisation with ninhydrin. Putrescine, spermidine and spermine were eluted after 17.2, 24.1 and 35.9 min retention times, respectively. ODC-apo-7/3-3, ODC-apo-7/3-4: T_2 transgenic lines expressing apoplasmic ODC; C: Wild type SR1 tobacco plants.

There was a significant difference ($P< 0.05$) in the putrescine levels between all transformed lines expressing apoplastic ODC and the wild type SR1 control plants (Figure III-11). There is no difference in the spermidine and spermine levels.

A 5.6-fold increase in putrescine levels was observed in ODC-apo-7/3-3 line (622 nmol/g fresh weight, compared to 110 nmol/g fresh weight in the control ($P<0.05$).

The line ODC-apo-7/3-4 exhibited a 4.5 fold increase (520 nmol/gfresh weight; $P<0.05$), while line ODC-apo-7/3-2 showed a 4-fold (462 nmol/g fresh weight; $P<0.05$) increase in putrescine levels, compared to control. No significant variation ($P> 0.05$) was detected in the levels of spermidine and spermine compared to control plants.

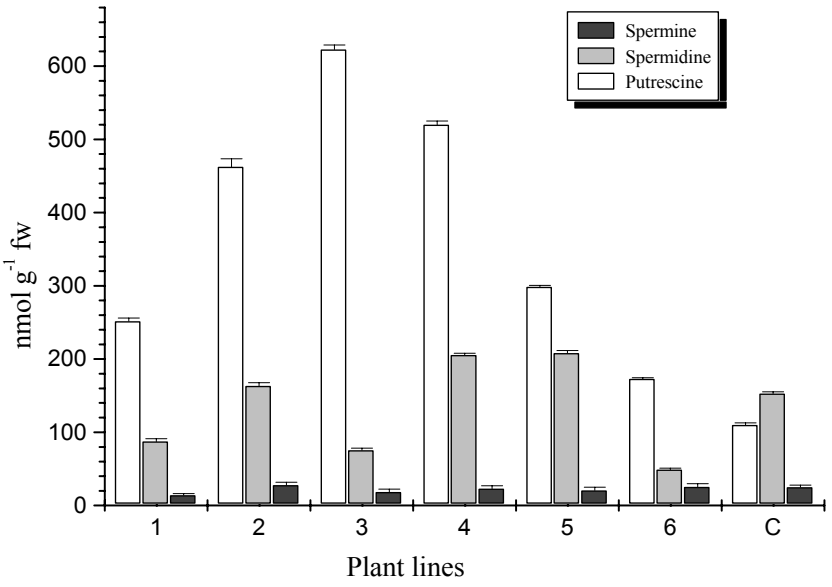

Figure III-11 Analyses of polyamine levels in T_2 generation of transgenic plants expressing human ODC.

Free polyamines were extracted by grinding leaf tissue in the presence of 10% TCA (1:3 w/v) (II.2.10). The levels of free polyamines were determined on a Biochrom 20 Amino acid analyser by post-column derivatisation with ninhydrin. Values are mean ± SE for three replicates for every transgenic plant. Control values were determined by analysing 4 different plants. 1-6: ODC-apo-7/3-1→6 different T_2 transgenic lines. C: wild type tobacco plant SR1.

III.5.2 Polyamine levels in transgenic plants co-expressing apoplasmic ODC and SDE enzymes

To investigate the effect of co-expressed ODC and SDE on the polyamine pool the levels of free polyamines were analyzed. Five transgenic T_1 lines (ODC x SDE/4; 6; 8; 9 and 11, please refer to the Figure III-9) showing the highest expression of both enzymes in immunoblot were examined (Figure III-12). A significant increase in the levels of putrescine and spermidine was measured in all transgenic lines. Putrescine levels ranged from 250-341 nmol per gram fresh weight. These values differed significantly from the non-transgenic control ($P<0.05$), which showed only 70 nmol/g fresh weight. Spermidine levels varied from 199 to 370nmol/g fw, representing an up to 4.5 fold increase ($P<0.05$) compared to the wild type control (82 nmol/g fw). Spermine levels did not show any significant change ($P>0.05$).

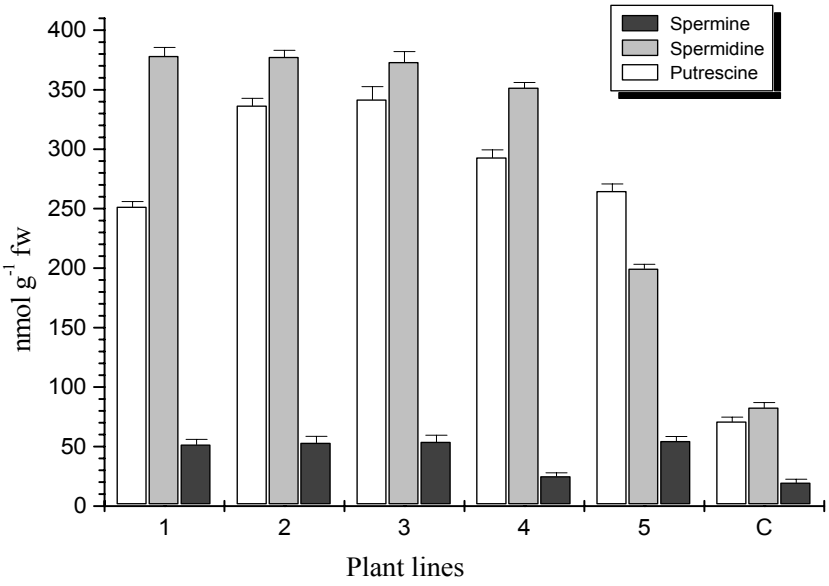

Figure III-12 Analyses of polyamine levels in T_1 generation of transgenic plants co-producing ODC and SDE in the apoplast.

Free polyamines were extracted by grinding leaf tissue in the presence of 10% TCA (1:3 w/v) (II.2.10). The levels of free polyamines were determined on a Biochrom 20 Amino acid analyzer by post-column derivatisation with ninhydrin. Values are mean ± SE for three replicates for every transgenic plant. Control values were determined by analyzing 4 different plants. 1-5: ODC x SDE/4; 6; 8; 9 and 11**,** different transgenic lines. C: wild type tobacco plant SR1.

III.6 Enzymatic activity of ODC in stable transformed plants overexpressing human ODC

To investigate whether the apoplastic human ODC is a functional and active enzyme in leaf extracts from T_2 transgenic plants were assays for ODC activity. The ODC activity was measured in 30-40 days old leaves of ODC-apo-7/3-1, -4, -5, -6, -7, -10 transgenic plants that showed high expression levels of ODC protein in western blot (Figure III-13).

Wild type tobacco plants were assayed for intrinsic plant ODC activity.

All the plants overexpressing ODC showed elevated ODC activity that was 1.6 to 32.8 fold greater than that of wild type plant (Figure III-14).

The highest increase of enzymatic activity, up to 32-fold, was found in line 1 (481 nmol $^{14}CO_2$ released per hour per mg total soluble protein; $P<0.001$) when compared to controls (14 nmol $^{14}CO_2$ / mg total soluble protein /hr). A 19-fold increase in activity was detected in line O6 ($P<0.005$).

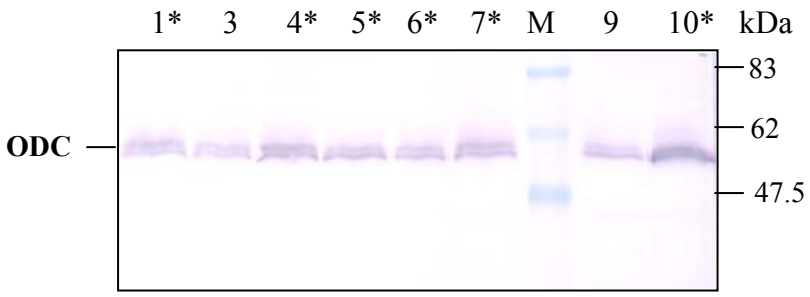

Figure III-13 Immunoblot analysis of 30-40 days old ODC-apo-7/3-O_1-O_{10} transgenic T_2 plants.

Total soluble leaf proteins were extracted by grinding leaf tissue in two volumes extraction buffer (II.2.2.4), separated by SDS-PAGE (II.2.4.2) and blotted onto a nitrocellulose membrane (II.2.4.3). Immunodetection was carried out with anti-c-myc antibody (1:5000), followed by goat anti-mouse antibody conjugated to alkaline phosphatase (1:5000) and NBT/BCIP detection for 1 min at RT. Lines 1-10: ODC-apo-7/3-1→10 individual T_2 transgenic lines. M: prestained protein marker. Lines that were analyzed for the ODC enzymatic activity are indicated by *.

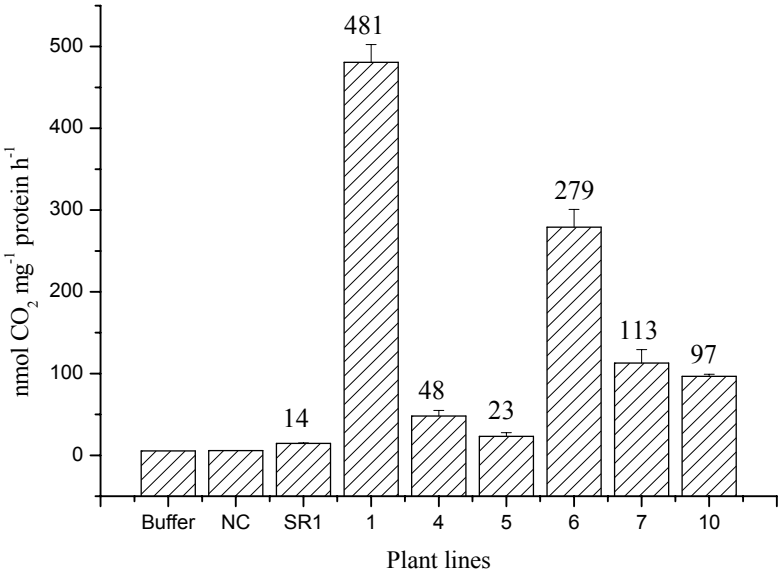

Figure III-14 ODC enzymatic activity analyses of T_2 generation of stable transformed tobacco plant with apoplastic ODC.

Tobacco leaf tissue was extracted in HEPES extraction buffer at ratio 500 mg/ml and the determination of ODC activity was performed as described previously (please refer to II.2.9). The control values are mean ± SE for four replicates from five wild type SR1 plants. The values for transgenic lines are mean ± SE (n=4). The indicated mean value of the ODC activity is expressed in nmol of CO_2/mg total soluble protein /h. Determination of plant total soluble protein was performed using BCA assay. Buffer: HEPES extraction buffer pH 7.0; NC: boiled plant extract used as negative control; SR1: wild type tobacco plant; 1, 4, 5, 6, 7, 10: stable transformed T_2 tobacco lines (ODC-apo-7/3-1; 4; 5; 6; 7; 10) (Figure III.13) expressing human ODC in apoplast.

III.7 Immunization of mice with recombinant ADC, ODC and PAO

Mice were immunised three times with the recombinant proteins ADC, ODC-GST and PAO-GST inclusion bodies at two week intervals (II.2.5). After the third boost, polyclonal antibodies were obtained from mouse blood serum and the titer was determined by direct ELISA (Figure III-15). To avoid cross reaction of antibodies against the GST domain, ELISA tests (II.2.5.1) were performed with ADC protein cleaved from GST moiety with Factor Xa (III.2), or ODC and PAO proteins purified from pET22b vector (III.3). GST was used as a control.

The antibody titer refers to the highest dilution at which antigen-specific binding was detectable above background binding to the GST. Titer of polyclonal mouse antibody specific for ADC and PAO ranged between 1:120,000-150,000, while the anti-ODC antiserum titer ranged between 1:60,000-70,000 indicating that ODC-GST triggered a lower immune response then ADC protein and PAO-GST inclusion bodies.

No cross reactivity of polyclonal antibodies with GST was observed for mice immunized with ADC, indicating the successful cleavage of the protein from GST with factor Xa. A reactivity to GST was observed for mice immunized with ODC-GST and PAO-GST fusion proteins.

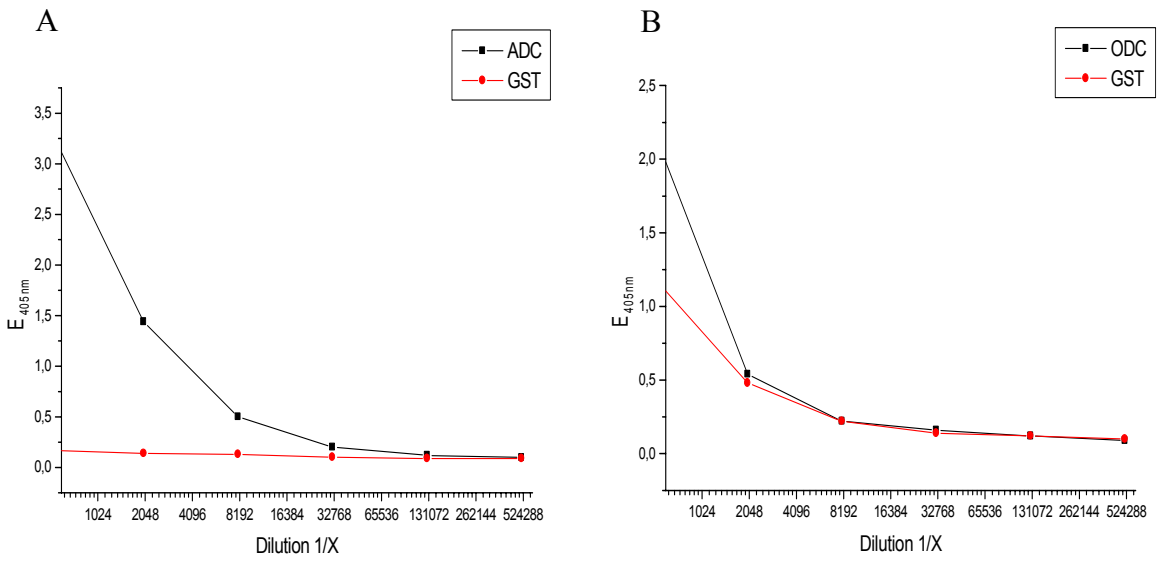

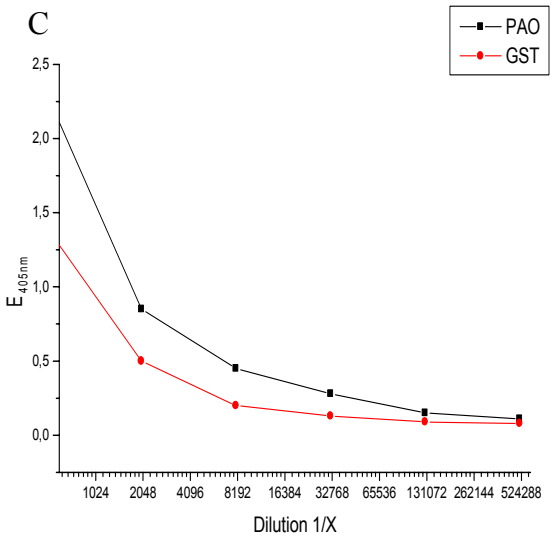

Figure III-15 Determination of polyclonal antibody titers from mouse antiserum by direct ELISA.

The ADC cleaved from GST with Factor Xa (II.2.3), ODC and PAO proteins purified from pET vector (II.2.3.2) (10 µg/ml each) were coated to ELISA plates (II.2.5.1). Serial dilutions of sera were added to the coated plates and incubated for 1.5 hours. Bound antibodies were detected by addition of GAM^{AP} polyclonal antibody (1:5000). ELISA readings were performed at $OD_{405\ nm}$ after 1 h min incubation with pNPP substrate at 37°C. A: Antisera from mice immunized with protein ADC cleaved from GST with Factor Xa. B: Antisera from mice immunized with ODC-GST fusion protein. C.: Antisera from mice immunized with PAO-GST inclusion bodies. Antigens used in ELISA for titer determination are indicated.

III.8 Construction of phage displayed libraries

III.8.1 Isolation of total RNA from mouse spleen cells

Total RNA was isolated from spleen cells of mice immunized with ADC, ODC-GST and PAO-GST inclusion bodies (II.2.6.1). The RNA concentration and the purity of isolated total RNA was determined by spectrophotometry. The yield of total RNA isolated from an individual mouse ranged between 1-1.5 mg, regardless of the antigen used for immunization. The integrity of the RNA was checked on a 1.2% (w/v) agarose gel (Figure III-16).

The 28S and 18S ribosomal RNA were visible as distinct bands whereas the mRNA was present as background smear indicating the quality and integrity of the isolated total RNA.

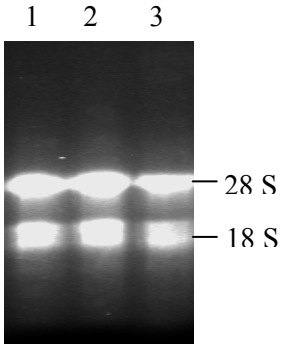

Figure III-16 Analysis of total RNA isolated from mouse spleen cells (II.2.6.1).

Total RNA was isolated from spleen cells of immunized mice (II.2.6.1) and separated on a 1% (w/v) agarose gel containing 2.4 M formaldehyde. The major ribosomal RNA species (28S and 18S rRNA) are indicated. 1: 1 μg total RNA isolated from ADC immunized mice; 2: 1 μg total RNA isolated from ODC-GST immunized mice; 3: 1 μg total RNA isolated from PAO-GST immunized mice

III.8.2 cDNA synthesis and PCR amplification of variable heavy and light chain fragments

Total RNA was used for PCR amplification of variable heavy (V_H) and light (V_L) chain fragments. Five μg RNA was reverse transcribed to synthesise first strand cDNA, using primers (II.1.8/3) binding to the constant regions of mouse heavy and light chains. Mouse IgG1 and IgG2a/b heavy chain variable region and variable fragments from the λ and κ light chain were amplified with primer combinations listed in Materials and Methods (II.1.8).

47 individual PCR reactions were performed to amplify V_H and V_L fragments for each library. From ADC, ODC and PAO cDNA 15 out of 16 primer combinations amplified a product for the heavy chain subclass IgG1. 14 primer combinations out of 16 amplified a product for subclass IgG2a/b. From the ADC cDNA PCR products were amplified from 12 out of 13 primer combinations for the κ light chain (Figure III-17).

The same procedure was applied for cDNA amplification of ODC-GST and PAO-GST immunized mice. All PCR products had the expected size of 400 to 450 bp. No visible band was detected when λ primers were used. Reamplification of λ variable domains failed to amplify a PCR product.

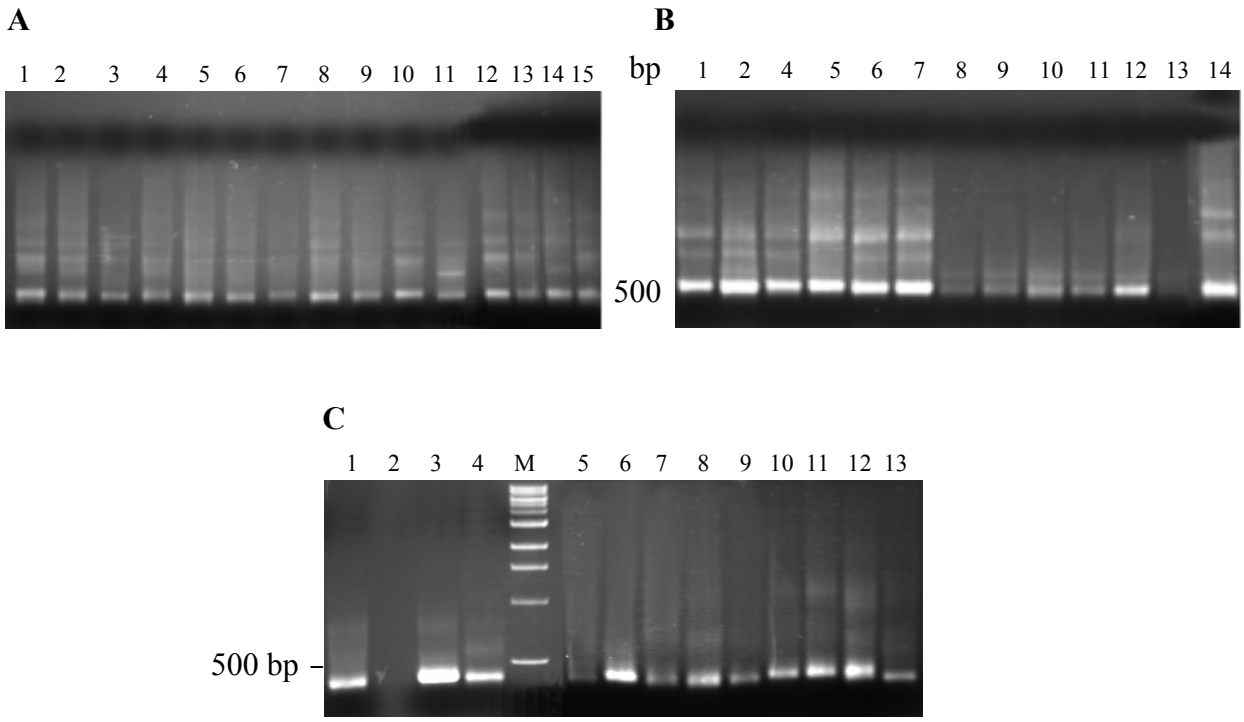

Figure III-17 Amplification of variable heavy and light chain fragments from ADC immunized mice using primers specific for murine: IgG1 (A); Ig2a/2b (B); κ (C).

Nucleic acids were separated on a 1.2% (w/v) agarose gel**.** M=1 kb DNA ladder. Lines 1-15 (A); 1-14 (B) and 1-13 (C) indicate the different MPDV forward primers used for the amplification of the IgG1, IgG2a/2b and κ, respectively (II.1.8).

Table III-1 summarizes the results of amplified variable light and heavy chain fragments from mice immunized with ADC, ODC-GST and PAO-GST antigens.

Table III-1 Summary of amplified variable heavy and light chain fragments from cDNAs of ADC, ODC-GST and PAO-GST immunized mice. Amplification was performed using primers specific for IgG1, Ig2a/2b, kappa (κ) and lambda (λ). '++': strong band; '+' band present; '(+)' faint band'; '-': no band visible. 1-16; 1-13 and 14-15 represent the different MPDV forward primers used for the amplification of the IgG1 (IgG2a/2b), κ and λ respectively (II.1.8).

IgG1	1	2	3	4	5	6	7	8	9	10	11	12	13	14	15	16
ADC	++	+	-	+	+	+	+	+	++	+	+	+	+	+	+	+
ODC	++	++	-	++	++	++	++	++	++	+	++	++	++	++	++	+
PAO	+	(+)	-	+	++	++	+	+	++	(+)	++	+	+	+	++	+

IgG2a/b	1	2	3	4	5	6	7	8	9	10	11	12	13	14	15	16
ADC	++	++	-	++	++	++	++	(+)	(+)	+	(+)	++	-	++	+	(+)
ODC	++	++	-	++	++	++	++	(+)	+	++	++	++	++	++	-	++
PAO	++	+	-	++	++	++	+	+	+	++	+	++	++	++	-	++

	κ													λ	
	1	**2**	**3**	**4**	**5**	**6**	**7**	**8**	**9**	**10**	**11**	**12**	**13**	**14**	**15**
ADC	++	-	++	++	(+)	++	+	++	+	+	++	++	+	-	-
ODC	++	++	++	++	++	++	++	++	++	++	++	++	++	-	-
PAO	+	+	+	+	+	+	+	+	+	(+)	+	++	(+)	-	-

III.8.3 Construction of phagemid-scFv libraries

The strategy shown in Figure III-8 was used to establish the scFv libraries expressing recombinant antibodies against ADC, ODC and PAO (II.2.6.3).

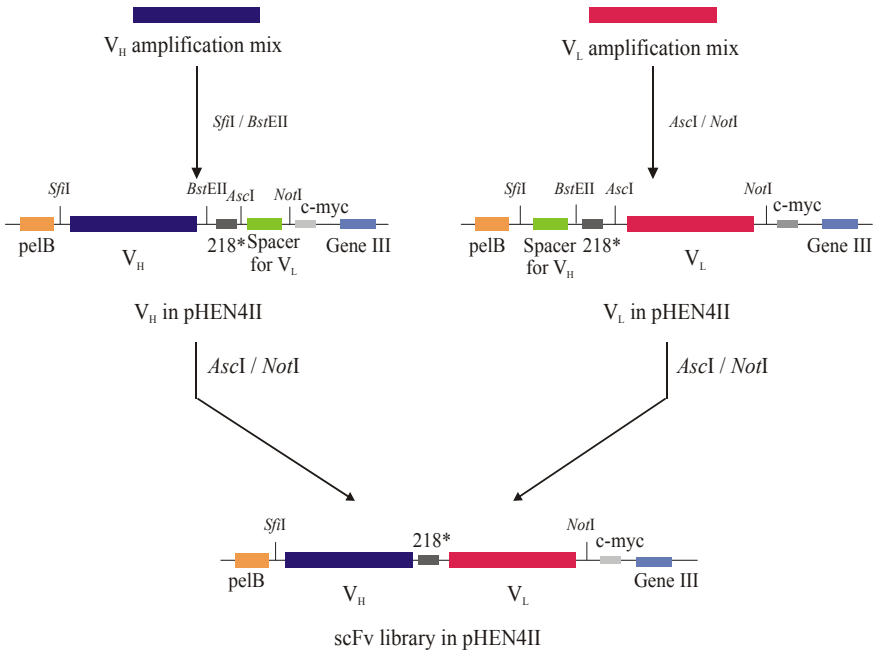

Figure III-18 Schematic presentation of cloning procedure followed for construction of murine scFv libraries.

The V_H and V_L amplification mixes were digested with *Sfi*I/*Bst*EII or *Asc*I/ *Not*I, respectively and ligated into the linearized pHEN4II vector. Then the V_L was excised with *Asc*I/*Not*I and subcloned into the pHEN4II vector containing the corresponding V_H fragment. *pel*B: *pel*B leader peptide; c-myc: myc epitope for the scFv detection; 218*: 218 linker.

Gel purified V_L fragments were digested with *Sfi*I/*BstE*II and *Asc*I/*Not*I, respectively, and ligated into pHEN4II vector resulting in construction of variable heavy and light chain libraries. The construction of scFv libraries were performed by recovering of V_L fragments from the V_L libraries and cloning them into the linearized pHEN4II vector containing the corresponding V_H fragment.

For determination of cloning efficiency 19 individual colonies were randomly selected from each scFv library and amplified by PCR using pHEN specific primers (II.1.8/2). The amplified PCR products had the expected size of 900-950 bp (Figure III-19).

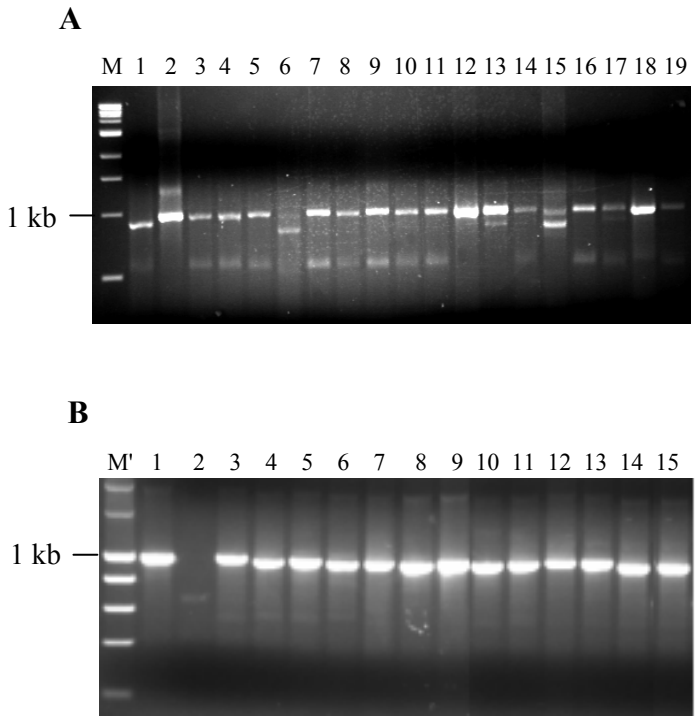

Figure III-19 Analysis of PCR product of randomly selected colonies from murine scFv libraries with specificity for ADC (A) and ODC (B).

1-19: PCR amplification of scFv-fragment of 19 or 15 independent colonies separated on a 1.2% (w/v) agarose gel. M: 1 kb ladder. M': 100 bp ladder.

Three final scFv libraries designated HA_1LA_2; HO_1LO_2; HP_1LP_2, were generated for ADC, ODC and PAO, respectively. Table III-2 summarizes results obtained from all Fv and scFv libraries created. The percentage of positive clones in these final libraries carrying a full size scFv fragment were 86.6% for ADC, 87.5% for ODC and 100% for PAO. The library size was $3.2x10^7$, $2.6x10^6$ and $1.4x10^6$ for ADC, ODC and PAO, respectively. Biopanning was performed with libraries HA_1LA_2; HO_1LO_2 only, since purification of soluble PAO was unsuccessful (III.2).

Table III-2 Summary of constructed murine phage displayed libraries. Library designation and their antigen specificity are indicated. The library size and cloning efficiency are indicated for V_H, V_L and scFv libraries generated for each of the three antigens.

Designation		**Antigen**	**Fv-Library size** (Cloning efficiency %)		**scFv-Library size** (Cloning efficiency %)
H	**L**		**H**	**L**	
A_1	A_2	ADC	$5.0x10^5$ (75)	$9.0x10^6$ (94)	$3.2x10^7$ (86.6)
O_1	O_2	ODC	$5.0x10^5$ (100)	$1.2x10^6$ (87)	$2.6x10^6$ (87.5)
P_1	P_2	PAO	$1.2x10^7$ (94)	$1.0x10^6$ (100)	$1.4x10^6$ (100)

To verify diversity of scFv HA_1LA_2 and HO_1LO_2 libraries before panning procedures PCR-amplified scFv fragments were subjected to *Bst*NI digestion (II.2.6.4). The RFLP analyses indicated that ~70% and ~80% of the clones tested from the HA_1LA_2 and HO_1LO_2 libraries respectively, had different RFLP pattern (Figure III-20).

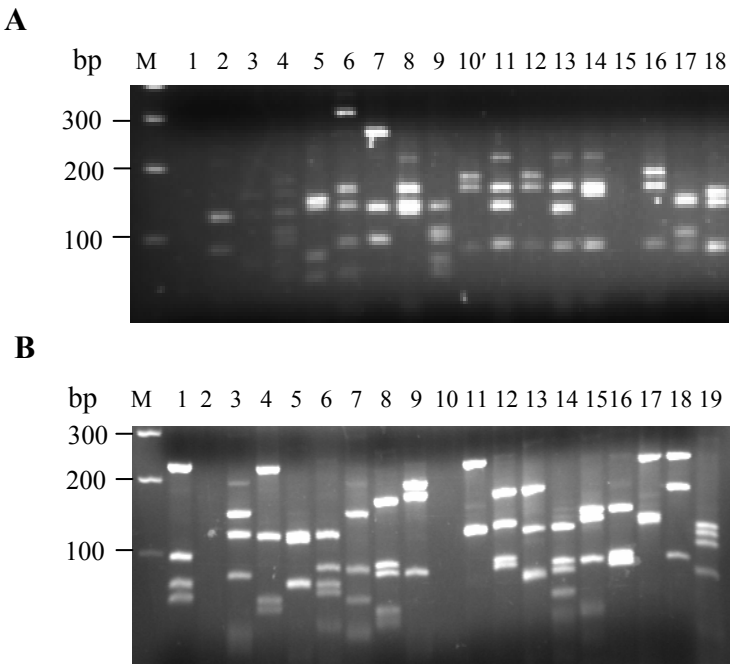

Figure III-20 Analysis of murine scFv fragments after *Bst*NI digestion.

Samples were analyzed on a 2.3% (w/v) agarose gel. A.: *Bst*NI fingerprinting of 18 randomly selected colonies from HA1LA2 scFv library. B.: *Bst*NI fingerprinting of 19 randomly selected colonies from HO_1LO_2 scFv library. M: 100 bp ladder. 10: empty line.

III.9 Selection and characterisation of specific scFvs

III.9.1 Solid phase panning of libraries HA_1LA_2 and HO_1LO_2 against recombinant fusion proteins ADC and ODC-GST

The phage libraries HA_1LA_2 and HO_1LO_2 were subjected to 3 rounds of panning against 25 µg/ml ADC and ODC-GST antigens immobilized on the surface of the immuno tubes (II.2.7). For each round of panning, 10^{12} recombinant phages were preabsorbed with GST (10 µg/ml) protein to exclude GST specific phages in the subsequent panning rounds. After each round the integrity of full size scFv-fragments was verified by PCR amplification using vector-specific primers followed by *Bst*NI fingerprinting to visualize diversity of the library (data not shown). As shown in Table III-3 there was a 152 and 382-fold enrichment of specific phages after the third round of panning of ADC and ODC phage displayed libraries, respectively.

Between the first and the second round of panning of HA_1LA_2 library an increase of insert free-phages from 4.5×10^4 (100% with insert) to 5.4×10^5 (70% with insert) was observed. However, the third round of panning led to an enrichment of the eluted phage to a library size of 4.7×10^6 (95% with insert).

Table III-3 Enrichment of ADC-GST and ODC-GST binding phage through panning. Fold enrichment was calculated by dividing the ratio of recovered number of phage to the input number of phage for each round by the same ratio from the preceding round. Total enrichment is obtained by dividing the ratio of recovered number of phage to input number of phage of round 3 by the same ratio from round 1. Enrichment of round 1 is considered as one.

scFv library	Panning Antigen	Panning rounds	Input phage	Recovered phage	Recovered to input ratio	Fold-enrichment
HA_1LA_2	ADC-GST	1	2×10^{12}	4.5×10^4	2.3×10^{-8}	1
		2	2.4×10^{12}	5.4×10^5	2.2×10^{-7}	9.7
		3	1.9×10^{12}	6.7×10^6	3.5×10^{-6}	15.9
HO_1LO_2	ODC-GST	1	3.1×10^{12}	5.3×10^4	1.7×10^{-8}	1
		2	2.6×10^{12}	6.2×10^5	2.4×10^{-7}	14
		3	1.3×10^{12}	8.4×10^6	6.5×10^{-6}	27

For the HO_1LO_2 library there was a significant increase in phage titer after each round of panning. The presence of insert-free phage during panning rounds was not observed for this library. The *Bst*NI fingerprinting performed with 20 randomly selected colonies from the HO_1LO_2 library after the third round of panning indicated four unique fragment profiles suggesting the enrichment of at least four distinct antibody clones. This observation was confirmed by DNA sequencing (III.9.3).

III.9.2 Screening and characterisation of scFv-fragments against ODC-GST fusion protein

After the third panning round of HO_1LO_2 phage display library 120 colonies were randomly selected and grown in microtiter plates. Expression of soluble scFv-fragments was induced by 1 mM IPTG. The specificity of scFv-fragments was tested in direct ELISA experiments against bacterially expressed ODC-GST. More than 60% of analyzed clones (Figure III-21) showed a specific binding to the ODC-GST antigen. To verify the presence of full size scFv-fragments, the DNA inserts of 30 clones that showed a high reactivity to ODC-GST were PCR-amplified followed by *Bst*NI fingerprinting. All clones analyzed showed an insert of about 1 kb and *Bst*NI digestion indicated the presence of four different band patterns (data not shown).

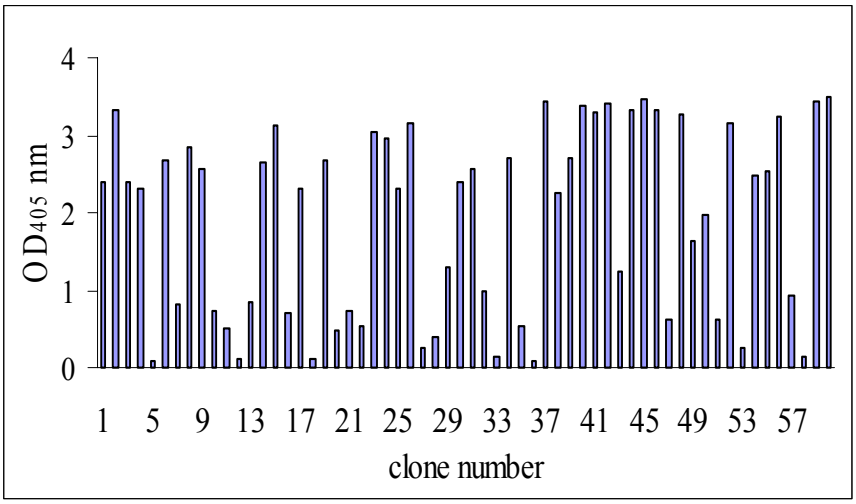

Figure III-21 Screening of selected clones from the library HO_1LO_2 in soluble ELISA.

Binding activity of 60 randomly selected soluble murine scFv binding to ODC-GST protein after the third round of panning was revealed by direct ELISA (II.2.8.1). 10µg/ml of ODC-GST was coated on microtiter plates. Bacterial supernatant was added in 2% (w/v) MPBS to a final volume of 100µl. Bound scFvs were detected by addition of 1:5000 diluted 9E10 monoclonal antibody, and goat-anti mouse polyclonal antibodies conjugated to alkaline phosphatase as secondary antibody (1:5000). ELISA readings ($OD_{405\ nm}$) were performed after 10 min incubation with pNPP substrate at 37°C

15 clones with the highest absorbance and with different RFLP patterns were subjected to medium scale periplasmic expression to overcome the differences based on expression in microtiter plates. Their reactivity to the ODC protein purified from pET vector, to ODC-GST fusion protein, and GST was evaluated in direct ELISA. All scFv-fragments reacted specifically to ODC and/or ODC-GST (Figure III-22). No cross reactivity to GST was observed. Clone number 3 and clone number 14 (Figure III-22) reacted only specifically to the ODC-GST fusion protein and could recognize a conformational epitope, which is not present in the denaturated form of ODC.

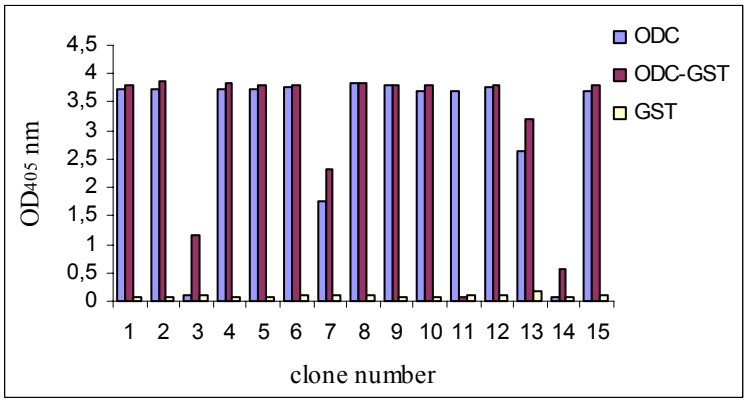

Figure III-22 Reactivity of selected murine scFv-fragments with ODC, ODC-GST and GST in direct ELISA.

10µg/ml of ODC-GST, ODC purified via IMAC under denaturated conditions and GST were coated on microtiter plates (II.2.8.1). Periplasmic supernatant (II.2.3.3) was added in 2% (w/v) MPBS to a final volume of 100 µl. Bound scFvs were detected by addition of 1:5000 diluted 9E10 monoclonal antibody, and GAM^{AP} polyclonal antibody (1:5000). ELISA readings ($OD_{405\ nm}$) were performed after 10 min incubation with pNPP substrate at 37°C.

To avoid false positives, and to insure that the engineered scFvs were specific for epitopes in ODC and not against GST or the linker present in the fusion protein, the reactivity of the 15 selected clones was analysed against ODC-GST, SME-GST and GST fusion proteins. None of the fifteen clones showed a reaction with GST and SME-GST, indicating that these clones bind specifically to ODC (data not shown).

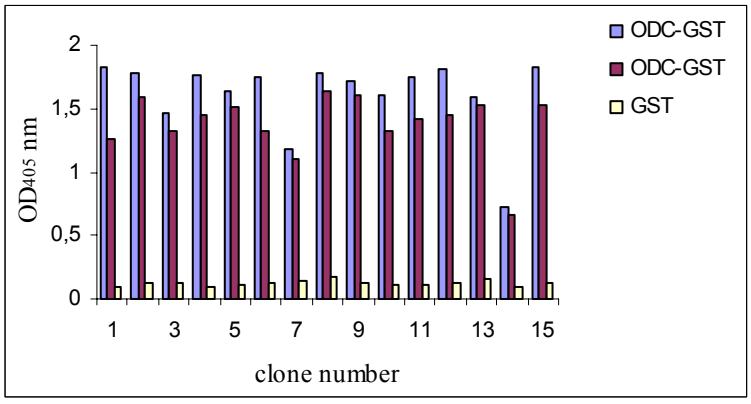

Figure III-23 Reactivity of selected murine scFv fragments to ODC-GST and GST in capture ELISA.

Chicken IgY's specific to ODC-GST fusion protein were coated o/n in dilutions 1:1000 (blue) and 1:5000 (red, yellow) (II.2.8.2). The ELISA plate was blocked for 2 h at RT, and then incubated with 10 µg/ml of ODC-GST and GST. Supernatant from the periplasmic expression of 15 selected scFvs (II.2.8.1) was added followed by addition of 1:5000 diluted 9E10 monoclonal antibody and GAM^{AP} polyclonal antibody (1:5000). ELISA readings ($OD_{405\ nm}$) were performed after 10 min incubation with pNPP substrate at 37°C

The capture ELISA (II.2.8.2) performed with the same 15 selected scFv fragments (Figure III-23) showed that the selected murine scFvs show a high specificity and reactivity for ODC-GST and a low reactivity to GST.

The clone Nr. 3 showed a relatively high signal in the indirect ELISA (Figure III-23) compared to the direct ELISA readings (Figure III-22), confirming that this scFv-fragment could recognize a conformational epitope in ODC.

III.9.3 Sequence analysis of scFv fragments specific to ODC clones

The fifteen scFv fragments selected from the library were sequenced. The 15 scFv fragments belonged to four different sequence groups. The most abundant sequence was represented by clone scFvODC1 (8/15) followed by scFvODC3 (3/15), scFvODC15 (3/15) and scFvODC7 (1/15).

One representative clone of each group named scFvODC1, scFvODC3, scFvODC7 and scFvODC15 was further analyzed. All scFv-fragments had open reading frames encoding proteins of about 28 kDa. The sequence alignment of the four scFv-fragments with the consensus sequence of Kabat database indicated that variable heavy and light chain fragments belong to murine IgG. Amino acid comparison of the selected scFv showed differences in the framework and CDR regions of both heavy and light chain fragments. The deduced amino acid alignment of four scFv is presented in Figure III-24.

Except for four amino acid differences (Ile^{54}→ Val^{54}; Ser^{58} → Asn^{58}; Gly^{69} → Asp^{69} and Met^{84} → Ile^{84}) the scFvODC7 and scFvODC15 have the same heavy chain, but two different light chains. In addition, scFv3 and scFv7 share the same light chain sequence (expect for two amino acid change: Try^{244} → Leu^{244}, Gly^{248} → Ala^{248},) with two different variable heavy chains. Table III-5 summarizes the sequencing results of the four selected scFvODCs.

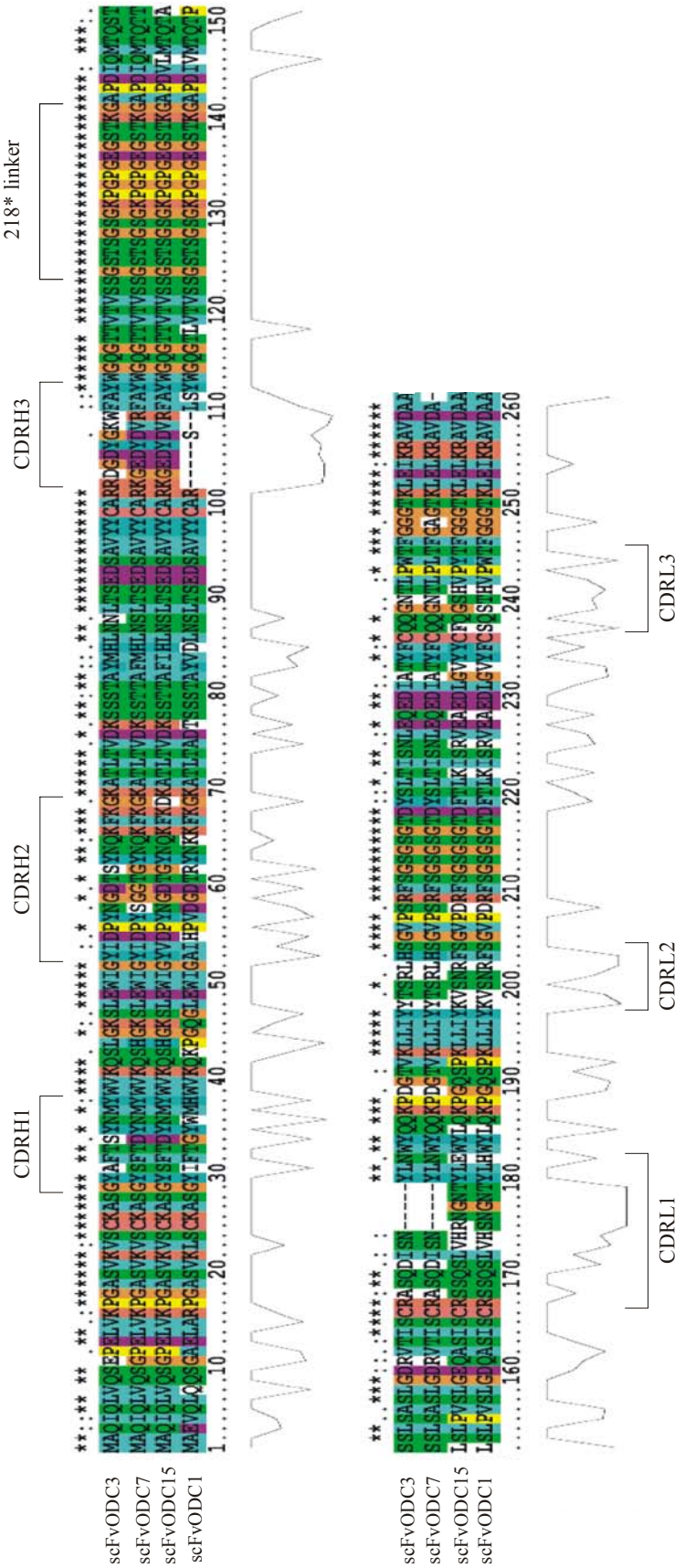

Figure III-24 Alignment of the deduced amino acid sequences of selected murine scFv-fragments with specificity for ODC: scFvODC1, scFvODC3, scFvODC7 and scFvODC15.

Framework regions and complementary determining regions (CDRs) were determined according to Kabat and Wu, (1991). '*': the same amino acid; '-': no amino acid at this position; ':' or '.' different amino acid. The complementary determining regions and the 218* linker have been indicated.

Table III-4 Summary of sequence analysis of murine derived scFvs with specificity for ODC. Deduced molecular weight is indicated.

Designation of scFv	Nucleotide length (bp)	Deduced MW (Da)	CDRH3 sequence
scFvODC1	759	26921	- - - - - S - - LSY
scFvODC3	765	27666	RDGDYGKWFAY
scFvODC7	765	27457	KGEDYDVRFAY
scFvODC15	777	28199	KGEDYDVRFAY

Sequence alignment with the nearest germline V-gene segments listed in the IMGT database indicated that the heavy and light chain variable domains of selected scFvODCs were members of the family I of murine VH and family I and 10 of the κ light chain respectively. Several differences were observed from the nearest germline V-gene segments both in the nucleotide and amino acid level as indicated in Table III-5.

Table III-5 V-gene family, germline deviation and extent of somatic hypermutation of four scFvs specific for ODC. Numbers in brackets indicate the nucleotide and amino acid differences observed in the primer region of scFv-fragments. The alignment of the four selected scFvODCs to their closest germline gene sequences was performed using the IMGT database (http://imgt.cnusc.fr:8104/).

scFvs	Mouse IgG Family		Closest germline gene sequences		Differences from germline			
					Nucleotides		Amino acid	
	H	L	H	L	H	L	H	L
scFvODC1	IGHV1	IGKV1	X02459	D00080	$49^{(4)}$	$5^{(2)}$	$22^{(2)}$	$2^{(2)}$
scFvODC3	IGHV1	IGKV10	AF304556	M15520	$13^{(5)}$	$4^{(2)}$	$10^{(4)}$	$2^{(1)}$
scFvODC7	IGHV1	IGKV10	AF304556	M15520	$7^{(4)}$	$3^{(2)}$	$6^{(3)}$	$2^{(0)}$
scFvODC15	IGHV1	IGKV1	AF304556	D00081	$11^{(4)}$	$8^{(1)}$	$9^{(3)}$	$3^{(1)}$

III.9.4 Screening and characterisation of scFv-fragments against ADC-GST fusion protein

After the third round of panning the HA_1LA_2 phage display library against purified ADC protein, 120 colonies were randomly selected and grown in microtiter plates. Expression of soluble scFv fragments was induced by IPTG. The specificity of scFv-fragments was

tested in ELISA experiments against ADC-GST. 40% of the analysed clones showed a specific binding to the antigen (data not shown). To examine the presence of full size scFv-fragments inserts from 15 clones that showed a high reactivity to ODC-GST in soluble ELISA were PCR-amplified followed by *Bst*NI fingerprinting. All clones analysed had an insert of about 1 kb and *Bst*NI digestion showed the presence of two RFLP patterns. 14 clones were subjected to periplasmic expression. Their reactivity to the ADC-GST fusion protein and to GST was reevaluated by direct ELISA (Figure III-25). The results indicated that all selected scFv-fragments reacted specifically to ADC and there was no cross reactivity to GST.

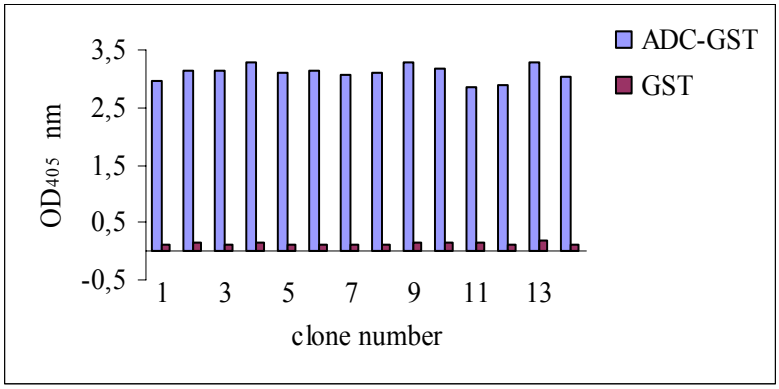

Figure III-25 Reactivity of selected murine scFv-fragments to ADC-GST and GST in direct ELISA.

10µg/ml of ADC-GST, and GST were coated on microtiter plates (II.2.8.1). Periplasmic supernatant (II.2.3.3) was added in 2% (w/v) MPBS to a final volume of 100 µl. Bound scFvs were detected by addition of 1:5000 diluted 9E10 monoclonal antibody, and GAM^{AP} polyclonal antibody (1:5000). ELISA readings ($OD_{405\ nm}$) were performed after 30 min incubation with pNPP substrate at 37°C.

The capture ELISA (II.2.8.2) was performed with the periplasmic preparation of the same 14 scFv fragments. Capture antibodies used for ELISA were IgY's from chickens immunized with ADC-GST protein cleaved off from GST with Factor Xa. Results presented in Figure III-26 indicated that there was a high specificity and reactivity of the scFv to the ADC-GST and the reactivity to the GST are significantly lower, but higher when compared to the reactivity of the ODC specific clones (refer to Figure III.23).

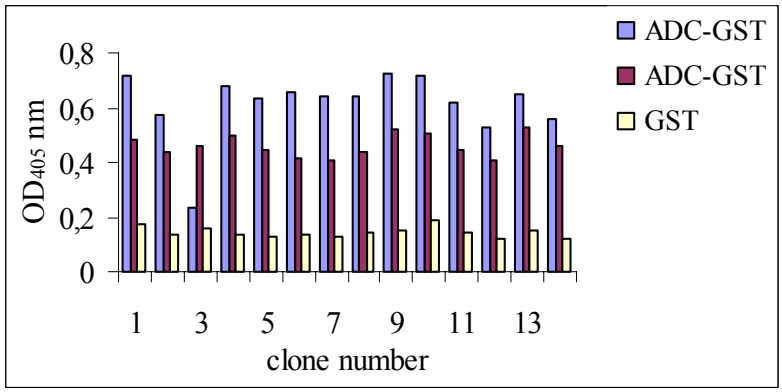

Figure III-26 Reactivity of selected murine scFv fragments to ADC-GST and GST in capture ELISA.

Chicken IgY's specific to ADC protein were coated o/n in dilutions: 1:1000 (blue) and 1:5000 (red, yellow) (II.2.8.2). The ELISA plate was blocked for 2 h at RT, and then incubated with 10 µg/ml of ADC-GST and GST. Supernatant from the periplasmic expression of 14 selected scFvs (II.2.8.1) was added followed by addition of 1:5000 diluted 9E10 monoclonal antibody and GAM^{AP} polyclonal antibody (1:5000). ELISA readings ($OD_{405\ nm}$) were performed after 10 min incubation with pNPP substrate at 37°C

III.9.5 Sequence analysis of selected scFv-ADC clones

The scFv inserts of 14 clones that showed the highest reactivity to the antigen in direct and capture ELISA were sequenced. All scFv-fragments had open reading frames comprising two different sequences (confirmation of RFLP pattern). The most abundant scFv fragment was present in thirteen of the 14 clones sequenced. Two clones showing a different sequence, named scFvADC3 and scFvADC7 were analysed further. Amino acid alignment (Figure III-27) showed that the selected scFvs share 55.9% identity and 65% similarity. Analysis of the amino acid sequence revealed significant differences in the framework and CDR regions of both, heavy and light chain fragments. Sequence alignment with the Kabat database showed that V_H of the scFvADC3 and 7 belonged to the murine V1 and V5 family. The V_L is member of V4 and V9 of murine κ light chain respectively. Table III-7 present a short summary of sequence analyses of scFvADC3 and scFvADC7. The comparison with the closest germline V-gene segments indicated large differences both in nucleotide and amino acid levels (Table III-7).

Table III-6 Summary of sequence analysis of murine derived scFvs with specificity for ADC. The deduced molecular weight is indicated. Matching amino acid is indicated in red.

Designation of scFv	Nucleotide length (bp)	Deduced MW (Da)	CDRH3 sequence
scFvADC3	759	27160	R - - DYYYAMDY
scFvADC7	762	27039	KGENYGNYFYV

Table III-7 V-gene family, germline deviation and extent of somatic hypermutation of two scFvs specific for ADC. Numbers in brackets indicate the nucleotide and amino acid differences observed in the primer region of scFv-fragments. The alignment of the four selected scFvADCs to their closest germline gene sequences was performed using the IMGT database (http://imgt.cnusc.fr:8104/).

scFvs	Mouse IgG Family		Closest germline gene sequences		Differences from germline			
					Nucleotides		Amino acid	
	H	L	H	L	H	L	H	L
scFvADC3	IGHV5	IGKV9	AF120474	V00804	>40(2)	6(4)	37(2)	1(1)
scFvADC7	IGHV1	IGKV4	AF304556	AJ231224	14(4)	5(3)	9(3)	2(1)

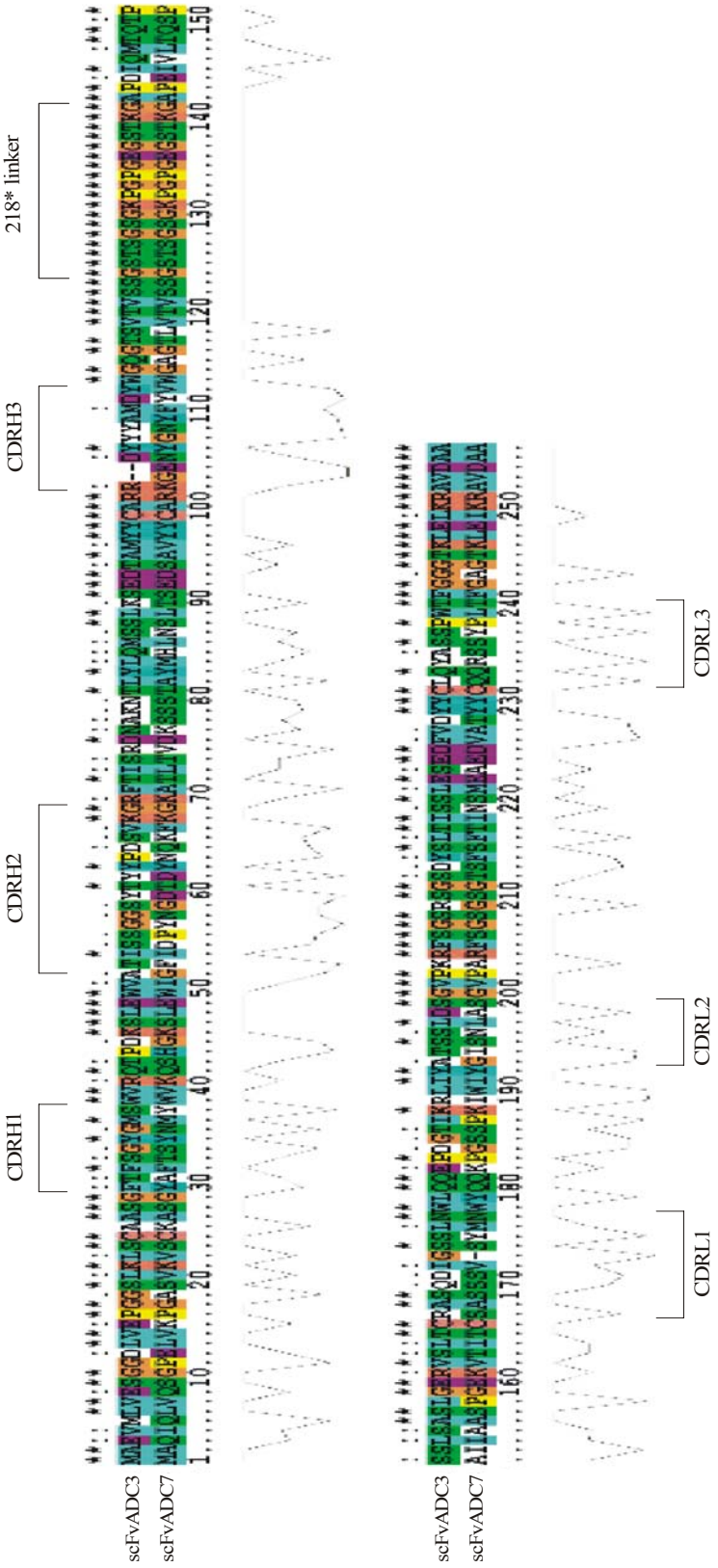

Figure III-27 Alignment of the deduced amino acid sequences of two selected murine scFv-fragments with specificity for ADC: scFvADC3 and scFvADC7.

Framework regions and complementary determining regions (CDRs) were determined according to Kabat and Wu, (1991). '*': the same amino acid as above; '-': no amino acid at this position; ':' or '.' different amino acid. The complementary determining regions and the 218* linker have been indicated.

III.10 Characterization of biological and physical features of the ODC-specific scFv antibodies

III.10.1 Cloning and expression of scFvODC1, scFvODC3, scFvODC7 and scFvODC15 in *E. coli*

Up scaled expression of scFvODC1, scFvODC3, scFvODC7 and scFvODC15 was performed using pSyn vector (III.10.1). Protein expression into the periplasmic space was achived by 1 mM IPTG at 30°C (II.2.8). scFvODC1 and scFvODC3 were subcloned downstream of the pelB leader peptide of pSyn vector using *Nco*I and *Not*I restriction sites. Because of an internal *Nco*I site at base pair position 125 of the V_H chains of the scFvODC7 and scFVODC15 *Sfi*I and *Not*I restriction enzymes were used for subcloning. Correct insertion was confirmed by sequencing (data not shown). Soluble expression of recombinant proteins was performed using *E. coli* strain HB2151.

The His6 tagged scFvs were purified by IMAC from the culture medium (III.10.1). SDS-PAGE analysis of the affinity purified scFvs' revealed the presence of a single band of approximately 30 kDa for all four scFvs (Figure III-28).

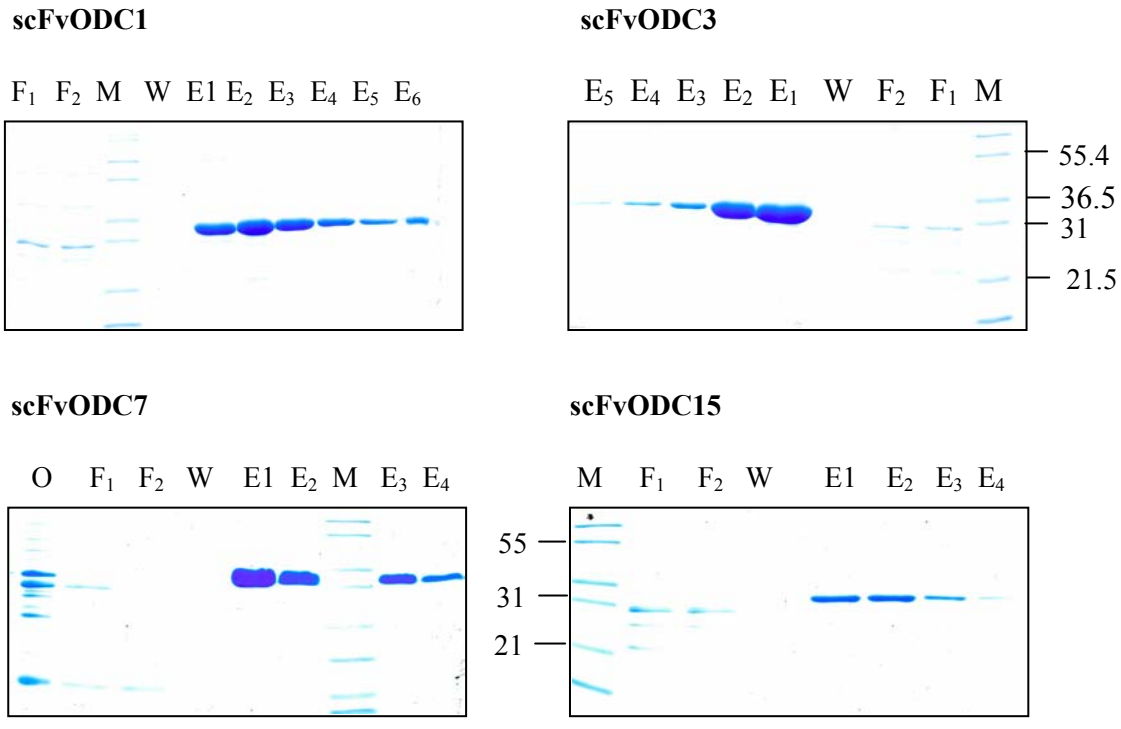

Figure III-28 SDS-PAGE analysis of affinity purified scFvODC1, scFvOSC3, scFvODC7 and scFvODC15.

Selected scFvODCs (1, 3, 7 and 15) were subcloned into the pSyn vector and expressed in the *E. coli* strain HB2151 upon induction with IPTG. The periplasmic expressed scFvs were purified by IMAC (II.2.8.1). Proteins were separated on 12% (w/v) SDS-PAGE and stained with Coomassie brilliant blue (II.2.4.2). O: 10 µl of osmotic fraction; F_1: 10 µl of the first flow through; F_2: 10 µl of the second flow through; W: 10 µl of washing fraction; E_1, E_2, E_3, E_4, E_5: 5 µl of five elution fractions; M Mark12 protein marker.

Pilot experiment showed that washing steps with 30 mM imidazol led to losses of recombinant protein (data not shown). This was avoided by increasing the matrix volume and decreasing the imidazol concentration to 10 mM in the wash buffer (data not shown). After purification the purified scFv were dialysed overnight in 1xPBS buffer pH 7.4 and the final concentration determined by either Bradford or BCA assay using BSA as a standard. The yield of purified scFvs ranged between 1.5-2.7 mg/L culture volume. Slight deviations were observed depending on the batch of preparation. All clones expressed a functional scFv as shown by their ability to bind specifically to ODC-GST in ELISA (III.10.3).

III.10.2 Stability of affinity purified scFvODCs

To generate more information about the stability of affinity purified scFvODC1, 3 and scFvODC7 and to ascertain whether scFvs were present as monomeric or dimeric forms, gel filtration analysis was performed (II.2.8.6). Proteins with known molecular weight were run as standards. A calibration curve was prepared by plotting the logarithms of the known molecular weights of protein standards versus their respective V_e/V_o values (V_e is the elution volume and V_o is the void volume). Molecular weight determination of scFvs was made by comparing the ratio V_e/V_o of the scFvs to the V_e/V_o of the protein standards of known molecular weight. Elution was monitored by UV absorption at 280 nm.

Figure III-29 shows results from gel filtration analysis of the scFvODC1, 3 and 7. Analyses of the scFvODC1 after 3-6 months storage at 4°C revealed that more than 80% of the scFvODC1 eluted as a 16 kDa degradation product. Degradation of scFvODC1 was confirmed by SDS-PAGE (data not shown). However, the degraded scFvODC1 retained 50% binding activity compared to the fresh purified scFvODC1 (data not shown). The scFvODC1 stored at -20°C for about 3-months was stable and eluted as a monomeric scFv form.

The elution profile from the scFvODC3 and scFvODC7 showed two peaks (Figure III-29) with a retention volume of 14.54 ml and 16.2 ml; the second peak corresponded to a molecular weight of 27-28 kDa, as determined from the standards, representing a monomeric scFv. The first peak (retention volume 14.54 ml) corresponded with 66 kDa to dimeric forms of scFvODC3 and 7. About 35% of scFvODC3 and 20% of the scFvsODC7 were present as dimers. The immunoblot analysis confirmed the monomeric and dimeric forms of scFvODC3 and 7 by showing the presence of 28 and 66 kDa protein bands (data not shown). The scFvODC7 used for this analysis was stored at -20°C for about 1 month. The scFvODC3 was analyzed directly after a fresh purification indicating that the dimer formation is a scFv property.

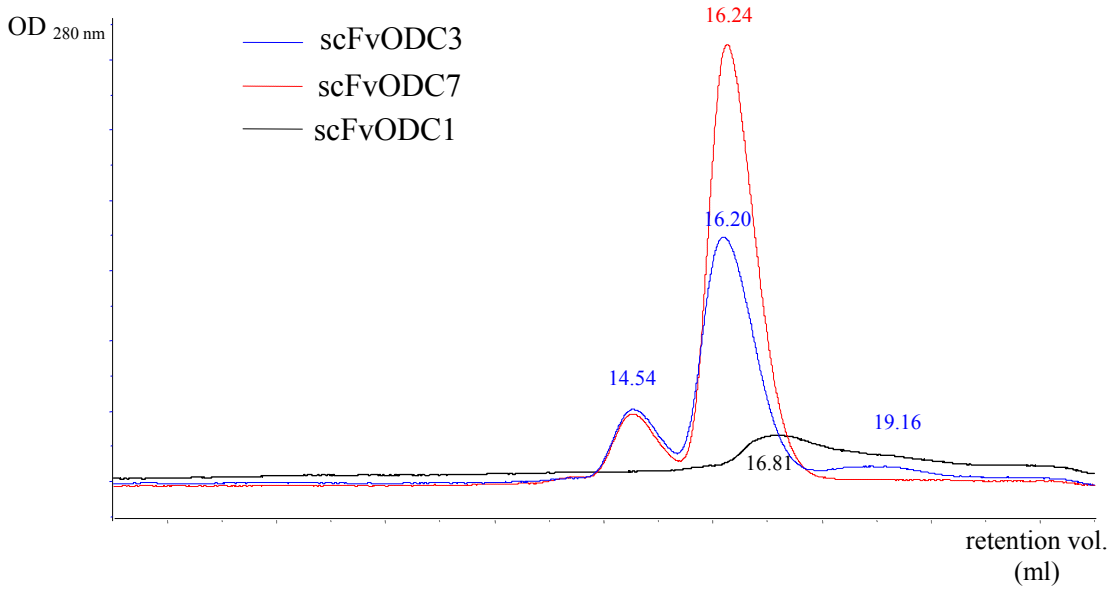

Figure III-29 Gel filtration chromatography of affinity purified ODC-specific scFvs.

scFv were purified via IMAC (II.2.3.3) and analyzed after dialyses by gel filtration on a Sephadex 200 column (II.2.8.6). Affinity purified scFvs were loaded and run at 1 ml/min after calibration with the MW standards (II.2.8.6). The scFvODC1 stored at 4°C eluted as a 16 kDa degradation product. The mobility of the scFv3 and 7 were consistent with a molecular mass of 27-28 kDa. Dimers of both scFvs were present (retention volume 14.54 ml).

III.10.3 Reactivity of ODC-specific scFvs with ODC-GST and GST

Direct ELISA was performed to examine the reactivity of the purified scFvODC1, 3, 7, and 15 to the ODC-GST and GST antigens. Several dilutions of purified scFvODCs were incubated on high binding ELISA plates coated with ODC-GST and GST (5µg/ml). The slope determined by linear regretion was taken as reactivity (Figure III-30).

The slope of the curves in the Figure III-30/B, D is a direct indication of reactivity of these scFv to their antigens. The results indicate that scFvODC1, scFvODC3 and scFvODC7 have a high, specific reactivity to ODC-GST and do not cross-react to GST. The signal to noise ratio indicated in Figure III-30/D presents the ratio between the scFv reactivity of ODC-GST antigen and GST. Even though the scFvODC15 did not show a high reactivity to the antigen, its signal to noise ratio (482.1) indicated a high specificity to ODC-GST. The specific binding of scFv was further assessed using surface plasmon resonance analysis (III.2.8.7).

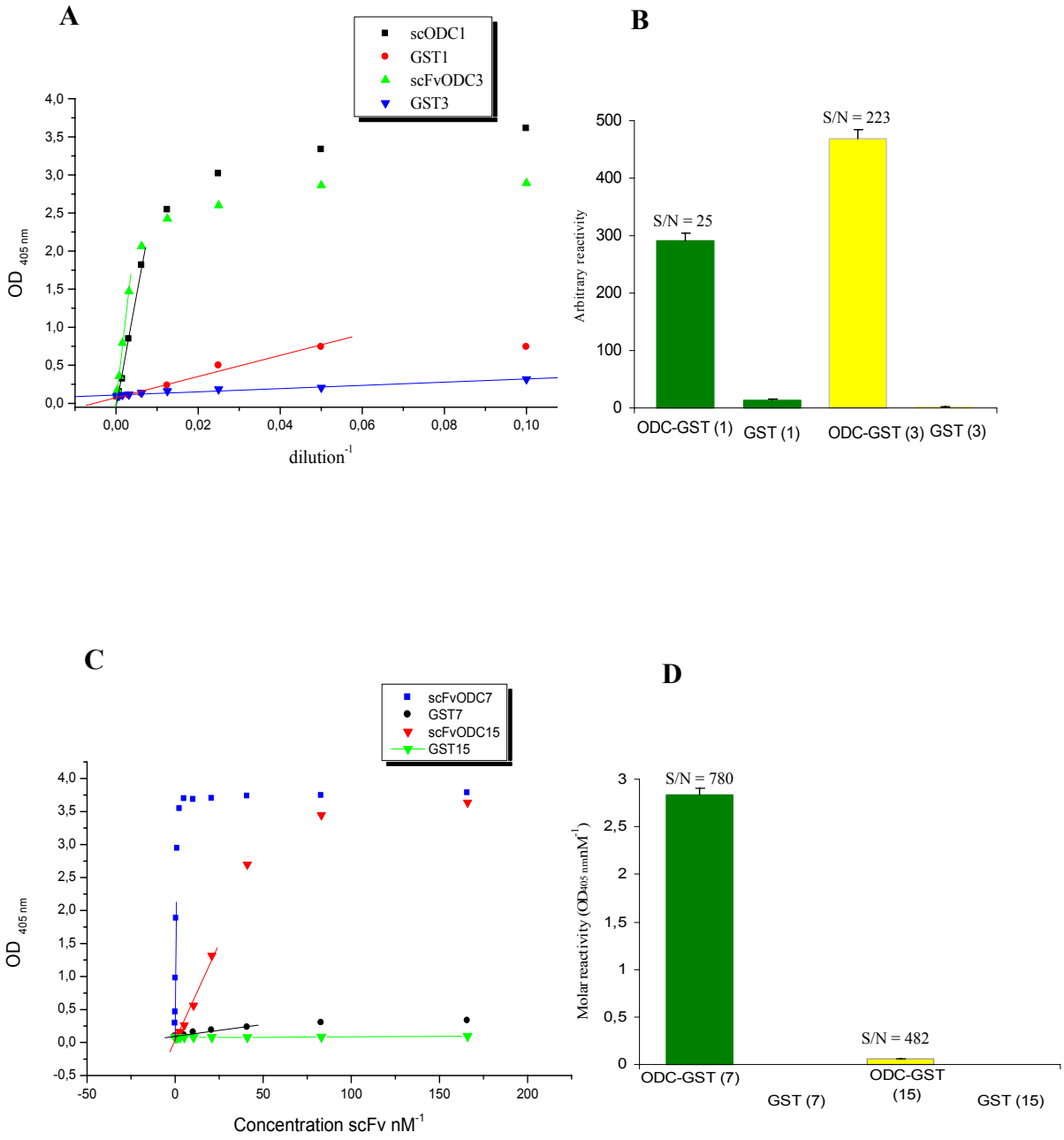

Figure III-30 Reactivity of affinity purified scFvODC1, 3, 7 and 15 to ODC-GST and GST.

1 µg/ml of ODC-GST and GST were coated on microtiter plates (II.2.8.1). Serial dilutions (concentrations) of affinity purified ODC specific scFvs were added in 1xPBS to a final volume of 100 µl. Bound scFvs were detected by using 9E10 monoclonal antibody (1:5000), and GAM^{AP} polyclonal antibody (1:5000). ELISA readings were performed at $OD_{405\ nm}$ after 30 min incubation with pNPP substrate at 37°C and presented in A, C. Using the Origin software the slope was determined by linear regression and then presented as the arbitrary reactivity of the scFvODC1 (green) and scFvODC3 (yellow) to the ODC-GST and GST (B), or as the molar reactivity of the scFvODC7 (green) and 15 (yellow) (D) to the ODC-GST and GST. The signal to noise ratio is calculated for all scFvs specific to ODC.

III.10.4 Epitope mapping of scFvODC1, scFvODC3 and scFvODC7 by surface plasmon resonance

Epitope mapping of affinity purified scFvs to ODC-GST was performed by surface plasmon resonance (BIAcore) using pair-wise epitope mapping analysis (II.2.8.5). In pair-wise epitope mapping assays the ability of two scFv to bind simultaneously to the same antigen is tested. One scFv ‘‘the ligand’’ is covalently bound to the sensor surface using amine-specific coupling. Then the antigen is passed over the prepared surface under flow to bind to the ligand, followed by the injection of the second scFv.

If the second scFv binds to the antigen, the two scFv recognize different epitopes. If two scFvs have identical or overlapping epitopes they compete for the binding site. Any interaction between proteins is recorded as a function of time in resonance units (RU). RU are arbitrary units that reflect the changes in refractive index (a function of mass) at the sensor surface as a result of the binding of solution-phase analyte to (or its release from) surface-bound ligand.

scFvODC1 was immobilized in the flow cell 1 (Fc1). In the second flow cell (Fc2) rabbit anti GST monoclonal antibody (Rα-GST) that does not have identical or overlapping epitopes with any of the scFvODCs was immobilized. The Rα-GST was used as positive control because it recognized an epitope present in GST part of the ODC-GST fusion protein. The scFvODC3 and 15 were immobilized in the Fc3 and Fc4 respectively. After immobilization the ODC-GST antigen was injected in the four flow cells at a concentration of 0.15 μM. Then, either scFvODC1 (Figure III-31/A) or scFvODC3 (Figure III-31/B) was injected to the flow cells after immobilization with ODC-GST and the changes in the RU was studied on the sensogram. Figure C, D represents the binding activity of the second injected scFv (scFvODC1 or scFvODC3) to the antigen bound in the four flow cells. The binding activity of the second scFv to the Fc2 where the rabbit anti GST has been immobilized was taken as 100% because the scFvODCs do not have identical or overlapping epitope with the R-α-GST antibody. Binding activity of scFvODC1 to Fc1 (Figure III-31/C) was taken as negative control. The binding activity of scFvODC1 in Fc3 and Fc4 ranged between 75-85% indicating that scFvODC1 did not have overlapping epitopes with scFv3 and 15.

In Figure III-31/B, D the pair wise epitope mapping of scFvODC3 with the scFvODC1 and scFvODC15 is analysed. The low binding activity of the scFvODC3 to the ODC-GST antigen in the Fc3 (negative control) and Fc4 indicated that scFvODC3 has an overlapping epitope with scFvODC15. scFvODC1 recognized a distinct epitope different to scFvODC3, 7 and 15.

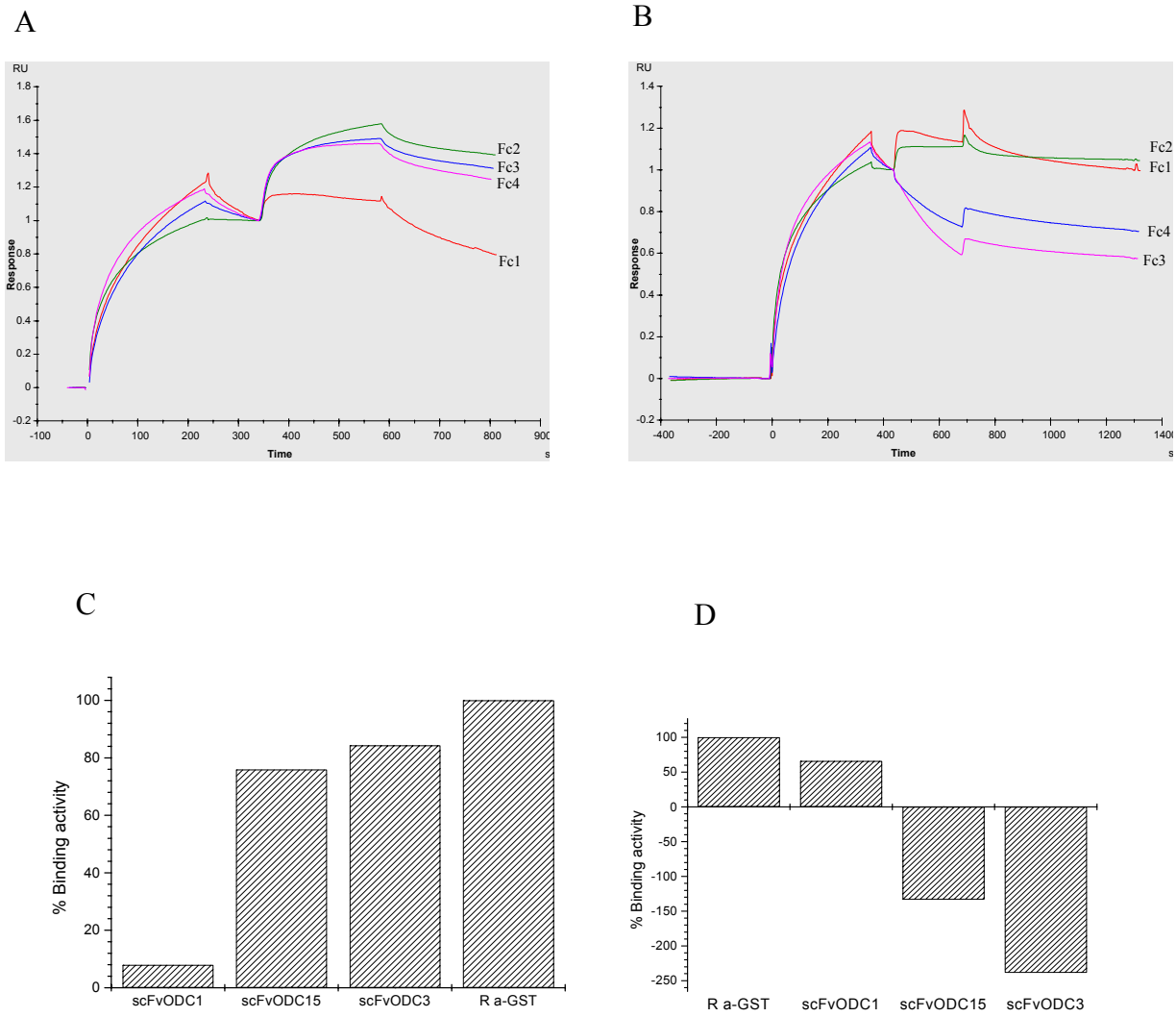

Figure III-31 Epitope mapping of scFvODC to ODC-GST by surface plasmon resonance. 0.3 µM scFvODC1, 3 and 15 were immobilized in flow cells 1, 3 and 4 (Fc1, Fc3 and Fc4) (II.2.8). Rabbit anti GST antibody was immobilized in the Fc2 at a concentration of 0.35 µM. First injection was performed by 0.15 µM ODC-GST antigen. After surface regeneration the second scFvODC (scFvODC1 (A) or scFvODC3 (B) were injected. The changes in the RU were measured after 800 (A) and 1200 (B) seconds of the second injection. C: binding activity of scFvODC1 to the ODC-GST antigen bound in the four flow cells. D: binding activity of scFvODC3 to the ODC-GST antigen bound in the four flow cells.

III.10.5 Comparative analysis of binding activity of scFvODC1 preincubated with ODC-GST

To analyze the binding activity of scFvODC1 to soluble ODC-GST a BIAcore assay was performed. The ODC-GST antigen was immobilized to a BIAcore CM5 sensor chip surface at a concentration of 0.15 µM. Constant concentrations of scFvODC1 (750 nM) were incubated with different molar ratio of soluble ODC-GST for 1 h at RT. Controls

without ODC-GST and scFvODC1 alone were prepared and analysed under the same conditions. Each sample was passed over the chip and the response units monitored. The obtained BIAcore curves shown in Figure III-32 indicate that the highest binding activity of scFvODC1 to the immobilized ODC-GST antigen was achieved in the sample without ODC-GST. Addition of increasing concentration of antigen from 0 to 7.5 µM reduced the binding activity of scFvODC1 to the immobilized antigen. The ratio of observed to maximal response units was calculated and plotted against the logarithmic concentration of soluble ODC-GST (Figure III-32). The graph shows that addition of soluble ODC-GST inhibits the interaction of scFvODC1 to the immobilized antigen in a dose-dependent fashion.

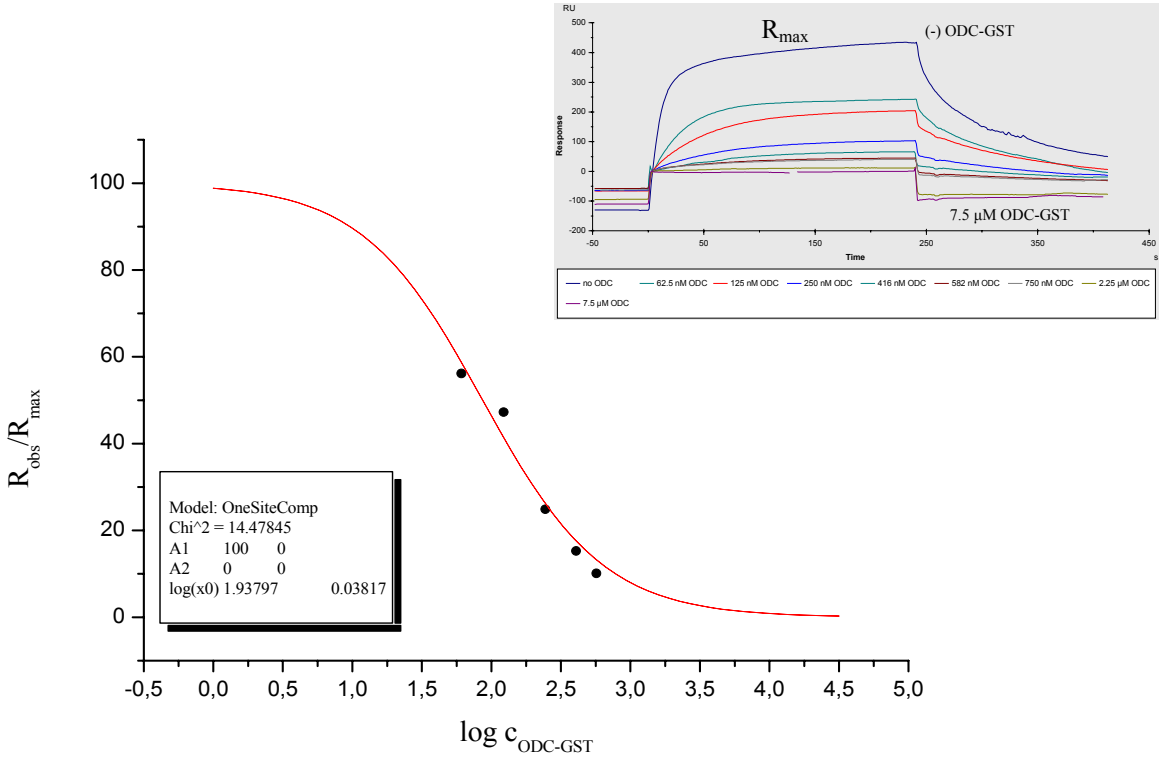

Figure III-32 Inhibition of scFvODC1 binding to immobilized ODC-GST by addition of soluble antigen.

The binding curves representing scFvODC1 binding to the immobilized ODC-GST in the absence of soluble ODC-GST (upper curve), or increasing amounts of up to 7.5 µM (lower curve) are shown in the inset figure. The changes in the RU were measured after 240 seconds of sample injections. One site competition model expressed the function between the R_{obs}/R_{max} ratio and the logarithmic concentration of soluble ODC-GST antigen. R_{max} reflect the response units measured after 240 seconds of the scFvODC1 (without soluble ODC-GST antigen) injection. R_{obs} reflect the RU measured after 240 seconds of any sample (scFvOSC1 + soluble ODC-GST) analyzed.

III.10.6 Electrophoretic mobility shift assay (EMSA)

The functionality of the affinity purified scFvODC1 and scFvODC3 to the ODC-GST antigen was confirmed by electrophoretic mobility shift assay (EMSA). EMSA is based on the observation that stable antibody-antigen complexes migrate slower through polyacrylamide gels than free antigen and antibody fragments (II.2.8.5). Two µg of the purified scFvODC1 and scFvODC3 were incubated for one h at RT with ODC-GST starting with a 1:1 molar ratio of antigen:scFv up to a 30:1 ratio. Incubation of the antigen with the scFv formed complexes that migrated slower than the ODC-GST and the scFv fragments alone (Figure III-33). Samples containing the scFvODC1, scFvODC3 and ODC-GST antigen were loaded in parallel.

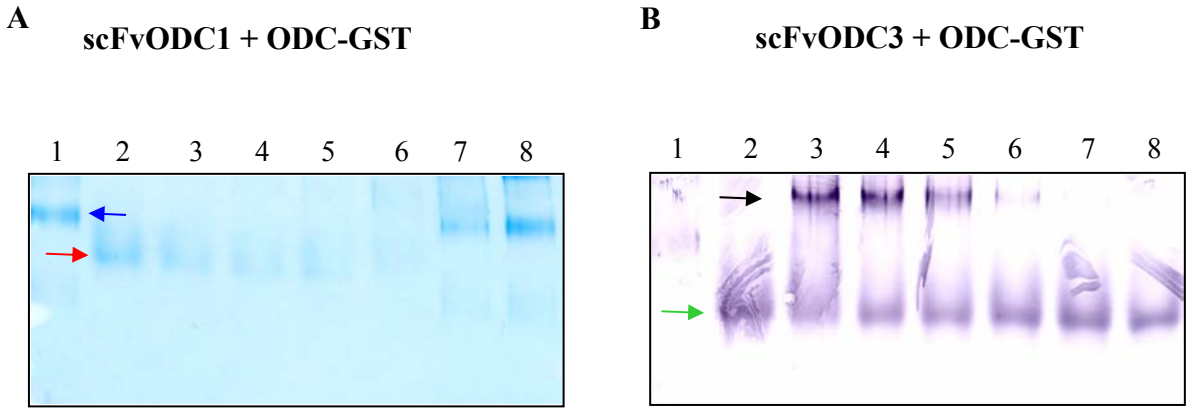

Figure III-33 The functionality analysis of the scFvODC1 (A) and scFvODC3 (B) to ODC-GST antigen by EMSA.

scFvODC1-ODC-GST complex formation was analyzed on a nondenaturating 12% (w/v) PAA-gel electrophores at RT for 5 h at 100 V. A-1: 1.5 µg ODC-GST; 2: 2 µg scFvODC1; 3: 0.16 µg ODC-GST + 2 µg scFvODC1; 4: 0.33 µg ODC-GST + 2 µg scFvODC1; 5: 0.5 µg ODC-GST + 2 µg scFvODC1; 6: 1 µg ODC-GST + 2 µg scFvODC1; 7: 1.5 µg ODC-GST + 2 µg scFvODC1; 8: 5 µg ODC-GST + 2 µg scFvODC1.

B- 1: 1.5 µg ODC-GST; 2: 2 µg scFvODC3; 3: 4 µg ODC-GST + 2 µg scFvODC3; 4: 2 µg ODC-GST + 2 µg scFvODC3; 5: 1 µg ODC-GST + 2 µg scFvODC3; 6: 0.5 µg ODC-GST + 2 µg scFvODC3; 7: 0.25 µg ODC-GST + 2 µg scFvODC3; 8: 0.125 µg ODC-GST + 2 µg scFvODC3. The scFvODC3-ODC-GST complex formation was separated on a nondenaturating PAA-gel run at 4°C for 5 h at 100 V and blotted onto a nitrocellulose membrane (II.2.2.3). Immunodetection was carried out by addition of 1:5000 diluted 9E10 mAb, and goat-anti mouse polyclonal antibodies conjugated to alkaline phosphatase as secondary antibody (1:5000). Detection was carried out with NBT/BCIP for 1 min at RT.

As indicated in Figure III-33/A the scFvODC1 (red arrow) migrated faster than the ODC-GST antigen (blue arrow). Although the concentration of scFvODC1 was kept constant in the assay, scFv band intensity decreased with increasing concentration of ODC-GST (Figure III-33/A lines 3-8) resulting in formation of higher MW complexes. These results

indicate that scFvODC1 and ODC-GST interacted and formed stable complexes. Thus, confirming the functionality of the scFvODC1 to the antigen.

Also scFvODC3 caused a band shift (Figure III-33/B lanes 3-6) when incubated with ODC-GST. Lanes 3, 4, 5 and 6 in Figure III-32/B show clearly the band shift resulting from addition of increasing amounts of ODC-GST using the constant scFvODC3 concentrations versus the scFvODC3 alone (lane 2). In lanes 3, 4, 5 and 6 two bands are observed, an intense band with decreased mobility (black arrow) corresponding to the scFvODC3-ODC-GST complex and a faint band corresponding to the free scFvODC3 (green arrow). The intensity of the scFvODC3-ODC-GST complex decreases with decreasing amounts of the antigen indicating that scFvODC3-ODC-GST complex formation is a dose dependent process.

III.10.7 *In vitro* effect of scFvODC1 and scFvODC3 on the enzymatic activity of bacterial purified ODC-GST

In order to examine the effect of ODC-specific murine scFvODC1 and scFvODC3 on the ODC enzymatic activity, radioactive assays were performed using bacterial purified ODC-GST (II.2.3.1). Prior to *in vitro* analyses the binding of freshly purified scFvODC1 and scFvODC3 with affinity purified bacterial ODC-GST was tested by direct ELISA (II.2.8.1). Both scFvs exhibited high binding activity to ODC (data not shown).

Serial dilutions of bacterial purified ODC-GST were analysed for ODC enzymatic activity, to determine the enzyme concentrations resulting in a significant signal in the assay. The ODC-GST concentration chosen was 13 nM (data not shown) and used as the 100% value.

The antibody concentration chosen for the *in vitro* enzyme assay was determined theoretically as indicated in the formula below based on the law of mass action, since it was crucial to be in the range giving inhibition effect.

$$[AB]_{1,2} = \frac{1}{2} * c^0(A) * \left\{1 + \beta + \frac{K_D}{c^0(A)}\right\} \pm \sqrt{\left(\frac{1}{2} * c^0(A) * \left\{1 + \beta + \frac{K_D}{c^0(A)}\right\}\right)^2 - \beta * c^0(A)^2}$$

$$= \frac{1}{2} * c^0(A) * \left[\left\{1 + \beta + \frac{K_D}{c^0(A)}\right\} \pm \sqrt{\left\{1 + \beta + \frac{K_D}{c^0(A)}\right\}^2 - 4 * \beta}\right]$$

where, $[AB]_{1,2}$ = complexed ODC-GST
$c^0(A)$ = ODC-GST molar concentration
$c^0(B)$ = scFv molar concentration
β = $c^0(B) / c^0(A)$

K_D = 500 nM (estimated by BIAcore experiments)

Five different concentrations of scFvODC1 and scFvODC3 (3.4 µM; 1.7 µM; 850 nM; 425 nM; 212 nM) were chosen for *in vitro* enzyme analyses (Figure III-34). The scFv4813 (in the same molar concentrations) was used as a negative control.

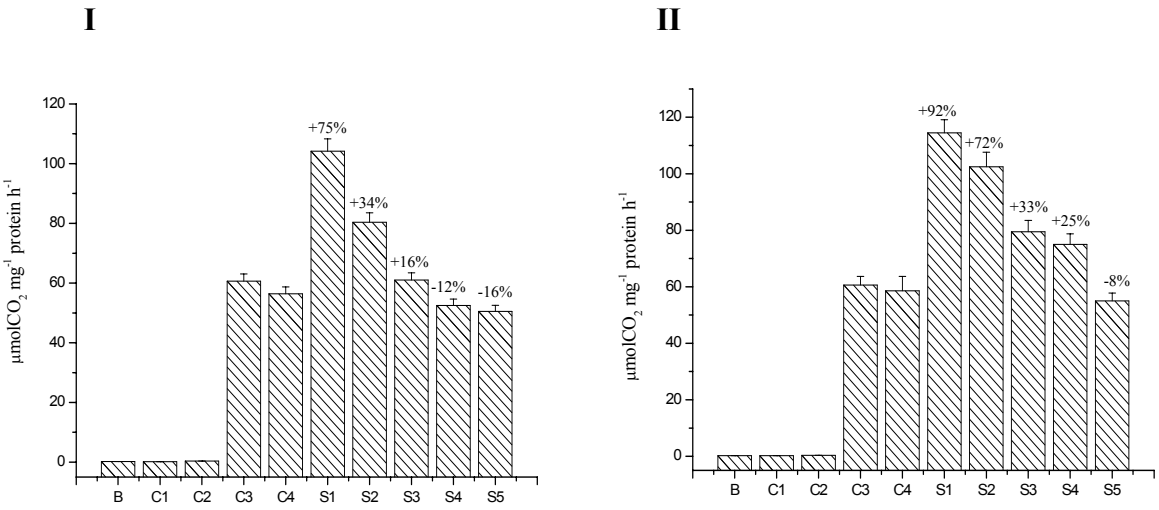

Figure III-34 ***In vitro*** **effect of scFvODC1 (A) and scFvODC3 (B) on the enzymatic activity of ODC.**

ODC-GST fusion protein was affinity purified using glutathione sepharose matrix (II.2.3.1). 13 nM of the ODC-GST were diluted in HEPES buffer (pH 7.5) and mixed with different concentrations of scFvODC1 and scFvODC3 (3.4 µM; 1.7 µM; 850 nM; 425 nM; 212 nM). Determination of ODC activity was performed as described (II.2.9). All the values indicated are mean ±SE (n=4). The indicated mean value of the ODC activity are expressed in µmol CO_2 mg^{-1} protein h^{-1}. The % change of the ODC activity after addition of scFvODc1 and scFvODc3 is indicated.

I: B: Hepes buffer pH 7.5; C1: 13 nM of heat inactivated ODC-GST enzyme; C2: 1.7 µM of scFvODC1; C3: 13 nM ODC-GST ≡100% value; C4: 13 nM ODC-GST + 3.4 µM scFv4813; S1: 13 nM ODC-GST + 3.4 µM scFvODC1; S2: 13 nM ODC-GST + 1.7 µM scFvODC1; S3: 13 nM ODC-GST + 850 nM scFvODC1; S4: 13 nM ODC-GST + 425 nM scFvODC1; S5: 13 nM ODC-GST + 212 nM scFvODC1.

II: B: Hepes buffer pH 7.5; C1: 13 nM of heat inactivated ODC-GST enzyme; C2: 1.7 µM of scFvODC3; C3: 13 nM ODC-GST; C4: 13 nM ODC-GST + 3.4 µM scFv4813; S1: 13 nM ODC-GST + 3.4 µM scFvODC3; S2: 13 nM ODC-GST + 1.7 µM scFvODC3; S3: 13 nM ODC-GST + 850 nM scFvODC3; S4: 13 nM ODC-GST + 425 nM scFvODC3; S5: 13 nM ODC-GST + 212 nM scFvODC3.

Results presented in Figure III-34 clearly indicate that addition of different of scFvODC1 and scFvODC3 concentrations stabilized the enzymatic activity of bacterial purified ODC

in a dose dependent manner. Addition of 3.4 µM scFvODC1 and scFvODC3 increased the enzymatic activity of ODC by 75% and 92%, respectively, indicating that the scFvODC3 could have a stronger stabilizing effect. In future experiments it would be interesting to invenstigate the additive effect of both scFvODC1 and scFvODC3 to 13 nM ODC.

III.10.8 Transient expression of scFvODC1, 3, 7 and 15 in vacuum-infiltrated tobacco leaves

To study recombinant antibody expression in tobacco plants scFvODC1, 3, 7 and 15 were subcloned into plant expression vector pTRA using *Nco*I/*Not*I restriction sites. Leader peptides or tags were added for either secretion into the apoplasmic space or retention in ER. Eight different plant expression constructs were generated and their sequences verified. Transient assays were performed and the scFv expression levels in the apoplast and ER were analysed by immunoblot analysis (Figure III-35).

The immunoblot analyses of the total soluble protein extracted from infiltrated leaves showed a distinct, single band of about 30 kDa for all four ODC-specific scFvs. No difference in expression level was observed among four leaves of the same construct. The constructs that retained the scFv in ER, carrying His6 and KDEL detection tags, were analyzed in parallel (Figure III-35). The immunoblot analyses revealed that all four scFvs specific to ODC had higher levels of expression in the ER than in the apoplast (Figure III-35/C).

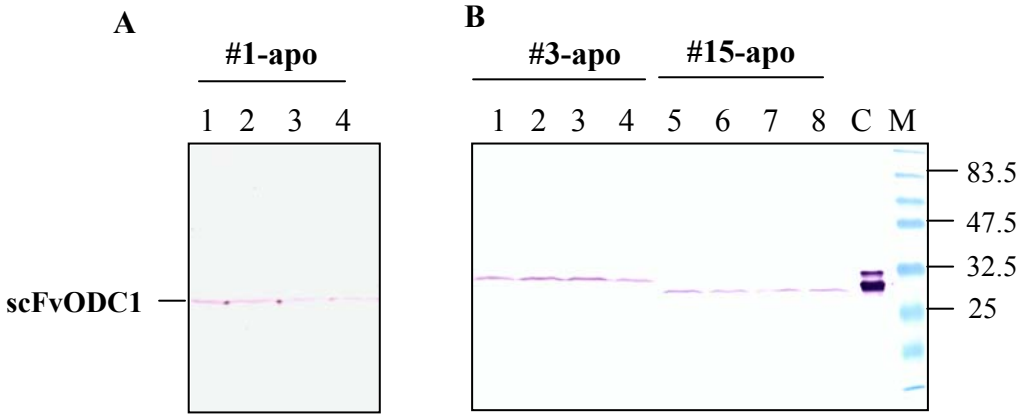

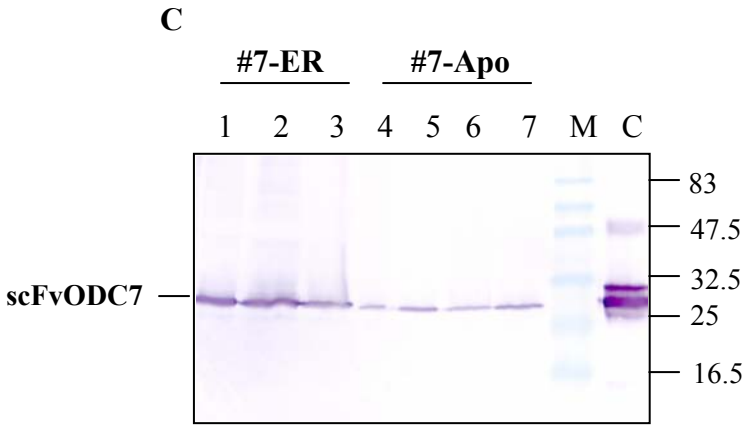

Figure III-35 Transient expression of ODC specific scFvs in tobacco leaves.

Four tobacco leaves were infiltrated for each construct either for retention of scFv in ER or for secretion of scFvs into apoplastic space. Total soluble leaf proteins were extracted by grinding tobacco leaf tissue in two volumes of extraction buffer (II.2.2.6). 5 µl of total soluble protein from each sample was separated by 12% SDS-PAGE (II.2.4.2) and blotted onto a nitrocellulose membrane (II.2.2.3). Immunodetection was carried out with anti-his6 antibody (1:5000), followed by 1 hr incubation with goat anti-mouse antibody conjugated to alkaline phosphatase (1:5000) and NBT/BCIP detection for 1 min at RT.

A: 1-4: different infiltrated leaves expressing scFvODC1 in apoplast. B: 1-4: different infiltrated leaves expressing scFvODC3 in apoplasm; 5-8: different infiltrated leaves expressing scFvODC15 in apoplasm. C: 1-3: different infiltrated leaves expressing scFvODC7 in ER; 4-7: different infiltrated leaves expressing scFvODC7 in apoplasm; M: prestained protein marker; C: 1 µg anti HCG diabody.

III.10.9 Functional analyses of cytosolic expressed scFvODC1 and scFvODC3

To study the accumulation level and the functionality of ODC-specific murine scFv fragments in the plant cytosol, the scFvODC1 and scFvODC3 that were fully functional in EMSA assays and recognized different epitopes in the ODC protein were chosen for cytosolic targeting.

The scFvODC1 and scFvODC3 were cloned via *Nco*I and *Sal*I restriction sites in the SCA24OmW cassette in pUC 18 downstream of the TMV 5′ UTR (omega (Ω) leader), and upstream of the c-myc/his-6 tags (Figure III-36). Then, the cassette containing the Ω leader, scFvODC cDNAs and c-myc/his6 tags was excised with *EcoR*I and *Xba*I and cloned between the enhanced 35S promoter and Pw untranslated region of pSS vector resulting in the pSS: scFvODC1-cyt and pSS: scFvODC3-cyt constructs (Figure III-36).

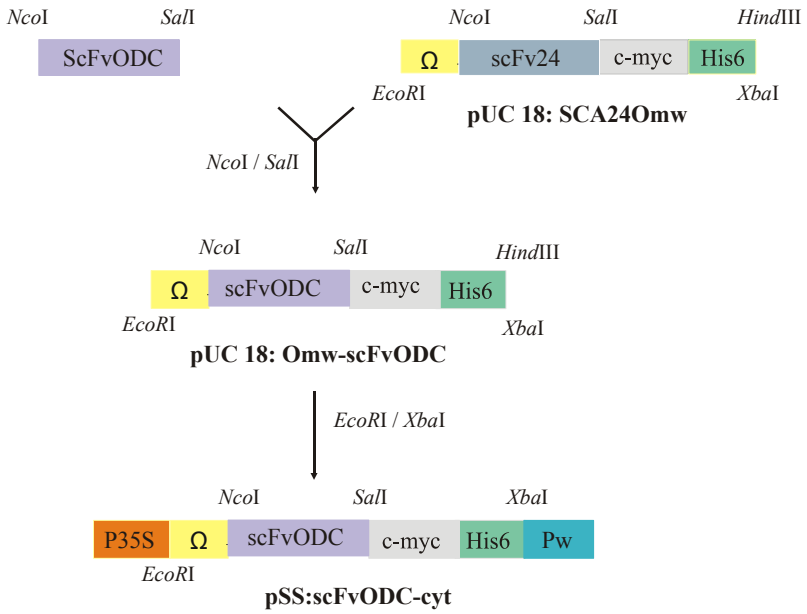

Figure III-36 Strategy for cloning of ODC specific murine scFvs into pSS plant expression vector for cytosolic targeting.

P35S: 35S promoter from CaMV with duplicated 35S enhancer; Ω: omega leader region of TMV RNA; Pw: 3' UTR of TMV RNA: scFv24: TMV specific single chain antibody 24; scFvODC: ODC specific murine scFv antibody (scFvODC1 or scFvODC3); c-myc: myc epitope for detection; His6: his-6 tag for purification and detection.

Transient expression experiments were performed. Four leaves for each construct were infiltrated with recombinant agrobacteria. After three days of incubation at 26°C total soluble proteins were extracted and detected by immunoblot analyses to verify accumulation and integrity of the recombinant proteins in the plant cytosol. Immunoblot analyses (Figure III-37) showed a distinct band of approximately 30 kDa, corresponding to the molecular weight of scFvODC1 and scFvODC3. No significant difference in accumulation level was observed among four leaves of the same construct. The immunoblot analyses revealed that scFvODC1 and scFvODC3 accumulated to high levels in the plant cytosol (~50-70 µg/g fresh weight), as indicated by comparison of band intensity with several concentrations of scFv standard (data not shown).

The total soluble protein extracts were analyzed for antigen-binding activity of cytosolic expressed scFv fragments. The binding of scFvODC1 and scFvODC3 to ODC-GST was analysed by direct ELISA (Figure III-38).

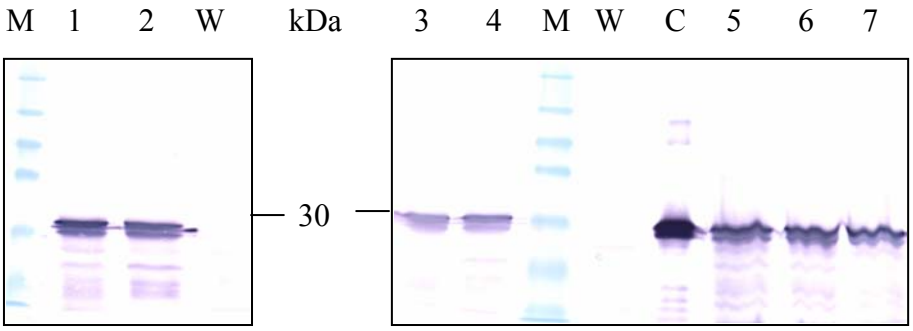

Figure III-37 Transient expression of cytosolic scFvODC1 and scFvODC3

Total soluble proteins were extracted by grinding tobacco leaf tissue (II.2.2.6) in two volumes extraction buffer, separated by SDS-PAGE (II.2.4.2) and blotted onto a nitrocellulose membrane. Immunodetection was carried out with 1:5000 diluted 9E10 as primary antibody, followed by 1:5000 diluted alkaline phosphatase conjugated goat anti mouse as secondary antibody. Detection was performed with NBT/BCIP for 1 min at RT.

Lane 1: 7 µl PPM; 2-4: 5 µl of total soluble protein extracted from individual leaves expressing scFvODC1 in the cytosol; 5-7: 5 µl of total soluble protein extracted from individual leaves expressing scFvODC3 in the cytosol; W: 5 µl of total soluble protein extracted from wild type tobacco leaves; C: 1 µg of bacterial purified scFvODC3.

To confirm the specific reactivity of the scFvs to the ODC antigen SME-GST and GST were coated onto ELISA plates as control. The reactivity of the wild type tobacco plant extract to ODC-GST was analysed as well.

ELISA results presented in Figure III-38 showed that the cytosolic expressed scFvODC1 and scFvODC3 had a high binding reactivity with ODC compared to the wild type tobacco extract. No cross reactivity with the GST and SME-GST was observed for both scFvs, indicating the ODC-specificity and functionality of the cytosolic expressed scFvODC 1 and scFvODC3.

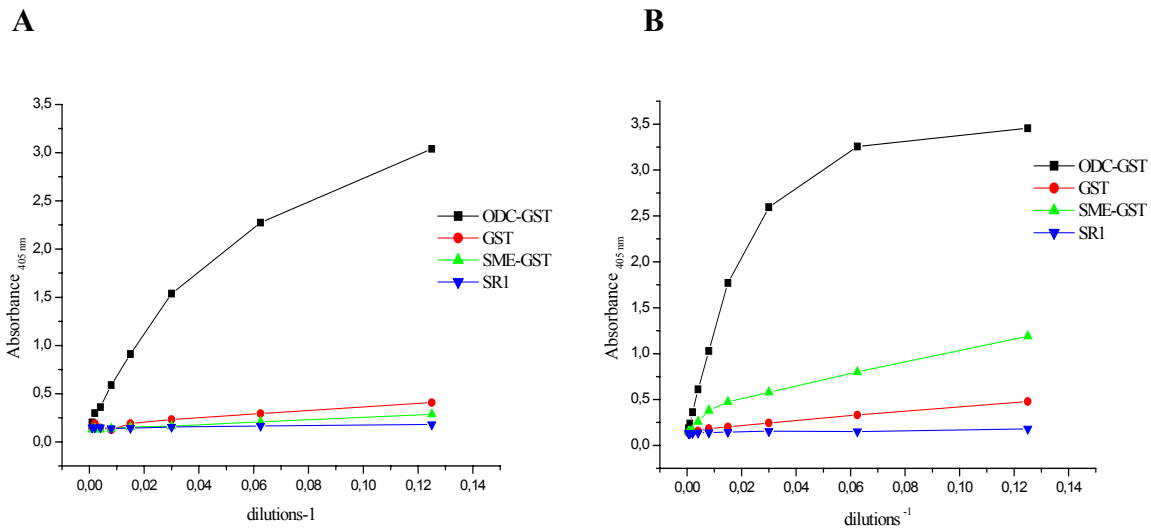

Figure III-38 ELISA analyses of cytosolic expressed murine scFvODC1 (A) and scFvODC3 (B) to ODC-GST, SME-GST and GST antigens.

Analyses of cytosolic expressed scFvODC1 to ODC-GST (black), SME-GST (green) and GST (red). The reactivity of wild type SR1 tobacco extract to ODC-GST is indicated (blue).

2.5 µg/ml of ODC-GST, GST and SME-GST were coated on microtiter plates. Wild type and transient infiltrated tobacco leaves accumulating the scFvODC1 and scFvODC3 in the plant cytosol were extracted 1:2 into protein extraction buffer. Plant extract was serially diluted into protein extraction buffer in a siliconized plate. After 3x washing with PBST 100 µl of the serially diluted plant extract was added into ELISA plates. The plates were incubated at 37°C for 1.5 h. Bound scFvs were detected by addition of 1:5000 diluted 9E10 mAb and GAM^{AP} secondary antibody (1:5000). ELISA readings ($OD_{405\ nm}$) were performed after 30 min incubation with pNPP substrate at 37°C.

III.10.10 Generation and characterisation of stable transformed plants overexpressing scFvODCs

ScFvODC1 and scFvODC3 recognize different epitopes in the ODC protein (III.10.4) and shown to be fully functional in EMSA assays (III.10.6) were chosen for generation of stable transformed plants accumulating ODC-specific scFvs in the plant apoplast and cytosol.

Stable transformed tobacco plants expressing apoplasmic scFvODC1 and scFvODC3 were generated for crossing experiments with stable transformed tobacco plants overexpressing recombinant human ODC into the apoplast (III.4.2). Transgenic plants accumulating the scFvODC1 and scFvODC3 in the apoplast were regenerated after leaf disc transformation of *N. tabacum* cv. Perite Havana SR1. The resulting transformed tobacco plants (T_0) were selected for kanamycin resistance. Nineteen regenerated T_0 plants (labeled scFvODC1-apo-1→19) from the transformation experiments with pTRA: scFvODC1-apo and 18 T_0 plants (labeled scFvODC3-apo-1→18) expressing pTRA: scFvODC3-apo were planted and

screened for expression of the recombinant protein. None of the transformed plants exhibited an altered morphology and all set seed normally upon self-fertilization. The presence of recombinant proteins in tobacco leaves was analysed by immunoblot using crude extracts of total soluble protein. Immunoblot experiments revealed that 16 out of 19 and 12 out of 18 T_0 plants accumulating scFvODC1 or scFvODC3 in the apoplast (Figure III-39).

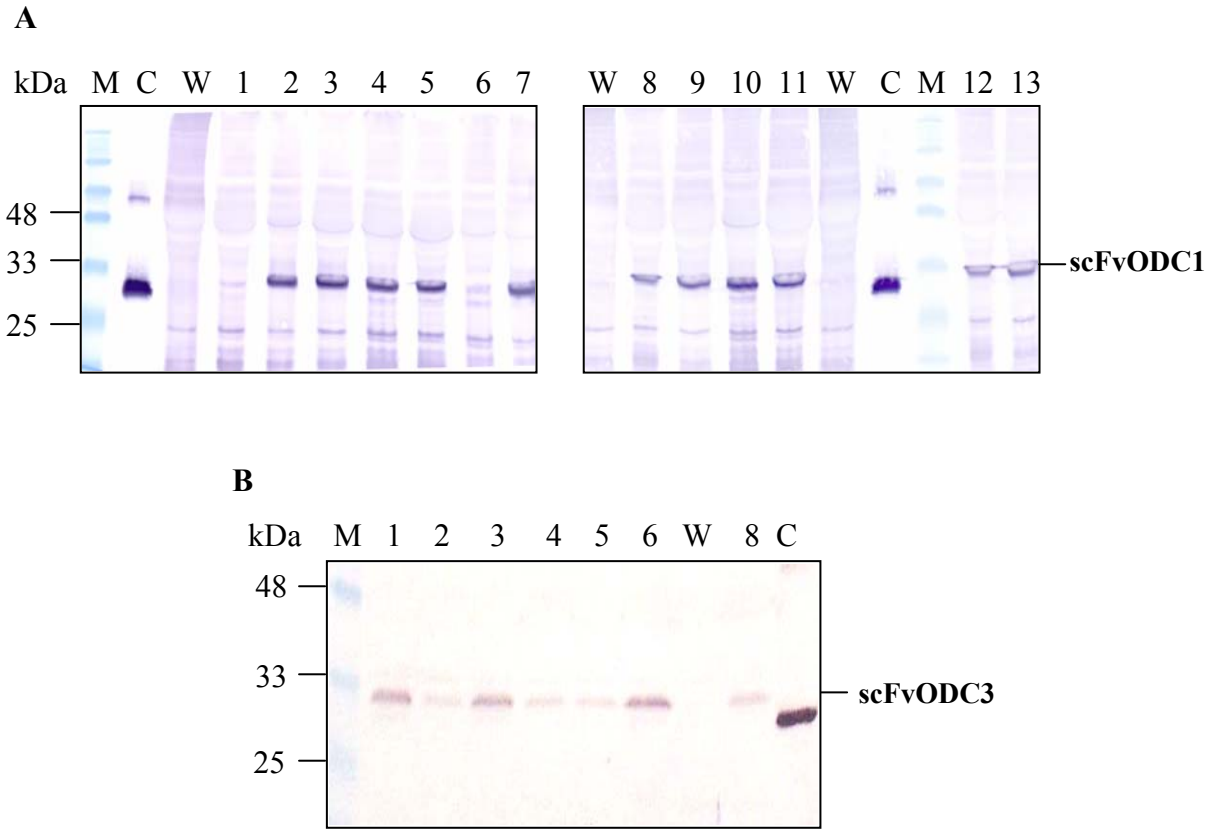

Figure III-39 Immunoblot analysis of stable tobacco T_0 plants producing apoplastic scFvODC1 (A) and scFvODC3 (B).

Total soluble proteins were extracted by grinding tobacco leaf tissue in two volumes extraction buffer (II.2.2.6). 5 µl of total soluble protein from each sample was separated by 12% SDS-PAGE (II.2.4.2) and blotted onto a nitrocellulose membrane (II.2.2.3). Immunodetection was carried out with 1:5000 diluted anti-his6 antibody, followed by incubation with 1:5000 diluted goat anti-mouse antibody conjugated to alkaline phosphatase and NBT/BCIP detection for 5 min at RT.

A: 1-13: 7 µl total soluble protein extracted from transgenic T_0 tobacco lines (scFvODC1-apo-1→19) producing apoplastic scFvODC1. M: prestained protein marker. C: 0.46 µg scFv4813 used as positive control.

B: 1-8: 7 µl total soluble protein extracted from transgenic T_0 tobacco lines (scFvODC3-apo-1→18) producing apoplastic scFvODC3. M: prestained protein marker. C: 0.46 µg scFv4813 used as positive control.

ScFvODC1 and scFvODC3 migrated according to their predicted molecular weight of 30 kDa (Figure III-39).

Transgenic T_0 lines with the highest level of accumulation of scFvODC1 in apoplast (scFvODC1-apo-2; scFvODC1-apo-3; scFvODC1-apo-4; scFvODC1-apo-8 and scFvODC1-apo13) and scFvODC3 (scFvODC3-apo-2; scFvODC3-apo-4; scFvODC3-apo-10; scFvODC3-apo-17; scFvODC3-apo-19) were kept for generation of the homozygous lines, that will be used for crossing experiments with the ODC-apo-7/3 lines that showed high ODC enzymatic activity (III.6).

Generation of stable transformed plants accumulating scFvODC1 and scFvODC3 into the cytosol is still ongoing. As soon as homozygous transgenic plants are available they will be analysed for enzymatic activity of ODC and polyamine levels.

III.11 Cloning and expression of scFvADC3 and scFvADC7 in *E.coli*

Large-scale expression of selected scFvADCs was performed using the bacterial expression vector pSyn. scFvADC3 was subcloned downstream of the pelB leader peptide of pSyn vector using *Nco*I and *Not*I restriction sites. Because of an internal *Nco*I site at the 126 bp position of V_H chain the scFvADC7 was subcloned into pSyn vector using *Sfi*I and *Not*I restriction sites. Correct insertion of the scFvs was confirmed by sequence analysis.

Both antibody fragments were expressed upon induction with 1 mM IPTG. The His6 tagged scFvs secreted into the culture medium were purified by IMAC. The affinity purified scFvs were analysed by SDS-PAGE (Figure III-40).

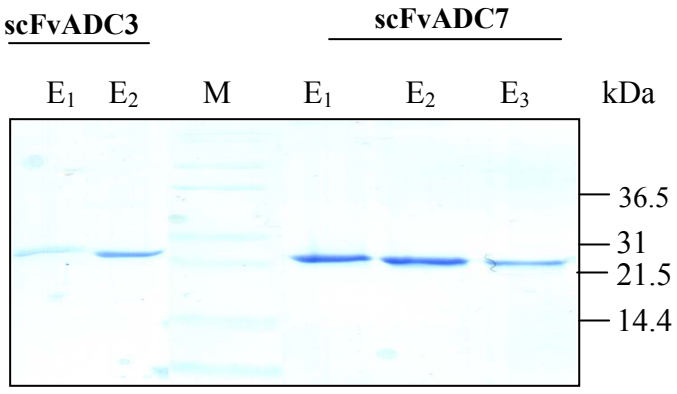

Figure III-40: SDS-PAGE analyses of affinity purified scFvADC3 and scFvADC7.

Two selected scFvADCs (3 and 7) were subcloned into the pSyn vector and expressed in the *E. coli* strain HB2151 upon induction with IPTG. The periplasmic expressed scFvs were purified by IMAC (II.2.8.1). Proteins were separated on 12% (w/v) SDS-PAGE and stained with Coomassie brilliant blue (II.2.4.2). E_1, E_2, E_3: 5 µl of three 1 ml elution fractions; M: Mark12 protein marker.

The purified scFv revealed the presence of a single band of approximately 30 kDa. The concentration of purified scFvs was determined by either Bradford or BCA assay using BSA as a standard. The yield of purified scFvs ranged between 1-1.5 mg/L culture volume with slight deviations depending on the batch of preparation. The purified scFv fragments (Figure III-36) retained their functionality as shown in ELISA test (Figure III-41).

III.11.1 Reactivity of purified scFvADC3 and scFvADC7

Direct ELISA was performed to examine the reactivity of the purified scFvADC3 and scFvADC7 to ADC-GST and GST antigens (Figure III-41/A).

Dilutions of purified scFvADC3 and scFvADC7 were incubated on high binding ELISA plates coated with ADC-GST and GST (5µg/ml). Quantitative analysis of the linear fit was performed for the data in linear range. The slope, the direct indication of reactivity of these scFv to the antigen has been calculated and presented in Figure III-41/B. The results indicated that scFvADC3 and scFvADC7 have a high, specific reactivity to ADC-GST and no cross-reactivity to GST.

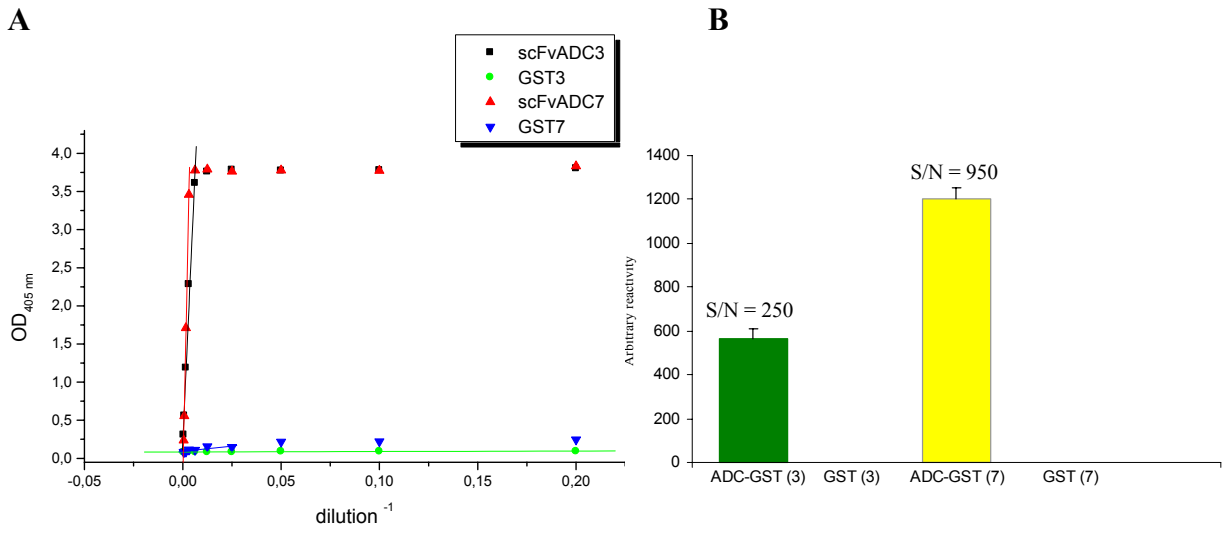

Figure III-41 Reactivity of affinity purified scFvADCs to ADC-GST and GST.

1 µg/ml of ADC-GST and GST were coated on microtiter plates (II.2.8.1). Serial dilutions of affinity purified scFvADCs (3 and 7) were added in 1xPBS to a final volume of 100 µl. Bound scFvs were detected by using 9E10 monoclonal antibody (1:5000), and GAM^{AP} polyclonal antibody (1:5000). ELISA readings were performed at $OD_{405\ nm}$ after 30 min incubation with pNPP substrate at 37°C and presented in A. Using the Origin software the slope was determined by linear regretion and then presented as the arbitrary reactivity of the scFvADC3 (green) and scFvADC7 (yellow) to the ADC-GST and GST (B). The signal to noise ratio is calculated for scFvADC3 and scFvADC7.

III.12 Epitope mapping of scFvADC3 and scFvADC7

Epitopes of the two scFvADC3 and scFvADC7 were analysed by competition to the ADC-GST antigen in ELISA experiment. In order to verify independent or overlapping epitopes the biotinylation of one scFv was necessary since both scFvs carried the same detection tags. scFvADC3 was biotinylated using biotin disulfide N-hydroxysuccinimide ester (II.2.8.3). Biotinylation efficiency of the scFvADC3 was determined by immunoblot analysis using non-biotinylated scFvADC3 and another biotinylated scFv with known concentration as standard (Figure III-42). The reactivity and functionality of the biotinylated scFvADC3 was analysed in the direct ELISA. Serial dilutions of biotinylated scFvADC3 were incubated on ELISA plates coated with a constant concentration of ADC-GST (1.5 µg/ml).

For the competition ELISA experiments the concentration of biotinylated scFvADC3 was chosen, which gave an $OD_{405\ nm}$ of one (Figure III-42) after 30 min incubation.

The scFvADC3 and scFvADC7 were serially diluted in a constant concentration of biotinylated scFvADC3 (1:80) determined by the direct ELISA and incubated for 2 hrs on ELISA plates coated with ADC-GST. Bound scFvADC3-bio was detected with AP-labeled Streptavidin.

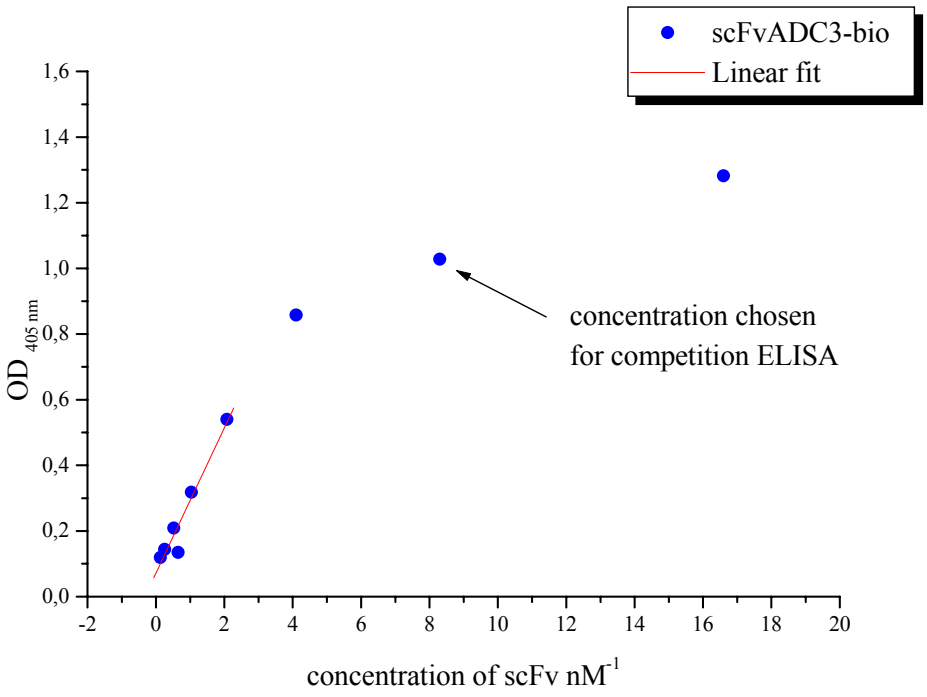

Figure III-42 Reactivity of biotinylated scFvADC3 to the ADC-GST antigen.

ADC-GST (1.5 µg/ml) was immobilised on ELISA plates and several dilutions of biotinylated scFvADC3 were added to the plate. Bound scFvs were detected with 1:3000 diluted AP-labeled Streptavidin. ELISA readings ($OD_{405\ nm}$)were performed after 30 min incubation with pNPP substrate at 37°C.

Results presented in Figure III-43 showed the ability of non-biotinylated scFvADC3 to inhibit the binding scFvADC3-bio to the antigen.

This indicated competition between biotinylated and not biotinylated scFvADC3 and proofed the correct set-up of the competition ELISA. Conversely, increasing amounts of scFvADC7 did not inhibit the binding of scFvADC3-bio to the ADC-GST antigen. Thus, no competition between scFvADC3 and scFvADC7 existed indicating that scFvs binds to two nonoverlapping epitopes.

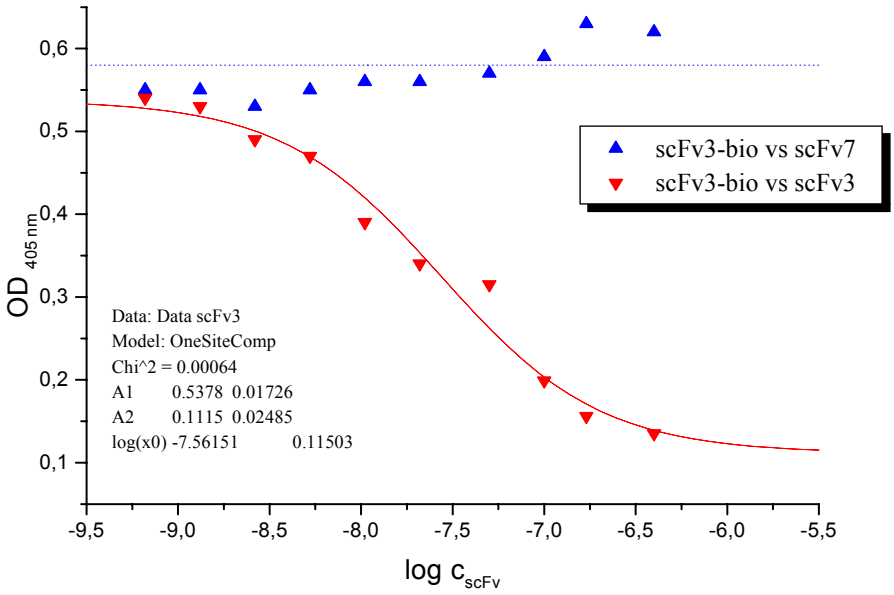

Figure III-43 Epitope mapping of scFvADC3 and scFvADC7.

ADC-GST fusion protein was coated to a microtiter plate at a concentration of 1 µg/ml (II.2.8.4). scFvADC3 and scFvADC7 were serially diluted in 1:80 dilution of biotinylated scFvADC3. Bound scFvADCs were detected with 1:3000 diluted AP-labelled Streptavidin. ELISA readings were performed at $OD_{405\ nm}$ after incubation at 37°C with pNPP for 1 h. One site competition model was performed by Origin program indicating the function between the scFvADC3 or scFvADC7 and the biotinylated scFvADC3.

III.13 Transient expression of scFvADC3 in tobacco plants

To examine the expression of scFvADC3 in *N. tabaccum*, scFvADC3 was subcloned into plant expression vector pTRA. Plant expression constructs were generated for targeting of expressed recombinant protein to the plant cytosol, secretion into the apoplast and retention in the ER. Transient assay experiments were performed, total soluble proteins extracted as described (II.2.2.6) and the presence of scFv fragments analysed by immunoblot analysis.

In immunoblots (Figure III-44) a distinct band of the expected molecular size of 30 kDa were detected in all analysed plant cell compartments. The level of expression of the ADC-specific murine scFvADC3 varied between the constructs. Higher level of expression was shown in ER.

Generation of stable transformed plants accumulating scFvADC3 in the cytosol is still on going.

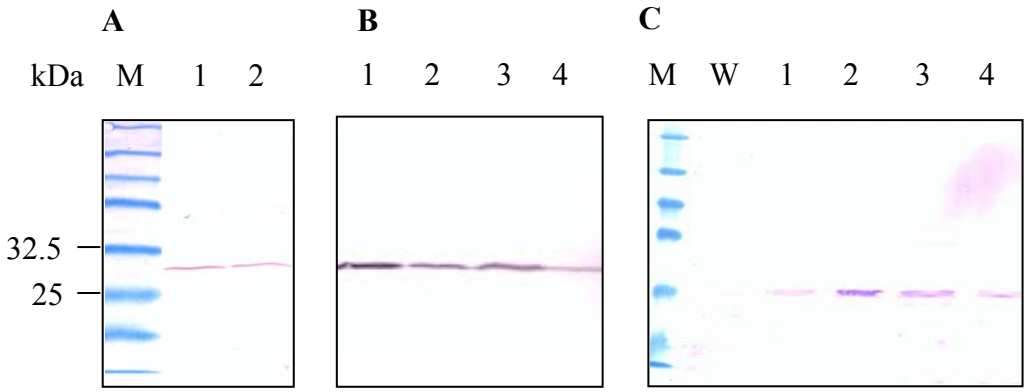

Figure III-44 Transient expression of scFvADC3 in tobacco plants.

Total soluble leaf proteins were extracted by grinding tobacco leaf tissue in two volumes of extraction buffer (II.2.2.6). 5 µl of total soluble protein from each sample was separated by 12% SDS-PAGE (II.2.4.2) and blotted onto a nitrocellulose membrane (II.2.2.3). Immunodetection was carried out with anti-his6 antibody (1:5000), followed by 1 h incubation with goat anti-mouse antibody conjugated to alkaline phosphatase (1:5000) and NBT/BCIP detection for 5 min at RT. A- 1-2: different infiltrated leaves expressing scFvADC3 in apoplast. B- 1-4: different infiltrated leaves expressing scFvADC3 in ER. C- 1-4: different infiltrated leaves expressing scFvADC3 in cytosol; W: wild type SR1 tobacco plant.

IV Discussion

The polyamine biosynthetic pathway has been the subject of intensive study for several decades (Smith, 1985; Pegg, 1986). All genes of the enzymes involved in the polyamine biosynthesis pathway are cloned permitting its manipulation. Strategies to manipulate the pathway are based on the overexpression of key anabolic enzymes in concert with the down regulation of catabolic enzymes such as diamine oxidase (DAO) and polyamine oxidase (PAO) (DeScenzo and Minocha, 1993; Bastola and Minocha, 1995; Kumar *et al*., 1996; Burtin and Michael, 1997; Capell *et al*., 1998; Malmberg *et al*., 1998; Noury *et al*., 2000). Conversely, Burtin and Michael (1997) speculate that the plant polyamine pathway is so rigidly controlled that changes in polyamine levels cannot be achieved by over-expressing key enzymes. The immunomodulation is an alternative approach for manipulating plant metabolism to change agronomic traits, 'immunize' the plants against pathogens, or blocking regulatory factors, such as immunomodulation of enzyme or signal molecule activity (De Jaeger *et al*., 2000; Giddings *et al*., 2000; Cattaneo and Biocca, 1997). The idea of this work was to achieve changes in the polyamine pathway by over-expression of ODC and SDE enzymes combined with the expression of recombinant antibodies to immunommodulate key enzymes. So far no data are available for modulation of the biosynthesis pathway by expressing specific scFv fragments binding to key enzymes.

Human ODC, a key enzyme of polyamine biosynthesis was overexpressed in different plant cell compartments. Stable transformed tobacco plants were generated and the effect of the recombinant protein on the polyamine metabolism investigated. Stable transformed tobacco plants co-expressing ODC and SDE were generated and the effect of the recombinant proteins investigated. Three phage display libraries were constructed from spleen cells of immunized mice with polyamine GST fusion proteins. Four scFv-fragments specific to ODC and two scFv fragments specific to ADC were selected from phage display libraries. Then, fully active scFvs were expressed in *Escherichia coli* and characterized for their reactivity and functionality to antigens by ELISA, EMSA and surface plasmon resonance analysis. *In vitro* assays were performed to analyse the effect of ODC-specific scFvs on the enzymatic activity of ODC. Transient expression experiments were performed with all selected scFvs to analyse their intracellular performance. In addition, stable transformed plants expressing two scFv-fragments specific to ODC were generated and characterized for scFv expression.

IV.1 Generation and characterization of transgenic plants

The human ODC gene was amplified from a prostate cDNA library (III.1) using gene specific primers (Gen-bank accession number M16650) The ODC-PCR product was cloned into pGEM-3zf vector and the sequence was verified. A single point mutation changing glutamic acid to glutamine ($Glu^{417} \rightarrow Gln^{417}$) in the position 417 was observed. An amino acid change in the protein sequence could be critical for the correct folding and may abolish the enzymatic activity especially when present in the catalytic site. Therefore it was important to investigate if this point mutation is an alternative form of the ODC gene (allele) or was introduced during PCR and RT-PCR amplification steps. The sequence analyses of six independent transformants carrying the ODC gene amplified from the human prostate c-DNA library using Expand high fidelity polymerase showed that the $Glu^{417} \rightarrow Gln^{417}$ change was not introduced during PCR amplification steps. Alignment of the ODC gene with database human ODC sequences confirmed that the amplified gene is an allele of ODC. In addition the most important residues for ODC activity are Lys^{69}, Cys^{360} and Asp^{361} (Tobias and Kahana, 1993; Osterman *et al*., 1995; Almrud *et al*., 2000). Variants mutated in these amino acids revealed that each one is required for full catalytic activity (Osterman *et al*., 1995; Toney and Kirsch, 1993; Coleman *et al*., 1993). The Glu^{417} is not involved in the catalytic site of the ODC enzyme suggesting that this point mutation does not abolish the enzymatic activity. Therefore the amplified human ODC gene was considered for further analyses. The analysis of ODC enzymatic activity in T_2 stable transformed plants overexpressing human ODC in apoplast showed that this point mutation did not affect the enzymatic activity.

The plant ODC is localized in cytosol, but has also been reported to be present in the nucleus, vacuole and mitochondria. Nevertheless, these data have to be interpreted with caution, because of the limitations of the subcellular fractionation studies and the electron microscopic autoradiography methods (Slocum, 1991). So far, overexpression of ODC has been only reported in plant cytosol (Bastola and Minocha, 1995; Andersen *et al*., 1998; Lepri *et al*., 2001). To investigate the stability and the activity of ODC in different plant cell compartments the human ODC gene was cloned into different pSS vector constructs suitable for expressing the recombinant protein in the plant cytosol, the apoplast and endoplasmic reticulum (ER) (III.4.1.1). Successful overexpression of functional enzymes in ‘‘non native’’ compartments may provide an additional alternative for polyamine pathway manipulation. Taking into consideration that ODC is a cytosolic protein the pSS: ODC-cyt construct was generated assuming that this would be the best environment for high level of accumulation and activity. Immunoblot analysis showed expression of human ODC protein in the plant cytosol and apoplasm with higher levels in the cytosol, while ER targeted ODC was not detected in Western blot assays. Northern blot analyses, however, showed that the level of ODC mRNA was similar for apoplastic and ER transcripts

demonstrating that transcript stability is not the reason for the observed difference. The failure to detect the ER targeted ODC could be the lower sensitivity of the anti-KDEL antibody compared to the anti-c-myc antibody. This assumption could be investigated by adding a tag to the ER construct for which a more sensitive detection antibody is available. Alternatively the stability of the protein in the ER might be lower than in the apoplast leading to low accumulation levels.

The transient state of transgene accumulation in vacuum-infiltrated leaves may not be fully comparable to results after stable integration into tobacco chromosomes and extended screening of different individual lines. However, data from transient and stable transformation experiments of different recombinant proteins indicate that the accumulation levels observed in agrobacterium-infiltrated leaves correlate to those obtained in best expressing lines. In addition, transient expression is not influenced by positional effects that potentially bias gene expression levels in stable transformed plants (Kapila *et al*., 1996; Schalthof *et al*., 1996). Therefore, transient gene expression seems particularly suited for rapidly verifying a gene construct and the gene product before moving into transgenic plants (Kapila *et al*., 1996; Fischer *et al*., 1999c).

Stable transgenic tobacco plants were generated only for the cytosolic and apoplastic targeted ODC. Generation of stable plants retaining the ODC in ER was not considered since the ER accumulation of ODC in transient assays was below the detection limit.

Western blot analyses showed that 15 out of 22 and 16 out of 23 independent transgenic lines expressed the human ODC in the apoplast and cytosol, respectively. Higher expression was observed in tobacco plants expressing the ODC in cytosol, the native compartment of ODC. Two ‘‘apoplastic’’ and four ‘‘cytosolic’’ lines with the highest level of expression were selected and self pollinated for establishment of homozygous lines. Further screening was carried out in the T_1 and T_2 generation to identify the lines with the highest accumulation levels.

The accumulation levels of the best expressing lines correlated with the accumulation levels obtained in the transient agroinfiltration thereby corroborating the suitability of transient expression to indicate the levels obtained in stable transformants.

IV.2 Enzymatic activity and polyamine analyses of stable transformed plants overexpressing human ODC

Seeds of the ODC-apo-7/3-T_1-line that showed the highest level of ODC protein accumulation in apoplast were selected on kanamycin and six resistant, individual T_2-plants were tested for ODC activity. For analysing enzymatic activity young leaves were chosen because it was reported that ODC expression is low in mature leaves (Kwak and

Lee, 2001). To exclude errors due to assay variation four replicates were analyzed. The control values were determined by analyzing 4 different SR1 wild type tobacco plants grown under the comparable conditions. The ODC enzymatic activity of the transgenic lines was 1.6- to 32-fold higher than in wild type plants. Although significantly higher amounts ($P<0.05$) of ODC activity were observed in all transgenic plants compared to the wild type controls, the enzyme activity varied significantly in different transgenic lines (Figure III-14). No variation was observed between the four different control plants. Such variations in transgene activity regulated by the CaMV 35S promoter are quite common (Nagata *et al*., 1987; Hamill *et al*., 1990; Fecker *et al*., 1993; Bastola and Minocha, 1995; Noury *et al*., 2000). Variations of ODC activity in different transgenic lines could also be due to different sites of integration of the foreign gene in the plant genome and its copy number. Therefore, Southern analyses may be necessary to determine the gene copy number.

The 1.6- to 32-fold increase of the enzymatic activity proofs that the mutation is not compromising the enzymatic activity. In addition the C-terminal addition of the c-myc epitope and hexa histidine tag for detection and/or purification does not interfere with enzymatic activity. However no studies have been done to investigate if these modifications affect the stability and/or activity of human ODC. A detailed analysis of the properties of the recombinant plant-expressed human ODC could be done after purification of his-tagged protein using IMAC.

To investigate if overexpression of human ornithine decarboxylase in a ‘‘non native compartment’’ affects the polyamine pools free levels of putrescine, spermidine and spermine were analysed. Six individual T2 plants of the GR1-7/3 line were analysed. As observed for the enzyme activities the levels of free polyamines varied significantly among individual transgenic plants. In addition polyamine levels were slightly dependent on the developmental stage of the tissues with higher amounts in young leaves. There was a significant 4-5.6 fold increase ($P<0.05$) of putrescine levels in all transgenic lines expressing apoplastic ODC compared to wild type SR1 control plants (III.5.1).

Elevated levels of ODC activity and putrescine were caused by the presence of the transgene indicating that the polyamine biosynthesis machinery was functional at the DNA, RNA and enzymatic level. However a direct correlation of enzyme activity to putrescine levels could not be done because it was not possible to analyse the same individual plants for both parameters. Nevertheless the results and the model of the polyamine biosynthesis strongly suggest that this correlation exist.

However, the increased putrescine levels did not result in elevated spermidine and spermine accumulation.

The results of this study are in line with results from the overexpression experiments of human ODC in mouse (Halmekytö *et al*., 1991), yeast ODC in hairy root cultures of *N. hesperis* (Hamill *et al*., 1990) and mouse ODC in tobacco (DeSenzo and Minocha, 1993). None of the ODC overexpressing systems produced a significant change in spermidine and spermine accumulation. Increased ODC activity in transgenic mice overexpressing human ODC did i.e. not result in a general increase in putrescine levels except in testes and brain (Halmekytö et al., 1993). Similarly, overexpression of yeast ODC in *N. hesperis* did not significantly increase putrescine levels (Hamill *et al*., 1990) and overexpression of mouse ODC in tobacco increased putrescine accumulation 2.5-fold in the most extreme case (DeSenzo and Minocha, 1993). Conversely, Lepri *et al*. (2001) reported that overexpression of a cDNA for human ODC gene in transgenic rice plants under the control of Ubi-1 exhibit significant changes in the levels of all three major polyamines in seeds and also in vegetative tissues. Increased ODC activity and putrescine levels might result in an increase in alkaloid production via putrescine. Nicotine is synthesized in the roots and transported to the leaves (Hibi *et al*., 1994). Hamill *et al*. (1990) reported that overexpression of yeast ODC in hairy root cultures of *Nicotiana hesperis* resulted in a slight increase (less then 2-fold) in nicotine accumulation.

IV.3 Polyamine analyses of transgenic tobacco plants co-expressing apoplasmic ODC and SDE enzymes

Previous studies (Hamill *et al*., 1990; DeSenzo and Minocha, 1993; Bastola and Minocha, 1995) indicated that increased ODC activity by overexpression of recombinant ODC gene is apparently not adequate to increase spermidine and spermine levels. It was then concluded that the polyamine pathway is tightly controlled and the system adjusts by regulation of other parts.

For this reason stable transformed lines co-expressing human ODC and chimeric human-mouse SDE enzymes were generated (III.4.3). Up to date this is the first study attempting to modulate the polyamine pathway by simultaneous expression of two enzymes involved in polyamine synthesis. Western blot analyses revealed that more than 80% of the lines tested co-expressed both enzymes. Despite the expression of both enzymes no change in growth and phenotypic appearance was observed compared to wild type plants. When free polyamine levels in four transgenic plants were measured, significantly higher ($P<0.05$) putrescine and spermidine levels were observed compared to SR1 control plants.

The parental transgenic plants overexpressing SDE were not analysed for their spermidine levels. However, Western blot experiments verified high SDE accumulation levels in the parental lines. In contrast the level of SDE in the crossed lines (ODCxSDE) was significantly lower than in the parental lines.

It is reasonable to postulate that increase in ODC and SDE enzyme activity cause this significant increase in putrescine and spermidine levels. However, spermine values were not altered. This could either indicate that catabolic enzymes such as PAO were activated to keep spermine levels low compensating accumulation of putrescine and spermidine or higher levels of spermine synthase is needed to bring the reaction forward.

The polyamine pathway is tightly regulated and it is very sensitive to changes in end product accumulation (Burtin and Michael, 1997). Consequently, there is a general notion that it is unlikely that any major changes in PA accumulation can be achieved. Previous experiments have indicated that a key element for changing polyamine levels in transgenic tissues is the strength of the promoter used to drive expression of transgenes (Capell *et al*., 1998; Bassie *et al*., 2000). The CaMV 35S promoter used in this study is a strong promoter for driving heterolous transgene expression in tobacco (Töpfer *et al*., 1988; Kay *et al*., 1987; Becker, 1990). The constitutive overexpression of the human ODC in apoplast appears to be sufficient to increase the putrescine pool, but a tight control of the polyamine pathway on the rate of spermidine and spermine synthesis does not lead to an accumulation of spermidine and spermine. The constitutive co-expression of ODC and SDE enzymes results in increased levels of putrescine and spermidine suggesting that the pathway can be brought ‘‘forward’’ by increasing the levels of subsequent enzymes. Due to time constrains no further crossing of stable transformed plants could be performed. However, in the future a cross between the stable transformed tobacco lines expressing SME and stable transformed tobacco co-expressing ODC and SDE is suggested. In case the spermine levels will be increased, this would indicate that the polyamine levels are not as tightly controlled as thought or that metabolic pathways cannot respond to an increase of polyamines.

This study shed further light on the complexity of polyamine biosynthesis in intact plants providing a basis for further manipulations of the pathway using additional genes of the pathway.

IV.4 Generation and Characterization of scFv-fragments specific to ADC, ODC and PAO

In this study arginine decarboxylase (ADC), ornithine decarboxylase (ODC) and polyamine oxidase (PAO) were chosen as antigens for generation of specific scFv antibody fragments. These proteins were chosen because they present key enzymes of the polyamine pathway. ADC and ODC convert L-arginine and L-ornithine, respectively to putrescine. The flavoprotein PAO deaminates oxidatively the higher polyamines such as spermidine and spermine. The idea was to immunomodulate ADC and ODC which might then result in increased levels of putrescine by improving their stability and catalytic activity.

Antibodies that inhibit PAO function might, on the other hand, increase spermidine and spermine levels by blocking their degradation.

So far, almost all antibodies that have been used for intracellular immunization derived from classical hybridoma technology. However, this technology is expensive and time-consuming resulting in scFv that express badly in the cytosol (McCafferty *et al*., 1990; Hoogenboom *et al*., 1991). Phage display technology, on the other hand allows the isolation of recombinant antibodies of the desired specificity *in vitro* directly from established libraries or from the spleen of immunized mice, thus obviating the need for hybridoma production. In this study, the phage display technology was used to provide high affinity antibodies against the above mentioned enzymes from antibody libraries of immunized mice.

Important for immunomodulation is the targeting of the recombinant antibody to the right subcelluar compartment were it should retain antigen binding activity. Therefore, the antibody has to be co-localised where the antigen is residing. Because ODC is localised in the cytosol, PAO in the cell walls and ADC in the chloroplast, scFv fragments (Bird *et al*., 1988; Huston *et al*., 1988) were chosen as recombinant antibody format. ScFv-fragments have lesser requirements for folding and assembly and have successfully been expressed in the reducing environment of the plant cytosol (Fecker *et al*., 1996; De Jaeger *et al*., 1999; Zimmermann *et al*., 1998) while accumulation of larger fragments like Fab or full size antibodies is not possible. Moreover, scFv-fragments can also be easily expressed in *E. coli* and are suitable for phage display, facilitating selection, identification and characterization of potential binding molecules.

IV.4.1 Expression and purification of recombinant antigens

To obtain polyamine proteins for immunization, panning and scFv characterization the ADC, ODC and PAO cDNAs were genetically fused to the carboxyl-terminal end of GST (III.2). Using GST as fusion partner allowed one step affinity purification of the fusion proteins under native conditions (Frangioni and Neel, 1993). Overexpression of all GST-fusion proteins resulted in formation of inclusion bodies. Thus, for altering amounts of soluble and correctly folded protein the culturing and induction conditions had to be optimized. Larger quantities of soluble ADC-GST and ODC-GST fusion proteins were obtained by increasing the culture volume, decreasing the IPTG concentration to 0.05 mM, increasing the induction time to 8 hrs and reducing the temperature to 18°C after induction. The positive effect of low temperature to reduce inclusion body formation has been demonstrated in many studies (Bishia *et al*., 1987; Schein, 1989; Burton *et al*., 1991). The rationale behind was based on the assumption that the rate of protein folding is only slightly affected at temperatures between 15 to 20°C, whereas the rates of transcription and

translation, being biochemical reactions, is substantially decreased. This, in turn provided sufficient time for protein folding, yielding active proteins and avoiding the formation of inactive protein aggregates, i.e., inclusion bodies, without reducing the final yield of the target protein (Oppenheim *et al*., 1996). The yields of purified ADC cleaved from GST domain with Factor Xa and ODC-GST fusion proteins after optimization were 2.0 and 1.5 mg per liter culture, respectively. Affinity purified proteins showed high purity in SDS-PAGE. In contrast, no soluble PAO fusion could be obtained even after optimizing the conditions suggesting that the formation of PAO inclusion bodies was not affected by the expression conditions used. The large size of the PAO-GST (83 kDa) could effect the proper refolding of the fusion protein as reported in other studies (Hackenbeck *et al*., 1998).

In some cases the change of expression vector or compartment can lead to soluble expression. Therefore the PAO gene was cloned into pET22b vector for periplasmic expression. Since the periplasm contains only 4% of the total cell protein (Nossal and Heppel, 1966) the target protein is effectively concentrated, and could be purified with less contaminants. In addition the oxidizing environment of the periplasm facilitates the proper folding of proteins. *In vivo* cleavage of the signal peptide during translocation to the periplasm is more likely to yield the authentic N terminus of the target protein. Protein degradation in the periplasm is also less extensive (Talmadge and Gilbert, 1982). However, attempts to express PAO in a soluble form failed, presumably *via* the aggregation of a folding intermediate. The yield of IMAC purified PAO under native conditions was very low. No reports so far are published describing a successful expression and purification of recombinant PAO.

IV.4.2 Immunization of mice with ADC, ODC-GST and PAO-GST inclusion bodies

The isolation of specific antibodies from a cloned immunological repertoire requires a large, diverse library, as well as an efficient selection procedure. The key to achieve this goal is the generation of a good immune response, isolation of high quality RNA and efficient cDNA synthesis from which the library is constructed.

Mice were immunized with ADC, ODC fusion proteins and PAO-GST inclusion bodies. A high serum antibody titer against the injected antigen usually indicates enrichment of an antigen-specific cell clone. Serum titers from immunized mice against ADC and PAO ranged between 1:120,000-150,000, while the anti-ODC antisera titer ranged between 1:60,000-70,000. The ODC protein is highly conserved in mammalians showing more than 90% homology between human and mouse. This could render a limited immune response in mouse due to immunologic tolerance invoked during fetal development (Barbas *et al*.,

2001) which would explain the low immunogenicity of human ODC in mice. The oat ADC and maize PAO were more immunogenic because they have a low homology with mammalian enzymes (Li *et al*., 1994; Tavladoraki *et al*., 1998; Bagni and Tassoni, 2001). Serum from mice immunized with ADC exhibited no cross reactivity against GST, indicating complete cleavage of the fusion partner by Factor Xa. Cross reactivity with GST was observed for serum from mice immunized with ODC-GST fusion protein and PAO-GST inclusion bodies. However, as shown in the ELISA experiments with the recombinant proteins expressed from pET22b vector the immune response against the ODC and PAO domain were greater than against GST carrier protein.

IV.4.3 Phage displayed antibody selection

For each target antigen a complex scFv-phage display library was generated from the spleen cells of immunized mice. The library sizes were $3.2x10^7$, $2.6x10^6$ and $1.4x10^6$ for ADC, ODC and PAO respectively (III.8.3). Previous studies have shown that the success of selection experiments depends to a large extent on the quality of the library. Complexity is a major factor determining the quality of a library and its complexity (Rader *et al*., 2001). The greater the complexity the higher is the possibility to select scFvs of the required affinity and/or specificity. Although the constructed phage display libraries were not very large, selection of specific, high affinity binders was anticipated from these libraries since: -an immunized source was used for library construction where affinity maturation and clonal expansion had already taken place; -the percentage of positive clones carrying a full size scFv fragment was high (86.6% for ADC, 87.5% for ODC and 100% for PAO); -analyses by *Bst*NI fingerprinting showed diverse RFLP pattern for all libraries.

Phage display is most successful when a purified antigen is used for selection. Selections on impure antigens are significantly more difficult, due to the problem of the limited amount of target antigen present in the mixture, and the enrichment of phage antibodies specific to non-relevant antigen (Hoogenboom *et al*., 1998). Because the purification of soluble PAO recombinant protein failed panning of library HP_1LP_1 was postponed. Work was continued with HA_1LA_2 and HO_1LO_2 libraries which were panned against purified ADC-GST and ODC-GST antigens.

Phage antibody library selection was carried out using antigens directly coated on a plastic surface (immunotubes). This method was chosen since it is easy to perform, has been shown to be very successful for a diverse set of antigens (for review see Winter *et al*., 1994) and does not require antigen biotinylation. The biotin is attached to the functional groups that are surface exposed and often reside in selection of binders that recognize only the biotinylated protein. Liquid phase panning using delayed infectivity panning selection

(DIP), biotinylated antigen and indirect coating (Dierks *et al*., 1986; Hawkins *et al*., 1992; Grob *et al*., 1998; Benhar *et al*., 2000; Chames et al., 2001) was regarded as an alternative backup strategy if no enrichment of specifically binding phages or/and characterization of isolated candidates would indicate the need for isolating higher affinity binders. Since suitable candidates have been successfully isolated from these libraries the alternative approaches were not performed.

For both libraries three rounds of selection were performed by panning on immunotubes coated with the antigen as recommended by Vaughan *et al*., (1996). Zhang *et al*., (2001) have reported selection of GST specific binders when using GST as a fusion partner Therefore soluble GST was incubated with phage pools before each round of panning. The presence of false and low-specificity binders was eliminated by applying more stringent washing conditions in panning (De Bruin *et al*., 1999) and by blocking the phage with milk proteins prior to selection.

The enrichment of ODC and ADC specific binders was followed by monitoring the ratio of input/output phage in each cycle. In the third round of panning the number of eluted phages was increased 152-fold for library HA_1LA_1 and 382-fold for library HO_1LO_1 compared to the number of phages eluted in the first round indicating enrichment of specific binding clones.

The integrity of the full size insert was verified in both libraries throughout the panning process. For the HA_1LA_1 library an increase of phages without scFv insert was observed between the first and the second round of panning. Plasmids carrying nonproductive, aberrant or truncated antibody fragments encoding sequences are often preferred by the *E. coli* host and frequently have a growth advantage over the scFv-expressing clones (Seehaus *et al*., 1992; Courtney *et al*., 1995; Dziegiel *et al*., 1995). This phenomenon seems to be related to the stringency of the washing procedures during the panning. Recovery of insert free phages is an indication of too low stringency of the washing procedures (Tur *et al*., 2001). Here, such clones were eliminated by applying more stringent washing and elution conditions. Therefore 95% of the eluted phages carried a full size insert after the third round of panning.

The diversity of the libraries was determined after each round of panning. The RFLP pattern of randomly selected clones revealed the presence of two and four unique patterns for ADC and ODC, respectively suggesting the efficient enrichment of specific clones.

For a first screen, soluble ELISA-based assays were used in combination with PCR and *Bst*NI fingerprinting to identify positive scFv-fragments (Marks *et al*., 1991). As indicated previously (Iacono-Connors, 1994; Murthy *et al*., 1999; Zhang, 2000) the ELISA method used for the recombinant phage characterization is critical for excluding false positives. Therefore, fifteen scFv-fragments with the highest ELISA readings and with different

RFLP patterns were selected for further characterization to increase the likelihood of selecting different DNA sequences. Their reactivity and functionality was assayed in direct and capture ELISA tests to avoid false positives. All clones analyzed from both libraries showed specific binding to ADC-GST and ODC-GST respectively. No cross reactivity to GST was observed in direct and capture ELISA tests. These results are in line with results from Songsivilai and Dharakul, (1998) who successfully used GST fusion proteins for selection of specific scFv against hepatitis C virus nucleocapsid protein by antibody phage display technology. Conversely, Zhang *et al*. (2001) described selection of false positives when GST fusion proteins were used for selection of antibodies specific to viral movement protein (TSWV). A similar phenomenon was observed by Murthy *et al*. (1999) while identifying a consensus motif specific for the PDZ2 domain of a cytosolic protein tyrosine phosphatase by peptide phage display.

Sequence analyses of fifteen selected mouse derived scFvs specific to ODC showed that all scFv-fragments were in frame with the cloning module and belonged to four different sequence groups. Four clones scFvODC1, scFvODC3, scFvODC7 and scFvODC15 were chosen from each sequence group for further analyses. Sequence alignment with the Kabat database showed that the heavy and light chain variable domains of selected ODC-specific scFvs were members of the murine family V_H1 and Vκ1/Vκ10 light chain respectively (Table III-6).

ScFvODC1-like antibodies dominated the mouse immune response sharing only 72% similarity with scFvODC3, 7 and 15. The sequence variation between scFvODC1 and scFvODC3, 7 and 15 could be the result of the diversity generated by somatic recombination as indicated by alignment of scFvODCs variable sequences with the nearest germline V-gene segments listed in the IMGT database. Additionally, some sequence variation at the N terminus of both light and heavy chain may have been introduced by degenerate primers used for cloning (H5: Val, Gln; L4: Ile, Val; L5: Gln, Leu or Val), while the internal variations may have resulted from somatic mutations or from errors introduced during PCR amplifications.

Comparison of the V_H sequence of the scFvODC1 with the nearest germline V-gene segments (X02459) indicated large differences, both at the nucleotide (49) and amino acid (22) level. These amino acid differences were mainly distributed between CDRH1, CDRH2, FR2 and FR3 representing an affinity maturated clone that arose through somatic mutation/antigen selection.

The variable heavy chain of the scFvODC3; 7 and 15 were most homologous to the AF304556 germline gene segment exhibiting a ratio of replacement to silent substitutions ranging from 3:1 to 6:1, respectively. The majority of the replacement substitutions fall within CDR1, CDR2 and FR3 with occasional changes in the FR1 and FR2 suggestive of an antigen-driven selection of the same maturated B-cell since somatic hypermutation of

antibody genes is triggered only after antigen-induced B-cell proliferation (Griffiths *et al*., 1984).

Furthermore, the homology between the scFvODC7 and 15 heavy chains and the scFvODC3 and 7 light chains respectively could be explained by mutations on an original V_H and V_L introduced during the PCR since low-fidelity polymerase such as *Taq* DNA polymerase was used to amplify the variable fragments. Although most of the mutations were neutral or detrimental, a small fraction could have improved the affinity of the scFvs for the target, and/or the folding or stability of a member, thereby yielding an advantage for this mutant in the next selection cycle (Schaffitzel and Plückthun, 2001).

Sequence analyses of fourteen selected scFvs specific for ADC showed that all scFv-fragments had open reading frames comprising two different sequences (proof by RFLP pattern). The most abundant scFv-fragment, was present in thirteen of the clones sequenced (13/14). This could be due to its predominant presence in the immune response of mouse or to its preferential amplification by PCR or phage multiplication as shown by Burmester and Plückthun, (2001) or due to the overselection of the library. Two clones scFvADC3 and scFvADC7 that shared 55.9% identity and 65% similarity were selected for further analyses. Sequence alignment with the Kabat database showed that V_H of the scFvADC3 and 7 belonged to the murine V5 and V1 family. The V_L is member of V9 and V4 of murine κ light chain respectively.

The comparison of V_H fragment of scFvADC3 with its nearest V germline gene fragments (AF120474) showed very large differences both in nucleotide and amino acid levels mainly distributed in the FR3 region. These mutations that possibly arose through somatic hypermutations could have an important positive effect on antibody affinity and stability considering that the scFvADC3 was the most abundant scFv specific to ADC selected. Most of the differences observed between the VH fragment of scFvADC7 and its closest germline gene segments (AF304556) were mainly distributed in CDR1, CDR2 and FR3 with occasional changes in the FR1.

The sequence analyses of both scFvADCs suggested the presence of two different affinity maturated clones arose by random rearrangment of antibody gene fragments and somatic hypermutations.

IV.4.4 Expression and purification of scFvs in *E. coli*

Since the production of functional recombinant antibody fragments in *E. coli* was first described (Skerra and Plückthun, 1988) it has become the method of choice in a variety of applications, ranging from immunochemical analyses to therapeutic treatment. The

bacterial synthesis of antibody fragments provides important advantages mainly due to facile handling of the prokaryotic organism (Fiedler and Skerra, 2001).

An important strategy for production of scFvs-fragments in *E. coli* is their secretion to the periplasmic space as it permits the production of soluble and functional proteins with correctly formed disulfide bonds. Therefore the scFvODC1; 3; 7 and 15 and scFvADC3 and 7 were cloned in pSyn vector preceded by a pelB leader sequence (Lei *et al*., 1987). Soluble scFv fragments were produced by induction with IPTG in *E. coli* HB2151. Immunoblots showed distinct bands with the expected molecular weight of about 28 kDa. The yield of purified scFvs was relatively high and ranged between 1.5-2.7 mg/L culture volume. Previous studies have indicated that bacterial expression systems secreting scFvs into the periplasmic space give typical yields of 0.1-2 mg/l in shake flask cultures for many scFv fragments. However, success of expressing antibody fragments in *E. coli* depends on the properties of the variable domain sequences and structure (Plückthun *et al*., 1996) and expression levels can vary widely for different antibody fragments. The relatively high yield of the scFvs in this study could be related with the particular amino acids located in the positions H6, H7 and H10 (H9) of the FR1 segment of the V_H domain. Particularly the residue in the position H6, a buried glutamine or glutamate residue, has been found to have a strong effect on antibody yield and functionality (Kipriyanov *et al*., 1997; de Haard *et al*., 1998; Langedijil *et al*., 1998). Honegger and Plückthun (2001) indicated that the mutations in the N-terminal part of FR1 of the V_H domain introduced by PCR cloning using degenerate primers can lead to severe impairment of production yield, stability and antigen binding. Gln H6 is relatively permissive concerning the identity of the amino acids in the position H7 and H10 (H9), while Glu has more stringent requirements: H7 cannot be a proline residue and H10 (H9) requires a positive phi torsion angle compatible only with a glycine residue in this position (Honegger and Plückthun, 2001). The PCR-induced substitutions of Gln H6 by Glu decreased the production yield of the scFv derived from the murine hybridoma OKT3 30-fold, while antigen binding was not affected (Kipriyanov *et al*., 1997). The scFvODCs and scFvADC7 share Gln residues at this position showing a high expression levels in bacterial periplasm. The scFvADC3 has Glu residues at the H6 position revealing a notable difference in the production yields of the scFvADC3 (Glu at H6) compare to scFvADC7 (Gln at H6). However, the presence of serine and glycine residues at the H7 and H9 position respectively could lead in relatively high expression levels.

IV.4.5 Characterization of engineered scFvs

The reactivity of affinity purified scFvODC1; 3; 7; and 15 with ODC antigen was analysed in direct ELISA tests (III.10.3). Comparative analyses of the reactivity of the affinity

purified scFvs to ODC-GST and GST indicated that scFvODC1; 3 and 7 had a high specific reactivity to the ODC and did not cross react to GST. Although the scFvODC15 did not show a high reactivity to the antigen, its signal to noise ratio (482) indicated a high specificity to ODC. Therefore the four selected scFv specific to ODC were further characterized.

The specific reactivity of scFvADC3 and scFvADC7 to ADC antigen was also directly compared indicating that scFvADC7 had a two fold higher reactivity to ADC.

In EMSA, complex formation with ODC-GST was observed between the scFvODC1 and scFvODC3. Both scFvs were completely shifted demonstrating that IMAC purified scFvs were fully functional. ELISA assays are not capable of revealing this information unless a standard probe is used for calibration and the concentration of the purified scFv's. Unfortunately for the scFvODC7 and scFvODC15 EMSA was not successful so further analyses are necessary. Therefore only scFvODC1 and 3 were considered for further *in vivo* analyses.

The binding properties of the scFvODC1 on the soluble antigen were further verified by competition in solution monitored by surface plasmon resonance (III.10.5). Binding of soluble scFv to immobilized ODC-GST was completely inhibited by addition of excess amounts of soluble ODC-GST confirming the previous EMSA results and clearly proving that the scFv recognized the antigen in solution in a dose-dependent fashion. These experiments indirectly demonstrated that the scFvODC1 recognize an epitope present in the native confirmation of the ODC antigen. This was of special concern since the passive adsorption of the antigen to the plastic surface of immunotubes could result in the complete denaturation of the bound protein and loss of the conformational epitopes. Under these conditions, 95% of adsorbed proteins are not functional (Butler *et al*., 1992; Davies *et al*., 1994) and the phage antibodies binding to epitopes only present in denaturated molecules could be selected (Chames *et al*., 2001).

The determination of the epitope specificity was an important part of the scFv characterization. The selected scFvs were analyzed whether they recognize overlapping epitopes by pair wise epitope mapping. Epitopes recognized by the two scFvADC3 and scFvADC7 were analysed by competition to ADC-GST antigen in ELISA experiments. Because both scFvADCs carried the same detection tags biotinylation of scFvADC3 was necessary for discriminating between the different scFvs. No competition was observed between the biotinylated scFvADC3 and scFvADC7 and therefore it was concluded that they recognize independent epitopes. Thus, without additional information available both scFvADCs were considered for further *in vivo* analyses in transgenic plants.

The pair wise epitope mapping of four generated scFvs specific to ODC was performed by surface plasmon resonance analyzes using immobilized scFv. This approach has the

advantage that whenever binding of the antigen to the immobilized scFv occurs this particular epitope is blocked. In contrast, a setup where the antigen is immobilized and the scFvs are serially injected is not optimal for two reasons. First, high scFv concentration have to be used to saturate all binding sites. Second, when the antigen-scFv interaction is characterized by fast off-rates, binding sites could become available for the second scFv affecting the reliability of the analyses.

The pair wise epitope mapping revealed that scFvODC3 had an overlapping epitope with scFvODC7 and scFvODC15. This may be explained either by the fact that these scFvs may belong to the same original B-cell population or their striking homology in the CDR3. ScFvODC1 recognized a distinct epitope to scFvODC3, 7 and 15. Further analyses are needed to proof whether the scFvODC3, 7 and 15 bind to overlapping or identical epitopes and their effect on the enzymatic activity of ODC.

After selection of high affinity from the low affinity scFv fragments, it was important to differentiate their binding kinetic. Preliminary experiments indicated an estimated K_d value of $5.0x10^{-7}$ M and $2.5x10^{-7}$ M for scFvODC1 and scFvODC3, respectively (data not shown). Despite several attempts, a precise determination of the affinity constant was not possible. Association and dissociation rate determination on the BIAcore device of scFv fragments is difficult due to the problem of multimerization behavior inherent to many scFv formats which complicates measurements of the antigen binding kinetics of scFv fragments as shown for other studies (Plückthun and Pack, 1997). The presence of monomeric and dimeric forms in affinity purified ODC-specific scFvs was revealed by gel filtration chromatography analyses (III.10.2). scFv fragments can associate to form dimers in bacterial supernatants (Griffiths *et al*., 1993; Holliger *et al*., 1993), and the dimers have higher binding avidity especially to solid phase (immobilized) antigen (Griffiths *et al*., 1993). Purification can also lead to the formation of multimers (Nissim *et al*., 1994). Presumably multimerisation is promoted by dissociation of V_H and V_L chain domains of the same chain, followed by pairing with another chain, especially during acid elution and neutralization in concentrated solutions. The phenomenon of dimerization or even higher oligomerization of scFv fragments has been reported previously (Essig *et al*., 1993; Griffiths *et al*., 1993; Whitlow *et al*., 1993; Kortt *et al*., 1994; Raag and Whitlow, 1995) and has been investigated in the context of the linker length and the scFv properties (Alfthan *et al*., 1995; Turner *et al*., 1997).

In addition, the affinity measurements are even more complicated when the antigen is present in multimeric forms as shown for the ODC-GST protein in the gel filtration analyses (data not shown).

IV.4.6 Generation of stable transformed tobacco plants overexpressing ODC-specific scFvs

Because of the complexity of the ODC activity regulation, a full understanding of the effect of the generated scFvs on the polyamine pathway can only be studied *in vivo*. However, *in vitro* assays for testing the effect of selected scFv fragments on the ODC activity are crucial prior to *in vivo* experiments. Therefore, scFvODC1 and scFvODC3 that recognize different epitopes on the ODC enzyme and shown to be fully functional in EMSA were chosen for *in vitro* assays. Both scFvs stabilized the activity of the human ODC in a dose dependent manner. Incubation with scFvODC1 and scFvODC3 increased the enzymatic activity of bacterial purified human ODC 16-75% and 25-92%, respectively. *In vitro* results indicated that scFvODC1 and scFvODC3 could be good candidates for the immunomodulation approach and further *in vivo* characterisation. Furthermore, the effect upon addition of two scFvs (scFvODC1 and scFvODC3) would be worth invenstigating, as well as enzyme crosslinking by bivalent diabodies or bispecific antibodies.

Since ODC enzyme is localized in the cytosol, co-localization of the scFvODCs in this plant cell compartment is necessary for the immunomodulation approach. To immunomodulate the ODC activity in the plant cytosol, the scFv fragments must be stable and functional in a reducing environment. Accumulation of scFvs in the cytosol is not straightforward due to the reducing conditions and the absence of protein disulphide isomerase and chaperones. In the majority of reported transgenic plants expressing cytosolic scFvs, levels were found to be very low or at the detection limit (Bruyns *et al*., 1996; Fecker *et al*., 1996; Owen *et al*., 1992; Schouten *et al*., 1996; Tavladoraki *et al*., 1993). Two exceptions were reported by De Jaeger *et al*. (1999) and Zhang (2000) in which cytosolic scFvs have accumulated to levels of up to 1% and 8% of total soluble protein, respectively. Preclusion of the scFv intradomain disulfide bridges often results in a loss of stability and antigen binding activity of the scFvs in the plant cytosol. However, examples of scFv fragments that are stable and able to bind their antigen without disulfide bridges have been described. The scFvODC1 and scFvODC3 were tested for their accumulation levels and functionality in the plant cytosol. Transient expression experiments showed high accumulation levels (50-70 μg/g fresh weight) of the scFvODC1 and scFvODC3 in the plant cytosol. Furthermore, ELISA results indicated that both scFvs retained antigen binding specificity and activity in the reducing environment of the plant cytosol. However, these results have to be interpreted carefully. Because ELISA was not performed under reducing conditions, it cannot be excluded that binding in ELISA occurs upon the formation of disulfide bonds *in vitro*. Nevertheless, the combined results from the *in vitro* enzyme assay and high accumulation levels of the functional scFvODC1 and scFvODC3 in the plant cytosol show that these scFv fragments are possible candidates for interfering with *in vivo* ODC activity and polyamine pathway and will be further

characterised in transgenic plants. Additionally, co-expression of cytosolic scFvODC1 and scFvODC3 in a monovalent, bivalent or bispecific form may be interesting to invenstigate their biological effect *in planta*.

Since ODC was expressed as an active enzyme in the apoplast, the apoplast was chosen as an alternative model to study the *in vivo* activity of scFvsODC. This experimental setup will indicate if any of the generated scFvODCs is capable of inhibiting or stabilizing the activity of human ODC.

However, a prerequisite of such a study was the generation of stable transformed tobacco plants targeting the scFvODC fragments to the apoplast. Therefore a straightforward approach was pursued to generate transgenic tobacco plants co-expressing both the polyamine enzymes and scFv fragments. Two scFvODC fragments (scFvODC1 and scFvODC3) that recognize different epitopes in ODC enzyme and shown to be fully functional in EMSA assays were targeted to the apoplast under control of the *35S* enhanced cauliflower mosaic virus promoter. Constructs retaining the scFvs in ER were generated in parallel and used as control. Transient expression method was used to quickly assess the scFv accumulation in tobacco plants before establishing transgenic plants. Western blot analyses confirmed the high levels of accumulation of scFvODC1 and scFvODC3 in the apoplast and ER. Following transient expression experiments stable transformed tobacco plants overexpressing the scFvODC1 and scFvODC3 in the apoplast were regenerated. The effect of the scFv expression on the immunomodulation of ODC will be studied by analyses of ODC enzymatic activity and free polyamine levels. Functional studies with stable transformed plants are ongoing.

In recent years, several reports have proven the value of the immunomodulation in plant research to modulate phytohormone activity and to block plant pathogen infection (De Jaeger et al., 2000; Conrad and Manteuffel, 2001). However, successful trials of immunomodulation of enzyme activity in plants have not yet reported, despite the success of this approach in mammalian cells (Marasco, 1995; Lener et al., 2000). Furthermore, only a few articles have been published dealing with the modulation of protein function in transgenic plants. One example is phytochrome, a plant regulatory receptor protein, whose activity has been changed by immunomodulation (Owen *et al*., 1992). Seeds of one homozygous transgenic tobacco line displayed an aberrant phytochrome mediated photocontrol of germination. On the other hand immunomodulation of flower pigment synthesis in *Petunia hybrida* was not successful (De Jaeger *et al*., 1999), although five different murine scFv against dihydroflavonol-4-reductase (DFR) were accumulated in the cytosol of transgenic plants. Recently, a specific scFv has been produced using phage display technology against CDC2a of *Arabidopsis* (Eckhout et al., 2000), which is a key regulator of the cell cycle in plants. This specific scFv against CDC2a was transiently

expressed in the cytosol of tobacco leaves and could recognize the antigen *in vitro*. Functional studies with stable transformed plants are still ongoing.

IV.5 Conclusion and future prospects

Data presented in this study demonstrated that the human ODC cDNA can be stably integrated in the tobacco genome. It is successfully expressed and produces an active human ODC enzyme in the apoplast, a non-native compartment of ODC. The increased enzymatic activity resulted in increased cellular levels of putrescine. Spermidine and spermine levels were unchanged. In transgenic tobacco lines co-expressing human ODC and chimeric human/mouse SDE putrescine and spermidine levels increased. Despite the co-expression of both enzymes spermine values did not show a significant increase.

Previous studies indicated that the polyamine pathway is sensitive to changes in end product accumulation. It has also been reported that the cellular content of spermidine and spermine in plants are much more tightly regulated than those of putrescine (Hiatt and Malmberg, 1988; Minocha *et al*., 1995; Minocha and Minocha, 1995). The question arises whether the tight regulation of the spermidine and spermine biosynthesis was due to the pathway compensating in some undetected manner for the increased putrescine and/or spermidine level. Therefore, to explore if the polyamine flux may have been channelled into other polyamine-derived metabolites, the rates of methylation, ethylene synthesis and nicotine production could be analysed in the stable transformed tobacco plants.

To further our understanding about the role of the anabolic and catabolic enzymes on the tight regulation of polyamine synthesis the enzymatic activity of PAO, SDE, SME and SAMDC could be investigated. This work will be carried out with selected progenies of transgenic tobacco plants overexpressing human ODC and co-expressing ODC and SDE enzymes.

Furthermore, analyses of transgenic plants overexpressing ODC in its native compartment could help understanding whether the putrescine and/or spermidine were not accessible to the rest of the pathway because of the rapid degradation or sequestration by compartmentation. This work is currently in progress.

In an alternative approach highly specific scFvs were generated by phage display technology for immunomodulation of ADC and ODC key enzymes in the polyamine biosynthesis. Transiently expressed scFvs were accumulated at high levels in the plant cytosol, apoplast and ER. The scFvODC1 and scFvODC3 stabilized the ODC activity of the bacterial purified human ODC in a dose dependent manner in an *in vitro* assay. In further experiments, transgenic tobacco plants expressing the scFvs in apoplast and/or

cytosol could be generated and characterized for their effect in the polyamine pathway by analysing changes in the ODC, ADC and PAO enzymatic activities and polyamine levels.

De Jaeger *et al*., (2000) suggested that applying antibodies with the same target specificity but with different binding affinities might permit different levels of epitope blocking and different effects on the protein enzymatic activity. As proteins often interact with more than one other protein, it is possible that blocking a signal epitope may leave other protein protein interaction intact, resulting in less pleiotropic effect than a total gene knock out.

Studies have indicated that successful immunomodulation depends not only on the expression of high affinity recombinant antibodies in a specific compartment and organ at the appropriate time but also on system-intrinsic factors, such as the sensitivity of a cellular process to the degree of inhibition of activities to be modulated (Conrad and Manteuffel, 2001). The ability to modulate levels of enzyme activity and end product accumulation by heterologous transgene expression suggested that the polyamine pathway can exhibit plasticity. Therefore, immunomodulation could be a promising approach for analysis and manipulation of metabolic polyamine pathway, including polyamine biosynthesis.

Optimized antibody gene isolation and expression, especially in reducing subcellular environments should turn immunomodulation into a powerful and attractive tool for gene inactivation, complementary or even as replacement to classical antisense and co-supression approaches.

V Summary

Polyamines are ubiquitous low-molecular weight polycationic compounds found in all living organisms and involved in crucial developmental, physiological and metabolic processes. The majority of information available about the polyamine pathway was obtained by using a wide range of metabolic inhibitors (Evans and Malmberg, 1989; Tiburcio *et al*., 1990) and modulation of specific enzymatic activities via heterologous gene expression in transgenic plants. Previous studies have indicated that the polyamine pathway is tightly controlled in the end product accumulation. The objective of this study was to achieve changes in the pathway by combining genetic engineering and antibody technology approaches.

ODC a key enzyme in the polyamine biosynthesis, was amplified from a human prostate cDNA library and subcloned into plant expression vector for transient expression in the apoplast, cytosol and endoplasmatic reticulum. ODC was accumulated to higher levels in plant cytosol and apoplast, while ODC targeted to ER was not detected in immunoblots. Stable transformed tobacco plants overexpressing heterologus ODC in cytosol and apoplast were generated. Lines with the highest accumulation levels were selected for establishment of homozygous lines. The T_2 generation of transgenic plants overexpressing human ODC in apoplast, ‘‘non-native compartment’’ of ODC revealed up to 32-fold elevated levels of ODC activity and accumulated significantly higher levels of putrescine. Additionaly, stable transformed tobacco plants co-expressing human ODC and chimeric human mouse SDE in apoplast were generated. Immunoblot analyses revealed that more than 80% of the lines tested co-expressed both enzymes. The best expressers showed significantly increased levels of putrescine (up to 5-fold) and spermidine (up to 4.5-fold). No increased levels of spermine were observed.

The ADC, ODC and PAO key enzymes in polyamine pathway were chosen as a target for generation of specific scFv recombinant antibody fragments by phage display technology. Mice were immunized with the bacterial produced and affinity purified ADC, ODC-GST fusion protein and PAO-GST inclusion bodies. High antibody titers showed successful immunization. Three phage display libraries were constructed using the immunized mice repertoire. Recombinant antibodies were isolated by solid phase panning using bacterial ADC- and ODC-GST fusion proteins. Their specific reactivity to ADC and ODC was analysed by direct and capture ELISA. Sequence analyses revealed selection of two and four scFvs specific to ADC and ODC, respectively. Electromobility shift assays confirmed the functionality of the affinity purified scFvODC1 and scFvODC3. The binding properties of scFvODCs on soluble antigen were further verified by solution competition as monitored by surface plasmon resonance. The epitope specificity of selected scFvs was

determined in ELISA and BIAcore assays. The pairwise epitope mapping indicated that scFvADC3 and scFvADC7 recognize independent epitopes in ADC, while scFvODC1 recognize a distinct epitope to scFvODC3, 7 and 15. Gel filtration assays indicated the presence of monomeric and dimeric forms of scFvODC3 and scFvODC7. *In vitro* assays indicated increase of the human ODC activity after addition of 3.4 μM of scFvODC1 and scFvODC3 of 75% and 92%, respectively.

All selected scFvs were cloned into pTRA plant expression vector and analysed for their stability and accumulation levels in the plant cytosol, apoplast and ER. Immunoblot analyses of tobacco leaves demonstrated accumulation of scFvs in apoplast and ER with higher levels in ER. Moreover, scFvODC1 and scFvODC3 accumulated in high levels (up to 50-70 μg/g fresh weight) in the plant cytosol retaining the antigen binding specificity and activity in the reducing environment of the plant cytosol. Stable transformed plants expressing scFvODC1 and scFvODC3 specific to ODC in the apoplast and cytosol were generated. More than 67% of the regenerated plants expressed the apoplastic scFvODC1 and scFvODC3.

The data presented in this study demonstrated changes in the polyamine pathway by constitutive expression of heterologous ODC and co-expression of ODC and SDE enzymes indicating that the polyamine pathway exhibit plasticity. Up to date this is the first study attempting to modulate the polyamine pathway by simultaneous expression of two enzymes involved in the polyamine synthesis. Moreover, generation of the scFvs specific to ADC and ODC key enzymes in the polyamine biosynthesis could be a valuable molecular tool for altering the pathway by using immunomodulation approaches and crossing experiments with the homozygous transgenic lines overexpressing ADC and/or ODC.

VI References

Alabadi, D., Carbonell, J. (1998) Expression of ornithine decarboxylase is transiently increased by pollination, 2,4-dichlorophenoxyacetic acid, and gibberellic acid in tomato ovaries. *Plant Physiol.* **118:** 323-328.

Alberts, B., Bray, D., Lewis, J., Raff, M., Roberts, K., Watson, J. (1989) In: *The immune system* (Robertson, M., Ed.), pp. 1001-1057, Garland, New York.

Alfthan, K., Takkinen, K., Sizmann, D., Soderlund, H., Teeri, T. T. (1995) Properties of a single-chain antibody containing different linker peptides. *Protein Eng.* **8:** 725-731.

Al-Lazikani, B., Lesk, A., Chothia, C. (1997 Standard conformations for the canonical structures of immunoglobulins. *J. Mol. Biol*. **273:** 927-948.

Almrud, J. J., Oliveira, M. A., Kern, A. D., Grishin, N. V., Phillips, M. A., Hackert, M. L. (2000) Crystal structure of human ornithine decarboxylase at 2.1 A resolution: structural insights to antizyme binding. *J. Mol. Biol*. 295: 7-16.

An, G. (1995) Binary Ti plasmid vectors. *Methods Mol. Biol.* **44:** 47-58.

Andersen, S. E., Bastola, D. R., Minocha, S. C. (1998) Metabolism of polyamines in transgenic cells of carrot expressing a mouse ornithine decarboxylase cDNA. *Plant Physiol.* **116:** 299-307.

Anehus, S., Pohjanpelto, P., Baldetorp, P., Längström, E., Heby, O. (1984a) Polyamine starvation prolongs the S and G2 phases of polyamine-dependent (arginase-deficient) CHO cells. *Mol. Cell. Biol.* **4:** 915-922.

Antognoni, F., Pistocchi, R., Casali, P., Bagni, N. (1995). Does calcium regulate polyamine uptake in carrot protoplasts? *Plant Physiol. Biochem.* **33:** 701-702.

Apelbaum, A., Goldlust, A; Icekson; I. (1985). Control by ethylene of arginine decarboxylase activity in pea seedlings and its implication for hormonal regulation of plant growth. *Plant Physiol.* **79:** 635.

Artsaenko, O. Kettig, B., Fiedler, U., Conrad, U., Düring, K. (1998) Potato tubers as a biofactory for recombinant antibodies. *Mol. Breeding* **4:** 313-319.

Artsaenko, O., Peisker, M., zur Nieden, U., Fiedler, U., Weiler, E. W., Müntz, K., Conrad, U. (1995) Expression of a single chain Fv antibody against abscisic acid creates a wilty phenotype in transgenic tobacco. *Plant J*. **8:** 745-750.

Artsaenko, O., Phillips, J., Fiedler, U., Peisker, M., Conrad, U. (1999) Intracellular immunomodulation in plants- a new tool for the investigation of phytohormones. In: K. Harper and A. Ziegler (eds.), *Recombinant Antibodies: Applications in Plant Science and Plant Pathology*, Taylor & Francis, London, pp. 145-156.

Ausubel, F. M., Brent, R., Kingston, R. F., Moore, D.D., Seidman, J.G., Smith, J.A., Struhl, K. (eds) (1995) *Current protocols in molecular biology.* John Wiley & Sons, Inc., New York.

Auvinen, M., Paasinen, A., Andersson., C. L., Hölttä, E. (1992) Ornithine decarboxylase activity is critical for cell transformation. *Nature* **360:** 355-358.

Aziz, S. M., Gillespie, M. N., Crooks, P. A., Tofiq, S. F., Tsuboi, C. P., Olson, J. W., Gosland M. P. (1996) The potential of a novel polyamine transport inhibitor in cancer chemotherapy. *J. Pharmacol. Exp. Ther.* **278**: 185-192.

Babal, P., Ruchko, M., Campbell, C. C., Gilmour, S. P., Mitchell, J. L., Olson, J, W., Gillespie, M. N. (2001) Regulation of ornithine decarboxylase activity and polyamine transport by agmatine in rat pulmonary artery endothelial cells. *J. Pharmacol.* **296:** 372-377.

Bagni, N. Torrigiani, P. (1992) Polyamines: A new class of growth substances. In: *Progress in Plant Growth Regulation* (C. M. Karssen, L. C. van Loon, D. Vreugdenhil, eds), pp 264-275. Kluwer Academic Publishers, Dordrecht. ISBN 0-7923-1617-7.

Bagni, N., Tassoni, A. (2001) Biosynthesis, oxidation and conjugation of aliphatic polyamines in higher plants. *Amino acids* **20:** 301-317.

Bajaj, S., Rajam, M. V. (1995) Efficient plant regeneration from long term callus cultures of rice by spermidine. *Plant Cell Rep.* **14:** 717-720.

Bajaj, S., Rajam, M. V. (1996) Polyamine accumulation and near-loss of morphogenesis from long-term callus cultures of rice: Restoration of plant regeneration by manipulation of cellular polyamine levels. *Plant Physiol.* **112**: 1343-1348.

Balasundaram, D., Tabor, C. W., Tabor, H. (1993) Oxygen toxicity in a polyamine-depleted spe2 delta mutant of Saccharomyces cerevisiae. *Proc. Natl. Acad. Sci. USA*. **90:** 4693-4697.

Ballestar, E., Abad, C., Franco, L. (1996) Core histones are glutaminyl substrates for tissue transglutaminase. *J. Biol. Chem*. **271:** 185-192.

Barbas, C. F. III. (1993) Recent advances in phage display. *Curr. Opin. Biotechnol*. **4:** 526-530.

Barbas, C., Kang, A. S., Lerner, R. A., Benkovic, S. J. (1991) Assembly of combinatorial antibody libraries on phage surfaces: the gene III site. *Proc. Natl. Acad. Sci. USA*. **88:** 7978-7982.

Bardocz, B., Grant, G., Brown, D. S., Ralph, A., Pusztai, A. J. (1993) Polyamines in food-implications for growth and health. *Nutr. Biochem*. **4:** 66-70.

Bass, S., Greene, R., Wells, J. A. (1990) Hormone phage: An enrichment method for variant proteins with altered binding properties. *Proteins* **8:** 309-314.

Bassie, L., Noury, M., Lepri, O., Lahaye, T., Christou, P., Capell, T. (2000) Promoter strength influencs polyamine metabolism and morphogenic capacity in transgenic rice tissues expressing the oat *adc* cDNA constitutively. *Transgenic Res*. **9:** 33-42.

Bastola, D. R., Minocha, S. C. (1995) Increased putrescine biosynthesis through transfer of mouse ornithine decarboxylase cDNA in carrot provides tolerance embryogenesis. *Plant Physiol*. **109:** 63-71.

Basu, H. S., Smirnov, IV., Peng, H. F., Tiffany, K., Jackson, V. (1999) Effects of spermine and its cytotoxic analogs on nucleosome formation on topologically stressed DNA in vitro. *Eur. J. Biochem*. **243:** 247-258.

Becker, I. (1990) Konstruktion chimärer Phosphoenolpyruvat-Carboxylase-Gene und ihre Expression in *Solanum tubersosum.* Dissertation. RWTH Aachen.

Bell, E., Malmberg, R. (1990) Analysis of cDNA encoding arginine decarboxylase from oat reveals similarity to the *Escherichia coli* arginine decarboxylase and evidence of protein processing. *Mol. Gen. Genet*. **224:** 431-436.

Bello-Fernandez, C., Packham, G., Cleveland, J. L. (1993) The ornithine decarboxylase gene is a transcriptional target of c-Myc. *Proc. Natl. Acad. Sci. USA*. **90:**7804-7808.

Benhar, I., Azriel, R., Nahary, L., Shaky, A., Berdichevsky, Y., Tamarkin, A., Wels, W. (2000) Highly efficient selection of phage antibodies mediated by display of antigen as lpp-OmpA′ fusion on live bacteria. *J. Mol. Biol*. **301:** 893-904.

Benvenuto, E., Ordas, R. J., Tavazza, R., Ancora, G., Biocca, S., Cattaneo, A., Galeffi, P. (1991) 'Phytoantibodies': a general vector for the expression of immunoglobulin domains in transgenic plants. *Plant Mol. Biol.* **17:** 865-874.

Berek, C., Milstein, C. (1988) The dynamic nature of the antibody repertoire. *Immunol. Rev*. **105:** 5-26.

Besford, R. T., Richardson, C., Campos, J. L., Tiburcio, A. F. (1993) Effect of polyamines on stabilization of molecular complexes in thylakoid membranes of osmotically stressed oat leaves. *Planta*. **189:** 201-206.

Bhatnagar, P., Glasheen, B. M., Bains, S. K., Long, S. L., Minocha, R., Walter, C., Minocha, S. C. (2001) Transgenic manipulation of the metabolism of polyamines in poplar cells. *Plant Physiol.* **125:** 2139-2153.

Biondi, S., Diaz, T., Iglesias, I., Gamberini, G., Bagni, N. (1990) Polyamines and ethylene in relation to adventitious root formation in *Prunus avium* shoot cultures. *Physiol. Plant*. **78:** 474.

Bird, R. E., Hardmann, K. D., Jacobson, J. W., Johnson, S., Kaufman, B. M., Lee, T., Pope, S. H., Riordan, G. S., Whitlow, M. (1988) Single-chain antigen binding proteins. *Science* **242:** 423-426.

Bishia, W. R., Rappuoli, R., Murphy, J. R. (1987) High level expression of a proteolytically sensitive diphtheria toxin fragment in *Escherichi coli. J. Bacteriol.* **169:** 5140-5151.

Borrell, A., Bestford, R. T., Altabella, T., Masgrau, C., Tiburcio, A. F. (1996) Regulation of arginine decarboxilase by spermine in osmotically-stressed oat leaves. *Physiol. Plant.* **98:** 105-110.

Borrell, A., Culianez-Macia, F. A., Altabella, T., Bestford, R. T., Flores, D., Tiburcio, A. F. (1995) Arginine decarboxylase is localized in chloroplast. *Plant Physiol*. 109: 771-776.

Boucherau, A., Aziz, A., Larher, J., Tanguy, M. J. (1999) Polyamines and environmental challenges: recent development. *Plant Sci.* **140:** 103-125.

Bradford, M. M. (1976) A rapid and sensitive method for the quantification of microgram quantities of protein utilizing the principle of protein dye binding. *Anal. Biochem*. **72:** 248-254.

Breitling, F., Dübel, S. (2000) Recombinant antibodies. John Wiley and Sons, New York.

Breitling, F., Dübel, S., Seehaus, T., Klewinghaus., Little, M. (1991) A surface infection vector for antibody screening. *Gene* **104:** 147-153.

Brinkmann, U. (2000) Recombinant antibody fragments and immunotoxin fusions for cancer therapy. *In Vivo* **14:** 21-27

Bryans, M., Harley, E., Gilmour, S. K. (1996) Elevated cellular polyamine levels enhance promoter activity in vivo. *Biochem. Biophys. Res. Commun*. **226:** 618-625.

Bruyns, A.M., De Jaeger, G., De Neve, M., De Wilde, C., Van Montagu, M., Depicker, A. (1996) Bacterial and plant-produced scFv proteins have similar antigen-binding properties. *FEBS Lett* **386:** 5-10

Burmester, J., Plückthun, A. (2001) Construction of scFv fragments from hybridoma or spleen cells by PCR assembly. In *Antibody Engineering* (Kontermann, R. and Dübel, S., eds). Pp. 19-40. Springer Verlag, Heidelberg.

Burtin, D., Michael, A. J. (1997) Overexpression of arginine decarboxylase in transgenic plants. *Biochem. J.* **325:** 331-337.

Burton, D. R., Barbas, C. F. III. (1994) Human antibodies from combinatorial libraries. *Adv. Immunol.* **57:** 191-280.

Burton, D. R. (2001) Antibody libraries. In: *Phage Display: A Laboratory Manual.* Barbas, C. F., Burton, D. R., Scott, J. S. (eds). Cold Spring Harbor Laboratory Press. pp: 3.1-3.18.

Butler, J. E., Ni, L., Nessler, R., Joshi, K. S., Suter, M., Rosenberg, B., Chang, J., Brown, W. R., Cantareno, L. A. (1992) The physical and functional behavor of capture antibodies adsorbed on polystyrene. *J. Immunol. Methods* **150:** 77-90.

Caffaro, S. V., Antognoni, F., Scaramagli, S., Bagni, N. (1994) Polyamine translocation following photoperiodic flowering induction in soybean. *Physiol. Plant.***91:** 251-256.

Caffaro, S. V., Viecente, C. (1994) Polyamine implication durino soybean flowering induction and early reproductive transition of vegetative buds. *Plant Physiol. Biochem.* **32:** 391-397.

Capell, T., Escobar, C., Lui, H., Burtin, D., Lepri, O., Christou, P. (1998) Over-expression of the oat arginine decarboxylase cDNA in transgenic rice (*Oriza sativa* L.) affects normal development patterns in vivo and results in putrescine accumulation in transgenic plants. *Theor. Appl. Genet*. **97:** 246-254.

Carbonell, J., Navarro, J. L. (1989) Correlation of spermine levels with ovary senescence and with fruit set and development in *Pisum sativum. Planta* **178:** 482-487.

Carter, C. (ed.) (1994) Neuropharmacology of polyamines. Academic Press, San Diego, CA.

Cattaneo, A., Biocca, S. (1997) Intracellular antibodies: development and applications. Berlin: Springer.

Celano, P., Baylin, S. B., Casero, R. A. (1989) Polyamines differentially modulate the transcription of growth-associated genes in human colon carcinoma cells. *J. Biol. Chem*. **264:** 8922-8927.

Chames, P., Baty, D. (2000) Antibody engineering and its applications in tumor targeting and intracellular immunization. *FEMS Microbiol. Lett.* **189:** 1-8.

Chames, P., Hoogenboom, H., Henderikx, P. (2001) Selection on biotinylated antigens. In *Antibody Engineering* (Kontermann, R. and Dübel, S., eds). Pp. 148-166. Springer Verlag, Heidelberg.

Chester, K. A., Begent, R. H., Robson, L., Keep, P., Pedley, R. B., Boden, J. A., Boxer, G., Green, A., Winter, G., Cochet, O. (1994) Phage libraries for generation of clinically useful antibodies. *Lancet.* **343:** 455-456.

Chomczynsky, P. (1992) One-hour downward alkaline capillary transfer for blotting of DNA and RNA. *Anal. Biochem.* **201:** 134-139.

Chowdhury, P. S., Viner, J. L., Beers, R., Pastan, I. (1998) Isolation of a high affinity stable single-chain Fv specific for mesothelin from DNA-immunized mice by phage display and construction of a recombinant immunotoxin with anti-tumor activity. *Proc. Natl. Acad. USA*. **95:** 669.

Christou, P. (1994) Rice Biotechnology and Genetic Engineering. *Biotechnology of Food Crops.* Technomic Publishing Company, Lancaster, PA.

Clackson, T., Hoogenboom, H. R., Griffiths, A. D., Winker, G. (1991) Making antibody fragments using phage display libraries. *Nature* **352:** 624.

Clackson, T., Wells, J. A. (1994) In vitro selection from protein and peptide libraries. *Trends Biotechnol* **12:** 173-184

Cohen, E., Arad, M., Heimer, Y. M., Mizrahi, Y. (1982) Participation of ornithine decarboxylase in early stages of tomato fruit development. *Plant Physiol*. **70:** 540-543.

Coleman, C. S., Stanley, B. A. Pegg, A. E. (1993) Effect of mutations at active site residues on the activity of ornithine decarboxylase and its inhibition by active-site-directed irreversible inhibitors. *J. Biol. Chem*. **268:** 24572-24579.

Coligan, J.E., Dunn, B.M., Ploegh, H.L., Speicher, D.W. and Wingfield, P.T. (eds.) (1995) *Current protocols in protein science.* John Wiley & Sons, New York

Conrad, U., Fiedler, U. (1998) Compartment-specific accumulation of recombinant immunoglobulins in plant cells: en essential tool for antibody production and immunomodulation of physiological functions and pathogen activity. *Plant Mol. Biol.* **38:** 101-109.

Conrad, U., Manteuffel, R. (2001) Immunomodulation of phytohormones and functional proteins in plant cells. *Trends in Plant Science* **6:** 399-402.

Cook, G. P., Tomlinson, I. M. (1995) The human immunoglobulin V_H repertoire. *Immunol. Today* **16:** 237-242.

Corley, E., Wolosluk, R. A., Hertig, C. M. (1983) Regulation of the activation of chloroplast fructose-1,6-bis phosphatase. Inhibition by spermidine and spermine. *Biochem. Biophys. Res. Commun.* **115:** 707.

Courtney, B. C., Williams, K. C., Schlager, J. J. (1995) A phage display vector with improved stability, applicability and ease of manipulation. *Gene* **165:** 139-140.

Coutinho, A., Freitas, A. A., Holmberg, D., Grandien, A. (1992) Expression and selection of murine antibody repertoires. *Int. Rev. Immunol*. **8:** 173-187.

Cumber, A. J., Ward, E. S., Winter, G., Parnell, G., Wawrzynczak, E. J. (1992) Comparative stabilities in vitro and in vivo of a recombinant mouse antibody FvCys fragment and a bisFvCys conjugate. *J. Immunol.* **149:** 120.

Datta, N., Schell, M. B., Roux, S. J. (1987) Spermine stimulation of a nuclear NII kinase from pea plumules and its role in the phosphorylation of a nuclear polypeptide. *Plant Physiol*. **84:** 1397.

Davies, J., Dawkes, A. C., Haymes, A. G., Roberts, C. J., Sunderland, R. F., Wilkins, M. J., Davies, M. C., Tendler, S. J., Jackson, D. E., Edwards, J. C. (1994) A scanning tunnelling microscopy comparison of passive antibody adsorption and biotinylated antibody linkage to streptavidin on microtiter wells. *J. Immunol. Methods* **167:** 263-269.

De Bruin, R., Spelt, K., Mol, J., Koes, R., Quattrocchio, F. (1999) Selection of high affinity phage antibodies from phage display libraries. *Nature Biotechnol.* **17:** 397-399.

De Haard, H. J., Kazemier, B., van der Bent, A., Oudshoorn, P., Boender, P., van Gemen, B., Arends, J. W., Hoogenboom, H. R. (1998) Absolute conservation of residue 6 of immunoglobulin heavy chain variable regions of class IIA is required for correct folding. *Protein Eng*. **11:** 1267-1276.

De Jaeger, G., Buys, E., Eeckhout, D., De Wilde, C., Jacobs, A., Kapila, J., Angenon, G., Van Montagau, M., Gerats, T., Depicker, A. (1999) High level accumulation of single-chain variable fragments in the cytosol of transgenic *Petunia Hybrida. Eur. J. Biochem.* **259:** 1-10.

De Jaeger, G., De Wilde, C., Eeckhout, D., Fiers, D., Depicker, A. (2000) The plantibody approach: expression of antibody genes in plants to modulate plant metabolism or to obtain pathogen resistance. *Plant Mol. Biol.* **43:** 419-428.

De Neve, M., De Loose, M., Jacobs, A. (1993) Assembly of an antibody and its derived antibody fragment in *Nicotiana* and *Arabidopsis. Transgenic Res.* **2:** 227-237.

De Scenco, R. A., Minocha, S. C. (1993) Modulation of cellular polyamines in tobacco by transfer and expression of mouse ornithine decarboxylase cDNA. *Plant Mol. Biol***. 22:** 113-127.

De Wilde, C., De Rycke, R., Beeckman, T., De Neve, M., Van Montagu, M., Engler, G., Depicker, A. (1998) Accumulation pattern of IgG antibodies and Fab fragments in transgenic Arabidopsis thaliana plants. *Plant Cell. Physiol.* **39:** 639-46

De Wilde, C., De Jaeger, G., De Neve, M., Van Montagu, M., Depicker, A. (1999) Production of antibodies in transgenic plants-a general introduction. In *Recombinant Antibodies*: *Applications in Plant Science and Plant Pathology* (Harper, K., Ziegler, A., eds), pp. 113-127.

Denecke, J., De Rycke, R., Botterman, J. (1992) Plant and mammalian sorting signals for protein retention in the endoplasmic reticulum contain a conserved epitope. *EMBO J.* **11:** 2345-2355.

Dierks, S. E., Butler, J. E., Richerson, H. B. (1986) Altered recognition of surface-adsorbed compared to antigen-bound antibodies in the ELISA. *Mol. Immunol*. **23:** 403- 411.

Dobrovinskaya, O. R., Muniz, J., Pottosin, I. I. (1999) Inhibition of vacuolar ion channels by polyamines. *J. Membrane Biol.* **167:** 127-140.

Douglas, J. T., Curiel, D. T. (1997) Strategies to accomplish targeted gene delivery to muscle cells employing tropism-modified adenoviral vectors. *Neuromuscul Disord.* **7:** 284-98

Dower, W.J., Miller, J.F. and Ragsdale, C.W. (1988) High efficiency transformation of *E.coli* by high voltage electroporation. *Nucleic Acids Res.* **16:** 6127-6145.

Dreyer, W. J., Bennett, J. C. (1965) The molecular basis of antibody formation: a paradox. *Proc. Natl. Acad. Sc.i USA*. **54:** 864-869.

Drolet, G., Dumbroff, E. B., Legge, R. L., Thompson, J. E. (1986) Radical scavenging properties of polyamines. *Phytochem.* **25:** 367-371.

Dypbukt, J. M., Ankarcrona, M., Burkitt, M., Sjoholm, A., Strom, K., Orrenius, S., Nicotera, P., (1994) Different prooxidant levels stimulate growth, trigger apoptosis, or produce necrosis of insulin-secreting RINm5F cells. The role of intracellular polyamines. *J. Biol. Chem.* **269:** 30553-30560.

Dziegiel, M., Nielsen, L. K., Andersen, P. S., Blancher, A., Dickmeiss, E., Engberg, J. (1995) Phage used for gene cloning of human recombinant antibody against the erythrocyte surface antigen, rhesus D. *J. Immunol. Methods* **182:** 7-19.

Eeckhout, D., Fiers, E., Sienaert, R., Snoeck, V., Depicker, A., De Jaeger, G. (2000) Isolation and characterization of recombinant antibody fragments against CD2a from *Arabidopsis thaliana*. *Eur. J. Biochem*. **267:** 6775-6783.

Ellman, J. A., Gallop, M. A. (1998) Combinational chemistry. *Curr. Opin. Chem. Biol*. **2:** 317-319.

Essig, N. Z., Wood, J. F., Howard, A. J., Raag, R., Whitlow, M. (1993) Crystallization of single-chain Fv proteins. *J Mol Biol* **234:** 897-901

Evans, P. T., Malmberg, R. L. (1989) Do polyamines have roles in plant development? *Annu. Rev. Plant Physiol.* **40:** 235-269.

Fecker, L., Kaufmann, N., Commandeur, U., Commandeur, J., Koenig, R., Burgemeister, W. (1996) Expression of single-chain antibody fragments (scFv) specific for beet necrotic yellow vein virus coat protein or 25 kDa protein in *Escherichia coli* and *Nicotiana benthamiana*. *Plant Mol. Biol*. **32:** 979-986.

Fecker, L. F., Rugenhagen, C., Berlin, J. (1993) Increased production of cadaverine and anabasine in hairy root cultures of *Nicotiana tabacum* expressing a bacterial lysine decarboxylase gene. *Plant Mol. Biol*. **23:** 11-21.

Fecker, L., Koenig, R., Obermeier, C. (1997) *Nicotiana benthamiana* plants expressing beet necrotic yellow vein virus (BNYVV) coat protein-specific scFv are partially protected against the establishment of the virus in the early stages of infection. *Arch. Virol*. **142:** 1857-1863.

Federico, R., Angelini, R. (1991) Polyamine catabolism. In: Clocum, R. D., Flores, H. E., (eds) *Biochemistry and physiology of polyamines in plants.* CRC Press, Boca Raton, pp, 41-56.

Feirer, R. P., Mignon, G., Litvay, J. D. (1984) Arginine decarboxylase and polyamines required for embryogenesis in the wild carrot. *Science* **223:** 1433-1434.

Fiedler, U., Conrad, U. (1995) High-level production and long term storage of engineered antibodies in transgenic tobacco seeds. *Bio. Technol*. **10:** 1090-1094.

Fiedler, M., Skerra, A. (2001) Purification and characterisation of His tagged antibody fragments. In *Antibody Engineering*. (Köntermann and Dübel, eds.). Springer Verlag. Heidelberg. pp. 243-256.

Fischer, R. (1990) Herstellung, Characterisierung und Klonierung der Immunoglobulingene von TMV-neutralisierenden Antikörpern. *Eberhard-Karls-Universität Tübingen, Dissertation*.

Fischer, R., Drossard, J., Emans, N., Commandeur, U., Hellwig, S. (1999a) Towards molecular farming in the future: Pichia pastoris-based production of single chain antibody fragments. *Biotechnol. Appl. Biochem*. **30:** 117-120.

Fischer, R., Drossard, J., Commandeur, U., Schillberg, S., Emans, N. (1999b) Towards molecular farming in the future: moving from diagnostic protein and antibody production in microbes to plants. *Biotechnol. Appl. Biochem*. **30:** 101-108.

Fischer, R., Emans, N., Schillberg, S. (2001) Achieving plant disease resistance by antibody expression. *Can. J. Plant. Pathol.* **23:** 236-245.

Fischer, R., Liao, Y. C., Hoffmann, K., Schillberg, S., Emans, N. (1999c) Molecular farming of recombinant antibodies in plants. *Biol. Chem.* **380:** 825-839.

Fischer, R., Schumann, D., Zimmermann, S., Drossard, J., Sack, M., Schillberg, S. (1999d) Expression and characterization of bispecific single chain-Fv fragments produced in transgenic plants. *Eur. J. Biochem.* **262:** 810-816.

Flores, H. E., Filner, P. (1985) Metabolic relationships of putrescine GABA and alkaloids in cell and root cultures, in: Newman, K. H., Barz, W., Reinhard, E. (Eds.) *Primary and Secondary Metabolism of Plant Cell cultures*. Springer, New York. pp: 37-42.

Flores, H. E., Galston, A. W. (1982) Polyamines and plant stress: activation of putrescine biosynthesis by osmotic shock. *Science*, **217:** 1259-1261.

Flores, H. E., Galston, A. W. (1984) Osmotic stress-induces polyamine accumulation in cereal leaves. I. Physiological parameters of the response. *Plant Physiol*. **75:** 101-109.

Fong, W. F., Heller, J. S., Canellakis, E. S. (1976) The appearance of an ornithine decarboxylase inhibitory protein upon the addition of putrescine to cell culture. *Biochem. Biophys. Acta* **428:** 456-465.

Fraley, R. T., Rogers, S. G., Horsch, R. B., Sanders, P. R., Flick, J. S., Adams, S. P., Bittner, M. L., Brand, L. A., Flink, C. L., Fry, J. S., Galluppi, G. R., Goldberg, S. B., Hoffmann, N. L., Woo, S. C. (1983) Expression of bacterial genes in plant cells. *Proc. Natl. Acad. USA*. **80:** 4803-4807.

Franken, E., Teuschel, U., Hain, R. (1997) Recombinant proteins from transgenic plants. *Curr. Opin. Biotechnol.* **8:** 411-416.

Frangioni, J. V., Neel, B. G. (1993) Solubilization and purification of enzymatically active glutathione S-transferase (pGEX) fusion proteins. *Anal. Biochem*. **210:** 179-187.

Galston, A. W., Kaur-Sawhney, R. (1990) Polyamines in plant physiology. *Plant Physiol.* **94:** 406-410.

Gao, C., Mao, S., Lo, C. H., Wirsching, P., Lerner, R. A., Janda, K. D. (1999) Making artificial antibodies: a format for phage display of combinatorial heterodimeric arrays. *Proc. Natl. Acad. Sci. USA*. **96:** 6025-6030.

Garrard, L. J., Yang, M., O'Connell, M. P., Kelley, R. F., Henner, D. J. (1991) Fab assembly and enrichment in a monovalent phage display system. *Biotechnol.* **9:** 1373-1377.

Ghoda, L., Phillips,M. A., Bass, K. E., Wang, C. C., Coffino, P. (1990) Trypanosome ornithine decarboxylase is stable because it lacks sequences found in the carboxyl terminus of the mouse enzyme which target the latter for intracellular degradation. *J. Biol. Chem*. **265:** 11823-11826.

Ghoda, L., van Daalen Wetters, T., Macrae, M., Ascherman, D., Coffino, P. (1989) Prevention of rapid intracellular degradation of ODC by carboxyl-terminal truncation. *Science* **243:** 1493-1495.

Giddings, G., Allison, G., Brooks, D., Carter, A. (2000) Transgenic plants as factories for biopharmaceuticals. *Nature Biotechnol.* **18:** 1151-1155.

Gilad, G. M., Gilad, V. H. (1988) Early polyamine treatment enhances survival of sympathetic neurons after postnatal axonal injury or imunohistosympathectomy. *Dev. Brain Res.* **38:** 175-181.

Gilad, G. M., Gilad, V. H. (1996) Arginine and ornithine decarboxylation in rodent brain-coincidental changes during development and after ischemia. *Neurosci. Lett*. **216:** 33-36.

Glockshuber, R., Malia, M., Pfitzinger, I., Plückthun, A., (1990) A comparison of strategies to stabilize immunoglobulin Fv fragments. *Biochem.* **29:** 1362-1367.

Goldberg, R., Pedrizet, E. (1984) Ratio of free to bound polyamines during maturation in mung-bean hypocotyls cells. *Planta* **161:** 531.

Griffiths, A. D., Malmqvist, M., Marks, J. D., Bye, J. M., Embleton, M. J., McCafferty, J., Baier, M., Holliger, K. P., Gorick, B. D., Hughes-Jones, N. C.Hoogenboom, H. R., Winter, G. (1993)

Human anti-self antibodies with high specificity from phage display libraries. *EMBO J.* **12:** 725-734.

Griffiths, A. D., Duncan, A. R. (1998) Strategies for selection of antibodies by phage display. *Curr. Opin. Biotechnol***. 9:** 102-108.

Griffiths, G. M, Berek, C, Kaartinen, M, Milstein, C. (1984) Somatic mutation and the maturation of immune response to 2-phenyl oxazolone. *Nature* **312:** 271-527.

Grob, P., Baumann, S., Ackermann, M., Suter, M. (1998) A system for stable indirect immobilization of multimeric recombinant proteins. *Immunotechnol.* 4, 155-163.

Guggisberg, G., Hesse, M. (1983) In: *The alkaloids: Chemistry and Pharmacology* (Brossi, A., ed.) vol. 22, pp. 85-188. Academic Press, New York.

Guo, Y., Zhao, J., Sawicik, J., Soler, A. P., O'Brien, T. G. (1999) Convertion of C57BI/6 mice from tumaor promotion-resistant to a sensitive phenotype by enhanced ornithine decarboxylase expression. *Mol. Carcinogenesis.* **26:** 32-36.

Hackenbeck, R., Konig, A., Kern, I., van der Linden, M., Keck, W., Billot-Klein, D., Legrand, R., Schoot, B., Gutmann, L. (1998) Acquisition of five high-Mr penicillin-binding protein variants during transfer of high-level β-lactam resistance from *Streptoccoccus pneumoniae*. *J. Bacteriol*. **180:** 1831-1840.

Halmekytö, M., Hyttinen, J. M., Sinervirta, R.M., Leppänen, P., Jänne, J., Alhonen, L. (1993) Regulation of the expression of human ornithine decarboxylase promoter-driven reported gene in transgenic mice. *Biochem. J.* **292:** 927-932.

Hamill, J. D., Robins, R. J., Parr, A. J., Evan, D. M., Furze, J. M., Rhodes, M. J. C. (1990) Over-expression of a yeast ornithine decarboxylase gene in transgenic roots of *Nicotiana rustica* can lead to enhanced nicotine accumulation. *Plant Mol. Biol*. **15:** 27-38.

Hanahan, D. (1983) Studies on transformation of *E. coli* with plasmids. *J. Mol. Biol.* **166:** 557-580.

Harris, B. (1999) Exploiting antibody based technologies to manage environmental pollution. *Trends Biotechnol*. **17:** 290-296.

Havelange, A., Lejeune, P., Bernier, G., Kaur-Sawhney, R., Galston, A. W. (1996) Putrescine export from leaves in relation to floral transition in *Sinapis alba*. *Physiol. Plant.*. **96:** 59-65.

Hawkins, R. E., Russell, S. J., Winter, G. (1992) Selection of phage antibodies by binding affinity. Mimicking affinity maturation. *J. Mol. Biol.* **226:** 889.

Hayashi, S., Murakami, Y. (1995) Rapid and regulated degradation of ornithine decarboxylase. *Biochem. J.* **306:** 221-230**.**

Heby, O., Persson, L. (1990) Molecular genetics of polyamine synthesis in eukaryotic cells. *Trends Biochem. Sci*. **15:** 153-158.

Heller, J. S., Fong, W. F., Canellakis, E. S. (1976) Induction of a protein inhibitor to ornithine decarboxylase by the end products of its reaction. *Proc. Nat. Acad. Sci. USA* **73:** 1858-1862.

Hiatt, A. C., Cafferkey, R., Bowdish, K. (1989) Production of antibodies in transgenic plants. *Nature* **342:** 76-78.

Hiatt, A. C., McIndoo, J., Malmberg, R. L. (1986) Regulation of polyamine biosynthesis in tobacco. *J. Biol. Chem.* **261:** 1293-1298.

Hiatt, A. C., Malmberg, R. L. (1988) Utilization of putrescine in tobacco cell lines resistant to inhibitors of polyamine synthesis. *Plant Physiol*. **86:** 441-446.

Hibi, N., Higashiguchi, S., Hashimoto, T., Yamada, Y. (1994) Gene expression in tobacco low-nicotine mutants. *Plant Cell* **6:** 723-35.

Hobbs, C. A., Gilmour, S. K. (2000) High levels of intracellular polyamines promote histone acetyltransferase activity resulting in chromatin hyperacetylation. *J. Cell. Biochem.* **77:** 345-360.

Holliger, P., Prospero, T., Winter, G. (1993) Diabodies: small bivalent and bispecific antibody fragments. *Proc. Natl. Acad. Sci. USA*. **90:** 6444-6448.

Holliger, P., Winter, G. (1997) Diabodies: small bispecific antibody fragments. *Cancer Immunol Immunother.* **45:** 128- 130.

Hölttä, E., Pohjanpelto, P. (1986) Control of ornithine decarboxylase in Chinese hamster ovary cells by polyamines. *J. Biol. Chem.* **261:** 9502-9508.

Hoogenboom, H. R. (1997) Designing and optimizing library selection strategies for generating high-affinity antibodies. *Trends Biotechnol.* **15:** 62-70.

Hoogenboom, H. R., Allen, D. J. and Roberts, A. J. (1996) Converting rodent into human antibodies to guided selection. In: *Antibody Engineering- A practical approach.* IRL Press at Oxford University Press, Ed. By J. Mc Cafferty, H. Hoogenboom and D. Chiswell, Chapter 8: 169-185.

Hoogenboom, H. R., Chames, P. (2000) Natural and designer binding sites made by phage display technology. *Immunol Today.* **21:** 371-378.

Hoogenboom, H. R., De Bruine, A. P., Hufton, S. E., Hoet, R. M., Arends, J. W., Roovers, R. C. (1998) Antibody phage display technology and its applications. *Immunotechnol.* **4:** 1-20.

Hoogenboom, H. R., Griffiths, A. D., Johnson, K. S., Chiswell, D. J., Hudson, P., Winter, G. (1991) Multi-subunit proteins on the surface of filamentous phage: methodologies for displaying antibody (Fab) heavy an light chains. *Nucl. Acids Res.* **19:** 4133-4137.

Horsch, R., Fry, J. E., Hoffman, N., Eicholtz, D., Rogers, S., Fraley, R. (1995) A simple and general method for transferring genes into plants. *Science.* **227:** 1229-1231.

Honegger, A., Plückthun, A. (2001) Yet another numbering scheme for immunoglobulin variable domains: an automatic modeling and analysis tool. *J. Mol. Biol.* **309:** 657-670.

Hougaard, D. M. (1992) Polyamine cytochemistry: localization and possible functions of polyamines. *Int. Rev. Cytol.* **138:** 51-88.

Hudson, P. J. (1999) Recombinant antibody constructs in cancer therapy. *Curr. Opin. Immunol.* **11:** 548-557.

Hudson, P. J., Kortt, A. A. (1999) High avidity scFv multimers: diabodies and triabodies. *J. Immunol. Methods.* **231:** 177-189.

Huston, J. S., Levinson, D., Mudgett, H. M., Tai, M. S., Novotny, J., Margolies, M. N., Ridge, R. J., Bruccoleri, R. E., Haber, E., Crea, R., Opperman, H. (1988) Protein engineering of antibody biding sites: recovery of specific activity in an anti-dioxin single chain Fv analogue produced in *Escherichia coli*. *Proc. Natl. Acad. Sci. USA*. **85:** 5879-5883.

Huston, J. S., McCartney, J., Tai, M. S., Mottola-Hartshorn, C., Jin, D., Warren, F., Keck, P. Oppermann, H. (1993) Medical applications of single-chain antibodies. *Int. Rev. Immunol*. **10:** 195-217.

Huston, J. S., Mudgett-Hunter, M., Tai, M. S., McCartney, J., Warren, F., Haber, E., Oppermann, H. (1991) Protein engineering of single-chain Fv analogs and fusion proteins. *Methods Enzymol*. **203:** 46-88.

Iacono-Connors, L. C., Novak, J., Rossi, C., Mangiafico, J., Ksiazek, T. (1994) Enzyme linked immunosorbent assay using a recombinant baculovirus-expressed Bacillius anthracis protective antigen (PA): measurement of human anti-PA antibodies. *Clin. Diagn. Lab. Immunol*. **1:** 78-82.

Iannolo, G., Minenkova, O., Petruzzelli, R., Cesareni, G. (1995) Modifying filamentous phage capsid: limits in the size of the major capsid protein. *J. Mol. Biol.* **248:** 835-844

Ichikawa, M., Maeda, T., Handa, J. (1997) Ornithine decarboxylase in developing brain

of normal and hydrocephalic rats. *Child's Nerv. Syst*. **13:** 578-583.

Igarashi, K., Kashiwagi, K., Kobayashi, H., Ohnishi, R., Kagegawa, T., Nagasu, A., Hirose, S. (1989) Effect of polyamines on mitochondrial FI ATPase-catalyzed reactions. *J. Biochem.* **106:**294-8

Iliades, P., Kortt, A. A., Hudson, P. J. (1997) Triabodies: single chain Fv fragments without a linker form trivalent trimers. *FEBS Lett.* **409:**437-441.

Irving, R. A., Kortt, A. A., Hudson, P. J. (1996) Affinity maturation of recombinant antibodies using *E. coli* mutator cells. *Immunotechnol.* **2:**127-143

Isomaa, V V., Pajuen, A. E. I., Bardin, C. W., Jänne, O. A. (1983) Ornithine decarboxylase in mouse kidney: purification, characterisation, and radioimmunological determination of the enzyme protein. *J. Biol. Chem*. **258:** 6735-6740.

Iyengar, R. V., Pawlik, C. A., Krull, E. J., Phels, D, A., Burger, R. A., Harris, L. C., Potter, P. M., Danks, M. K. (2001) Use of modified ornithine decarboxylase promoter to achive efficient c-MYC- or N-MYC-regulated protein expression. *Cancer Research.* **61:** 3045-3061.

Jackson, L. K., Brooks, H. B., Osterman, A. L., Goldsmith, E. J., Phillips, M. A. (2000) Altering the reaction specificity of eucaryotic ornithine decarboxylase. *Biochem.* **39:** 11247-11257.

Jänne, J., Pösö, H., Raina, A. (1978) Polyamines in rapid growth and cancer. *Biochim. Biophys.* **473:** 241-293.

Jesnowski, R., Nähring, J., Wolf, K. (1995) A rapid and reliable method for PCR-based amplification of chromosomal and mitochondrial DNA from intact yeast cells. *Current Genetics.* **27:** 318-319.

Jokela, A., Sarjala, T., Kaunisto, S., Huttunen, S. (1997) Effects of foliar potassium concentration on morphology, ultrastructure and polyamine concentration of Scots pine needles. *Tree Physiol.* **17:** 677-685.

Kabat, E. A. (1978) The structural basis of antibody complementarity. *Adv. Protein Chem*. **32:** 1-75.

Kabat, E. A., Wu, T. T., Bilofsky, H. (1977) Unusual distributions of amino acids in complementarity-determining (hypervariable) segments of heavy and light chains of immunoglobulins and their possible roles in specificity of antibody-combining sites. *J. Biol. Chem*. **252:** 6609-6616.

Kabat, E. A., Wu, T. T. (1991) Identical V region amino acid sequences and segments of sequences in antibodies of different specificities. Relative contributions of VH and VL genes, minigenes, and complementarity-determining regions to binding of antibody-combining sites. *J. Immunol.* 147: 1709-1719

Kapila, J., De Rycke, R., van Montagu, M., Agenon, G. (1996) An *Agrobacterium* mediated transient gene expression system for intact leaves. *Plant Sci*. **122:** 101-108.

Kaur-Sawhney, R., Kandpal, F., McGonigle, B., Galston, A. W. (1990) Further experiments on spermidine mediated floral bud formation in thin layer explants of Wisconsin 38 tobacco. *Planta* **181:** 212-215.

Kay, R., Chan, A., Daley, M., Mcpherson, J. (1987) Duplication of CaMV 35S promoter sequences creates a strong enfancer for plant genes. *Science* **236:** 1299-1302.

Khan, A. J., Minocha, S. C. (1989) Biosynthetic arginine decarboxylase in phytopathogenic fungi. *Life Sciences* **44:** 1215-1222.

Kipriyanov, S. M., Moldenhauer, G., Martin, A. C., Kupriyanova, O. A., Little, M. (1997) Two amino acid mutations in an anti-human CD3 single chain Fv antibody fragment that affect the yield on bacterial secretion but not the affinity. *Protein Eng*. **10:** 445-453.

Koc, E., Dong, N., Gardner, J. Y., Dharma, A., Phillips, G. C., Kuehn, G. D. (1995) Isolation and expression of the gene for polyamine oxidase from *Medicago sativa* and *Avena sativa. FASEB. J.* **9:** 54.

Königshofer, H. (1991) Distribution and seasonal variation of polyamines in shoot-axes of spruce (*Picea abies* (L.) Karst.). *J. Plant Physiol*. **137:** 607-612.

Konz, C., Schell, J. (1986) The promoter of TL-DNA gene 5 controls the tissue-specific expression of chimaeric genes carried by a novel type of *Agrobacterium* binary vector. *Mol. Gen. Genet*. **204:** 382-396.

Korolev, N., Lyubartsev, A. L., Nordenskiöld, L., Laaksonen, A. (2001) Spermine: An 'invisible' component in the crystals of B-DNA. A grand canonical Monte Carlo and molecular dynamics simulation study. *J. Mol. Biol*. **308:** 907-917.

Kortt, A. A., Malby, R. L., Caldwell, J. B., Gruen, L. C., Ivancic, N., Lawrence, M. C., Howlett, G. J., Webster, R. G., Hudson, P. J., Colman, P. M. (1994) Recombinant anti-sialidase single chain variable fragment antibody. Characterisation, formation of dimer and higher-molecular-mass multimers and the solution of the crystal structure of the single-chain variable. *Eur. J. Biochem*. **221:** 151-157.

Kotzabasis, K. (1993) Polyamines in the photosynthetic apparatus. Photosystem II highly resolved subcomplexes are enriched in spermine. *Photosynth. Res*. **38:** 83-88.

Krebber, A., Burmester, J., Plückthun, A. (1996) Inclusion of an upstream transcriptional terminator in phage display vectors abolishes background expression of toxic fusions with coat protein g3p. *Gene* **178:** 71-74.

Kumar, A., Altabella, T., Taylor, M., Tiburcio, A. (1997) Recent advances in polyamine research. *Trends Plant Science*: **2:** 124-130.

Kumar, A., Taylor, M. A., Mad Arif, S. A., Davies, H. V. (1996) Potato plants expressing antisense and sense S-adenosylmethionine decarboxylase (SAMDC) transgenes show altered levels of polyamine and ethylene: antisense plants display abnormal phenotypes. *Plant J.* **9:** 147-158.

Kushad, M. M., Dumbroff, E. B. (1991) In: *The Biochemistry and Physiology of Polyamines in Plants* (Slocum, R. D., Flores, H. E., eds). Boca Raton, FL: CRC Press, pp. 77-92.

Kwak, S. H., Lee, S. H. (2001) The regulation of ornithine decarboxylase gene expression by sucrose and small upstream open reading frame in tomato (*Lycopersicon esculentum* Mill). *Plant Cell Physiol*. **42:** 314- 323.

Lamberts, B., Dewey, L., Byerrum, R. (1959) Ornithine as a precursor for the pyrrolidone ring of nicotine. *Biochimica Biophysica Acta* **33:** 22-26.

Langedijik, A. C., Honegger, A., Matt, J., Planta, R. J., van Shaik, R. C., Plückthun, A. (1998) The nature of antibody heavy chain residue H6 strongly influences the stability of a V_H domain lacking the disulfide bridge. *J. Mol. Biol*. **283:** 95-110.

Larsson, L., Morch-Jorgensen, L., Hougaard, D. M. (1982) Cellular and subcellular localization of polyamines cytochemical methods providing new clues to polyamine function in normal and neoplastic cells. *Histochem.* **76:**159-174.

Lei, S. P., Lin, H. C., Wang, S. S., Callaway, J., Wilcox, G. (1987) Characterization of the *Erwinia carotovora pelB* gene and its product pectate lyase. *J. Bacteriol*. **169:** 4379-4383.

Lener, M., Horn, I. R., Cardinale, A., Messina, S., Nielsen, U. B., Rybak, S. M., Hoogenboom, H. R., Cattaneo, A., Biocca, S. (2000) Diverting a protein from its cellular location by intracellular antibodies. The case of p21Ras. *Eur. J. Biochem.* **267:** 1196-1205.

Lepri, O., Basie, L., Safwat, G., Thu-Hang, P-. Trung-Nghia, P., Hölttä, E., Christou, P., Capell, T. (2001) Over-expression of a cDNA for human ornithine decarboxylase in transgenic rice plants alters the polyamine pool in a tissue-specific manner. *Mol. Genet. Genomics* **266:** 303-312.

Lesk, A., Chothia, C. (1982) Evolution of proteins formed by beta-sheets. II. The core of the immunoglobulin domains. *J. Mol. Biol*. **160:** 325-342.

Leveque, J., Burtin, F., Cartos-Quemener, V., Havouis, R., Moulinoux, J. P. (1998) The gastrointestinal polyamine source depletion enhances DFMO induced polyamine depletion in MCF-7 human brest cancer cells in vivo. *Anticancer Res.* **18:** 2663-2668.

Li, G., Regunathan, S., Barrow, C. J., Eshraghi, J., Cooper, R., Reis, D. J. (1994) Agmatine-an endogenous clonidine-displacing substance in the brain. *Science* **263:** 966-969.

Li, X., Coffino, P. (1992) Regulated degradation of ornithine decarboxylase requires interaction with the polyamine-induced protein antizyme. *Mol. Cell. Biol***. 12:** 3556-3562.

Li, X., Coffino, P. (1993) Degradation of ornithine decarboxylase: Exposure of the C-terminal target by the polyamine-inducible inhibitory protein. *Mol. Cell. Biol***. 13:** 2377-2383.

Lorimer, I. A., Keppler-Hafkemeyer, A., Beers, R. A., Pegram, C. N., Bigner, D. D., Pastan, I. (1996) Recombinant immunotoxins specific for a mutant epidermal growth factor receptor: targeting with a single chain antibody variable domain isolated by phage display. *Proc. Natl. Acad. USA*. **93:** 14815-14820.

Low, N. M., Holliger, P., Winter, G. (1996) Mimicking somatic hypermutation: affinity maturation of antibodies displayed on bacteriophage using bacterial mutator strain. *J. Mol. Biol.* **260:** 359-368.

Lu, L., Stanley, B. A., Pegg, A. E. (1991) Identification of residues in ornithine decarboxylase essential for enzymatic activity and for rapid protein turnover. *Biochem J.* **277:** 1493-1495

Ma, J. Hiatt, A., Hein, M., Vine, N. D., Wang, F., Stabila, P., van, Dolleweerd, C., Mostov, K., Lehner, T. (1995) Generation and assembly of secretory antibodies in plants. *Science.* **268:** 716-719

Ma, J. K. C., Hein, M. B. (1996) Antibody production and engineering in plants. In *Engineering Plants for Commercial Products and Applications*. (eds Collins, G. B. & Sheperd, R. J.) (New York Academy of Sciences, NY). pp. 72-81.

Ma, J. K. C., Hiatt, A. (1996) Expressing antibodies in plants for immunotherapy. In *Transgenic plants: a production system for industrial and pharmaceutical proteins*. Owen, M. R. L. & Pen, P. (eds), pp 229-243 (John Wiley and Sons, London, UK.

Malik, P., Terry, T. D., Gowda, L. R., Langara, A., Petukhov, S. A., Symmons, M. F., Welsh, L. C., Marvin, D. A., Perham, R. N. (1996) Role of capsid structure and membrane protein processing in determining the size and copy number of peptides displayed on the major coat protein of filamentous bacteriophage. *J. Mol. Biol.* **260:** 9-21

Malmberg, R. L., Cellino, M. L. (1994) Arginine decarboxylase of oats is activated by enzymatic cleavage into two polypeptides. *J. Biol. Chem*. **28:** 2703-2706.

Malmberg, R. L., Watson, M. B., Galloway, G., Yu, W. (1998) Molecular genetic analyses of plant polyamines. *Crit. Rev. Plant Sci*. **17:** 199-224.

Marasco, W. A. (1995). Intracellular antibodies (intrabodies) as research reagents and therapeutic molecules for gene therapy. *Immunotechnol.* **1:** 1-19.

Marks, J. D., Hoogenboom, H. R., Bonnert, T. P., Mc Cafferty, J., Griffiths, A. D. and Winter, G. (1991) By-passing immunisation. Human antibodies from V-gene libraries displayed on phage. *J. Mol. Biol*. **222:** 581-597.

Marks, J. D, Griffiths, A. D., Malmqvist, M., Clackson, T. P., Bye ,J. M., Winter, G. (1992) By-passing immunization: building high affinity human antibodies by chain shuffling. *Biotechnology* **10:** 779-783.

Masgrau, C., Altabella, T., Farras, R., Flores, D., Thompson, A. J., Besford, R. T., Tiburcio, A. F. (1997) Inducible overexpression of oat arginine decarboxylase in transgenic tobacco plants. *Plant J.* **11:** 465-473.

Matsufuji, S., Matsufuji, T., Miyazaki, Y., Murakami, Y., Atkins, J. F., Gesteland, R. F., Hayashi, S. (1995) Autoregulatory frameshifting in decoding mammalian ornithine decarboxylase antizyme. *Cell* **80**: 51-60

McCafferty, J., Griffiths, A. D., Winter, G., Chiswell, D. J. (1990) Phage antibodies: filamentous phage displaying antibody variable domains. *Nature* **348:** 552-554.

McCann, P. P., Pegg, A. E. (1992) Ornithine decarboxylase as an enzyme target for therapy. *Pharmacol Ther.* **54:**195-215.

McConlogue, L., Dana, S. L., Coffino, P. (1986) Multiple mechanisms are responsible for altered expression of ornithine decarboxylase in overproducing variant cells. *Mol. Cell. Biol*. **6:** 2865-2871.

McConnell, S. J., Uveges, A. J., Fowlkes, D. M., Spinella, D.G. (1996) Construction and screening of M13 phage libraries displaying long random peptides. *Mol. Divers*. **1:** 165-176

McGuinness, B. T., Walter, G., FitzGerald, K., Schuler, P., Mahoney, W., Duncan, A. R., Hoogenboom, H. R. (1996) Phage diabody repertoires for selection of large numbers of bispecific antibody fragments. *Nat. Biotechnol*. **14:** 1149-1154.

Metcalf, B. W., Bey, P., Danzin, C. (1978) Catalytic irreversible inhibition of mammalian ornithine decarboxylase by substrate and product analogues. *J. Am. Chem. Soc*. **100:** 2551-2563.

Michael, A. J., Furze, J. M., Rhodes, M. J. C., Burtin, D. (1996) Molecular cloning and functional identification of a plant ornithine decarboxylase cDNA. *Biochem. J.* **314:** 241-248.

Michael, N. P., Chester, K. A., Melton, R. G., Robson, L., Nicholas, W., Boden, J. A., Pedley, R. B., Begent, R. H., Sherwood, R. F., Minton, N.P. (1996) In vitro and in vivo characterisation of a recombinant carboxypeptidase G2: anti-CEA scFv fusion protein. *Immunotechnol.* **2:** 47-57

Minocha, S. C., Minocha, R. (1995) Role of polyamines in somatic embryogenesis. *Biotechnology in Agriculture and Forestry* **30:** 53-70.

Minocha, R., Minocha, S. C., Simola, L. K. (1995) Somatic embryogenesis and polyamines in woody plants. In. *Somatic embryogenesis in woody plants.* S Jain, P Gupta, R Newton, (eds). Vol1. Kluwer Academic Publishers, Dordrecht. The Netherlands. pp 337-359.

Molinoux, J. P., Darcel, F., Quemener, V., Havouis, R., Seiler, N. (1991) Inhibition of the growth of U-251 Human glioblastoma in nude mice by polyamine deprivation. *Anticancer Res.* **11:** 175-180.

Morea, V., Leplae, R., Tramontano, A. (1998) In: Protein structure prediction and design. El-Gewely, M. R., (ed.), pp. 177-214. Elsevier, Amsterdam.

Morea, V., Lesk, A., Tramontano, A. (2000) Antibody modelling: Implications for engineering and design. *Methods* **20:** 267-279.

Morgan, D. M. L. (1998) Polyamine protocols-Methods in molecular biology. *Humana Press Inc.*

Morrison, L. D., Becker, L., And, L. C., Kish, S. J. (1995) Polyamines in human brain: Regional distribution and influence of aging. *J. Neurochem.* **65:** 636-642.

Morrison, L. D., Kish, S. J. (1995) Brain polyamine levels are altered in Alzheimer's disease. *Neurosci. Lett.* **197:** 5-8

Morrissey, J., McCracken, R., Ishidoya, S., Klahr, S. (1995) Partial cloning and characterisation of an arginine decarboxylase in the kidney. *Kidney International* **47:** 1458-1461.

Moshier, J. S., Dosescu, J., Skunca, M., Luk, G. (1993) Transformation of NIH/3T3 cells by ornithine decarboxylase overexpression. *Cancer Res*. **53:** 2618-2622.

Müller, H., Ziegler, B. and Schweizer, B. (1993) UV/VIS-Spektroskopie in der Nukleinsäureanalytik. *BioTec*. **4:** 25-29.

Munro, S., Pelham, H. R. (1987) A C-terminal signal pervents secretion of luminal ER proteins. *Cell* **48:** 899-907.

Murakami, Y., Matsufuji, S., Hayashi, S., Tanahashi, N., Tanaka, K. (2000) Degradation of ornithine decarboxylase by the 26S proteasome. *Biochem. Biophys. Res. Commun.* **267:** 1-6.

Murakami, Y., Matsufuji, S., Hayashi, S., Tanahashi, N., Tanaka, K. (1999) ATP-dependent inactivation and sequestration of ornithine decarboxylase by the 26S proteosome are prerequisites for degradation. *Mol. Cell. Biol.*, **19**: 7216–7227.

Murakami, Y., Matsufuji, S., Kameji, T., Hayashi, S., Igarashi, K., Tamura, T., Tanaka, K., Ichihara, A. (1992) Ornithine decarboxylase is degraded by the 26S proteasome without ubiquitination. *Nature*, **360**: 597–599.

Murthy, K. K., Ekiel, I., Shen, S. H., Banville, D. (1999) Fusion proteins could generate false positives in peptide phage display. *Biotech.* 26: 142-149.

Nagata, T., Okada, K., Kawazu, T., Tabeke, I. (1987) Cauliflower mosaic virus 35S promoter directs S-phase specific expression in plant cells. *Mol. Gen. Genet*. **207:** 242-244.

Nilsson, T., Warren, G. (1994) Retention and retrieval in the endoplasmic reticulum and the Golgi apparatus. *Curr. Opin. Cell Biol*. **6:** 517-521.

Nishioka, K., Melgarejo, A. B., Lyon, R. R., Mitchell, M. F. (1995) Polyamines as biomarkers of cervical intraepithelial neoplasia. *J. Cell. Biochem*. **23:** 87-95.

Nissim, A., Hoogenboom, H. R., Tomlinson, I. M., Flynn, G., Midgley, C., Lane, D., Winter, G. (1994) Antibody fragments from a 'single pot' phage display library as immunochemical reagents. *EMBO J.* **13:** 692-698.

Noh, E. W., Minocha, S. C. (1994) Expression of a human S-adenosylmethionine decarboxylase cDNA in transgenic tobacco and its effect on polyamine biosynthesis. *Transgenic. Res.* **3:** 26-35.

Nossal, N. G., Heppel, L. A. (1966) The release of enzymes by osmotic shock from Escherichia coli in experimental phase. *J. Biol. Chem.* **241:** 3055-3062.

Noury, M., Bassie, L., Lepri, O., Kurek, I., Christou, P., Capell, T. (2000) A transgenic rice cell lineage expressing the oat arginine decarboxylase (*adc*) cDNA constitutively accumulates putrescine in callus and seeds but not in vegetative tissues. *Plant Mol. Biol*. **43:** 537-544.

Oppenheim, A. B., Giladi, H., Goldenberg, D., Kobi, S., Azar, I. (1996) Vectors and transformed host cells for recombinant protein production at reduced temperatures. International patent application. WO 96/03521.

Orlandi, R., Gussow, D. H., Jones, P. T., Winter, G. (1989) Cloning immunoglobulin variable domains for expression by the polyamerase chain reaction. *Proc. Natl. Acad. Sci. USA*. **86:** 3833-3837.

Orum, H., Andersen, P. S., Oster, A., Johansen, L. K., Rise, E., Bjornvad, M., Svendsen, I., Engberg, J. (1993) Efficient method for constructing comprehensive murine Fab antibody libraries displayed on phage. *Nucleic Acids Res.* **21:** 4491-4498

Osterman, A. L., Kinch, L. N., Grishin, N. V., Phillips, M. A. (1995) Acidic residues important for substrate binding and cofactor reactivity in eukaryotic ornithine decarboxylase identified by alanine scanning mutagenesis. *J. Biol. Chem.* **270:** 11797-11802.

Owen M, Gandecha A, Cockburn B, Whitelam G. (1992) Synthesis of a functional anti-phytochrome single-chain Fv protein in transgenic tobacco. *Bio Technol.* **10:** 790-794.

Owen, M. R. L., Cockburn, B., Whitelam, G. (1996) The expression of recombinant antibody fragments in plants. In: *Transgenic Plants: A production system for Industrial and Pharmaceutical Proteins.* Owen, M. R. Pen, J. (eds) pp. 245-260. John Wiley, Chichester, UK.

Packham, G., Cleveland, J. L. (1994) Ornithine decarboxylase is a mediator of c-Myc-induced apoptosis. *Mol. Cell. Biol*. **14:** 5741-5747.

Pandit, M., Ghosh, B. (1988) Ornithine decarboxylase from embryos of jute seeds. *Phytochem.* **27:** 1609-1610.

Peeters, K., De Wilde, C., De Jaeger, G., Angenon, G., Depicker, A. (2001) Production of antibodies and antibody fragments in plants. *Vaccine* **19:** 2756- 2761.

Pegg, A. E. (1986) Recent advances in the biochemistry of polyamines in eukaryotes. *Biochem. J.* **234:** 249-262.

Pegg, A. E. (1988) Polyamine metabolism and its importance in neoplastic growth and a target for chemotherapy. *Cancer Res*. **48:** 759-774.

Pegg, A. E., McCann, P. P. (1992) S-adenosylmethionine decarboxylase as an enzyme target for therapy. *Pharmacol. Ther*. **56:** 359-377.

Pegg, A. E., McCann, P.P. (1982) Polyamine metabolism and function. *J. Physiol*. **243:** 212-221.

Perez-Amador, M. A., Carbonell, J. (1995) Arginine decarboxylase and putrescine oxidase in ovaries of Pisum sativum L. Changes during ovary senescence and carly stages of fruit development. *Plant Physiol.* **107:** 865-872.

Perisic O, Webb PA, Holliger P, Winter G, Williams RL. (1994) Crystal structure of a diabody, a bivalent antibody fragment. *Structure* **2:**1217-1226.

Phillips, J., Artsaenko, O., Fiedler, U., Horstmann, C., Mock, H. P., Müntz, K., Conrad, U. (1997) Seed specific immunomodulation of abscisic acid activity induces a developmental switch. *EMBO J*. **16:** 4489-4496.

Phillips, R., Press, M. C., Bingham, L., Grimmer, G. (1988) Polyamines in cultured artichoke explants: effects are primarily on xylogenesis rather then cell division. *J. Exp. Bot.* **39:** 473-480.

Piazenza, L., Peluffo, G., Radi, R. (2001) L-arginine-dependent suppression of apoptosis in *Trypanosoma cruzi*: Contribution of the nitric oxide and polyamine pathways. *Proc. Natl. Acad. Sci. USA*. **98:** 7301-7306.

Pistocchi, R., Keller, F., Bagni, N., Matile, P. (1988) Transport and subcellular localisation of polyamines in carrot protoplasts and vacuoles. *Plant Physiol.* **87:** 514-518.

Plückthun, A., Krebber, A., Horn, U., Knüpfer, U., Wenderoth, R., Nieba, L., Proba, K. Riesenberg, D. (1996) Producing antibodies in *Escherichia coli:* from PCR to fermentation. In *Antibody Engineering, A practical Approach.* McCafferty, J., Hoogenboom, H. R., Chiswell, D. J., (eds), pp. 203-252, IRL Press, Oxford University Press, New York.

Plückthun, A., Pack, P. (1997) New protein engineering approaches to multivalent and bispecific antibody fragments. *Immunotechnol.* 3: 83-106.

Primikirios, N. I., Roubelakis-Angelakis, K. (1999) Cloning and expression of an arginine decarboxylase cDNA from *Vitis vinifera* L. cell-suspention cultures. *Planta* **208:** 574-582.

Primikirios, N. I., Roubelakis-Angelakis, K. A. (2001) Indication for post-translational regulation of *Vitis vinifera* L. arginine decarboxylase. *Plant Mol. Biol*. **45:** 669-678.

Quemener, V., Blanchard, Y., Chamaillard, L., Havouis, R., Cipolla, B., Moulinoux, J. P. (1994) Polyamine deprivation: a new tool in cancer treatment. *Anticancer Res.* **14**: 443-448.

Raag, R., Whitlow, M. (1995) Single-chain Fvs. *FASEB J.* 9: 73-80.

Rakonjac, J., Jovanovic, G., Model, P. (1997) Filamentous phage infection-mediated gene expression: construction and propagation of the gIII deletion mutant helper phage R408d3. *Gene* **198:** 99-103.

Rajam, M. V. (1997) Polyamines. In: *Plant Ecophysiology*, M. N. V. Prasad (ed.), pp. 343-374. John Wiley and Sons, New York,

Rastogi, R., Sawhney, V. (1990) Polyamines and flower development in the male sterile stamenless-2 mutant of tomato. *Plant Physiol.* **93:** 439-445.

Rechsteiner, M (1987) Regulation of enzyme levels by proteolyses: the role of PEST regions. *Adv. Enzyme Regul*. **27:** 135-151.

Regunathan, S., Reis, D. J. (2000) Characterisation of arginine decarboxylase in rat brain and liver: distinction from ornithine decarboxylase. *J. Neurochem*. **74**: 2201-2208.

Roch, A. M., Nicolas, M. T., Quash, G. (1997) Ultrastructural immunolocalisation of polyamines in HeLa cells subjected to fast-freezing fixation and freeze substitution. *Histochem. Cell Biol.* **107:** 303-312.

Rogers, S., Wells, R., Rechsteiner, M. (1986) Amino acid sequence common to rapidly degraded proteins. The PEST hypothesis. *Science* **234:** 364-368.

Russell, D. H. (1980) Ornithine decarboxylase as a biological and pharmacological tool. *Pharmacology* **20:** 117-129.

Russell, M., Kidd, S., Kelley, M. R. (1986) An improved filamentous helper phage for generating single-stranded plasmid DNA. *Gene* **45:** 333-338.

Sambrook, J., Fritsch, E.F. and Maniatis, T. (1989) *Molecular cloning-A laboratory Manual*. Cold Spring Harbor Laboratory, New York.

Sambrook, J., Fritsch, E.F. and Maniatis, T. (1996) *Molecular cloning-A laboratory Manual*. Cold Spring Harbor Laboratory, 3rd edition.

Sanger, F., Nicklen, S., Coulsen, A. R. (1977) DNA sequencing chain terminating inhibitors. *Proc. Natl. Acad. Sci. USA*. **74:** 5463-5467.

Sanz, I. (1991) Multiple mechanisms participate in the generation of diversity of human H chain CDR3 regions. *J. Immunol*. **147:** 1720-1729.

Sarhan, S., Seiler, N. (1991) Effect of polyamine deprivation on the survival of intracranial glioblastoma bearing mice. *Anticancer Res.* **11:** 987-992.

Satriano, J., Matsufuji, S., Murakami, Y., Lortie, M. J., Schwartz, D., Kelly, C.J., Hayashi, S., Blantz, R. C. (1998) Agmatine suppresses proliferation by frameshift induction of antizyme and attenuation of cellular polyamine levels. *J Biol. Chem.* **273:** 15313-15316.

Schable, K. F., Zachau, H. G. (1993) The variable genes of the human immunoglobulin kappa locus. *Biol. Chem. Hoppe Seyler.* **374:** 1001-1022.

Schaffitzel, C., Plückthun, A. (2001) Protein-fold evolution in the test tube. *Trends Biochem. Sci.* **26:** 577-579.

Schein, C. H. (1989) Production of soluble recombinant proteins in bacteria. *Bio Technol*. **7:** 1141-1149.

Schillberg, S., Zimmermann, S., Voss, A., Fischer, R. (1999) Apoplastic and cytosolic expression of full-size antibodies and antibody fragments in Nicotiana tabacum. *Transgenic Res.* **8:** 255-263

Schillberg, S., Zimmermann, S., Zhang, M. Y., Fischer, R. (2001) Antibodies-based resistance to plant pathogens. *Transgenic Res*. **10:** 1-12.

Scholthof, H., Scholthof, K., Jackson, A. (1996) Plant virus gene vectors for transient expression of foreign proteins in plants. *Annu. Rev. Phytopathol*. **34:** 299-323

Schouten, A., Roosien, J., van Engelen, F. A., De Jong, G. A., Borst-Vrenssen, A. W., Zilverentant, J. F., Bosch, D., Stiekema, W. J., Gommers, F. J., Schots, A., Bakker, J. (1996) The C-terminal KDEL sequence increases the expression level of a single-chain antibody designed to be targeted to both the cytosol and the secretory pathway in transgenic tobacco. *Plant Mol. Biol.* **38:** 781-793.

Schröder, G., Schröder, J. (1995) cDNA from *Catharantus roseus*, heterologus expression, identification of the proenzyme-processing site, evidence for the presence of both subunits in the active enzyme, and a conserved region in the 5'-mRNA leader. *Eur. J. Biochem*. **228:** 74-78.

Schröder, H. W., Jr, Mortary, F., Shiokawa, S., Kirkham, P. M., Elgavish, R. A., Bertrand, F. E., III. (1995a) Developmental regulation of the human antibody repertoire. *Annu. N. Y. Acad. Sci.* **764:** 242-260.

Seehaus, T., Breitling, F., Dübel, S., Klewinghuas, I., Little, M. (1992) A vector for removal of deletion mutants from antibody libraries. *Gene* **114:** 235-237.

Seidenfeld, J., Block, A. L., Komar, K. A., Naujokas, M. F. (1986) Altered cell cycle phase distributions in cultured human carcinoma cells partially depleted of polyamines by treatments with difluoromethylornithine. *Cancer Res.* **46:** 47-53.

Sharma, P., Rajam, M. V. (1995) Spatial and temporal changes in endogenous polyamine levels associated with somatic embryogenesis from different hypocotyl segments of eggplant (*Solanum melongera* L.). *J. Plant. Physiol.* **146:** 658-664.

Sharma, P., Yadav, J. S., Rajam, M. V. (1997) Induction of laterals in root cultures of eggplant (*Solanum melongena* L.) in hormone–free liquid medium: A novel system to study the role of polyamines. *Plant Sci.* **125:** 103-111.

Shimada, N., Suzuki, Y., Nakajima, M., Conrad, U., Murofushi, N., Yamaguchi, I. (1999) Expression of a functional single chain antibody against $GA_{24/19}$ in transgenic tobacco. *Biosci. Biotechnol. Biochem*. **63:** 779-783.

Shore, L. J., Soler, A. P., Gilmour, S. K. (1997) Ornithine decaroxylase expression leads to translocation and activation of protein kinase CK2 *in vivo*. *J. Biol. Chem*. **272:** 12536-12543.

Skerra, A., Plückthun, A. (1988) Assembly of functional immunoglobulin Fv fragment in *Escherichia coli. Science* **240:** 1038-1040.

Slocum, R. D. (1991) Polyamine biosynthesis in plants. In: *The Biochemistry and Physiology of Polyamines in Plants.* Slocum, R. D., Flores, H. E., (eds). pp. 23-40. Boca Raton, FL: CRC Press.

Slocum, R. D. (1991a) Tissue and subcellular localisation of polyamines and enzymes of polyamine metabolism. In: *The Biochemistry and Physiology of Polyamines in Plants.*

Slocum, R. D., Flores, H. E., (eds). pp. 93-103. Boca Raton, FL: CRC Press.

Slocum, R. D., Kaur-Sawhney, R., Galston, A. W. (1984) The physiology and biochemistry of polyamines in plants. *Arch. Biochem. Biophys.* **235:** 283-303.

Slocum, R. D., Weinstein, L. H. (1990) Stress-induced putrescine accumulation as mechanism of ammonia detoxification in cereal leaves. In: *Polyamines and ethylene: biochemistry, physiology, and interactions. Current topics in plant physiology*. Flores, H. E., Arteca, R. N., Shannon, J. C. (eds). Vol 5. pp. 157-165. *Soc. Plant Physiologists*.

Rockville, Slotkin, T. A., Bartolome, J. (1986) Role of ornithine decarboxylase and the polyamines in nervous system development: a review. *Brain Res. Bull*. **17:** 307-320.

Smith, D. B. (1993) Purification of glutathione S-transferase fusion proteins. *Meth. Mol. Cell Biol.* **4:** 220-229

Smith, M. D., and Glick, B. R. (2000) The production of antibodies in plants. *Biotechnol. Adv.* **18:** 85-89.

Smith, P. K., Krohn, R. I., Hermanson, G. T., Mallia, A. K., Gartner, F. H., Provencano, M. D., Fujimoto, E. K., Goeke, N. M., Olson, B. J. and Klenk, D. C. (1985) Measurement of protein using bicinchoninic acid. *Anal. Biochem*. **150**: 76-85.

Smith, T. A. (1985) Polyamines. *Annu. Rev. Plant Physiol*. **36:** 117-143.

Smith., G. P. (1985) Filamentous fusion phage: Novel expression vectors that display cloned antigens on the virion surface. *Science* **228:** 1315-1317.

Smith, T. A. (1988) The di- and poly-amine oxidases of higher plants. *Biochem. Soc. Trans*. **13:** 319-322.

Smith, T. A. (1990) Plant polyamines: metabolism and function. In: *Polyamine and Ethylene: Biochemistry, Physiology, and Interactions*. H. E. Flores, R. N. Arteca, J. C. Shannon, (eds.), pp 1-17. American Society of Plant Physiologists, Rockville, MD.

Smith, G. P., Scott, J. K. (1993) Libraries of peptides and proteins displayed on filamentous phage. *Methods Enzymol.* **217:** 228-257.

Snyder, R. D., (1989) Polyamine depletion is associated with altered chromatin structure in HeLa cells. *Biochem. J.* 260: 697-704.

Songsivilai, S., Dharakul, T. (1998) Genetically engineered single-chain Fvs of human immunoglobulin against hepatitis C virus nucleocapsid protein derived from universal phage display library. *Asian. Pac. J. Allergy Immunol.* **1:** 31-41.

Sorensen, K. and Brodbeck, U. (1986) A sensitive protein assay method using micro titer plates. *Experimentia* **42:** 161-162.

Spiegelberg, H. L. (1974) Biological activities of Igs of different classes and subclasses. *Adv. Immunol.* **19:** 259.

Stemmer, W. P. (1994a) DNA shuffling by random fragmentation and reassembly: in vitro recombination for molecular evolution. *Proc. Natl. Acad. Sci. USA.* **91:** 10747-10751.

Stemmer, W. P. (1994b) Rapid evolution of a protein in vitro by DNA shuffling. *Nature* **370:** 389-391.

Stoger, E., Vaquero, C., Torres, E., Sack, M., Nicholson, L., Drossard, J., Williams, S., Keen, D., Perrin, Y., Christou, P., Fischer, R. (2000) Cereal crops as viable production and storage systems for pharmaceutical scFv antibodies. *Plant Mol. Biol*. **42:** 583-590.

Tabor, C.V., Tabor, H. (1984) Polyamines. *Annu. Rev. Biochem*. **53:** 749-790.

Tabor, H., Tabor, C. W., Irreverre, F. (1973) Quantitative determination of aliphatic diamines and polyamines by an automated liquid chromatography procedure. *Anal. Biochem*. **55:** 457.

Takahashi, Y., Mai, M., Nishioka, K. (2000) α-difluoromethylornithine induces apoptosis as well as anti-angiogenesis in the inhibition of tumor growth and metastasis in human gastric cancer model. *Int. J. Cancer*: **85:** 243-247.

Talmadge, K., Gilbert, W. (1982) Cellular localization affects protein stability in *Escherischia coli. Proc. Natl. Acad. Sci. USA.* **79:** 1830-1833.

Tarenghi, E., Martin-Tanguy, J. (1995) Polyamines, floral induction and floral development of strawberry (*Fragaria ananassa* duch). *Plant Growth Reg.* **17:** 157-165.

Tavladoraki, P., Benvenuto, E., Trinca, S., Martinis, D. D., Cattaneo, A., Galeffi, P. (1993) Transgenic plants expressing a functional single-chain Fv antibody are specifically protected from virus attack. *Nature* **366:** 469-472.

Tavladoraki, P., Schinina, M. E., Lecconi, F., Di Agostino, S., Manera, F., Rea, G., Mariottini, P., Federico, R., Angelici, R. (1998) Maize polyamine oxidase: primary structure from protein and cDNA sequencing. *FEBS Lett.* **426:**62-66.

Taylor, M. A., Mad Arif, S. A., Kumar, A., Davies, H. V., Scobie, L. A., Pearce, S. R., Flavell, A. J. (1992) Expression and sequence analysis of cDNAs induced during the early stages of tuberisation in different organs of potato plant (*Solanum tuberosum*). *Plant Mol. Biol*. **20:** 641-651.

Terano, S., Suzuki, Y. (1978) Formation of β-alanine from spermine and spermidine in maize shoots. *Phytochem.* **17:** 148-149.

Thomas, T., Gallo, M. A., Klinge, C. M., Thomas, T. J. (1995) Polyamine-mediated conformational perturbations in DNA alter the binding of estrogen receptor to poly(dG-m5dC).poly(dG-m5dC) and a plasmid containing the estrogen response element. *J. Steroid Biochem. Mol. Biol.* **54:** 89-99.

Thomas, T., Thomas, T. J. (2001) Polyamines in cell growth and cell death: molecular mechanisms and therapeutic applications. *Cell Mol. Life Sci*. **58:** 244-258.

Tiburcio, A. F., Gendy, C. A., Tran Thanh Van, K. (1989) Morphogenesis in tobacco subepidermal cells: Putrescine as a marker of root differentiation. *Plant Cell Tiss. Org. Cult.* **19:** 43-54.

Tiburcio, A. F., Kaur-Sawhney, R., Galston, A. W. (1990) Polyamine metabolism. in *Intermedatory Nitrogen Metabolism* (Vol 16, *The Biochemistry of Plants*). Miflin, B. and Lea, P. J., (eds), pp. 283-325. Academic Press.

Tiburcio, A. F., Altabella, T., Borrel, A., Masgrau, C. (1997) Polyamine matabolism and its regulation. *Physiol. Plant.* **100:** 664-674.

Tobias, K. E., Khahana, C. (1993) Intersubunit location of the active site of mammalian ornithine decarboxylase as determined by hybridization of site-directed mutants. *Biochem.* **32:** 5842-5847.

Tomlinson, I. M., Cook, G. P., Walter, G., Carter, N. P., Riethman, H., Buluwela, L., Rabitts, T. H., Winter, G. (1995) A complete map of the human immunoglobulin VH locus. *Annu. N. Y. Acad. Sci.* **764:** 43-46.

Toney, M. D., Kirsch, J. F. (1993) Lysine 258 in aspartate aminotransferase: enforcer of the Circe effect for amino acid substrates and general-base catalyst for the 1,3-prototropic shift. *Biochem.* **32**: 1471-1479.

Töpfer, R., Pröls, M., Schell, J., Steinbiss, H. H. (1988) Transient gene expression in tobacco protoplasts: II. Comparison of the reporter gene systems for CAT, NPT II and GUS. *Plant Cell Rep.* **7:** 225-228.

Tur, M. K., Huhn, M. Sasse, S., Engert, A., Barth, S. (2001) Selection of phages on intact cells under low pH conditions lead to a significant loss of insert-free phages. *Biotech.* **30:** 404-408.

Vaughan, T. J., Williams, A. J., Pritchard, K., Osbourn, J. K., Pope, A. R., Earnshaw, J. C., McCafferty, J., Hodits, R. A., Wilton, J., Johnson, K. S. (1996) Human antibodies with sub-nanomolar affinities isolated from a large non-immunized phage display library. *Nature Biotechnol*. **14:** 309-314.

Vaquero, C., Sack, M., Chandler, J., Drossard, J., Schuster, F., Monecke, M., Schillberg, S., Fischer, R. (1999) Transient expression of a tumor-specific single-chain fragment and a chimeric antibody in tobacco leaves. *Proc. Natl. Acad. Sci*. **96:** 11128-11133.

Verma, R., Boleti, E., George, A. J. T. (1998) Antibody engineering: comparison of bacterial, yeast, insect and mammalian expression systems. *J. Immunol. Methods*. **216:** 165-181.

Virnekäs, B., Ge, L., Plückthun, A., Schneider, K. C., Wellnhofer, G., Moroney, S. E. (1994) Trinucleotide phosphoramidites: ideal reagents for the synthesis of mixed oligonucleotides for random mutagenesis. *Nucl. Acids. Res*. **22:** 5600-5607.

Vitetta, E., Uhr, J. (1985) Immunotoxins. *Annu. Rev. Immunol*. **3:** 197-212.

Voss, A., Niersbach, M., Hain, R., Hirsch, H. J., Liao, Y., Kreuzaler, F., Fischer, R. (1995) Reduced virus infectivity in *N. tabacum* secreting a TMV-specific full-size antibody. *Mol. Breed*. **1:** 15-26.

Vaughan, T. P., Williams, A. W., Pritchard, K., Osbourn, J. K., Pope, A., McCaffety, J., Hodits, R. A., Wilton, J., Johnson, K. S. (1996). Human antibodies with sub-nanomolar affinities isolated from a large non-immunized phage display library. *Nature Biotechnol*. **14:** 309-314.

Wagner, A. J., Meyers, C., Laimins, A. L., Hay, N. (1993) c-Myc induces the expression and activity of ornithine decarboxylase. *Cell Growth Differ.* **4:** 879-883.

Whitlow, M., Bell, B. A., Feng, S. L., Filpula, D., Hardman, K. D., Hubert, S. L., Rollence, M. L., Wood, J. F., Schott, M. E., Milenic, D. E. (1993) An improved linker for single chain Fv with reduced aggregation and enhanced proteolytic stability. *Protein Eng*. **6:** 989-995.

Wiechelman, K., Braun, R. And Fitzpatric, J. (1988) Invenstigation of the bicinchoninic acid protein assay: Identification of the groups responsible for color formation. *Anal. Biochem*. **175:** 231-237.

Williams, K. (1994) Modulation of the N-methyl-D-aspartate receptor by polyamines: molecular pharmacology and mechanisms of action. *Biochem. Soc. Trans.* **22:** 884-887.

Williams, K. (1997) Interaction of polyamines with ion channels. *Biochem. J.* **325:** 289-297.

Williams, K., Romano, C., Dichter, M. A., Molinoff, P. B. (1991) Modulation of the NMDA receptor by polyamines. *Life Sci.* **48:** 469-498.

Winter, G., Griffiths, A. D., Hawkins, R. E., Hoogenboom, H. R., (1994) Making antibody by phage display technology. *Annu. Rev. Immunol*. **12:** 433-455.

Winter, G., Milstein, C, (1991) Man-made antibodies. *Nature* **349:** 293-299.

Wörn, A., Plückthun, A. (2001) Stability engineering of antibody single-chain Fv fragments. *J. Mol. Biol*. **305:** 989-1010.

Wright, R. M., Gram, H., Vattay, A., Byme, S., Lake, P., Dottavio, D. (1995) Binding epitope of somatostatin defined by phage-displayed peptide libraries. *Biotechnology* **13:** 165-169

Wu, D. Y., Ugozzoli, L., Pal, B. K., Wallace, R. B. (1991) The effect of temperature and oligonucleotide primer length on the specificity and efficiency of amplification by polymerase chain reaction. *DNA Cell Biol.* **10:** 233-238.

Yang, W. P., Green, K., Prinz-Sweeney, S., Briones, A. T., Burton, D. R., Barbas, C. F. III. (1999) CDR walking mutagenesis for the affinity maturation of a potent human anti-HIV-1 antibody into the picomolar range. *J. Mol. Biol.* **254:** 392-403.

Yanisch-Perron, C., Vieira, J., Messing, J. (1985) Improved M13 phage cloning vectors and host strains: nucleotide sequences of the M13mp18 and pUC19 vectors. *Gene* **33:** 101-119.

Yokota, T., Milenic, D. E., Whitlow, M., Schlom, J. (1992) Rapid tumor penetration of a single-chain Fv and comparison with other immunoglobulin forms. *Cancer Res.* **53:** 3402.

Young, N. D., Galston, A. W. (1983) Putrescine and acidic stress. *Plant Physiology* **71:** 767-771.

Young, N. D., Galston, A. W. (1984) Physiological control of arginine decarboxylase activity in K^+ deficient oat shoots. *Plant Physiol.* **76:** 331-335.

Zhang, M. Y. (2000) Generation, characterization and expression of single chain antibody fragments (scFvs) specific fort he NSM movement protein of tomato spotted wilt virus (TSWV). RWTH Aachen. Dissertation.

Zhang, M.Y., Schillberg, S., Zimmerman, S., Liao. Y.C., Breuer, G., Fischer, R. (2001) GST fusion proteins cause false positives during selection of viral movement protein specific single chain antibodies. *J. Virol. Methods*. **91**: 139-147.

Zheliaskova, A., Naydenova, S., Petrov, A. G. (2000) Interaction of phospholipid bilayers with polyamines of different length. *Eur. Biophys*. **29:** 153-157.

Zimmermann, S., Schillberg, S., Liao, Y. C., Fischer, R. (1998) Intracellular expression of TMV-specific single chain Fv fragments leads to improved virus resistance in *Nicotiana tabacum*. *Mol. Breeding* **4:** 369-379.

VII Appendices

VII.I Abbreviations

ABTS	2,2'-Azino-di-(3-ethylbenzthiazoline sulphonate)
Ab	Antibody
ADC	Arginine decarboxylase
Ag	Antigen
Amp	Ampicillin
AP	Alkaline phosphatase
AZ	Antizyme
B cell	Bone-marrow-derived lymphocyte
BCIP	5-bromo-4-chloro-3-indolyl phosphate
bp	Baise pair
BSA	Bovine serum albumin
$CaCl_2$	Calcium chloride
CaMV	Cauliflower mosaic virus
Carb	Carbenicillin
CB	Cleavage buffer
CDR	Complementarity determining region
cDNA	Complementary DNA
cfu	Colony-forming units
CHS	Chalcone synthase
CI	Chloroform/isoamyl alcohol (24:1)
C_H/C_L	Heavy/Light constant domains
CLB	Cell lysis buffer
Cys	Cysteine
cv.	Cultivar
D	Diversity gene segments
DAO	Diamine oxidase
DEAE	Diethylaminoethyl
DFMO	Difluoromethylornithine
DEPC	Diethylpyrocarbonate
DMSO	Dimethyl sulfoxide
DNA	Deoxyribonucleic acid
dNTP	Deoxyribonucleoside triphosphate
DTT	1,4-dithiothreitol
E. coli	*Escherichia coli*
EDC/NHS	N-Ethyl-N′-(Dimethylaminopropyl)
EDTA	Ethylenediamine tetraacetic acid

ELISA	Enzyme-linked immunosorbent assay
EMSA	Electrophoretic mobility shift assay
ER	Endoplasmatic reticulum
EtOH	Ethanol
Fab	Fragment antigen binding
Fc	Fragment crystalline
FRs	Framework regions
FV channels	fast-activating vacuolar channel
g	Relative centrifugal force (RCF)
GABA	Gamma-aminobutiric acid
gIII	Gene III (encoding minor coat protein III)
gVIII	Gene VIII (encoding major phage coat protein VIII)
GST	Glutathione S-transferase
GSM	*Agrobacteria* glycerol stock media
h	Hour(s)
HCl	Hydrochloride
his	Histidine
HRP	Horse radish peroxidase
IPTG	Isopropyl B-D-thiogalactopyranoside
IMAC	Immobilized metal ion affinity cgromatography
J	Joining gene segments
Lys	Lysine
kb	Kilobase pair
kDa	Kilodalton
KDEL	ER retention signal
Km	Kanamycin
M	Molarity
MES	2-(N-morpholino)-ethanesulphonic acid
min	Minute(s)
MPBS	Non-fat skrim milk powder in PBS
$MgSO_4$	Magnesium sulfate
MOPS	3-(morpholino)propanesulfonic acid)
mRNA	Messenger RNA
NaCl	Sodium chloride
OD	Optical density
ODC	Ornithine decarboxylase
o/n	Overnight
ORF	Open reading frame
Ori	Origin of replication
PAO	Polyamine oxidase
PBS	Phosphate buffered saline
PBST	0.1% Tween-20 in PBS

PCI	Phenol/chloroform/isoamyl alcohol (25:24:1)
PCR	Polymerase chain reaction
PEG	Polyethylene glycol
PLP	pyridoxal 5′-phosphate
poly A	Polyadenylation signal
pH	A logarithmic measure of hydrogen ion concentration
pIII	Phage minor protein III
pVII	Phage minor coat protein VII
pVIII	Phage major protein VIII
pIX	Phage minor coat protein VII
pNPP	p-nitrophenyl phosphate
PVDF	Polyvinylidene fluoride
Pw	Tobacco mosaic virus RNA termination sequence
Rif	Rifampicilin
RNA	Ribonucleic acid
RNase	Ribonuclease
rpm	Rounds per minute
RT	Reverse transcription
S	Segment; small
SAM	S-adenosynmethgionine
SAMDC	S-adenosynmethionine decarboxylase
SB	Stripping buffer
scFv	Single-chain variable fragment
SDE	Spermidine synthase
SDS-PAGE	Sodium dodecyl sulphate-polyacrylamide gel electrophoresis
SME	Spermine synthase
SV channels	Slow vacuolar channels
TBE	Tri- buffered saline electrophoresis buffer
TEMED	N,N,N′, N′-tetramethylene-ethylenediamine
TMV	Tobacco mosaic virus
UTR	untranslated region
Ω	Omega leader region of TMV
V	Volt; variable region
V_H/V_L	Heavy/Light chain variable region
v/v	Volume per volume
w/v	Weight per volume
w/w	Weight per weight

VII.2 Nucleic acid and amino acid sequence of amplified human ODC

- Alignment between database entry M16650 (HSODC) and #103, ODC_L/TOPO (ODC)

Percent Similarity: 100.000 Percent Identity: 99.783

```
                .         .         .         .         .
ODC       4 NNFGNEEFDCHFLDEGFTAKDILDQKINEVSSSDDKDAFYVADLGDILKK 53
            |||||||||||||||||||||||||||||||||||||||||||||||||||
HSODC     2 NNFGNEEFDCHFLDEGFTAKDILDQKINEVSSSDDKDAFYVADLGDILKK 51
                .         .         .         .         .
ODC      54 HLRWLKALPRVTPFYAVKCNDSKAIVKTLAATGTGFDCASKTEIQLVQSL 103
            |||||||||||||||||||||||||||||||||||||||||||||||||||
HSODC    52 HLRWLKALPRVTPFYAVKCNDSKAIVKTLAATGTGFDCASKTEIQLVQSL 101

ODC     104 GVPPERIIYANPCKQVSQIKYAANNGVQMMTFDSEVELMKVARAHPKAKL 153
            |||||||||||||||||||||||||||||||||||||||||||||||||||
HSODC   102 GVPPERIIYANPCKQVSQIKYAANNGVQMMTFDSEVELMKVARAHPKAKL 151
                .         .         .         .         .
ODC     154 VLRIATDDSKAVCRLSVKFGATLRTSRLLLERAKELNIDVVGVSFHVGSG 203
            |||||||||||||||||||||||||||||||||||||||||||||||||||
HSODC   152 VLRIATDDSKAVCRLSVKFGATLRTSRLLLERAKELNIDVVGVSFHVGSG 201
                .         .         .         .         .
ODC     204 CTDPETFVQAISDARCVFDMGAEVGFSMYLLDIGGGFPGSEDVKLKFEEI 253
            |||||||||||||||||||||||||||||||||||||||||||||||||||
HSODC   202 CTDPETFVQAISDARCVFDMGAEVGFSMYLLDIGGGFPGSEDVKLKFEEI 251
                .         .         .         .         .
ODC     254 TGVINPALDKYFPSDSGVRIIAEPGRYYVASAFTLAVNIIAKKIVLKEQT 303
            |||||||||||||||||||||||||||||||||||||||||||||||||||
HSODC   252 TGVINPALDKYFPSDSGVRIIAEPGRYYVASAFTLAVNIIAKKIVLKEQT 301
                .         .         .         .         .
ODC     304 GSDDEDESSEQTFMYYVNDGVYGSFNCILYDHAHVKPLLQKRPKPDEKYY 353
            |||||||||||||||||||||||||||||||||||||||||||||||||||
HSODC   302 GSDDEDESSEQTFMYYVNDGVYGSFNCILYDHAHVKPLLQKRPKPDEKYY 351
                .         .         .         .         .
ODC     354 SSSIWGPTCDGLDRIVERCDLPEMHVGDWMLFENMGAYTVAAASTFNGFQ 403
            |||||||||||||||||||||||||||||||||||||||||||||||||||
HSODC   352 SSSIWGPTCDGLDRIVERCDLPEMHVGDWMLFENMGAYTVAAASTFNGFQ 401
                .         .         .         .         .
ODC     404 RPTIYYVMSGPAWQLMQQFQNPDFPPEVEEQDASTLPVSCAWESGMKRHR 453
            |||||||||||||:|||||||||||||||||||||||||||||||||||||
HSODC   402 RPTIYYVMSGPAWELMQQFQNPDFPPEVEEQDASTLPVSCAWESGMKRHR 451
                .
ODC     454 AACASASINV 463
            ||||||||||
HSODC   452 AACASASINV 461
```

- Length 1394; 364A, 297C, 359G, 374T

```
CCATGGGTAACAACTTTGGTAATGAAGAGTTTGACTGCCACTTCCTCGAT
GAAGGTTTTACTGCCAAGGACATTCTGGACCAGAAAATTAATGAAGTTTC
TTCTTCTGATGATAAGGATGCCTTCTATGTGGCAGACCTGGGAGACATTC
TAAAGAAACATCTGAGGTGGTTAAAAGCTCTCCCTCGTGTCACCCCCTTT
TATGCAGTCAAATGTAATGATAGCAAAGCCATCGTGAAGACCCTTGCTGC
TACCGGGACAGGATTTGACTGTGCTAGCAAGACTGAAATACAGTTGGTGC
AGAGTCTGGGGGTGCCTCCAGAGAGGATTATCTATGCAAATCCTTGTAAA
CAAGTATCTCAAATTAAGTATGCTGCTAATAATGGAGTCCAGATGATGAC
TTTTGATAGTGAAGTTGAGTTGATGAAAGTTGCCAGAGCACATCCCAAAG
CAAAGTTGGTTTTGCGGATTGCCACTGATGATTCCAAAGCAGTCTGTCGT
CTCAGTGTGAAATTCGGTGCCACGCTCAGAACCAGCAGGCTCCTTTTGGA
ACGGGCGAAAGAGCTAAATATCGATGTTGTTGGTGTCAGCTTCCATGTAG
```

GAAGCGGCTGTACCGATCCTGAGACCTTCGTGCAGGCAATCTCTGATGCC
CGCTGTGTTTTTGACATGGGGGCTGAGGTTGGTTTCAGCATGTATCTGCT
TGATATTGGCGGTGGCTTTCCTGGATCTGAGGATGTGAAACTTAAATTTG
AAGAGATCACCGGCGTAATCAACCCAGCGTTGGACAAATACTTTCCGTCA
GACTCTGGAGTGAGAATCATAGCTGAGCCCGGCAGATACTATGTTGCATC
AGCTTTCACGCTTGCAGTTAATATCATTGCCAAGAAAATTGTATTAAAGG
AACAGACGGGCTCTGATGACGAAGATGAGTCGAGTGAGCAGACCTTTATG
TATTATGTGAATGATGGCGTCTATGGATCATTTAATTGCATACTCTATGA
CCACGCACATGTAAAGCCCCTTCTGCAAAAGAGACCTAAACCAGATGAGA
AGTATTATTCATCCAGCATATGGGGACCAACATGTGATGGCCTCGATCGG
ATTGTTGAGCGCTGTGACCTGCCTGAAATGCATGTGGGTGATTGGATGCT
CTTTGAAAACATGGGCGCTTACACTGTTGCTGCTGCCTCTACGTTCAATG
GCTTCCAGAGGCCGACGATCTACTATGTGATGTCAGGGCCTGCGTGGCAA
CTCATGCAGCAATTCCAGAACCCCGACTTCCCACCCGAAGTAGAGGAACA
GGATGCCAGCACCCTGCCTGTGTCTTGTGCCTGGGAGAGTGGGATGAAAC
GCCACAGAGCAGCCTGTGCTTCGGCTAGTATTAATGTGGTCGAC

Figure VII-1 Nucleic acid and amino acid sequences of human ornithine decarboxylase (ODC) amplified from prostate cDNA library. Plasmid ODC_L/TOPO reference number #103. Sequences were compared to the database entries M16650 (HSODC) from which the primers for PCR amplification were derived. The single point mutation is highlighted in the sequence. Comparison was performed with program GAP or Pileup of the GCG sequence analysis software package.

VII.3 Schematic presentation of vector maps

A

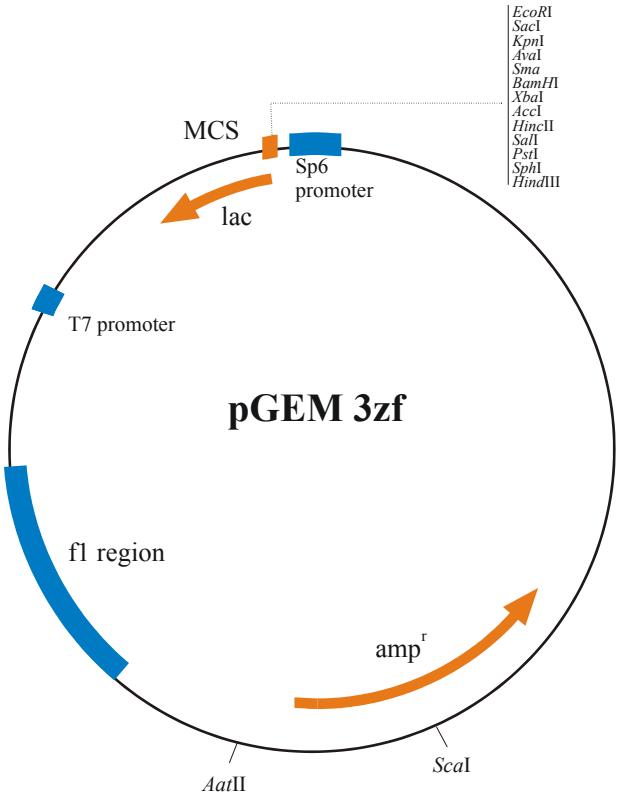

B

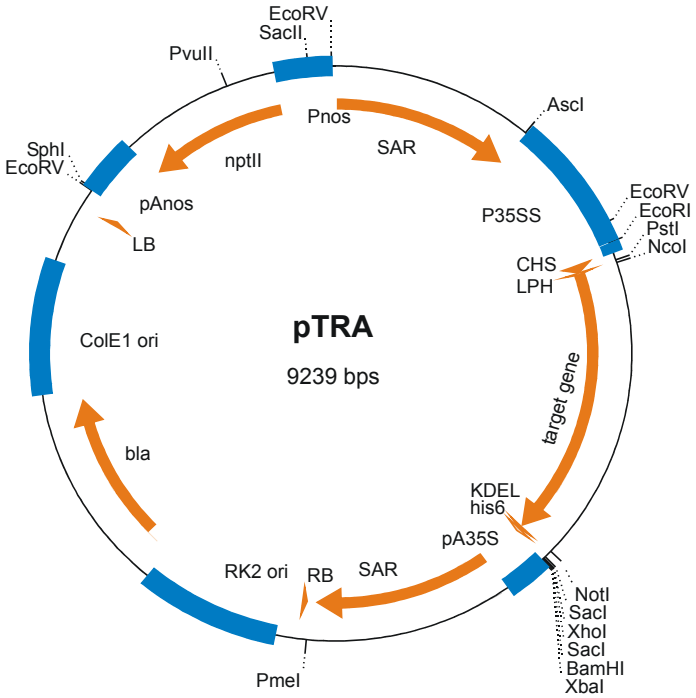

C

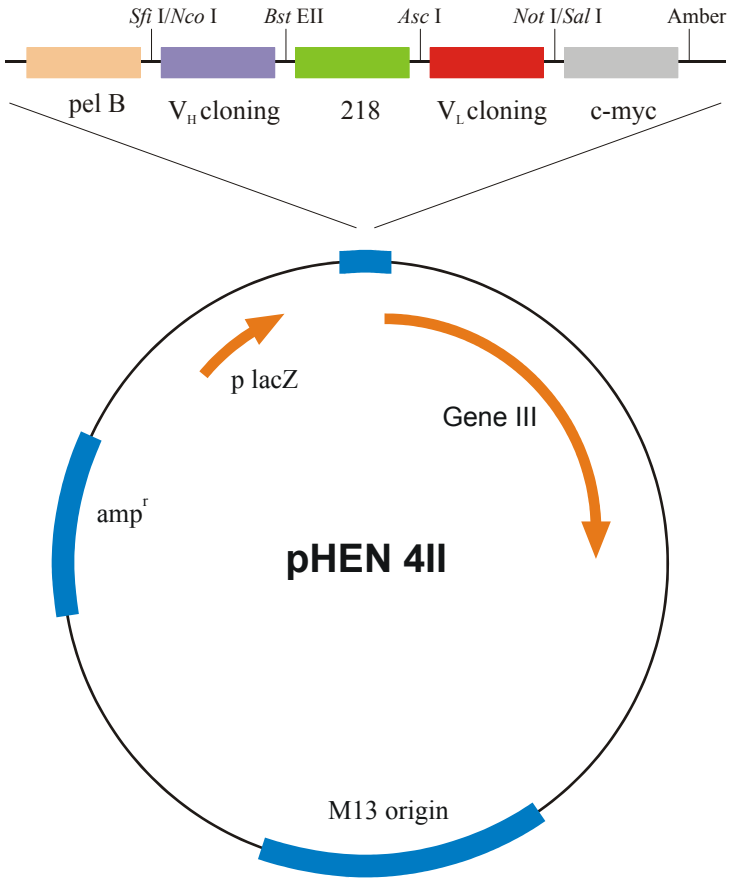
Sfi I/Nco I
Bst EII
Asc I
Not I/Sal I
Amber
pel B
V_H cloning
218
V_L cloning
c-myc
p lacZ
Gene III
amp^r
pHEN 4II
M13 origin

D

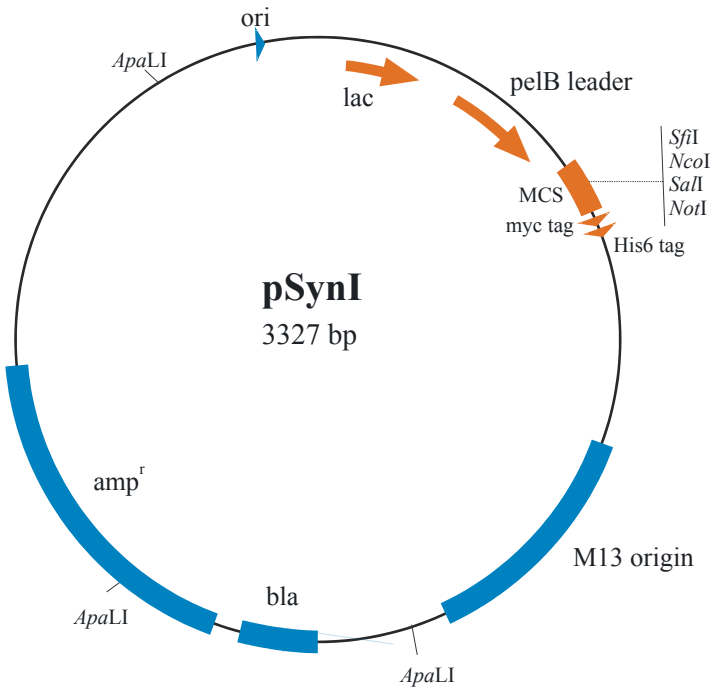
ori
ApaLI
lac
pelB leader
SfiI
NcoI
SalI
NotI
MCS
myc tag
His6 tag
pSynI
3327 bp
amp^r
M13 origin
bla
ApaLI
ApaLI

E

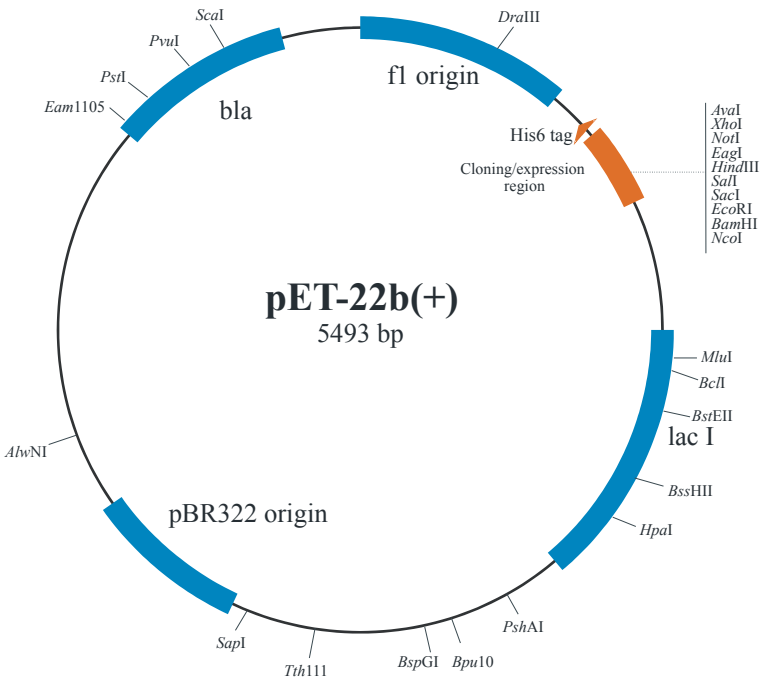
ScaI
PvuI
PstI
Eam1105
bla
DraIII
f1 origin
His6 tag
Cloning/expression region
AvaI
XhoI
NotI
EagI
HindIII
SalI
SacI
EcoRI
BamHI
NcoI
pET-22b(+)
5493 bp
MluI
BclI
BstEII
lac I
BssHII
HpaI
PshAI
BspGI
Bpu10
Tth111
SapI
AlwNI
pBR322 origin


T7 promoter primer
BglII
T7 promoter
lac operator
XbaI
rbs
AGATCTCGATCCCGCGAAATTAATACGACTCACTATAGGGGAATTGTGAGCGGATAACAATTCCCCTCTAGAAATAATTTTGTTTAACTTTAAGAAGGAGA
NdeI
pelB leader
MscI
NcoI
BamHI
EcoRI
SacI
TATACATATGAAATACCTGCTGCCGACCGCTGCTGCTGGTCTGCTGCTCCTCGCTGCCCAGCCGGCGATGGCCATGGATATCGGAATTAATTCGGATCCGAATTCGAGCTCC
Met Lys Tyr Leu Leu Pro Thr Ala Ala Ala Gly Leu Leu Leu Leu Ala Ala Gln Pro Ala Met Ala Met Asp Ile Gly Ile Asn Ser Asp Pro Asn Ser Ser Ser
signal peptidase
SalI
HindIII
NotI
XhoI
His Tag
GTCGACAAGCTTGCGGCCGCACTCGAGCACCACCACCACCACCACTGAGATCCGGCTGCTAACAAAGCCCGAAAGGAAGCTGAGTTGGCTGCTGCCACCGCTGAGCAATC
Val Asp Lys Leu Ala Ala Ala Leu Glu His His His His His His End
T7 terminator primer
T7 terminator
TAGCATAACCCCTTGGGGCCTCTAAACGGGTCTTGAGGGGTTTTTTG
pET-22b(+) cloning/expression region

F

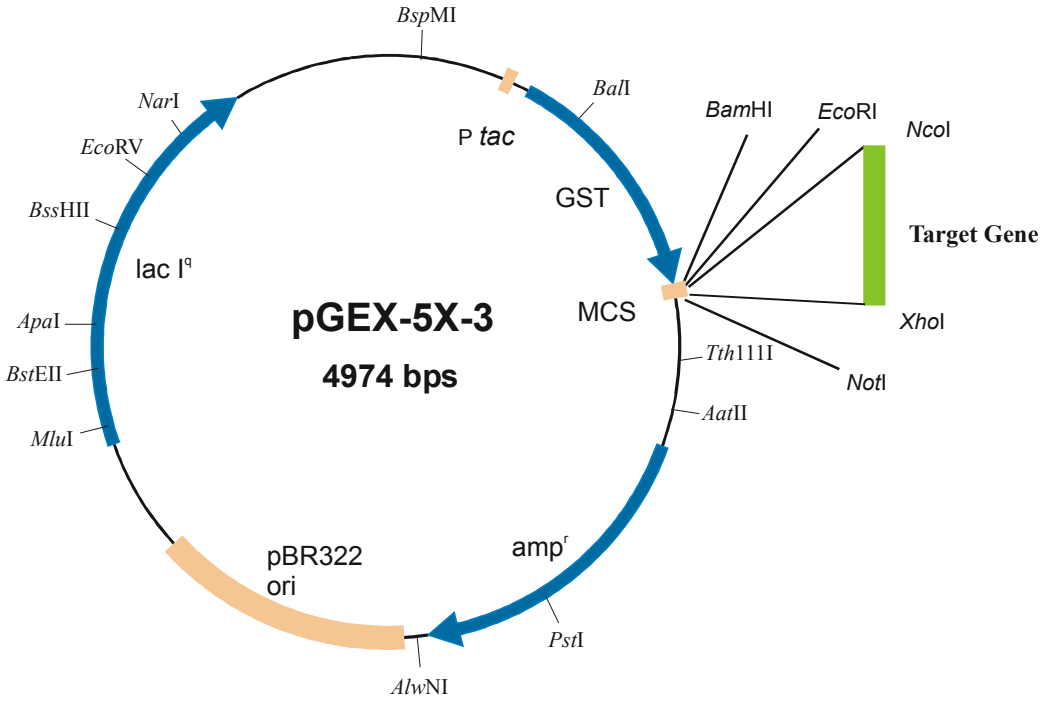

Figure VII-2 Schematic presentation of the vector maps. A: pGEM 3zf; B: pTRA; C: pHEN 4II; D: pSynI; E-pET22b(+) vector map. The nucleotide sequence of the expression region is indicated. F- pGEX-5x-3.

VII.4 Figures

Figure I-1 Structure of polyamines. 1
Figure I-2 Schematic representation of the polyamine biosynthetic pathway and its interrelationship with the ethylene pathway. 6
Figure I-3 Crystal structure of human ODC homodimer with the PLP as cofactor. 8
Figure I-4 Schematic presentation of IgG molecule and antibody fragments. 12
Figure I-5 Schematic overview of the project 21
Figure III-1 PCR amplification and cloning of human ODC gene. 51
Figure III-2 SDS-PAGE analysis of affinity purified GST fusion proteins. 52
Figure III-3 SDS-PAGE analysis of purified PAO proteins. 53
Figure III-4 SDS-PAGE analysis of purified ODC protein from pET22b vector via IMAC. 54
Figure III-5 Strategy for cloning of human ODC gene into pSS plant expression vector for cytosolic, apoplastic expression and ER retention. 55
Figure III-6 Transient expression of cytosolic and apoplastic ODC. 57
Figure III-7 Northern blot analysis of transcript levels of apoplastic and ER retained ODC.. 58
Figure III-8 Screening of stable transgenic tobacco plants expressing apoplastic and cytosolic ODC. 59
Figure III-9 Analysis of ODC-apo-7/3-2 x SDE-11-1/1 or (ODC x SDE/1→11) stable transformed tobacco plants co-expressing apoplasmic ODC and SDE. 60
Figure III-10 The polyamine profiles of the two T2 transgenic lines (ODC-apo-7/3-3 and ODC-apo-7/3-4) compared to wild type tobacco plants. 62
Figure III-11 Analyses of polyamine levels in T2 generation of transgenic plants expressing human ODC. 63
Figure III-12 Analyses of polyamine levels in T1 generation of transgenic plants co-producing ODC and SDE in the apoplast. 64
Figure III-13 Immunoblot analysis of 30-40 days old ODC-apo-7/3-O1-O10 transgenic T2 plants. 65
Figure III-14 ODC enzymatic activity analyses of T2 generation of stable transformed tobacco plant with apoplastic ODC. 65
Figure III-15 Determination of polyclonal antibody titers from mouse antiserum by direct ELISA. 67
Figure III-16 Analysis of total RNA isolated from mouse spleen cells . 68
Figure III-17 Amplification of variable heavy and light chain fragments from ADC immunized mice using primers specific for murine: IgG1; Ig2a/2b; κ. 69
Figure III-18 Schematic presentation of cloning procedure followed for construction of murine scFv libraries. 70

Figure III-19 Analysis of PCR product of randomly selected colonies from murine scFv libraries with specificity for ADC (A) and ODC (B). 71
Figure III-20 Analysis of murine scFv fragments after BstNI digestion. 72
Figure III-21 Screening of selected clones from the library HO_1LO_2 in soluble ELISA . 74
Figure III-22 Reactivity of selected murine scFv-fragments with ODC, ODC-GST and GST in direct ELISA. 75
Figure III-23 Reactivity of selected murine scFv fragments to ODC-GST and GST in capture ELISA. 75
Figure III-24 Alignment of the deduced amino acid sequences of selected murine scFv-fragments with specificity for ODC: scFvODC1, scFvODC3, scFvODC7 and scFvODC15. 77
Figure III-25 Reactivity of selected murine scFv-fragments to ADC-GST and GST in direct ELISA. 79
Figure III-26 Reactivity of selected murine scFv fragments to ADC-GST and GST in capture ELISA. 80
Figure III-27 Alignment of the deduced amino acid sequences of two selected murine scFv-fragments with specificity for ADC: scFvADC3 and scFvADC7. 82
Figure III-28 SDS-PAGE analysis of affinity purified scFvODC1, scFvOSC3, scFvODC7 and scFvODC15. 83
Figure III-29 Gel filtration chromatography of affinity purified ODC-specific scFvs. 85
Figure III-30 Reactivity of affinity purified scFvODC1, 3, 7 and 15 to ODC-GST and GST. 86
Figure III-31 Epitope mapping of scFvODC to ODC-GST by surface plasmon resonance.. 88
Figure III-32 Inhibition of scFvODC1 binding to immobilized ODC-GST by addition of soluble antigen. 89
Figure III-33 The functionality analysis of the scFvODC1 (A) and scFvODC3 (B) to ODC-GST antigen by EMSA. 90
Figure III-34 *In vitro* effect of scFvODC1 (A) and scFvODC3 (B) on the enzymatic activity of ODC 92
Figure III-35 Transient expression of ODC specific scFvs in tobacco leaves. 94
Figure III-36 Strategy for cloning of ODC specific murine scFvs into pSS plant expression vector for cytosolic targeting. 95
Figure III-37 Transient expression of cytosolic scFvODC1, scFvODC3 96
Figure III-38 ELISA analyses of cytosolic expressed murine scFvODC1 (A), scFvODC3 (B) to ODC-GST, SME-GST and GST. 97
Figure III-39 Immunoblot analysis of stable tobacco T_0 plants expressing apoplastic scFvODC1 and scFvODC3. 98
Figure III-40: SDS-PAGE analyses of affinity purified scFvADC3 and scFvADC7. 99
Figure III-41 Reactivity of affinity purified scFvADCs to ADC-GST and GST. 100
Figure III-42 Reactivity of biotinylated scFvADC3 to the ADC-GST antigen. 101

Figure III-43 Epitope mapping of scFvADC3 and scFvADC7. 102
Figure III-44 Transient expression of scFvADC3 in tobacco plants. 103
Figure VII-1 Nucleic acid and amino acid sequences of human ornithine decarboxylase (ODC) amplified from prostate cDNA library.. 149
Figure VII-2 Schematic presentation of the vector maps. A: pGEM 3zf; B: pTRA; C: pHEN 4II; D: pSynI; E-pET22b(+) vector map 153

VII.5 Tables

Table II-1 Names, suppliers and genotypes of *Escherichia coli* strains used throughout the work. 23
Table II-2 Murine phage display primer sequences for first strand cDNA generation from total RNA in 5′-3′ orientation. 26
Table II-3 Sequences of murine V_H domain specific front primers MPDVHF1-MPDVHF16 in 5′-3′ orientation..... 26
Table II-4 Sequences of murine V_L-domain specific front primers MPDVLF1-MPDVLF15 in 5′-3′ orientation. 27
Table II-5 Sequences of murine VH-domain specific back primers MPDVHB1-MPDVHB5 in 5′-3′ orientation 27
Table II-6 Sequences of murine κ V_L-domain specific back primers MPDVLB1-MPDVLB5 in 5′-3′ orientation..... 28
Table II-7 Primers used for DNA sequencing [LI-COR IR2-DNA sequencer, labelled with IRD 700 or IRD 800 (USB/Amersham)]..... 28
Table III-1 Summary of amplified variable heavy and light chain fragments from cDNAs of ADC, ODC-GST and PAO-GST immunized mice. 69
Table III-2 Summary of constructed murine phage displayed libraries 72
Table III-3 Enrichment of ADC-GST and ODC-GST binding phage through panning.. 73
Table III-4 Summary of sequence analysis of murine derived scFvs with specificity for ODC 78
Table III-5 V-gene family, germline deviation and extent of somatic hypermutation of four scFvs specific for ODC. 78
Table III-6 Summary of sequence analysis of murine derived scFvs with specificity for ADC. 81
Table III-7 V-gene family, germline deviation and extent of somatic hypermutation of two scFvs specific for ADC 81

Acknowledgements

Prof. Dr. Rainer Fischer for the opportunity to complete this thesis at the Institut für Biologie VII in Aachen, for his helpful suggestions and corrections of this thesis. I thank him very much for the help he offered to me when I started living in Aachen.

Prof. Dr. Fritz Kreuzaler for reviewing the thesis and agreeing to be co-examiner.

Dr. Bernd Schneider for his guidance, many comments and discussions at any time of the day and for giving this thesis a face-lift in english.

Dr. Stefan Schillberg for the continued interest and in-time encouragement during writing of this thesis.

Markus Sack for his help completing the BIAcore analyses, many influencal and constructive discussions, and his motivating enthusiasm.

Special thanks go to Dr. Flora Schuster for her friendship and help in stable transformation of tobacco plants.

I thank Dr. Jürgen Drossard for his help in polyamine analyses.

Dr. B. Schmidt for offering the opportunity to perform the radioactive assays in the Institut für Biologie V.

Furthermore, I would like to thank Dr. Carmen Vaquero-Martin and Dr. Stefano di Fiore for their support and useful discussions.

Many thanks go to Richa, Siham and Holger for their help, for the discussions, for their friendship and the funny times in the box 212.

Special thanks go to Sonal, Meltem, Simone, Kerstin, Rajan, Hatice, Jörg for making life inside and outside of the lab easier, funnier and more interesting.

To all members of the group I am very greatful for the cooperative spirit and the excellent working atmosphere, creating a unique setting for intellectual explorations as well as for culinary adventures.

Last, but not least I want to thank my parents and my brother for their love, their support and their patience throughout the last three decades. Without them none of this would have been possible. ‘‘Faleminderit nga zemra per gjithçka’’.

I thank Daniel who probably experienced most closely of all that writing a thesis can be a miserable business, not only for the author, but for all those in his immediate orbit. ‘‘Danke für Deine Geduld und unendliche Liebe’’.

Lebenslauf

Persönliche Daten

Name:	Greta Nölke, geb. Kondi
Geburtsdatum:	18. Mai 1972
Geburtsort:	Korce, Albanien
Familienstand:	verheiratet
Staatsangehörigkeit:	albanisch

Ausbildung

1986 – 1990	Raqi Qirinxhi Gymnasium, Korce, Albanien
1990 – 1995	Universität der Naturwissenschaften, Tirana, Albanien Abschluß: Diplom Biologie Thema der Arbeit: "Microalgae of Albanian lagoons: A case study approach"
1996 – 1997	Mediterranean Agronomic Institute of Chania (MAICH), Griechenland, Aufbaustudium des Umweltmanagements natürlicher Resourcen
1997 – 1998	Mediterranean Agronomic Institute of Chania (MAICH), Griechenland Abschluß: Master of Sciences Thema der Arbeit: "Biochemical characterisation of desaturase engineered rice and first steps towards antibody production of chloroplastic ω-3 desaturase"
seit Dezember 1998	Promotion am Institut für Biologie VII der RWTH Aachen unter Anleitung von Prof. Dr. Rainer Fischer

Berufserfahrung

1995 – 1996	Fan Noli Universität, Korce, Albanien Lehrtätigkeit aus Biologie, Anatomie, Tierphysiologie und Anorganische Chemie
1998	Lehrassistentin in den Kursen "Mikrobiologische Techniken" und "Molekularbiologische Techniken" Mediterranean Agronomic Institute of Chania (MAICH), Griechenland
seit Dezember 1998	Wissenschaftliche Hilfskraft am Institut für Biologie VII der RWTH Aachen